

Synthesis and Implication of 3d Transition Metal Catalysts for the Hydrogenative Transformations of Alkynes, Chalcones and Nitriles

by

Sharma Dipesh Mamraj
10CC17J26006

A thesis submitted to the
Academy of Scientific & Innovative Research
for the award of the degree of

DOCTOR OF PHILOSOPHY

in

SCIENCE

Under the supervision of

Dr. Benudhar Punji



CSIR- National Chemical Laboratory, Pune



Academy of Scientific and Innovative Research
AcSIR Headquarters, CSIR-HRDC campus
Sector 19, Kamla Nehru Nagar
Ghaziabad, U.P. – 201 002, India

Aug-2022

Certificate

This is to certify that the work incorporated in this Ph. D. thesis entitled, “Synthesis and Implication of 3d Transition Metal Catalysts for the Hydrogenative Transformations of Alkynes, Chalcones and Nitriles”, submitted by Mr. Dipesh Mamraj Sharma to the Academy of Scientific and Innovative Research (AcSIR) in fulfillment of the requirements for the award of the Degree of Doctor of Philosophy in Science, embodies original research work carried out by the student. We, further certify that this work has not been submitted to any other University or Institution in part or full for the award of any degree or diploma. Research material(s) obtained from other source(s) and used in this research work have been duly acknowledged in the thesis. Image(s), illustration(s), figure(s), table(s) etc., used in the thesis from other source(s), have also been duly cited and acknowledged.



Mr. Dipesh M. Sharma

Research Student

Date: 06/08/2022



Dr. Benudhar Punji

Research Supervisor

Date: 06/08/2022

STATEMENTS OF ACADEMIC INTEGRITY

I Mr. Dipesh Mamraj Sharma, a Ph. D. student of the Academy of Scientific and Innovative Research (AcSIR) with Registration No. 10CC17J26006 hereby undertake that, the thesis entitled “Synthesis and Implication of 3d Transition Metal Catalysts for the Hydrogenative Transformations of Alkynes, Chalcones and Nitriles” has been prepared by me and that the document reports original work carried out by me and is free of any plagiarism in compliance with the UGC Regulations on “*Promotion of Academic Integrity and Prevention of Plagiarism in Higher Educational Institutions (2018)*” and the CSIR Guidelines for “*Ethics in Research and in Governance (2020)*”.



Signature of the Student

Date: 06/08/2022

Place: Pune

It is hereby certified that the work done by the student, under my supervision, is plagiarism-free in accordance with the UGC Regulations on “*Promotion of Academic Integrity and Prevention of Plagiarism in Higher Educational Institutions (2018)*” and the CSIR Guidelines for “*Ethics in Research and in Governance (2020)*”.



Signature of the Supervisor

Name: Dr. Benudhar Punji

Date: 06/08/2022

Place: Pune



Dedicated to
To My Beloved Parents

CONTENTS

	Page No.
Acknowledgements	i
Abbreviations	iii
General Remarks	vi
Synopsis Report	vii
Chapter 1. Introduction	1
1.1 INTRODUCTION	2
1.2 HYDROGENATION OF ALKYNES	4
1.2.1 Hydrogenation using Manganese	5
1.2.2 Hydrogenation using Iron	8
1.2.3 Hydrogenation using Cobalt	10
1.2.4 Hydrogenation using Nickel	13
1.2.5 Hydrogenation using Copper	15
1.3 HYDROGENATION OF NITRILES	17
1.3.1 Hydrogenation using Manganese	18
1.3.2 Hydrogenation using Iron	21
1.3.3 Hydrogenation using Cobalt	24
1.3.4 Hydrogenation using Nickel	28
1.3.5 Hydrogenation using Copper	29
1.4 HYDROGENATION OF α,β-UNSATURATED KETONES	30
1.4.1 Hydrogenation using Manganese	31
1.4.2 Hydrogenation using Iron	32
1.4.3 Hydrogenation using Cobalt	33
1.4.4 Hydrogenation using Nickel and Copper	34
1.5 OBJECTIVES OF THE PRESENT STUDY	35
1.6 REFERENCES	38

CONTENTS

Chapter 2. Room Temperature (Z)-Selective Transfer Hydrogenation of Alkynes by NNN-Cobalt Catalyst	44
2.1 INTRODUCTION	45
2.2 RESULTS AND DISCUSSION	46
2.2.1 Synthesis and Characterization of Cobalt Catalysts	46
2.2.2 Optimization of Reaction Condition for Hydrogenation of Alkynes	49
2.2.3 Scope for Synthesis of (Z)-Alkenes	52
2.2.4 Mechanistic Study	54
2.2.4.1 Significance of N-H Proton of Ligands	54
2.2.4.2 Rate of Reaction (Electronic Effect)	54
2.2.4.3 Deuterium Labelling Experiments	55
2.2.4.4 Over-reduction and Isomerization Experiments	55
2.2.5 Probable Catalytic Cycle	56
2.3 CONCLUSION	57
2.4 EXPERIMENTAL SECTION	58
2.4.1 General Experimental	58
2.4.2 Procedure for Synthesis of Cobalt Complexes	59
2.4.3 Crystallographic Data	61
2.4.4 Representative Procedure for Hydrogenation	66
2.4.5 Gram Scale Synthesis	66
2.4.6 Characterization Data of (Z)-Alkenes	66
2.4.7 Mechanistic Experiments	72
2.4.7.1 Procedure for Rate of Reaction (Electronic Effect)	72
2.4.7.2 Procedure for Competition Experiment	72
2.4.7.3 Procedure for Deuterium Labelling Experiment	73
2.4.7.4 Procedure for Attempted Over-Hydrogenation with Excess of H ₃ NBH ₃ (from 5a)	73
2.4.7.5 Procedure for Attempted Isomerization of (Z)-Stilbene	73

CONTENTS

2.4.8	^1H and ^{13}C NMR Spectra for Selected (<i>Z</i>)-alkenes	74
2.5	REFERENCES	79
Chapter 3. Selective Synthesis of Secondary Amines from Nitriles by (Xantphos)CoCl₂ Complex		82
3.1	INTRODUCTION	83
3.2	RESULTS AND DISCUSSION	84
3.2.1	Optimization of Reaction Condition for the Synthesis of Symmetrical Secondary Amines	84
3.2.2	Scope for Synthesis of Symmetrical Secondary Amines	87
3.2.3	Optimization of Reaction Condition and Scope for the Synthesis of Unsymmetrical Secondary Amines	88
3.2.4	Gram Scale Synthesis of Secondary Amine	91
3.2.5	Probable Catalytic Cycle	91
3.3	CONCLUSION	92
3.4	EXPERIMENTAL SECTION	93
3.4.1	General Experimental	93
3.4.2	Representative Procedure for the Synthesis of Symmetrical Secondary Amines	94
3.4.3	Representative Procedure for the Synthesis of Unsymmetrical Secondary Amines	94
3.4.4	Procedure for Gram Scale Synthesis of Dibenzylamine (4a)	94
3.4.5	Characterization Data of Symmetrical Secondary Amines	95
3.4.6	Characterization Data of Unsymmetrical Secondary Amines	102
3.4.7	^1H and ^{13}C Spectra of Selected Secondary Amines	113
3.5	REFERENCES	119

CONTENTS

Chapter 4. Catalytic Hydrogenation of Nitriles to Secondary Amines and Imines using Cobalt Catalyst and Molecular H₂	123
4.1 INTRODUCTION	124
4.2 RESULTS AND DISCUSSION	125
4.2.1 Optimization of Reaction Condition for the Hydrogenation of Nitriles to Symmetrical Secondary Amines	125
4.2.2 Scope for the Synthesis of Symmetrical Secondary Amines	128
4.3 CONCLUSION	130
4.4 EXPERIMENTAL SECTION	130
4.4.1 General Experimental	130
4.4.2 Representative Procedure for the Hydrogenation of Nitriles to Secondary Amines	131
4.4.3 Characterization Data of Symmetrical Secondary Amines	132
4.4.4 ¹ H and ¹³ C NMR Spectra of Selected Secondary Amines	138
4.5 REFERENCES	143
Chapter 5. Synthesis of PN³N Based Mn(I) and Mn(II) Pincer Complexes and their Application in Selective Transfer Hydrogenation of Chalcones	
5.1 INTRODUCTION	146
5.2 RESULTS AND DISCUSSION	147
5.2.1 Synthesis and Characterization of Manganese Complexes	147
5.2.2 Optimization of Reaction Condition	150
5.2.3 Scope for Synthesis of Saturated Ketones	152
5.2.4 Mechanistic Study	155
5.2.4.1 Significance of N–H Proton of PN ³ N Ligand	155
5.2.4.2 Source of Hydrogen	156
5.2.4.3 Competition Experiment (Electronic Effect)	156

CONTENTS

5.2.5	Plausible Catalytic Cycle	157
5.3	CONCLUSION	158
5.4	EXPERIMENTAL SECTION	159
5.4.1	General Experimental	159
5.4.2	Procedure for Synthesis of Manganese Complexes	159
5.4.3	Crystallographic Data	161
5.4.4	Representative Procedure for Hydrogenation	163
5.4.5	Gram Scale Synthesis	163
5.4.6	Characterization Data of Hydrogenated Compounds	163
5.4.7	^1H and ^{13}C Spectra of Selected Saturated Ketone Compounds	178
5.5	REFERENCES	183
	Summary and Outlook	187
	Abstract for Indexing	189
	List of Publications	190
	List of Posters and Conferences	191
	Copy of SCI Publications	193
	Erratum	200

Acknowledgements

*I would like to thank all the people who contributed in some way to the work described in this thesis. First of all, I would like to express my enormous gratitude to my research supervisor **Prof. Benudhar Punji** for his valuable guidance and scholarly inputs. His enthusiasm, encouragement and faith in me have been extremely helpful. I am thankful to him for giving me an opportunity to work under his valuable guidance. It had been always a fruitful discussion with him which gave me a liberty to plan and execute my ideas in research without any pressure. The disciplines whatever he taught me, I will follow them throughout my life.*

I would also like to thank Dr. C. P. Vinod, Dr. Ravindar Konatham, Dr. B. Senthilkumar and Dr. E. Balaraman for being my doctoral advisory committee (DAC) members and providing me valuable suggestions during the DAC meetings. I am grateful to Prof. Ashish K. Lele, Director, CSIR-NCL, A. K. Nangia (Former Director, NCL), for giving me this opportunity and providing all necessary infrastructure and facilities. I also acknowledge the financial support of CSIR, New Delhi in terms of junior and senior research fellowships. I extend my thanks to our collaborator Dr. Rajesh Gonnade for XRD analysis. I would also like to thank Mrs. B. Santhakumari, for HRMS analysis, Dr. Rajamohanam, Dr. Ajithkumar, Dr. Uday Kiran for NMR facilities.

*I was fortunate enough to work in a lab that was really united, uniform, and clean. I enjoyed the cheerful co-operation and accompany of my seniors Drs. Shrikant Khake, Hanuman Prasad Pandiri, Vineeta Soni, Ulhas Patel, Dilip Pandey, **Rahul Jagtap**, Abad Ali and juniors, Sidheshwar Ankade, Vijaykumar M, Surydev Kumar Verma, Anand Shabade, Sadhna Bansal, Chandini Pradhan, Rameshwar Pawar, Anupriya, Shana, Pragnya, Sandip, Chandrakant, Banamali, Tamal, and Shuvajit for their valuable time and cooperation. Also I would like to thank research trainees of our lab Haripriya, Janhavi, Vaishali, Mahesh, Jagnyesh, Ankita, Tejaswini, Ishita and Harshada for their cooperation. The warm memories of my days in Polyolefin Lab and Lab-226 will remain with me forever.*

Special thanks goes to Dr. Samir Chikkali and his group members, Drs. Shahaji, Vijay, Satej, Nilesh, Swechchha, and Bhausahab for their valuable scientific advice and help in lab practices. I greatly acknowledge other lab colleagues Dr. Ketan, Dnyaneshwar, Ravi, Anirban, Rohit, Dr. Dipa, Dr. Sandip Pawal, Amol, Kishor, Rajkumar, Tanuja, Dr. Shailaja and Uday for keeping healthy environment in the lab and for their valuable scientific discussions.

Acknowledgements

My sincere thanks to the people in various parts of the institute and SAC office staff for their cooperation. I would also like to acknowledge all the staff members of NMR, Mass spectroscopy, Microanalysis, Library, Administration and technical divisions of NCL for their assistance during the course of my work.

*I am very much thankful to my teachers, **Prof. V. D. Bobade, Prof. A. V. Borade, Dr. S. V. Patil, Dr. Suryawanshi, Mr. B. U. Patil, Mrs. M. D. Patil, Mrs. S. S. Gosavi, Mr. Y. G. Bhadane, Dr. D. P. Jaiswal, Mrs. Udavant, Dr. Anand Patil, Dr. Sachin Kale and seniors Drs. Ravindra Phatake, Milind Ahire, Aslam Sheikh, Amol Sonavane** for their help and valuable suggestions. I am thankful to the staff of the chemistry department of RYK Science College, Nashik and ACS College, Navapur for immense support and encouragement during my M. Sc. and B. Sc. days.*

*Special thanks goes to all my friends from CSIR-NCL, **Subramanyam, Pawan Dhote, Kishor Mane, Satish More, Amit Gavit, Kailas, Samir, Swapnil Halnor, Rohit, Balasaheb, Lal Singh, Nitin, Sushil** and many others for the cherished friendships and creating wonderful atmosphere around me outside the lab. Also I would like to take this opportunity to thank all my childhood and college friends, **Krunal Panchal, Krunal Prajapat, Kalpesh Mahale, Nilesh Mankar, Chetan Mankar, Mahesh Bondarde, and Mukesh Valvi** for their support and motivation.*

*My family is always source of inspiration and great moral support for me in perceiving my education, I am thankful to God for having me such a supportive family. The words are insufficient to express my gratitude towards my family. I take this opportunity to express gratitude to my mother **Ramaben** and father **Mamraj Sharma** for their tons of love, sacrifice, blessings, unconditional support and encouragement. I express my deep and paramount gratitude to my sisters **Hemlata** and **Kirti** and brothers **Mukesh** and **Umesh** who stood up behind me throughout my Ph.D. career and became my strong moral support. Without their constant support and encouragement, I could not stand with this dissertation.*

Above all, I owe it all to Almighty God for granting me the wisdom, health and strength to undertake this research task and enabling me to its completion.

-DIPESH

2-MeTHF	2-Methyl tetrahydrofuran
Ag	Silver
<i>n</i> -BuLi	<i>n</i> -Butyllithium
<i>t</i> -BuOH	<i>tert</i> -Butyl alcohol
CaCO ₃	Calcium Carbonate
CF ₃	Trifluoromethyl
CH ₃ CN	Acetonitrile
CHCl ₃	Chloroform
CN	Cyanide
Co	Cobalt
CO	Carbon monoxide
Co(OAc) ₂	Cobalt(II) acetate
CoBr ₂	Cobalt(II) bromide
CoCl ₂	Cobalt(II) chloride
Co(OAc) ₂ ·4H ₂ O	Cobalt(II) diacetate tetrahydrate
Co(ClO ₄) ₂ ·6H ₂ O	Cobalt(II) perchlorate hexahydrate
Cu	Copper
CuI	Copper(I) iodide
CuBr	Copper(I) bromide
CuCN	Copper(I) cyanide
Cu(OAc) ₂	Copper(II) acetate
DBA	Dibenzyl amine
DCE	1,2-Dichloroethane
DCM	Dichloromethane
DMSO	Dimethyl sulphoxide
DMF	<i>N,N</i> -Dimethylformamide
DIBAL-H	Diisobutylaluminium hydride
DEPT	Distortionless enhancement by polarization Transfer
dippe	1,2-Bis(diisopropylphosphino)ethane
dppp	1,3-Bis(diphenylphosphino)propane
dppf	1,1'-Ferrocenediyl-bis(diphenylphosphine)
dpre	1,2-bis(di- <i>n</i> -propylphosphino)ethane
2 D NMR	Two-dimensional nuclear magnetic resonance spectroscopy
Et ₂ O	Diethyl ether
<i>ee</i>	<i>Enantiomeric excess</i>
Et	Ethyl
EtOH	Ethanol
EtOAc	Ethyl acetate
Et ₃ N	Triethylamine
(EtO) ₃ SiH	Triethoxy silylhydride
Fe	Iron
FeBr ₂	Iron(II) bromide
FeCl ₂	Iron(II) chloride
FeCl ₃	Iron(III) chloride
Fe ₂ (CO) ₉	Diiron nonacarbonyl
g	Gram
h	Hour

Abbreviations


HFIP	Hexafluoroisopropanol
HPLC	High performance liquid chromatography
HRMS	High resolution mass spectrometry
HCl	Hydrochloric acid
<i>i</i> PrOH	Isopropanol
IR	Infra-red
LiO ^t Bu	Lithium tert-butoxide
KHMDS	Pottasium hexamethyldisilazide
KO ^t Bu	Pottasium tert-butoxide
KBH ₄	Pottasium borohydride
K ₃ PO ₄	Tripotassium posphate
K ₂ CO ₃	Potassium carbonate
LiHMDS	Lithium hexamethyldisilazide
LiBH(Et) ₃	Lithium triethylborohydride
LiAlH ₄	Lithium aluminium hydride
LiBH ₄	Lithium borohydride
<i>m</i> -CPBA	<i>meta</i> -Chloroperoxybenzoic acid
M ⁺	Molecular ion
Me	Methyl
MeI	Iodomethane
MeOH	Methanol
Min	Minute
Mg	Magnesium
mg	Miligram
mL	Milliliter
Mn	Manganese
MnCl ₂	Manganese(II) chloride
MnBr ₂	Manganese(II) bromide
MnI ₂	Manganese(II) iodide
Mn(CO) ₅ Br	Bromopentacarbonylmanganese(I)
MS	Molecular sieves
NaBH ₄	Sodium borohydride
NaBH ₃ CN	Sodium cyanoborohydride
NaBH(OAc) ₃	Sodium triacetoxyborohydride
NaH	Sodium hydride
NaCl	Sodium chloride
NaOH	Sodium hydroxide
NaOMe	Sodium methoxide
NaBH ₃ CN	Sodium cyanoborohydride
NH ₃ -BH ₃	Ammonia borane
Me ₂ NH-BH ₃	Dimethylammonia-borane
NH ₄ Cl	Ammonium chloride
Ni	Nickel
Ni(COD) ₂	Bis(cyclooctadiene)nickel(0)
NiBr ₂	Nickel(II) bromide
NiCl ₂	Nickel(II) chloride
NiI ₂	Nickle(II) iodide
Ni(OTf) ₂	Nickel(II) triflate
NMR	Nuclear magnetic resonance

Abbreviations

NO	Nitrogen monoxide
Ome	Methoxy
OCF ₃	Trifluoromethoxy
Pd/C	Palladium on activated charcoal
KOH	Potassium hydroxide
<i>t</i> -BuOK	Potassium <i>tert</i> -butoxide
Ph	Phenyl
PHIP	<i>para</i> -Hydrogen Induced Polarization
Ph ₂ SiH ₂	Diphenyl silane
PPh ₃	Triphenylphosphine
[PPh ₃ CuCl] ₄	Chlorotris(triphenylphosphine)copper(I)
P ^t Bu ₃	Tritert-butylphosphine
Pd	Palladium
PdCl ₂	Palladium(II) chloride
Pd(OAc) ₂	Palladium(II) acetate
Py	Pyridine
Pyz	Pyrazole
Rf	Retention factor
(PPh ₃) ₃ RhCl	chloridotris(triphenylphosphine)rhodium(I)
H ₂ SO ₄	Sulfuric acid
Na ₂ SO ₄	Sodium sulfate
^t BuONa	Sodium <i>tert</i> -butoxide
TBP	Trigonal bipyramidal
THF	Tetrahydrofuran
TiCl ₄	Titanium tetrachloride
TLC	Thin layer chromatography
TOF-MS	Time-of-flight mass spectrometer
Zn	Zinc
ZnCl ₂	Zinc chloride

General Remarks

- All reagents, starting materials, and solvents were obtained from commercial suppliers and used as such without further purification. Solvents were dried using standard protocols.
- All reactions were carried out in oven-dried glassware in glove box or under a positive pressure of argon unless otherwise mentioned with magnetic stirring.
- Air sensitive reagents and solutions were transferred *via* syringe or cannula and were introduced to the apparatus *via* rubber septa.
- Progresses of reactions were monitored by thin layer chromatography (TLC) with 0.25 mm pre-coated silica gel plates (60 F254). Visualization was accomplished with either UV light, Iodine adsorbed on silica gel.
- Column chromatography was performed on silica gel (100-200 or 230-400 mesh size).
- Deuterated solvents for NMR spectroscopic analyses were used as received.
- All ^1H NMR, ^{13}C NMR spectra were obtained using a 200 MHz, 400 MHz, 500 MHz spectrometer. Coupling constants were measured in Hertz. The following abbreviations were used to explain the multiplicities: s = singlet, d = doublet, t = triplet, q = quartet, m = multiplet, br = broad.
- HRMS (ESI) were recorded on ORBITRAP mass analyzer (Thermo Scientific, QExactive).
- Infrared (IR) spectra were recorded on a FT-IR spectrometer as a thin film.
- Chemical nomenclature (IUPAC) and structures were generated using Chem Bio Draw Ultra.

	Synopsis of the thesis to be submitted to the Academy of Scientific and Innovative Research for the award of the degree of Doctor of Philosophy in Chemical Science
Name of the Candidate	Mr. Sharma Dipesh Mamraj
Enrollment No. and Date	Ph. D. in Chemical Sciences (10CC17J26006); 2 nd January, 2017
Title of the Thesis	Synthesis and Implication of 3d Transition Metal Catalysts for the Hydrogenative Transformations of Alkynes, Chalcones and Nitriles
Research Supervisor	Dr. Benudhar Punji

1. Introduction:

The thesis title is “**Synthesis and Implication of 3d Transition Metal Catalysts for the Hydrogenative Transformations of Alkynes, Chalcones and Nitriles**”. This thesis is divided into five different chapters. The first chapter describes a detailed literature survey on applying 3d transition metal catalysts in the selective hydrogenative transformation of unsaturated bonds, i.e., alkynes, nitriles, and α,β -unsaturated ketones. In particular, advances made with the late 3d transition metals such as manganese, iron, cobalt, nickel, and copper catalysts in selective hydrogenation reactions are discussed; those proceed either *via* the transfer hydrogenation process *or* by using molecular hydrogen. Chapter-2 deals with synthesizing unified (NNN)-pincer and non-pincer anionic cobalt complexes and their application in selective room temperature transfer hydrogenation of internal aromatic alkynes to respective *Z*-alkenes. A preliminary mechanistic investigation has been performed, and a plausible reaction proposal is drawn. Chapter-3 presents the selective transfer hydrogenation of nitriles to secondary amines using a friendly (xantphos)CoCl₂ catalyst. Selective synthesis of secondary imines and symmetrical secondary amines from nitriles using cobalt(II) catalysts and molecular hydrogen (H₂) is illustrated in Chapter-4. Chapter-5 contains the synthesis of PN³N-based pincer Mn(I) and Mn(II) complexes for the selective transfer hydrogenation of C=C on chalcones using ammonia-borane as a hydrogen source. Lastly, the summary of the thesis work, including the future direction related to the field, is elaborated.



Dr. Benudhar Punji (Supervisor)



Dipesh M. Sharma (Candidate)

2. Statement of the Problem: Catalytic hydrogenation of unsaturated bonds is a crucial synthetic path for achieving saturated bonds. Traditionally, two approaches are involved in this process, i) catalytic hydrogenation with molecular hydrogen (H_2) and ii) transfer hydrogenation using a hydrogen-donor. Over the past few decades, there has been significant advancement perceived in both methods. However, this growth was primarily accomplished using noble transition metal catalysts, *i.e.* 4d/5d transition metals. These rare metals are high in cost and are naturally limited, affecting their usage in sustainable hydrogenative transformation. To cope with the challenges related to using 4d/5d transition metals, researchers employed naturally abundant and cost-effective 3d transition metals for catalytic hydrogenations. Though the use of 3d transition metals could resolve the issue of high cost and sustainability, the harsh reaction conditions and use of highly reactive reagents restrict their practical applicability. Thus, there is an enormous demand to design concise, practical, sustainable synthetic approaches using 3d transition metal catalysts through which one can perform the hydrogenative transformations at milder reaction conditions in a stereoselective manner.

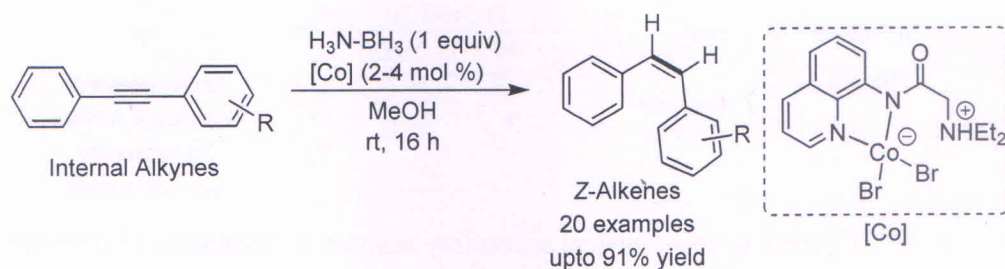
3. Objectives: As discussed in the above section, the hydrogenative transformation of unsaturated bonds, particularly alkynes, nitriles, and chalcones, is restricted by the utilization of costly noble metals or limited to harsh reaction conditions and the use of sensitive reagents. In addition, the stereoselective product formation is disturbed by extreme reaction parameters. Thus, our objective is to look into the problem related to these hydrogenative modifications and attempt to resolve those by designing easy-to-use catalytic systems to achieve the mild reaction conditions and high product selectivity by employing the earth-abundant 3d transition metals.

4. Methodology and Result:

Chapter 2. Development of NNN-Cobalt Catalysts for Room Temperature Z-Selective Transfer Hydrogenation of Alkynes

Controlled hydrogenation of alkynes is an important synthetic tool to access the desired stereoselective alkenes. Though the last few decades saw a huge advancement in the catalytic semi-hydrogenation of alkynes, several limitations are associated with them, such as controlling stereoselectivity and using a sensitive phosphine-based catalytic system and/or harsh reaction conditions. Thus, this chapter discussed the design and development of

hemilabile and phosphine-free quinolinyl-based (*NNN*)-type pincer and non-pincer cobalt complexes for the room temperature catalytic transfer semi-hydrogenation of alkynes to *Z*-alkenes.¹ The well-defined anionic non-pincer cobalt complexes $\kappa^2\text{-}(\text{QNN})\text{CoX}_2(\text{N}^{\text{C(O)HNEt}_2})$ ($\text{X} = \text{Cl}, \text{Br}$) efficiently catalyzed the semi-hydrogenation of diverse alkynes to deliver highly chemoselective and stereodivergent *Z*-alkenes at room temperature (Scheme 1). This hydrogenation exhibited broad substrate scope with the tolerance of sensitive functional groups, such as $-\text{Cl}$, $-\text{Br}$, $-\text{I}$, $-\text{OH}$, $-\text{NH}_2$, $-\text{COOMe}$, and pyridinyl, employing a stable and friendly ammonia borane as the hydrogen source. The anionic non-pincer cobalt complex was also active in the isomerization of *Z*- to *E*-alkene at 60 °C. Furthermore, the mechanistic studies put forward the crucial role of amide *N-H* of ligand backbone in room temperature activation of a non-pincer cobalt catalyst.



Scheme 1. Room temperature transfer hydrogenation of alkynes to *Z*-alkenes by anionic non-pincer cobalt complex.

Chapter 3. Selective Synthesis of Secondary Amines from Nitriles by (xantphos)CoCl₂ Complex

Secondary amines are an essential part of numerous drug and pharmaceutical molecules.² Nitrile hydrogenation is one of the courses of action to access secondary amines. However, literature in the context of conversion of nitrile to secondary amines is scarce and limited to a handful of reports. Consequently, this chapter describes the room temperature transfer hydrogenation of nitriles to symmetrical secondary amines using $\text{H}_3\text{N-BH}_3$ as a hydrogen source and a user-friendly (xantphos)CoCl₂ catalyst (Scheme 2a).³ The optimized mild reaction parameters were reliable with different functional groups like $-\text{F}$, $-\text{Cl}$, $-\text{Br}$, $-\text{I}$, $-\text{CH}_2\text{OH}$, $-\text{COOMe}$, and thiophenyl.

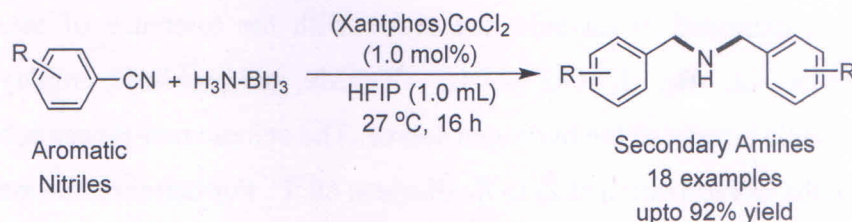
Similarly, the unsymmetrical secondary amines are obtained by adding an external amine source using a cheaper hydrogen source, i.e. $\text{Me}_2\text{NH-BH}_3$ (Scheme 2b). An excellent substrate

Dr. Benudhar Punji (Supervisor)

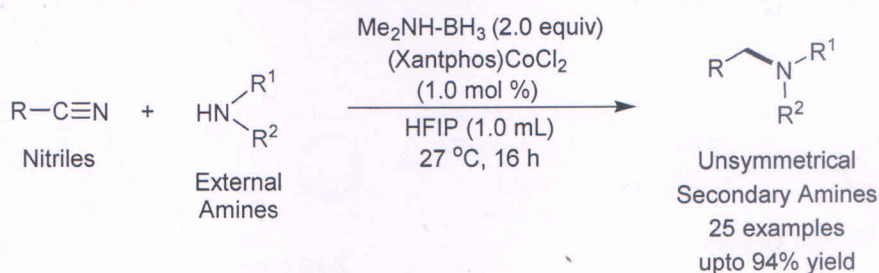
Dipesh M. Sharma (Candidate)

scope with various functional group tolerance has been observed under the optimized reaction protocol. The synthetic utility is shown by carrying out the reaction at a gram scale with an 82% isolated yield.

a) Synthesis of symmetrical secondary amines



b) Synthesis of unsymmetrical secondary amines



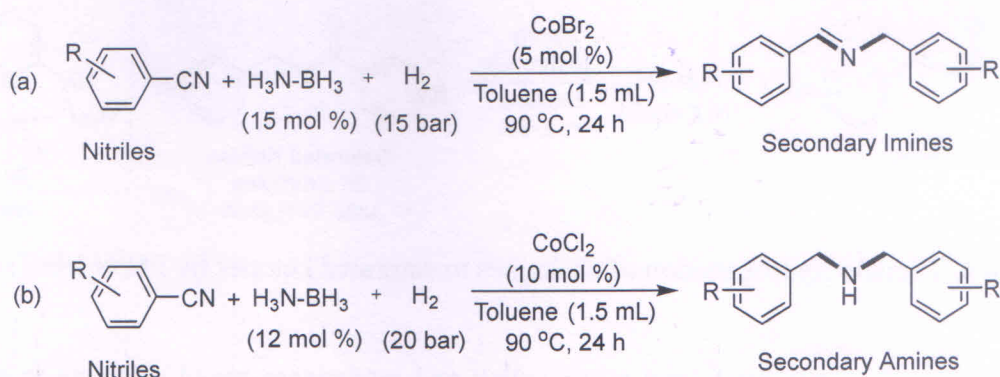
Scheme 2. a) TH of nitrile to symmetrical secondary amines, b) Synthesis of unsymmetrical secondary amines by reductive coupling of nitriles with amines.

Chapter 4. Catalytic Hydrogenation of Nitriles to Secondary Amines and Imines using Cobalt Catalyst

This chapter describes the catalytic hydrogenation of nitriles to secondary amines and imines. In this context, the CoBr_2 (5 mol %) and 15 mol % of ammonia-borane as an additive catalyze the hydrogenation of nitriles into secondary imines. This reaction needs 15 bar hydrogen pressure to transform nitriles into secondary imines (Scheme 3a). In contrast, when the CoBr_2 was replaced with CoCl_2 , a change in the product selectivity was observed and the reaction resulted in the significant formation of secondary amines. Thus, the catalytic amount of CoCl_2 with ammonia-borane (12 mol %) led to the hydrogenation of nitriles to secondary amines at 20 bar hydrogen pressure (Scheme 3b). The reaction protocol is tolerable with distinct functional groups like synthetically important $-\text{F}$, $-\text{Cl}$, $-\text{Br}$, $-\text{CF}_3$, $-\text{OMe}$ moieties and gave moderate to good yield for the respective secondary amine. Interestingly, an ester moiety remained intact during the reaction course and regioselectively nitrile was hydrogenated.

Dr. Benudhar Punji (Supervisor)

Dipesh M. Sharma (Candidate)



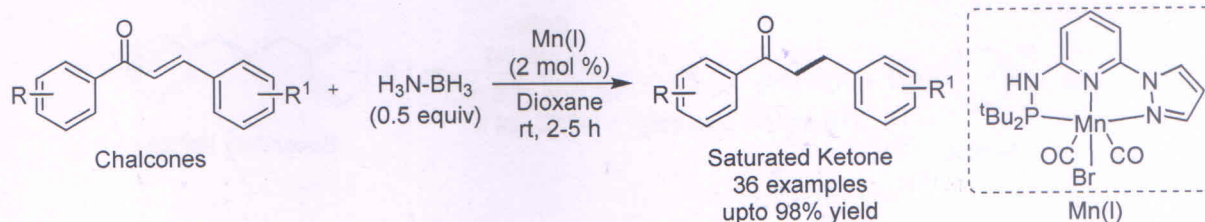
Scheme 3. (a) Catalytic hydrogenation of nitrile to secondary imines by CoBr_2 (b) Catalytic hydrogenation of nitrile to symmetrical secondary amines by CoCl_2

Chapter 5. Synthesis of PN^3N Based Mn(I) and Mn(II) Pincer Complexes and Application towards Selective Transfer Hydrogenation of Chalcones

This chapter discusses the synthesis and characterization of a series of PNN -based Mn(I) and Mn(II) complexes and their application toward the selective transfer hydrogenation of the $\text{C}=\text{C}$ bond in chalcones. The tridentate ${}^t\text{Bu}_2\text{PNpyrN}^{\text{imid}}$ (PN^3N) ligand synthesized following the literature procedure on treatment with $\text{Mn(CO)}_5\text{Br}$ and MnX_2 salts led to the development of $\text{PN}^3\text{N-Mn(I)}$ and $\text{PN}^3\text{N-Mn(II)}$ pincer complexes, respectively. These complexes have an acidic N-H at the ligand backbone, which could assist in the metal-ligand cooperation (MLC) during catalysis. Among the newly synthesized complexes, Mn(I) complex catalyzes the transfer hydrogenation of $\text{C}=\text{C}$ bonds in chalcones under milder conditions, whereas the Mn(II) complexes are catalytically inactive. The Mn(I) complex selectively hydrogenates the $\text{C}=\text{C}$ bond of chalcone at room temperature using ammonia-borane as a hydrogen source (Scheme 4). Interestingly, the reaction occurs smoothly with the 0.5 equivalent of ammonia-borane. The range of functional groups such as $-\text{F}$, $-\text{Cl}$, $-\text{Br}$, $-\text{CF}_3$, $-\text{NO}_2$, $-\text{OMe}$, alkyl, and heterocycles like thiophene, pyrrole, furan, indoles endure the reaction condition and provide respective reduced saturated ketones in high yields. Surprisingly, trisubstituted $\text{C}=\text{C}$ of chalcone didn't show any conversion into a reduced product. In addition, the isolated alkenes and alkynes also remained unaffected in the optimized reaction condition.

Dr. Benudhar Punji (Supervisor)

Dipesh M. Sharma (Candidate)



Scheme 4. Transfer hydrogenation of chalcones to saturated ketones by PN^3N Mn(I) catalyst.

5. Summary: We have developed novel cobalt and manganese-based catalysts to carry out (transfer)hydrogenation reactions under mild reaction conditions. Thus, internal aromatic alkynes are stereoselectively hydrogenated to *Z*-alkenes using cobalt catalyst and ammonia-borane as a hydrogen source (Chapter-2). Similarly, nitriles are converted into secondary amines by (xantphos)CoCl₂ catalytic system and ammonia-borane or dimethylammonia-borane as hydrogen sacrificial (Chapter-3). In addition, we have also optimized the reaction protocol for unprecedented hydrogenation of nitriles with molecular hydrogen using cobalt precursors (Chapter-4). Further, selective TH of activated C=C bond of chalcones at milder conditions was achieved by employing PN^3N -based Mn(I) catalyst and a half equivalent of ammonia-borane as a hydrogen source (Chapter-5). These transformations were carried out at very mild reaction conditions using robust catalytic systems. High regioselectivity and excellent functional group tolerance have been exhibited in all transformations.

6. Future Directions: We have successfully attempted to resolve the problems related to existing methodologies for the selected hydrogenation reaction. However, still, there is a scope to achieve better conditions to access controlled hydrogenation. The alkyne TH to *Z*-alkene is limited to aromatic internal alkynes. The focus should be centered on attaining *E*-selectivity. Also, the terminal alkynes and alkyl alkynes should be considered for such mild transfer hydrogenation. In the transfer hydrogenation of nitriles to secondary amines, aliphatic nitriles are rarely explored, and thus, they need significant attention. Similarly, chapter 4 shows unprecedented catalytic hydrogenation of nitriles to secondary imines/amines. However, this method is limited to moderate product yields, and there is a need for improvised catalytic conditions to get increased product yields. The last chapter deals with selective TH of C=C of chalcone by PN^3N -Mn(I) catalyst. The reaction works very well with the chalcone derivatives; however, trisubstituted alkenes of chalcone are unreactive. Also, aliphatic α,β -unsaturated ketones don't undergo selective C=C hydrogenation. Therefore, it is worth exploring the

Dr. Benudhar Punji

Dr. Benudhar Punji (Supervisor)

Dipesh M. Sharma

Dipesh M. Sharma (Candidate)

catalytic system/condition that reaches the targets as mentioned earlier. These future directions of the thesis would help find a better catalytic condition/system for milder and selective hydrogenation reactions.

7. List of Publications:

1. **D. M. Sharma**, C. Gouda, R. G. Gonnade and B. Punji, "Room Temperature Z-Selective Hydrogenation of Alkynes by Hemilabile and Non-innocent (NNN) Co (II) Catalyst" *Catal. Sci. Technol.*, **2022**, *12*, 1843-1849
2. **D. M. Sharma** and B. Punji, "Nickel-Catalyzed Benzylic C-H Functionalization", Book Chapter for "*Handbook of CH-Functionalization (CHF)*" **2021**
3. **D. M. Sharma** and B. Punji, "3 d Transition Metal-Catalyzed Hydrogenation of Nitriles and Alkynes" *Chem. Asian J.*, **2020**, *15*, 690-708
4. **D. M. Sharma** and B. Punji, "Selective Synthesis of Secondary Amines from Nitriles by a User-Friendly Cobalt Catalyst" *Adv. Synth. Catal.*, **2019**, *361*, 3930-3936
5. V. Soni, **D. M. Sharma** and B. Punji, "Nickel-Catalyzed Regioselective C(2)-H Difluoroalkylation of Indoles with Difluoroalkyl Bromides" *Chem. Asian J.*, **2018**, *13*, 2516-2521
6. H. Pandiri, **D. M. Sharma**, R. G. Gonnade and B. Punji, Synthesis and Characterization of Six-Membered Pincer Nickelacycles and Application in Alkylation of Benzothiazole" *J. Chem. Sci.*, **2017**, *129*, 1161-1169
7. **D. M. Sharma**, A. B. Shabade and B. Punji, "Synthesis of PN³N Based Mn(I) and Mn(II) Pincer Complexes and Application in Selective Transfer Hydrogenation of Chalcones". *Manuscript Under Preparation*

8. References:

1. Room Temperature Z-Selective Hydrogenation of Alkynes by Hemilabile and Non-innocent (NNN) Co (II) Catalyst, Sharma D. M.; Gouda; C.; Gonnade R. G.; Punji B., *Catal. Sci. Technol.*, **2022**, *12*, 1843-1849.
2. 3 d Transition Metal-Catalyzed Hydrogenation of Nitriles and Alkynes, Sharma D. M.; Punji B., *Chem. Asian J.*, **2020**, *15*, 690-708.
3. Selective Synthesis of Secondary Amines from Nitriles by a User-Friendly Cobalt Catalyst, Sharma D. M.; Punji B., *Adv. Synth. Catal.*, **2019**, *361*, 3930-3936.



Dr. Benudhar Punji (Supervisor)



Dipesh M. Sharma (Candidate)

Chapter 1

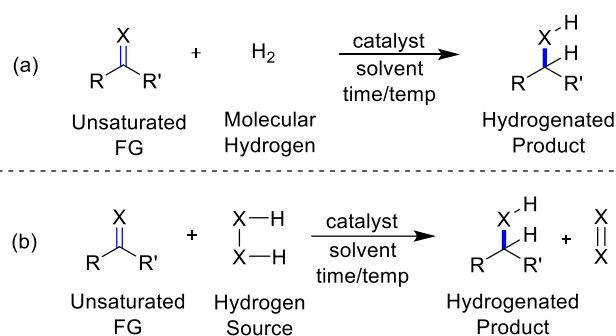
Introduction

This chapter has been partly adapted from the publication "3d Transition Metal-Catalyzed Hydrogenation of Nitriles and Alkynes" **Sharma, D. M.**; and Punji, B. *Chem. Asian J.* **2020**, *15*, 690–708.

1.1 INTRODUCTION

The hydrogenation reaction is one of the prime synthetic modifications practiced in organic synthesis due to its applications ranging from the production of fine chemicals to pharmaceuticals and industrial commodities.¹⁻⁴ Starting from the early 20th century, tremendous growth and development have been perceived in catalytic hydrogenative transformations with the help of numerous transition metal catalysts. For example, palladium on carbon and platinum on carbon are well-known heterogeneous catalysts for the diverse unsaturated bond hydrogenation.⁵ Similarly, prominent hydrogenation catalysts such as Raney Ni and Lindlar's catalyst (Pd/BaSO₄) are applied for the catalytic hydrogenation of multiple bonds.⁶ However, the selectivity issues in the product formation and harsh reaction conditions for such heterogeneous hydrogenation process led the researchers to move towards relatively milder and more product selective homogeneous hydrogenation.⁷⁻⁹

The term 'homogeneous' refers to the reaction mixture with the co-existence of reactants and catalyst in a similar phase. This phenomenon helps to control and tune the product selectivity by using milder reaction conditions. Among the homogeneous hydrogenation with molecular hydrogen explored, the 4d and 5d transition metals, i.e., ruthenium, rhodium, palladium, and iridium have taken the central role over the decades (Scheme 1.1a).¹⁰⁻¹¹ Wilkinson's rhodium-based (PPh₃)₃RhCl catalyst and Crabtree's (COD)Ir(PCy₃)₂(Pyr) are one of the important examples of homogeneous hydrogenation catalysts developed for the transformation of alkynes to alkenes under mild reaction conditions using hydrogen pressure.¹⁰ Transfer hydrogenation (TH) is another approach to carry out the hydrogenative transformation of C–X (X = C, N, O) multiple bonds using the proton/hydride sacrificials (Scheme 1.1b).¹² Pioneering work on TH with late transition metals catalysts was unfolded by Henbest and Mitchell where cyclohexanones and α,β -unsaturated ketones hydrogenated to respective alcohols using isopropanol as hydrogen sacrificial with iridium-hydride complex.^{13,14} Since then a huge advancement is seen in TH process with 2nd and 3rd row transition metals catalysts.¹² Although the homogeneous hydrogenation reactions accomplished at milder conditions and furnished better product-selectivity; the cost, natural-abundance, and toxic nature of these heavy 4d/5d transition metals demanded are placement by more economical, naturally-abundant and relatively low-toxic 3d transition metals.



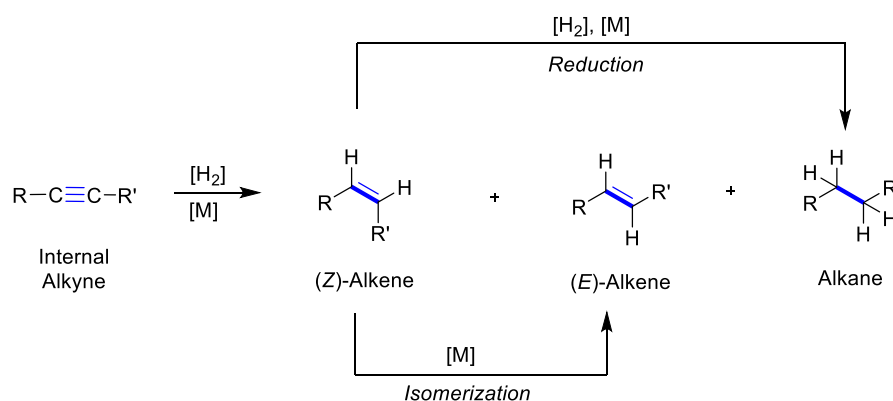
Scheme 1.1(a) Metal-catalyzed hydrogenation with molecular hydrogen, (b) Metal-catalyzed transfer hydrogenation with hydrogen source.

The first row 3d transition metals are considered attractive for the hydrogenative transformations, credit to their distinct features, such as being capable of inducing a range of variable oxidation states, which makes them more appropriate for redox chemistry.¹⁵⁻¹⁶ Despite this, the participation of 3d base metal catalysts in homogeneous hydrogenation straggled significantly, which could be rationalized with the low intrinsic reactivity of many 3d metal catalysts and relatively low stability of organometallic (M–C) intermediates formed during the reaction. In fact, the momentary existence of the M–C bond in the case of 3d metals should enhance their catalytic reactivity compared to their 4d and 5d congeners. But, the low stability of 3d metal-carbon intermediates makes the catalytic system challenging to control, leading to either no reaction or unintended side reactions. In addition, the comprehensive study of mechanistic insights in 3d transition metal-catalyzed hydrogenation is difficult in light of the fragile stability of the catalytic transition states. Although many challenges stand in the course of the usage of 3d metals as catalysts, the designing and implication of an appropriate ligand backbone for the catalyst could help in controlling the metal reactivity and product selectivity. In this direction, hydrogenation reactions catalyzed by the first-row transition metals have witnessed a scintillating growth in the last two decades.^{11,17-19} Notably, the first-row late transition metals are more prominent in the direction of hydrogenation of a variety of unsaturated bonds like C≡N, C≡C, C≡O and double bonds (C=C, C=N) to the respective reduced products. Among the diverse unsaturated bonds, the alkynes, nitriles and conjugated double bonds (chalcones) are of particular interest in regard to the demand for their reduced products in pharmaceuticals and industries.^{20-25,27} Thus, in this chapter, a brief introduction to the use of late 3d-transition metals (mainly Mn,

Fe, Co, and Ni) for catalytic hydrogenation of $C\equiv C$, $C\equiv N$, and chalcones using molecular hydrogen pressure or hydrogen source has been discussed.

1.2 HYDROGENATION OF ALKYNES

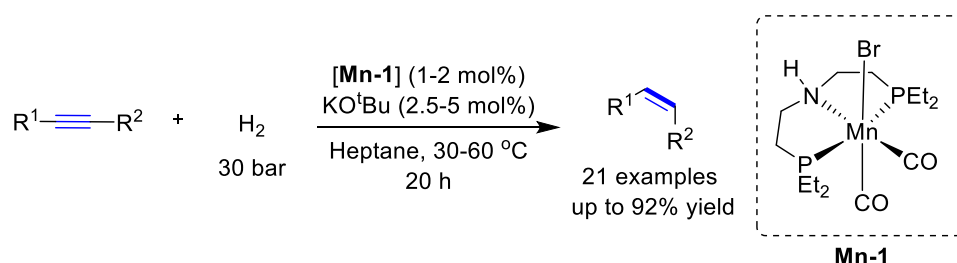
The hydrogenation of alkyne is an important reaction in synthetic chemistry, which can provide different reduced products, i.e., (*Z*)- or (*E*)-alkenes and alkanes (Scheme 1.2). Particularly, the controlled semi-hydrogenation of alkynes is a highly significant process considering the wide applications of resulted alkenes in the field of pharmaceutical chemistry.²⁸ Numerous drugs moieties constitute an olefin functional group with particular (*E*) or (*Z*) geometry, such as Combretastatin A4,^{29,30} Cruentaren A,²⁰ and Amphotericin.³¹ Similarly, naturally occurring compounds like *Lepidoptera* pheromones and polyunsaturated fatty acids contain olefin functionality in their molecular structure.³² Traditionally, the hydrogenation of alkyne to (*Z*)-alkene is well known by Lindlar (Pd/CaCO₃) catalyst.⁶ Apart from palladium, the reduction of alkynes is also executed by employing other precious metals catalysts such as ruthenium,³³ iridium,^{34,35} gold,³⁶ and Cu-Ag.³⁷ However, in last two decades, the earth-abundant 3d metals have emerged as a highly applied catalysts for the alkyne hydrogenation to achieve stereo-selective (*E*)- or (*Z*)-alkenes.¹⁸ Keeping focus on the sustainable synthesis, present-day research is being inclined towards the development of catalytic systems based on earth-abundant 3d metals, such as Mn, Fe, Co, Ni and Cu for the hydrogenative transformations of alkynes.



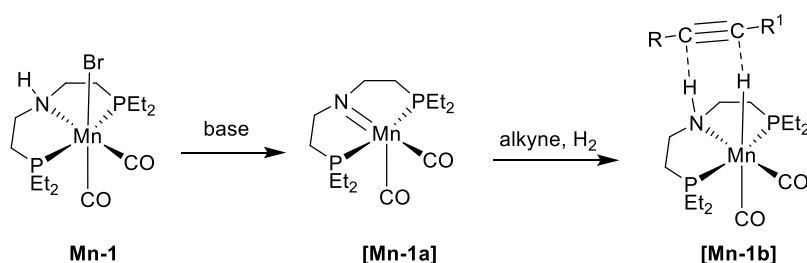
Scheme 1.2 Hydrogenation products of alkyne.

1.2.1 Hydrogenation using Manganese

Manganese is the fifth element in the first-row transition metals with high natural abundance. The oxidation state of the manganese varies from +1 to +7 among which +2, +3, +4, +6, and +7 are the most common. However, the manganese complexes in the +1 oxidation state are reported to be active for the hydrogenation reactions.³⁸ In recent years, manganese stands out as one of the most utilized 3d metal for the hydrogenation reaction. Nonetheless, the reports on unsaturated hydrocarbon hydrogenation with manganese catalysts are scarce. In 2020, the semi-hydrogenation of alkynes to (*Z*)-alkenes with molecular hydrogen disclosed by Junge and Beller.³⁹ Thus, the phosphine based Mn(I) complex **Mn-1** performs hydrogenation of internal diaryl alkynes at comparatively mild condition with 30 bar H₂ pressure and 30-60 °C temperature (Scheme 1.3). The mechanistic investigation carried out by authors revealed an outer sphere mechanism for alkyne hydrogenation. The pre-catalyst **Mn-1** on reaction with base (KO^tBu) and hydrogen produces manganese-amido intermediate **Mn-1a** which reacts with hydrogen to give an intermediate with proton on central nitrogen of ligand and hydride on the manganese. This intermediate hydrogenates alkyne to *cis*-alkene *via* the formation of **Mn-1c** intermediate and gives amido-manganese intermediate [**Mn-1a**] back after release of alkene product (Scheme 1.4).

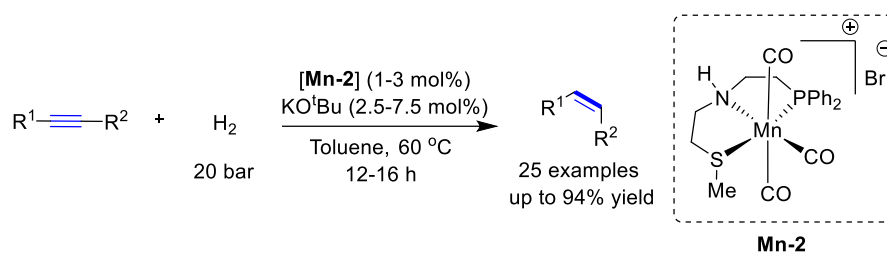


Scheme 1.3 Hydrogenation alkynes to (*Z*)-alkenes by **Mn-1**.



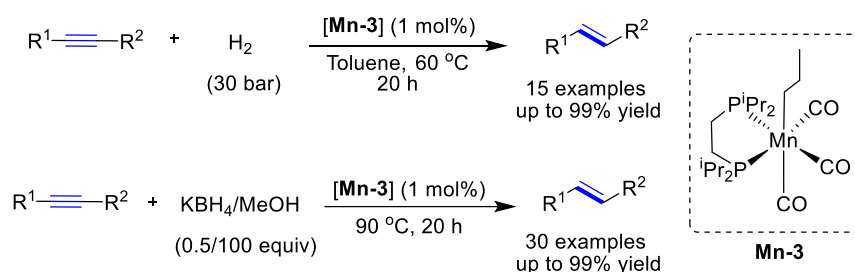
Scheme 1.4 Outer-sphere mechanism of hydrogenation of alkynes to (*Z*)-alkenes by **Mn-1**.

In the same year, Rueping and co-workers came up with an air-stable cationic Mn(I) complex **Mn-2** which could transform internal alkynes to (*Z*)-alkenes selectively.⁴⁰ The authors showed a broad substrate scope with the optimized reaction condition. The involvement of metal-ligand co-operativity *via* a bifunctional activation during the catalysis was concluded by the mechanistic experiments (Scheme 1.5).



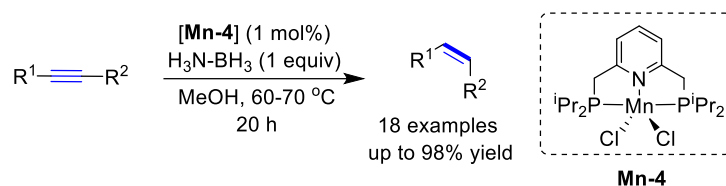
Scheme 1.5 **Mn-2** catalyzed hydrogenation alkynes to (*Z*)-alkenes.

Recently, in 2022, Kirchner group synthesized a robust Mn(I)-alkyl catalyst **Mn-3** which could hydrogenate alkynes to (*E*)-alkenes using external molecular hydrogen or in-situ generated hydrogen (from KBH_4/MeOH).⁴¹ Thus, either 30 bar hydrogen pressure or mixture of KBH_4/MeOH (0.5/100 equiv) could be employed to semi-hydrogenate alkynes into (*E*)-alkenes (Scheme 1.6).



Scheme 1.6 **Mn-3** catalyzed hydrogenation/TH of alkynes to (*E*)-alkenes.

El-Sepegly and co-workers developed a penta-coordinated PNP-based pincer Mn(II) complex **Mn-4** that catalyzed semi-hydrogenation of internal alkynes to (*Z*)-alkenes employing ammonia-borane as hydrogen source (Scheme 1.7).⁴² The catalysis proceeded without the use of any additives, base or super-hydride and tolerated by variety of functional groups. The active $[\text{Mn-4}]-\text{H}$ complex, produced upon the reaction of ammonia-borane with **Mn-4**, hydrogenated the alkyne into (*Z*)-alkene *via* the interaction of alkyne to Mn followed by insertion of an alkyne into **Mn-H** bond (Figure 1.1). The protonation by MeOH gave (*Z*)-alkene and regenerate catalyst.



Scheme 1.7 Alkyne transfer hydrogenation by **Mn-4**.

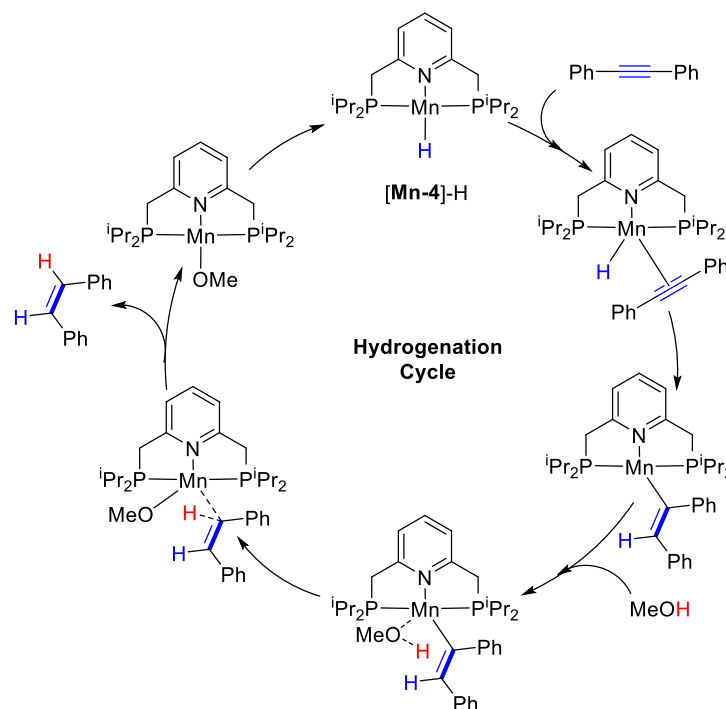
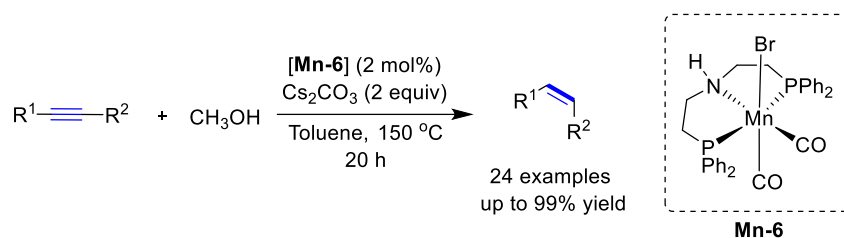


Figure 1.1 Catalytic cycle for alkyne transfer hydrogenation by **Mn-4**.

In the same year, Driess group prepared *N*-heterocycle based silylene-Mn(II) complex **Mn-5** which affords semi-hydrogenation of alkynes to (*E*)-alkenes using ammonia-borane as a hydrogen source.⁴³ This methodology work smoothly with di-aryl or aryl-alkyl or TMS protected internal alkynes. Rueping and co-workers in 2020 developed a methodology to semi-hydrogenate internal alkynes to (*Z*)-alkenes using a phosphine based pincer Mn(I) catalyst **Mn-6**, Cs₂CO₃ and MeOH as a hydrogen source (Scheme 1.8).⁴⁴ The **Mn-6** complex found robust enough to dehydrogenate MeOH to produce hydrogen for the reduction of alkynes to alkenes. The MeOH is considered as one of the best hydrogen sources as it also serves as hydrogen storage material. In addition the **Mn-6** catalyst is air and moisture-stable in nature. In addition, recently, a bidentate phosphine-based Mn(I) complex **Mn-7** [(*i*Pr²PCH₂CH₂P^{iPr²)Mn(CO)₃Br] used by Garcia and co-workers for the transfer hydrogenation of alkyne to (*E*)-alkenes selectively.⁴⁵ Isopropanol as a hydrogen source is}

used in this protocol. Unfortunately, this protocol found to be limited with very few substrates with moderate to good *Z/E* selectivity for alkene.



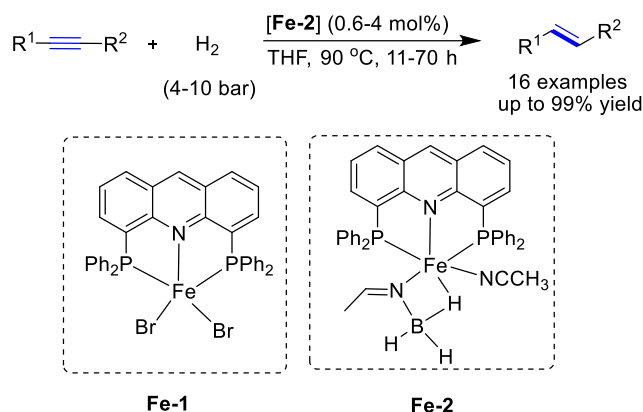
Scheme 1.8 Alkyne transfer hydrogenation by **Mn-6**.

1.2.2 Hydrogenation using Iron

Iron is the most abundant transition metal, which contributes 5.63% of the metals in the earth's crust. The oxidation states of the iron range from +2 to +7, which enhances the use of iron metal in the various redox reactions. The plentiful availability and the less biological toxicity of iron make it the most appealing metal for the organometallic transformations. In that direction the catalytic hydrogenation to synthesize important organic compounds employing iron based complexes is very significant. Similarly, it is also highly desirable to use an iron complex for the alkyne semi-hydrogenation. In that background, in 1989, Bianchini and co-workers reported an octahedral iron catalyst $[P(CH_2CH_2PPh_2)_3FeH(N_2)](BPh_4)$ for the semi-reduction of terminal alkynes to the respective alkenes.⁴⁶ In the last decade, enormous growth has been seen in the field of iron-catalyzed alkyne semi-hydrogenation, wherein various iron precursors combined with phosphine ligand, such as $Fe_2(CO)_9/P^tBu_3$ was employed as catalysts and $(EtO)_3SiH$ was used as hydrogen source.^{47,48} This method provided mixture of (*Z*)- and (*E*)-alkenes with higher selectivity towards the former. Similarly, Beller has employed $Fe(BF_4)_2 \cdot 6H_2O$ /tetracosylphosphine (PP_3) catalyst and formic acid as hydrogen source to hydrogenate terminal alkynes to alkenes. Moreover, the silanes are also used as hydrogen source to synthesize alkenes from alkynes employing $[Fe(PPh_3)_2H(CO)(NO)]$ or $(NHC)Fe(II)$ catalysts.^{49,50}

The report on alkyne hydrogenation using molecular hydrogen emerged in 2013. The molecularly defined $Fe(II)$ complexes **Fe-1** and **Fe-2** have been synthesized using previously developed PNP ligands and tested for the hydrogenation of terminal and internal alkynes (Scheme 1.9).⁵¹ Complex **Fe-1** is synthesized by the simple reaction of PNP ligand with $FeBr_2$ at room temperature. However, the treatment of PNP ligand with $FeBr_2$ in the presence of $NaBH_4$ in acetonitrile resulted in the formation of complex **Fe-2**. The investigation of both

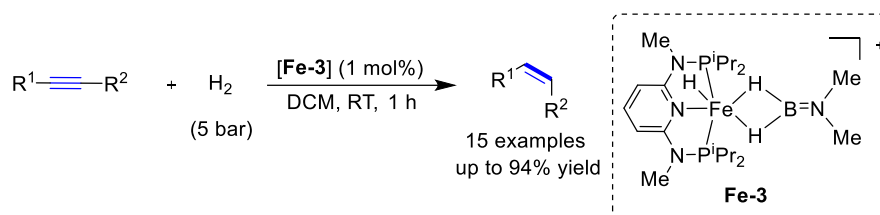
complexes for hydrogenation reaction revealed inactiveness of complex **Fe-1** while the imino-borohydride complex **Fe-2** converts internal alkynes to (*E*)-alkenes. Diversely substituted aryl alkynes, i.e., nitro, cyano, ester, methoxy were hydrogenated to respective (*E*)-alkenes with excellent yield. Notably, the keto functional group remained unharmed during alkyne hydrogenation. The complex is highly robust and doesn't require any activator. The authors hypothesized that the initially formed (*Z*)-alkenes isomerized to (*E*)-alkenes.



Scheme 1.9 Semi-hydrogenation of alkynes by iron catalyst **Fe-2**.

Kirchner group disclosed a protocol for the (*Z*)-selective semi-hydrogenation of internal alkynes by a bench-stable cationic iron complex, $[\text{Fe}(\text{PNPNMe}^i\text{Pr})(\text{H})(\eta^2\text{-H}_2\text{B}=\text{NMe}_2)]^+$ **Fe-3** (Scheme 1.10).⁵² The reaction proceeded with 5 bar H_2 pressure at room temperature. A broad range of functional groups, i.e., $-\text{F}$, $-\text{CF}_3$, $-\text{OH}$, as well as heterocycles like thiophene and pyridine were tolerated under the reaction conditions. The conjugated systems like 1,3-diynes and 1,3-enynes were hydrogenated to give selectively (*Z,Z*)-1,3-diene compounds in excellent yield. However, terminal alkynes underwent over-reduction to respective alkanes under the optimized reaction condition. The DFT study performed by the authors revealed that the energy requirement for the hydrogenation of internal alkyne to alkenes is lower than the energy needed for further hydrogenation of alkenes to alkanes. This energy difference restricts the internal alkenes for further reduction to alkanes. Notably, this energy difference is opposite in the case of a terminal alkyne, and thus, the over-reduction occurred in terminal alkynes. The proposed catalytic cycle proceeded *via* the initial conversion of complex **Fe-3** to **Fe-3a** in the presence of alkyne and hydrogen (Figure 1.2). The insertion of alkyne to the $\text{Fe}-\text{H}$ bond would give alkenyl-iron intermediate

Fe-3b. In the last step, the oxidative addition of H₂ followed by elimination of (*Z*)-alkene completes the cycle.



Scheme 1.10 Hydrogenation of alkyne to (*Z*)-alkene by **Fe-3**.

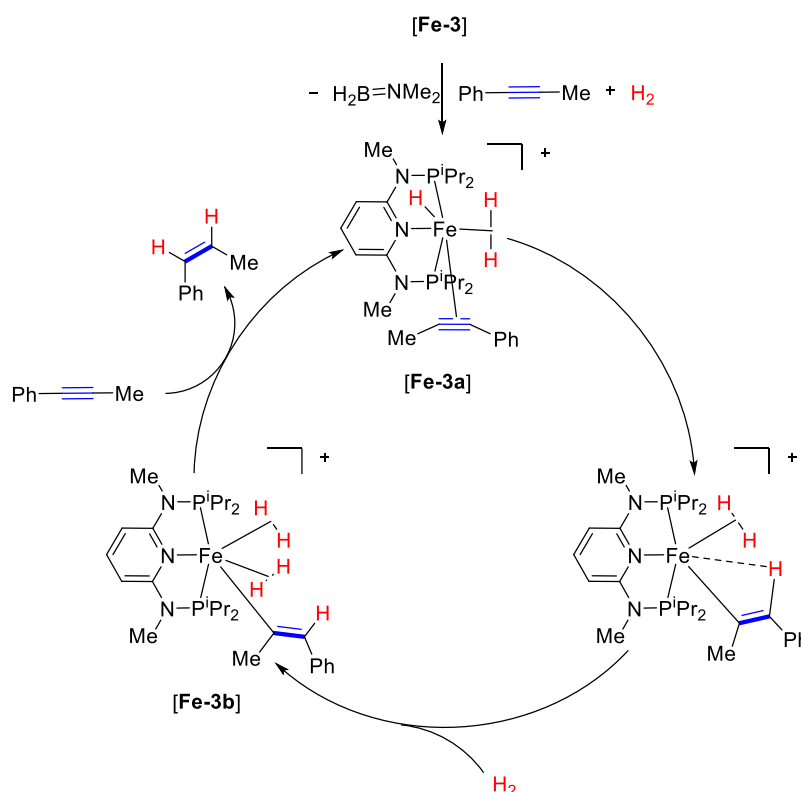
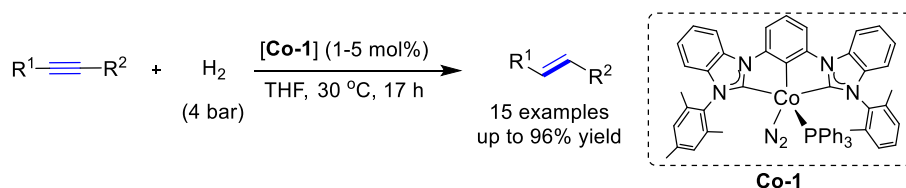


Figure 1.2 Proposed catalytic cycle for alkyne semi-hydrogenation by **Fe-3**.

1.2.3 Hydrogenation using Cobalt

Cobalt is one of the most utilized 3d metals for hydrogenation reactions. In recent years, cobalt-catalyzed alkyne hydrogenation has seen meteoric growth. Diverse approaches are followed for the cobalt-catalyzed hydrogenation of alkynes using various hydrogenation sources, such as hydrosilane, ammonia-borane or molecular hydrogen. In 2016, Fout and co-workers came up with a carbene based pincer cobalt complex **Co-1** that hydrogenate alkynes into selectively (*E*)-alkenes using molecular hydrogen (Scheme 1.11).⁵³ The catalyst **Co-1** could hydrogenate differently substituted (hetero)aryl internal alkynes as well as aliphatic

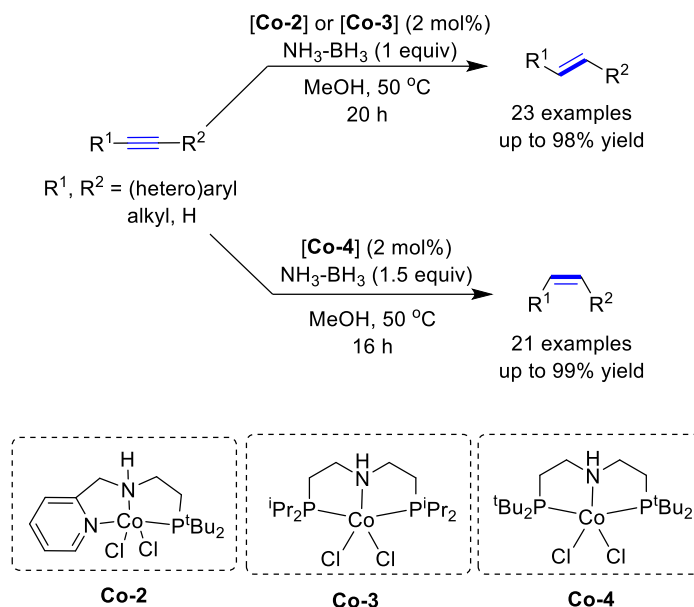
internal alkynes using 4 bar H₂ pressure at 30 °C. The authors have proposed the Co–H₂ complex as an active catalyst during the reaction.



Scheme 1.11 Carbene-cobalt catalyzed hydrogenation of alkynes.

A cobalt precursor Co(OAc)₂·4H₂O with ethylenediamine as a ligand was demonstrated for the hydrogenation of alkynes by Zhang and co-workers.⁵⁴ The catalytic amount of NaBH₄ and mixture of solvent (EtOH/THF/H₂O 10:10:1) was essential for the desired hydrogenation. The reaction afforded (*Z*)-alkenes, along with traces of (*E*)-alkenes and alkanes. The control study conducted by the authors revealed that the H₂ is the sole hydrogen source for the hydrogenation.

The stereo-divergent transfer hydrogenation of alkynes to (*E*)- and (*Z*)-alkenes is reported by Liu and Luo.⁵⁵ The molecularly defined PNN and PNP pincer Co(II) complexes **Co-2**, **Co-3**, and **Co-4** were developed and applied for the alkyne hydrogenation using ammonia-borane as a hydrogen source (Scheme 1.12). The stereo-selectivity generally controlled by the ligand design. Thus, catalysts **Co-2** and **Co-3** selectively produced (*E*)-alkenes, whereas catalyst **Co-4** provided (*Z*)-alkenes. This methodology operated at the mild condition and tolerated various functional groups like halides, alcohol, amine, cyano, ester, methoxy, and nitro on (hetero)aromatic and aliphatic nitriles. The authors proposed a mechanism which involves formation of a cobalt-hydride intermediate [**Co-Xa**] via the reaction of [**Co-X**]-H [X = 2, 3, or 4] with NH₃-BH₃. This [**Co-X**]-H can operate two cycles, i.e., hydrogenation cycle and isomerization cycle. The co-ordination of alkyne to cobalt, followed by insertion into Co-H bond gives intermediate [**Co-Xc**] which on protonation with MeOH provides (*Z*)-alkene and active catalytic species [**Co-X**]-H. In the next cycle, [**Co-X**]-H catalyzes the isomerization of (*Z*)-alkene to (*E*)-alkene via the co-ordination of (*Z*)-alkene to cobalt [**Co-Xd**], followed by the insertion into Co-H and rotation around C–C of intermediate [**Co-Xe**] would form [**Co-Xf**] which on β-hydride elimination gives (*E*)-alkene product (Figure 1.3).



Scheme 1.12 Stereo-divergent hydrogenation of alkyne.

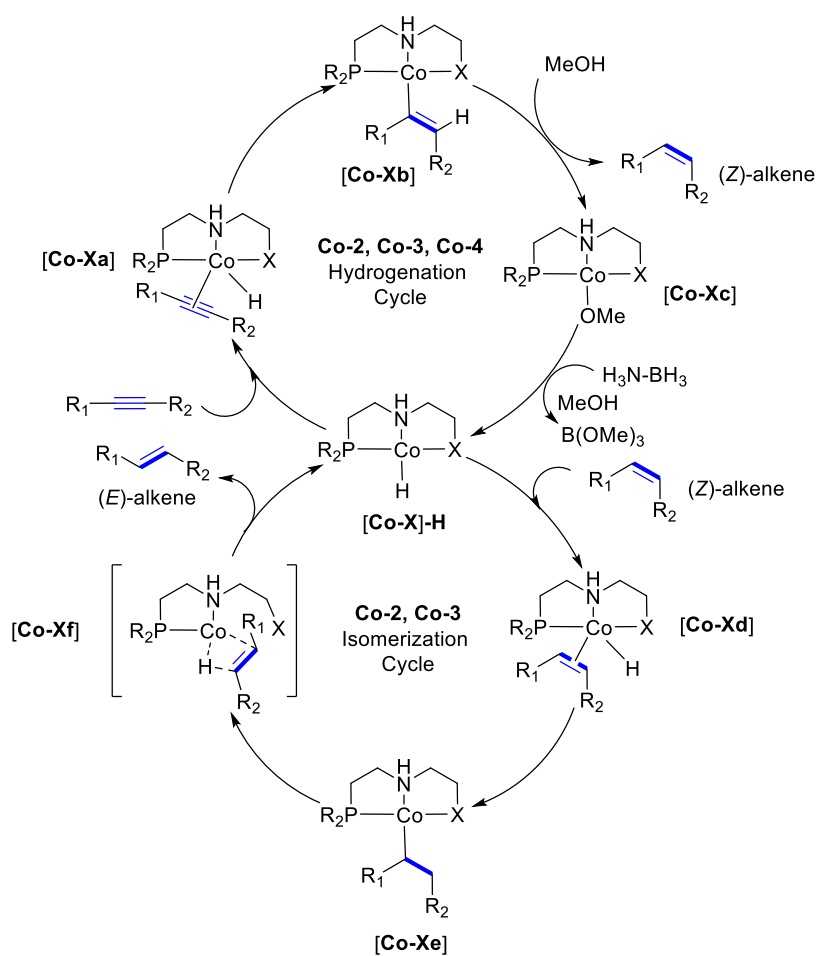
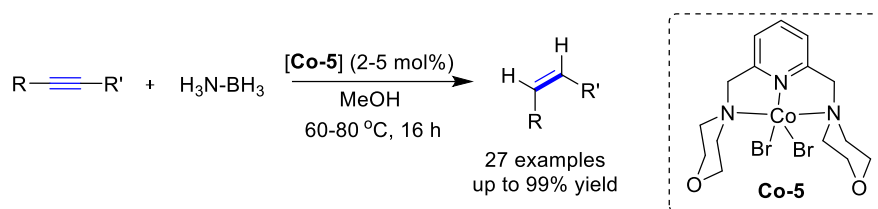


Figure 1.3 Catalytic cycle for hydrogenation of alkyne and isomerization of (Z)-alkene to (E)-alkene.

Balaraman and co-workers have shown a phosphine-free NNN pincer cobalt complex **Co-5** for the transfer hydrogenation of alkynes to alkenes using 1.2 equiv of $\text{NH}_3\text{-BH}_3$ (Scheme 1.13).⁵⁶ The method provided an excellent yield for the hydrogenation of aryl and alkyl internal and terminal alkynes. With increasing catalyst loading (4 mol%) and temperature (80 °C), the alkenes were converted to alkanes. The chemo-selectivity was demonstrated for the alkyne reduction in the presence of nitriles and esters.



Scheme 1.13 Transfer hydrogenation of alkyne by NNN ligated cobalt complex.

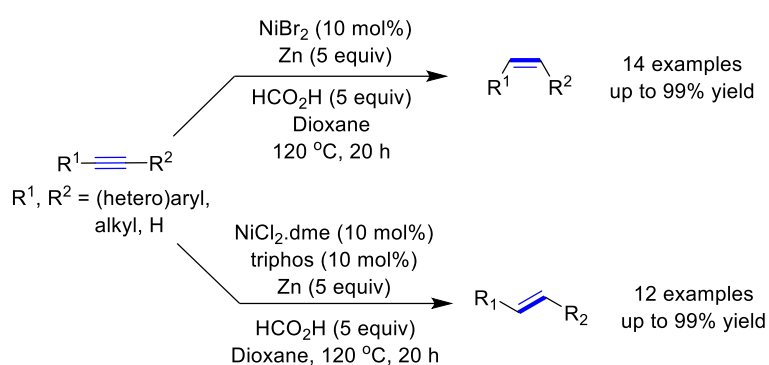
In 2021, a dinuclear cobalt complex supported by macrocyclic bispyridyl-diimine ligand synthesized, which catalyzed the switchable selective transfer hydrogenation of alkynes to (*E*)- or (*Z*)-alkenes employing Ph_2SiH_2 and H_2O as hydrogen sources.⁵⁷ The stereo-selectivity for the product found to be dependent of amount (equivalents) of H_2O used. The optimized methodology tolerated by different functionalities including some biologically relevant skeletons. Both diaryl and aryl-alkyl internal alkynes semi-hydrogenated to respective (*E*)- or (*Z*)- alkenes depending on the amount of water used.

Recently, Jiao and Beweries developed a phosphine based $\text{PNN}^{\text{H}}\text{Co(II)}$ pincer complex **Co-6** [$(\text{pyzN}^{\text{Pyr}}\text{N}^{\text{CH}_2}\text{P}^{\text{tBu}_2})\text{CoCl}_2$] for the transfer hydrogenation of diaryl internal alkynes to (*E*)-alkenes at 25 °C using ammonia-borane as a hydrogen source.⁵⁸ The mechanistic and spectroscopic studies revealed involvement of various active species like, $\text{PNN}^{\text{H}}\text{CoCl}$, $\text{PNN}^{\text{H}}\text{CoH}_2$, $\text{PNN}^{\text{H}}\text{CoH}$, $\text{PNN}^{\text{H}}\text{CoOMe}$ during the catalysis. Variety of reducible functional groups like, $-\text{CN}$, $-\text{COMe}$, $-\text{NO}_2$ remained unaffected during the catalysis and chemo-selectively alkyne was reduced.

1.2.4 Hydrogenation using Nickel

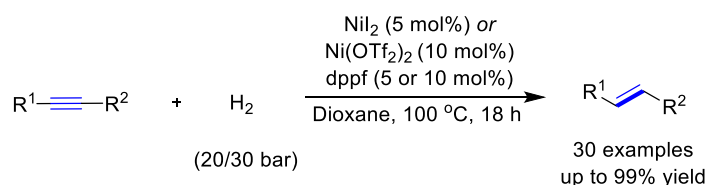
The alkyne hydrogenation by nickel has been demonstrated way back in 1973 by Brown using NaBH_4 as hydrogen source.⁵⁹ García has recently shown the semi-hydrogenation of alkynes using Ni(0) /diphosphine as a catalyst and ammonia-borane as hydrogen source.⁶⁰ The hypophosphorous acid as a hydrogen source for the (*E*)-selective semi-hydrogenation of alkynes was reported under $\text{NiCl}_2/\text{dppp}$ catalysis. In 2015, Moran and

Richmond developed a protocol to carry out alkyne hydrogenation to get both (*E*)- and (*Z*)-alkenes by suitable nickel catalyst (Scheme 1.14).⁶¹ Thus, NiBr₂ (10 mol%) catalyzed semi-hydrogenation of alkyne using 3 equiv of Zn and formic acid as a hydrogen source to obtain selectively (*Z*)-alkenes, whereas, a selective formation of (*E*)-alkenes was observed by employing NiCl₂(dme)/triphos as a catalyst. Notably, the reaction tolerated by a wide range of functional groups and doesn't require an inert atmosphere. The authors observed that the isomerisation of (*Z*)-stilbene occurred only in the presence of the triphos ligand.



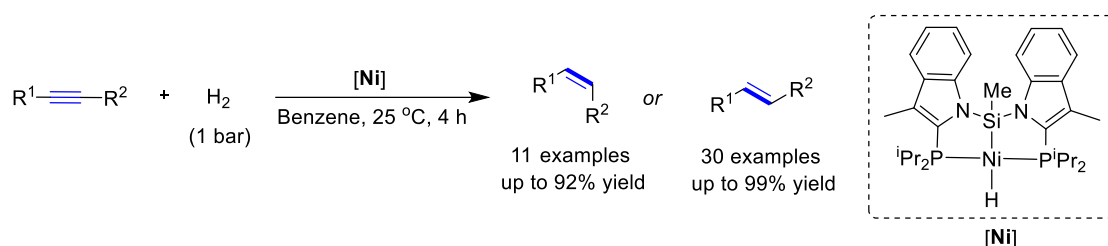
Scheme 1.14 Ligand controlled nickel-catalyzed hydrogenation of alkynes to (*E*)- or (*Z*)-alkenes.

Hydrogenation of internal alkynes to (*E*)-alkenes with hydrogen pressure was demonstrated by the Teichert group in 2020. Using the Ni(II) precursors [NiI₂ and Ni(OTf)₂] with dppf ligand system, both the aryl-aryl and aryl-alkyl internal alkynes were hydrogenated to respective (*E*)-alkenes with 20-30 bar H₂ pressure (Scheme 1.15).⁶² The optimized system was relevant with number of important functional groups and biomolecules. In addition, this optimized protocol was found to be dynamic as it also catalyzed migration of double bond from terminal position to internal. In the same line, Lu group synthesized a rare earth metal, gallium (Ga) supported nickel catalysts for the (*E*)-selective semi-hydrogenation of alkynes using 4.6 bar hydrogen pressure.⁶³



Scheme 1.15 Ni(OTf)₂/NiI₂ catalyzed hydrogenation of alkynes.

Recently, a bis(phosphino)silyl Ni-hydride complex ($i^{\text{Pr}}\text{-PSiP}^{\text{Ind}}\text{NiH}$) reported by the Turculet group for hydrogenative transformation of alkynes to (*E*)-alkenes (Scheme 1.16).⁶⁴ However, in some cases, authors observed reversal of selectivity for product as (*Z*)-alkene found to be major one. This newly synthesized Ni–H complex is highly robust and efficient for hydrogenation of alkynes at atmospheric pressure and room temperature. The authors were able to isolate the Ni–alkenyl intermediate which was then characterized by spectroscopic methods and single crystal XRD. A number of functional groups like –CN, –NO₂, –COOMe, –NH₂, –Cl were well tolerated. This report brought huge increment in the mild hydrogenation of alkynes to (*E*)-alkenes.



Scheme 1.16 Mild hydrogenation of alkyne to (*E*)- or (*Z*)-alkenes.

1.2.5 Hydrogenation using Copper

The semi-hydrogenation of alkynes with copper catalysts using molecular hydrogen has been demonstrated by Nakao group wherein the use of $[\text{PPh}_3\text{CuCl}]_4$ as a catalyst and 50 mol% LiO^tBu , the alkynes could be hydrogenated to (*Z*)-alkenes at 5 bar H_2 pressure (Figure 1.4).⁶⁵ The authors have reported very limited substrate scope for the aryl and alkyl internal alkynes. Notably, the hydrogenation of a terminal alkyne led to only trace amount of alkene formation (5%). The reaction mechanism depicted by the authors showed the formation of Cu–alkoxide followed by heterolytically cleavage of H_2 to produce an active intermediate Cu–H (Figure 1.4). The alkyne coordination to Cu–H, insertion in a stereo-selective manner followed by protonation led to the formation of (*Z*)-alkene.

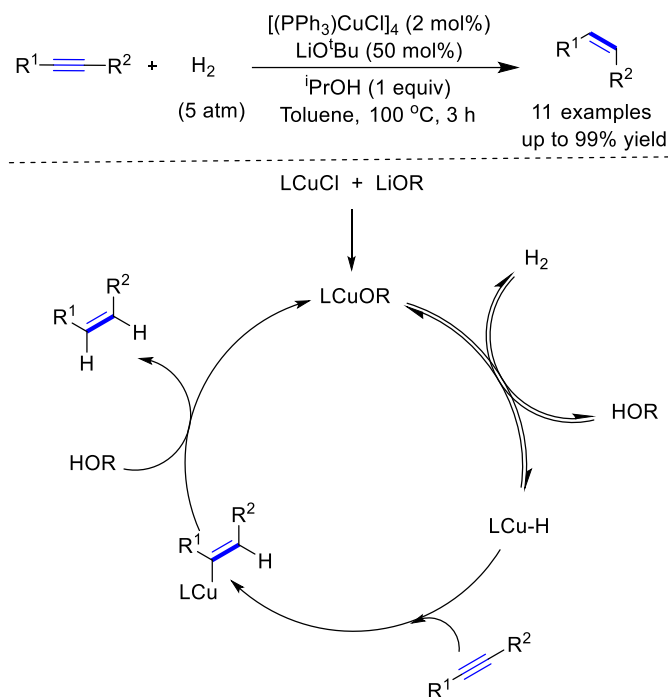
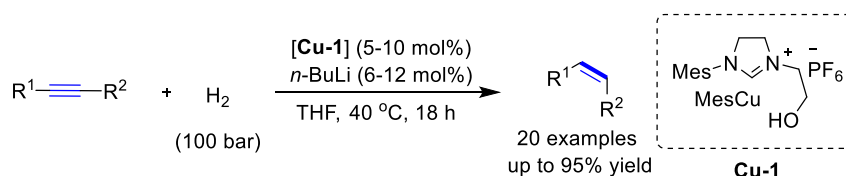


Figure 1.4 Catalytic cycle for copper-catalyzed alkyne hydrogenation.

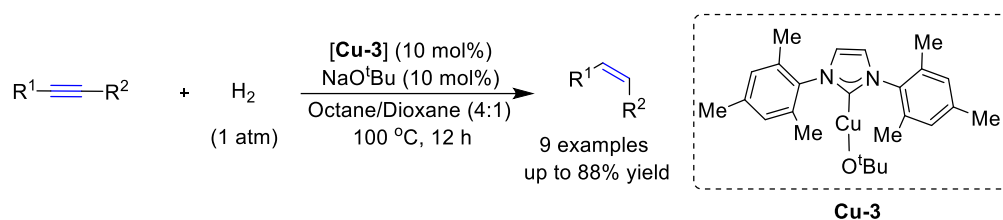
Teichert has shown the semi-hydrogenation of internal alkynes using 100 bar H_2 pressure employing a carbene-based copper complex, **Cu-1** (Scheme 1.17).⁶⁶ The catalyst is highly selective for semi-hydrogenation of alkyne in the presence of other reductive groups like ester, cyanide as well as ketone. Other functionalities like pyridine, thiophene, alcohol, and methoxy were compatible under the optimized reaction parameters and provided excellent yield of (Z) -alkenes. The authors have also shown that the simple carbene ligated catalyst **Cu-2** [iPrCuOH] can do the semi-hydrogenation of alkynes using molecular hydrogen without using an activator.⁶⁷



Scheme 1.17 Carbene ligated copper-catalyzed hydrogenation of alkynes.

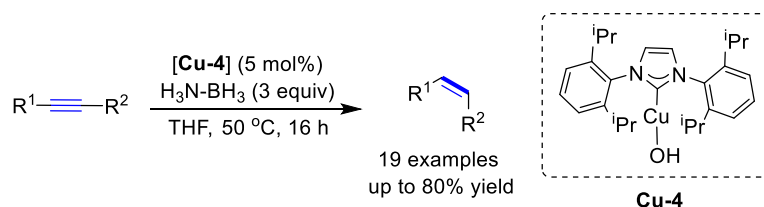
Ohmiya and Sawamura reported alkyne semi-hydrogenation at atmospheric hydrogen pressure (1 atm) using a commercially handy N -heterocyclic carbene ligated complex, $[(sIMes)CuCl]$ **Cu-3** (Scheme 1.18).⁶⁸ This catalyst hydrogenates alkyl and aryl internal alkynes to an alkenes with (Z) -selectivity upon activation with NaO^iBu . The catalytic

cycle follows the same pathway as described for the catalyst $[\text{PPh}_3\text{CuCl}]_4$ as shown in Figure 1.4.



Scheme 1.18 Catalytic cycle of alkyne hydrogenation by $[(\text{sIMes})\text{Cu}(\text{I})]$ catalyst.

The use of ammonia-borane as a hydrogen source in the copper-catalyzed hydrogenation of alkyne to (*Z*)-alkene was shown by Teichert (Scheme 1.19).⁶⁹ The use of carbene-ligated copper complex, $\text{IPrCu}(\text{I})\text{OH}$ **Cu-4** and 3 equivalents of ammonia-borane hydrogenated a range of internal alkynes to (*Z*)-alkenes at 50 °C. The developed methodology was also suitable for the hydrogenation of conjugated enolates. In the same line, Kusy and Grela demonstrated the transfer semi-hydrogenation of alkynes to afford (*Z*)-alkenes by oxidizable copper nanoparticles.⁷⁰ $\text{CuCl}_2 \cdot 2\text{H}_2\text{O}$ with ammonia-borane in the reaction mixture forms a copper-ammonia-borane adduct or nanoparticles which performs TH of alkynes. These nanoparticles are re-oxidizable with oxygen in the air and are re-usable up to 6 runs.

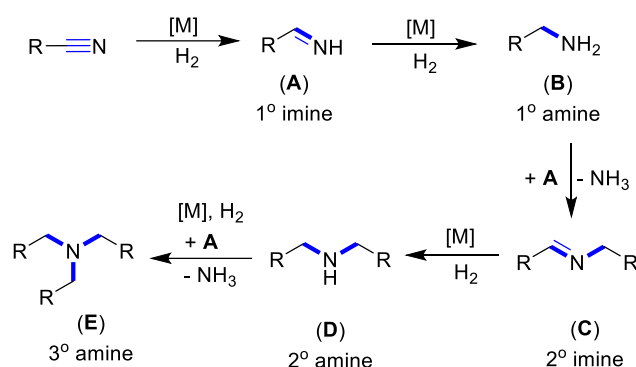


Scheme 1.19 Cu-catalyzed transfer hydrogenation of alkynes using $\text{NH}_3\text{-BH}_3$.

1.3 HYDROGENATION OF NITRILES

Catalytic hydrogenation of nitriles is amongst the essential organic modifications that lead to the formation of multiple imines and amines. In industries, these imines and amines are highly coveted organic constituent as they found application in agrochemicals, dyes, pigments, and fungicides.^{21,71} They have also significant role as intermediate and precursor for the synthesis of various pharmaceutically important compounds.⁷²⁻⁷⁴ In view of the significant importance and applicability of imines and amines, the advancement and growth in the field of nitrile hydrogenation is reasonable. The major challenge associated

with the nitrile hydrogenation is the regio-selectivity issues. For example, the hydrogenation of nitrile produces several products like primary imine (**A**) which then reduces to primary amine (**B**) (Scheme 1.20). Further, the condensation of in-situ formed imine **A** with primary amine (**B**) results in the formation of new intermediate secondary imine (**C**) with the evolution of ammonia gas. The secondary imine (**C**) can again hydrogenate to secondary amine (**D**), which is upon condensation with imine (**A**) can form tertiary amine (**E**). In general, the product selectivity in the nitrile hydrogenation is highly dependent on the design of catalyst, reaction solvents as well as on the additives used. Among the recent years, 3d transition metal-catalyzed nitrile hydrogenation has garnered much attention which is reflected in the form of various reports. Thus, in this section, a detailed note illustrated on the late 3d metal-catalyzed hydrogenation of nitriles to diverse compounds. The focus is broadly on the Mn, Fe, Co, Ni and Cu-catalyzed hydrogenation reactions.

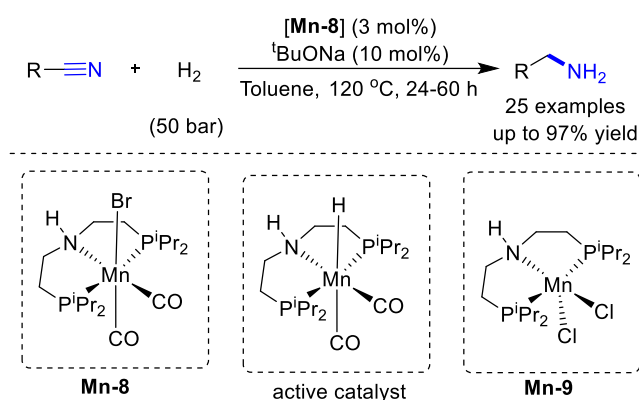


Scheme 1.20 Representation of nitrile hydrogenation showing various products.

1.3.1 Hydrogenation using Manganese

In recent years, manganese has turned up as one of the most utilized 3d metal for the hydrogenation reaction. Based upon previously reported Mn pincer catalysts,⁷⁵⁻⁷⁶ Beller reported the first catalytic hydrogenation of nitriles (Scheme 1.21).⁷⁷ The PNN pincer ligand-based manganese complex **Mn-8** selectively catalyzes the hydrogenation of the nitriles to the primary amines. The reaction needed a strong base ^tBuONa to activate the manganese catalyst. Various aromatic as well as heteroaromatic nitriles with both the electron-donating and electron-withdrawing functionality were well tolerated under the reaction conditions to give the respective primary amines. Moreover, aliphatic, benzylic and α,β -unsaturated nitriles provided good to excellent yield at 50 bar hydrogen pressure. Notably, the manganese

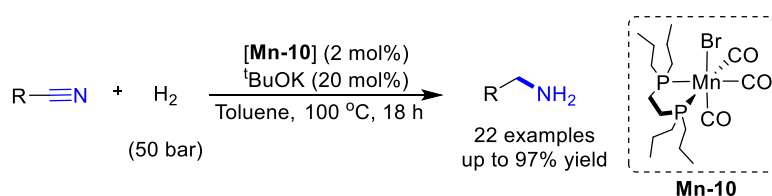
complex **Mn-9** with oxidation state +2 was found to be inert for the hydrogenation of nitriles. This study flourishes the activeness of Mn(I) complexes for the hydrogenation reactions.



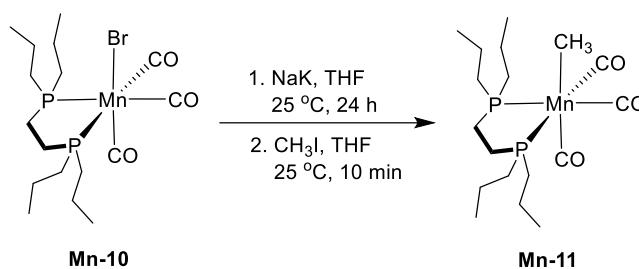
Scheme 1.21 Hydrogenation of nitriles by pincer-manganese catalyst.

In 2018, Kirchner and co-workers synthesized an air-stable non-pincer biphosphine manganese(I) complex **Mn-10** and employed for the hydrogenation of nitriles (Scheme 1.22).⁷⁸ The spectroscopic studies revealed that the geometry of the complex is facial, where all three CO are lying on the same side of the metal center. This bisphosphine ligated manganese complex hydrogenated various type of aromatic and aliphatic nitriles to the primary amines at 100 °C with 50 bar H₂ pressure. This catalyst showed chemo-selectivity towards the nitrile hydrogenation in the presence of ester and alkyne functionalities. The hydroxyl substituted benzonitrile did not undergo hydrogenation, which is attributed to the chelation of the oxygen with the open side of the manganese.

The same group synthesized a defined bench-stable alkyl biphosphine-Mn(I) complex fac-[Mn(dpre)(CO)₃(CH₃)] (dpre = 1,2-bis(di-*n*-propylphosphino)ethane) **Mn-11** by treatment of complex **Mn-10** with NaK followed by CH₃I (Scheme 1.23).⁷⁹ This alkyl biphosphine-Mn(I) complex acts as an active catalyst for nitrile hydrogenation to give corresponding primary amines without the use of an additive.

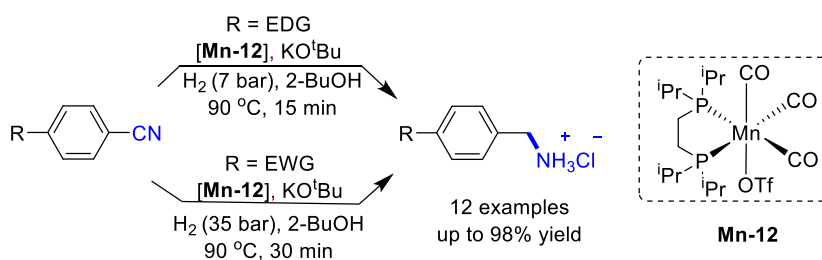


Scheme 1.22 Nitrile hydrogenation by bisphosphine manganese catalyst.



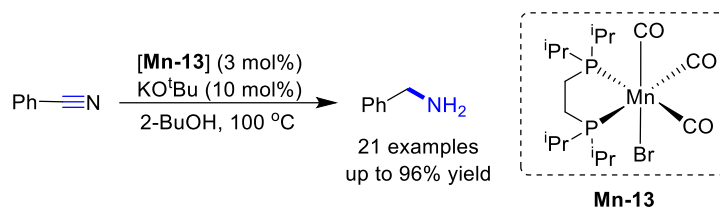
Scheme 1.23 Synthesis of alkyl-Mn complex.

Encouraged by the reactivity of the bidentate phosphine Mn complex for the nitrile hydrogenation, García *et. al.* reported a non-pincer Mn catalyst **Mn-12** having iso-propyl substituents on phosphorus center (Scheme 1.24).⁸⁰ The synthesized complex fac-[(CO)₃Mn(OTf)] **Mn-12** catalyzes hydrogenation of nitrile in the presence of KO^tBu using 2-butanol as a solvent. Particularly, the electron-rich substituted benzonitriles hydrogenated to the primary amines at the mild condition with 7 bar H₂ pressure, whereas the electron-deficient benzonitriles requires 35 bar hydrogen pressure to give an excellent yield of the desired primary amines.



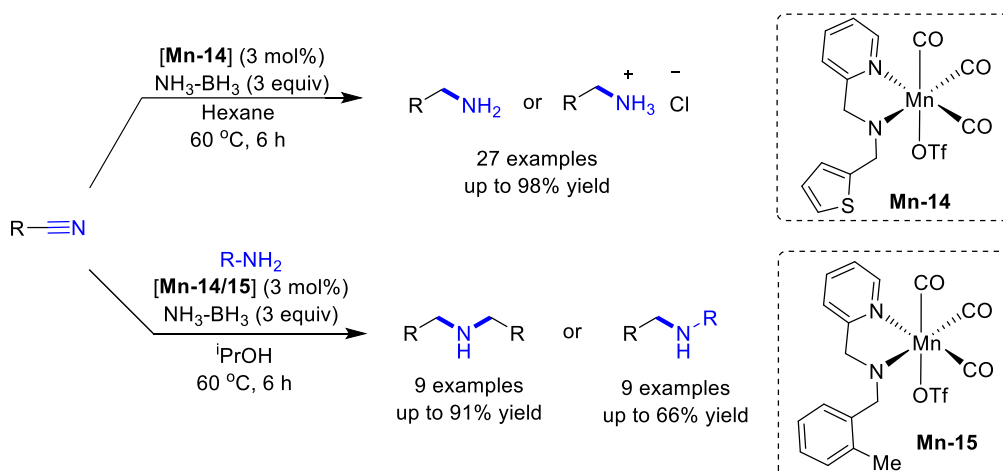
Scheme 1.24 Hydrogenation of nitriles by bisphosphine manganese catalyst.

Apart from the hydrogenation of nitriles using molecular H₂, the transfer hydrogenation has been preceded using manganese complex. Thus, García and co-workers have shown that the bromo-derivative **Mn-13** catalyzes the transfer hydrogenation of nitriles using 2-butanol as a hydrogen source (Scheme 1.25).⁸¹ The complex **Mn-13** generates the active catalyst **Mn-13a** in the presence of ^tBuOK and 2-butanol through the dehydrogenation of alcohol. The resulted active metal hydride complex **Mn-13a** reduces the nitrile to primary amine.



Scheme 1.25 Transfer hydrogenation of nitriles by complex **Mn-13**.

Recently, Maji and co-workers developed a phosphine-free sulphur based Mn(I) complexes **Mn-14** and **Mn-15** for the TH of nitriles to primary and secondary amines using ammonia-borane as a hydrogen source under different reaction solvents (Scheme 1.26).⁸² Thus, reaction in hexane solvent gives primary amine product using **Mn-14** while in the isopropanol solvent with **Mn-15** complex, secondary amine observed as the major product. The reaction parameters seems favourable with range of functional groups like, ester and halides on the nitriles and provided respective primary or secondary amines in good amount depending on the solvent used. Kinetic analysis revealed that the rate of the reaction is first order with respect to ammonia-borane and catalyst, while it is independent of nitrile substrate. This means, the nitrile hydrogenation step is not involved in rate determination.

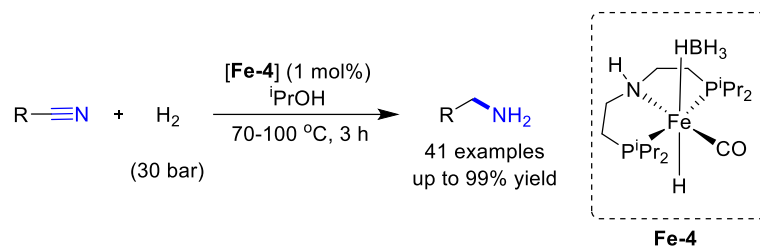


Scheme 1.26 Nitrile TH to primary/secondary amines by **Mn-14/15**.

1.3.2 Hydrogenation using Iron

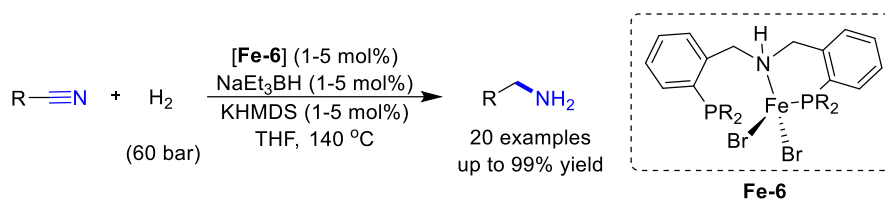
In 2014, the pioneering work on the iron-catalyzed nitrile hydrogenation was demonstrated by Beller and co-workers (Scheme 1.27),⁸³ wherein a previously synthesized PNP pincer iron complex was employed.⁸⁴ Hence, the PNP ligated complex **Fe-4** required 30 bar hydrogen pressure and 70°C to catalyze the hydrogenation of the nitriles to provide primary amines. Diversely substituted (hetero)aromatic and aliphatic nitriles were

hydrogenated to the respective amines using 1 mol% loading of catalyst **Fe-4**. Particularly, this catalyst showed regio-selectivity for the nitrile hydrogenation in the presence of amide and ester functionalities. Moreover, the α,β -unsaturated nitrile hydrogenated to synthetically important allylic amine with 75% isolated yield. The authors also synthesized a new catalyst **Fe-5** [$(i\text{Pr}_2\text{PN}^{\text{Me}}\text{P}i\text{Pr}_2)\text{Fe}(\text{CO})(\text{HBH}_3)\text{H}$] with methyl-substituent ($N\text{-Me}$) on the nitrogen of the ligand, which failed to perform the hydrogenation of nitrile.



Scheme 1.27 Nitrile hydrogenation by complex **Fe-4**.

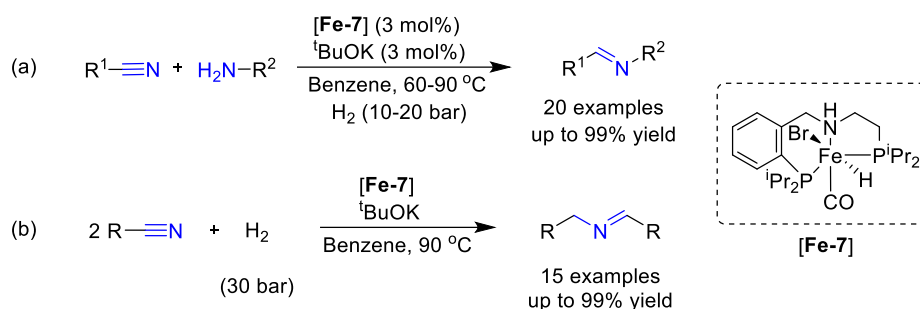
Milstein et al. synthesized a novel iron(II) complex by treating PNP pincer ligand with the FeBr_2 , wherein the complex doesn't have a pincer geometry (Scheme 1.28).⁸⁵ The complex formed a tetrahedral geometry with a non-coordinated phosphine side-arm, which was well established by the crystal structure analysis. Interestingly, this non-pincer complex **Fe-6** without having an ancillary CO ligand catalyzes the hydrogenation of diverse (hetero)aromatic and aliphatic nitriles using NaHBET_3 and KHMDs . The reaction condition for the hydrogenation seems to be harsh as it required 60 bar H_2 pressure and 140 °C of reaction temperature.



Scheme 1.28 Nitrile hydrogenation by iron complex [**Fe-6**].

The reports for the nitrile hydrogenation are mostly focused on a synthesis of primary amine. However, in 2017, Milstein group demonstrated the first example for the synthesis of secondary imine through nitrile hydrogenation (Scheme 1.29a).⁸⁶ The structurally modified PNP iron hydride pincer complex **Fe-7** hydrogenated the nitrile to unsymmetrical secondary imine in the presence of an external amine source. Generally, the

complex **Fe-7** reduces the nitriles to imines at relatively mild conditions, i.e., 10-20 bar H₂ pressure and 60°C. Under the reaction conditions, diverse functionalities on the aliphatic and (hetero)aromatic nitrile as well as numerous external amines were compatible, thus, leading to multiple types of unsymmetrical secondary imines.



Scheme 1.29 Synthesis of unsymmetrical secondary imine by catalyst **Fe-7**.

The synthesis of symmetrical secondary imines by the catalyst **Fe-7** is shown by the same group (Scheme 1.29b).⁸⁷ The symmetrical imines formed by the in-situ self-coupling of a hydrogenated amine with intermediate imine. Although the reaction required slightly elevated hydrogen pressure (30 bar) and temperature (90 °C), the compatibility of functional groups like halides, methoxy, amine, heteroaromatics, aliphatic cyanides is excellent. Interestingly, this secondary imine does not reduce further to the secondary amine when subjected to hydrogenation under the similar condition. The proposed catalytic cycle showed formation of iron-amido complex (**Fe-7a**) by the reaction of **Fe-7** with base (KO^tBu). This intermediate **Fe-7a** on the treatment with H₂ forms **Fe-7b** which is an active catalyst for the hydrogenation of nitrile and primary imine (Figure 1.5).

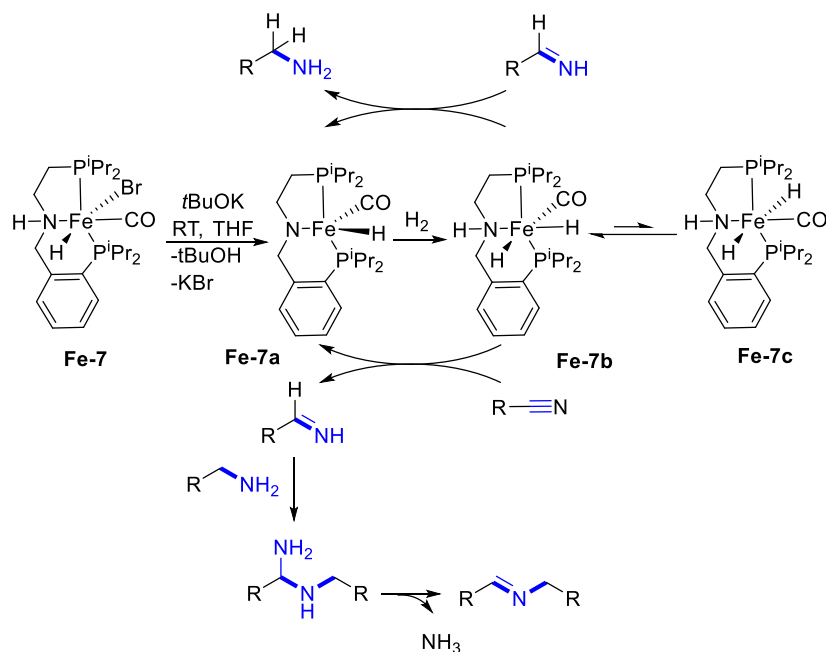
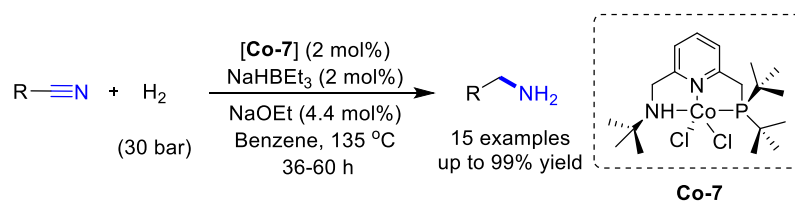


Figure 1.5 Catalytic cycle for **Fe-7** catalyzed nitrile hydrogenation.

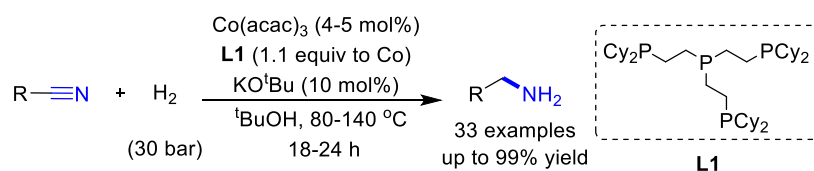
1.3.3 Hydrogenation using Cobalt

Cobalt is one of the most utilized 3d metals for hydrogenation reactions. In 2015, the Milstein group showed the first example of homogeneous cobalt catalyst to carry out the nitrile hydrogenation (Scheme 1.30).⁸⁸ The cobalt complex **Co-7** co-ordinated through PNN pincer ligand hydrogenated the nitriles to primary amines. This complex **Co-7** is activated by the use of two bases, i.e., a super-hydride base (NaHBET_3) and NaOEt . It was believed that the double-deprotonation of both N–H and methylene proton of the nitrogen side-arm of the pincer produces mono-anionic Co(I) complex. The activated complex hydrogenated the nitriles into primary amines employing 30 bar H_2 pressure at 135 °C in benzene. A variety of aromatic and heteroaromatic nitriles selectively reduced to primary amines in good yields. Generally, the aliphatic and benzylic cyanides required significantly longer reaction time (60 h) for the completion.



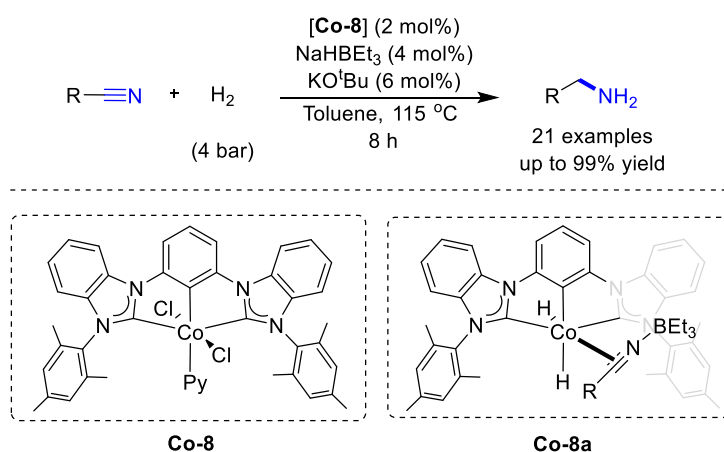
Scheme 1.30 PNN pincer cobalt catalyzed hydrogenation of nitriles.

Apart from the pincer (PNN)Co(II) complex, a cobalt catalyst with tetradentate phosphine ligand was demonstrated for the hydrogenation of nitriles to primary amines at relatively mild conditions (Scheme 1.31).⁸⁹ Thus, hydrogenation of different aromatic nitriles was carried out using 4 mol% of Co(acac)₃, 4.4 mol% of phosphine ligand **L1** and 30 bar H₂ pressure at 80-120 °C. A wide range of functional groups survived the reaction condition.



Scheme 1.31 Tetradentate Co-phosphine catalyzed hydrogenation of nitriles.

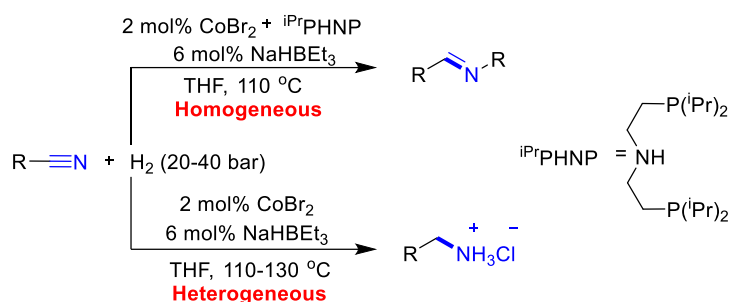
In 2017, Fout group developed an air-stable cobalt (bis)carbene pincer complex [**Co-8**] and utilized for the hydrogenation of nitriles.⁹⁰ The complex **Co-8** is activated by the use of NaHBET₃. Based on the *para*-Hydrogen Induced Polarization (PHIP) transfer NMR studies, it was shown that the in-situ generated Lewis acid helps in the side-on coordination of the nitrile to the metal center, **Co-8a** (Scheme 1.32). This adduct permits the pair-wise transfer of H₂ to nitrile through a Co(I)/Co(III) redox process. The catalyst [**Co-8**] exclusively gave primary amines when subjected to nitrile hydrogenation at low hydrogen pressure (4 bar H₂). A wide range of aromatic, aliphatic, and benzylic nitriles were hydrogenated to provide an excellent yield of corresponding products.



Scheme 1.32 Carbene ligated cobalt catalyzed hydrogenation of nitriles.

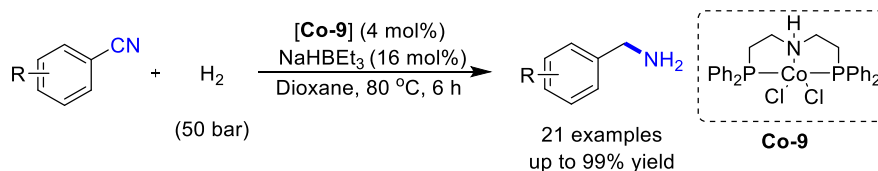
Dai and Guan demonstrated a twin catalytic system for switching the selectivity of the nitrile hydrogenation by including or omitting the HN(CH₂CH₂PⁱPr₂)₂ (ⁱPrPN^HP) ligand

(Scheme 1.33).⁹¹ The treatment of simple CoBr_2 with 3 equivalents of NaHBET_3 catalyzes the hydrogenation of nitriles into primary amines, whereas, employment of ($i\text{PrPN}^{\text{H}}\text{P}$) ligand with CoBr_2 and NaHBET_3 led to the formation of secondary aldimine as an exclusive product. The authors have proposed that the treatment of NaBET_3H with CoBr_2 generated heterogeneous cobalt particles, which reduced the nitriles to primary amines at 20–40 bar H_2 pressure. However, when $\text{HN}-(\text{CH}_2\text{CH}_2\text{P}^i\text{Pr}_2)_2$ ligand added to the cobalt system, the reaction forms a homogenous pincer catalyst $(\text{PN}^{\text{H}}\text{P})\text{CoBr}_2$ that showed selectivity for the formation of secondary aldimine.



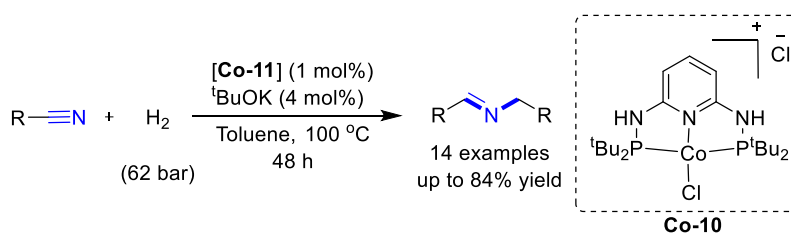
Scheme 1.33 Switchable selective hydrogenation of nitriles.

Recently, Junge and Beller synthesized the pincer complex $(\text{PN}^{\text{H}}\text{P})\text{CoCl}_2$ [**Co-9**] having phenyl-substituent on the phosphine ligand. This complex homogeneously catalyzed the hydrogenation of nitriles to respective primary amines at 50 bar H_2 pressure (Scheme 1.34).⁹² The homogenous nature of the complex **Co-9** during the reaction was evaluated by different control experiments. The kinetic profile of the standard reaction did not show significant induction period suggesting a homogeneous pathway of the reaction. Furthermore, the standard reaction in the presence of PPh_3 scavenger furnished 97–99% of the primary amine, whereas the reaction with cobalt nanoparticles completely quenched in the presence of PPh_3 . These observations ultimately confirmed the homogeneous nature of catalyst **Co-9**.



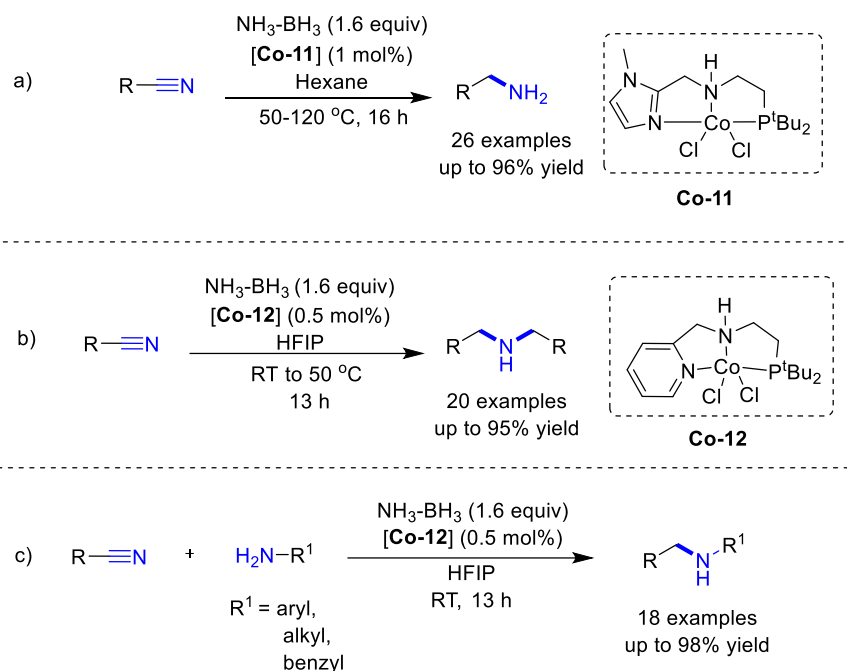
Scheme 1.34 (PhPNHP) CoCl_2 catalyzed hydrogenation of nitriles.

Cobalt-catalyzed selective synthesis of symmetrical secondary imine through nitrile hydrogenation has also been precedented. Huang group developed a cobalt pincer complex **Co-10** from a previously reported PN³P ligand,⁹³ which selectively catalyzed hydrogenation of nitriles to symmetrical secondary imines (Scheme 1.35).⁹⁴ The complex **Co-10** is activated by abstraction of an acidic proton from the NH side-arm of the pincer ligand with the help of KO^tBu. The catalytic cycle proposed to proceeds through metal-ligand co-operation. Although this was the first report for symmetrical secondary imine synthesis with cobalt, the reaction condition seems harsh as it needed 62 bar H₂ pressure for 48 h for the quantitative conversion.



Scheme 1.35 Synthesis of symmetrical secondary imines by catalyst **Co-10**.

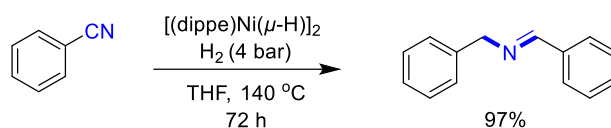
The cobalt-catalyzed hydrogenation of nitriles is mainly reported to synthesize primary amines and secondary (ald)imines. Unfortunately, the protocol for the hydrogenation of nitriles to secondary amines with molecular hydrogen was not known till this end. However, in 2016, Liu and Zhou came up with PNN pincer cobalt complexes **Co-11** and **Co-12** as catalysts for the transfer hydrogenation of the nitriles to primary and secondary amines.⁹⁵ The catalyst shows selectivity for the synthesis of primary or secondary amine based on the polarity of solvent used. Thus, nitriles can be selectively converted to primary amines using **Co-11** and NH₃-BH₃ as a sacrificial source in non-polar solvent hexane at mild conditions (Scheme 1.36a). However, the hydrogenation reaction in polar solvent, HFIP (Hexafluoroisopropanol), furnished symmetrical secondary amines as an exclusive product using catalyst **Co-12** and NH₃-BH₃ as hydrogen source (Scheme 1.36b). Additionally, the use of external amines in HFIP solvent produced unsymmetrical secondary amines in excellent yield (Scheme 1.36c). The catalyst is highly robust and TON was obtained up to 2366.



Scheme 1.36 Transfer hydrogenation of nitriles to primary/secondary amines.

1.3.4 Hydrogenation using Nickel

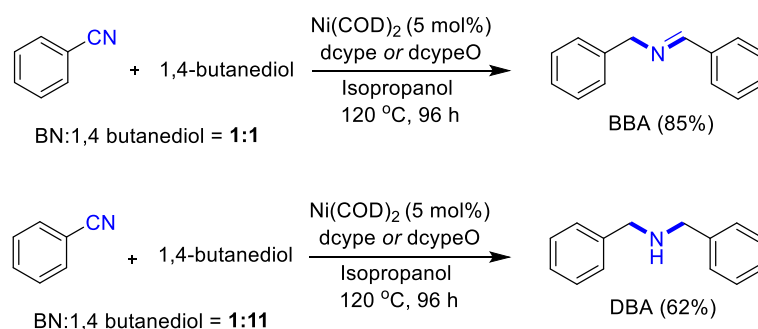
Nickel is the first 3d transition metal that was used for the homogeneous hydrogenation of the nitriles to aldimines. García demonstrated that the Ni(I) complex $[(\text{dippe})\text{Ni}(\mu\text{-H})_2]$ converts to Ni(0) $[(\text{dippe})\text{Ni}(\eta^2\text{-NC-Ph})]$ in the presence of benzonitrile and H_2 (Scheme 1.37).⁹⁶ The Ni(0) complex could hydrogenate the benzonitriles to aldimines using 4 bar hydrogen pressure at 140 °C for 72 h. However, benzodinitriles needed 8 bar hydrogen pressure and 180 °C to give the desired secondary imine. The developed methodology has a very limited substrate scope.



Scheme 1.37 Nickel-catalyzed hydrogenation of benzonitrile.

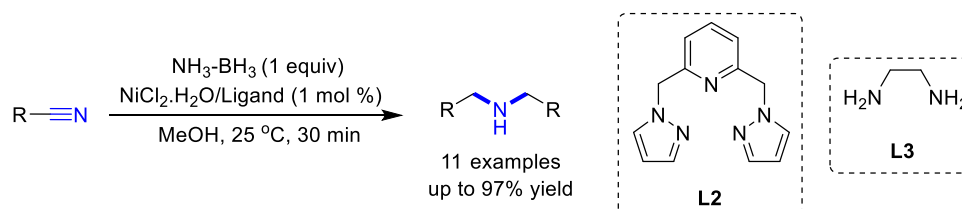
The same group has reported the homogeneous transfer hydrogenation of benzonitrile to aldimine or secondary amine. Thus, the use of $\text{Ni}(\text{COD})_2$ along with a mixture of $\text{Cy}_2\text{P}(\text{CH}_2)_2\text{P}(\text{O})\text{Cy}_2$ and $\text{Cy}_2\text{P}(\text{CH}_2)_2\text{PCy}_2$ as ancillary ligands and 2-propanol or 1,4-dibutanol as a hydrogen source led to the hydrogenation of benzonitrile (Scheme 1.38).⁹⁷ Generally, the 1,4-dibutanol acts as a better hydrogen source than 2-propanol and generated

γ -butyrolactone as a product after transfer dehydrogenation. The concentration of the 1,4-butanediol plays an important role, as an equivalent amount of 1,4-butanediol with benzonitrile (BN) produced BBA up to 85%, whereas 11 equivalents of the same furnished DBA as a major product (62%).



Scheme 1.38 Nickel-catalyzed transfer hydrogenation of benzonitrile.

Swartz and co-workers recently demonstrated chemo-selective transfer hydrogenation of nitriles to secondary amines with $\text{NiCl}_2 \cdot 6\text{H}_2\text{O}$ salt and bi/tridentate nitrogen based ligand (**L2/L3**).⁹⁸ Ammonia-borane as a hydrogen source converts nitriles into secondary amines at room temperature within 30 minutes. This protocol found efficient with aromatic as well as aliphatic nitriles and provided excellent isolated yields for respective secondary amines (Scheme 1.39).

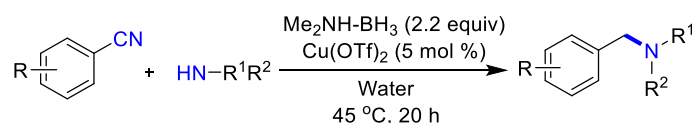


Scheme 1.39 Nickel-catalyzed hydrogenation of nitriles to secondary amines.

1.3.5 Hydrogenation using Copper

Copper as a catalyst has not been explored much for the nitrile hydrogenation reaction, which might be due to the strong end-on coordination of nitriles to Cu(I) that could inhibit the turnover of the catalyst. The first report for nitrile hydrogenation was preceded in 2014, where Cu(OTf)_2 as a sole catalyst catalysed the reductive amination of nitriles with aliphatic amines to form unsymmetrical secondary amines using $\text{Me}_2\text{NH-BH}_3$ as hydrogen source (Scheme 1.40).⁹⁹ Notably, the reaction was performed in the water medium at 45°C .

The heterogeneous nature of the copper catalyst was revealed by the mercury addition experiment, wherein the reaction was completely quenched.

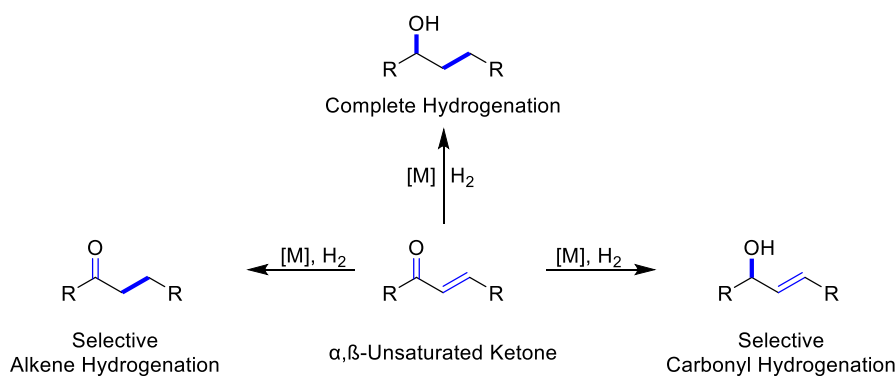


Scheme 1.40 Nitrile hydrogenation by copper.

In the same line, recently, Zhou group presented a copper triflate-catalyzed transfer hydrogenation of nitriles with oxazaborolidine complex as a hydrogen source.¹⁰⁰ This protocol showed solvent dependent product formation, where reaction in water solvent provided secondary amine as a sole product while, in THF solvent, primary amine was obtained as a major one. Moreover, external amines added to the reaction resulted in the formation of unsymmetrical secondary amines. This operationally simple methodology provides exceptional advancement in mild transfer hydrogenation of nitriles.

1.4 HYDROGENATION OF α,β -UNSATURATED KETONES

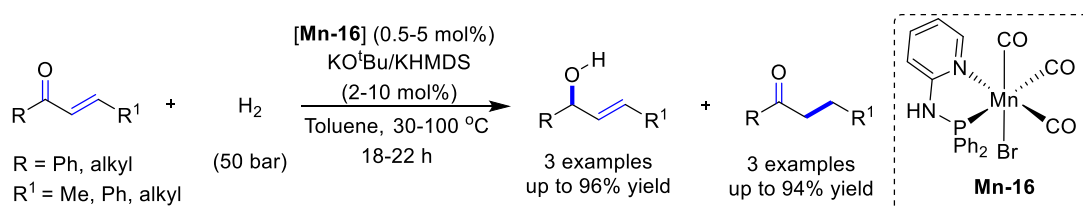
Hydrogenative transformation of α,β -unsaturated carbonyl compounds, particularly enones could provide variety of products, i.e., allylic alcohol or saturated ketone/alcohol which are significantly useful in the academics or industrial sector (Scheme 1.41).^{22-25,27} Thus, the transition metal catalyzed selective hydrogenation of C=C or C=O in the α,β -unsaturated ketone is very important and has progressed significantly in the recent decades. In particular, 3d-transition metal catalysed hydrogenative transformation of enones has been studied widely in the recent past and hence, here, collective information on the late 3d base-metals (Mn, Fe, Co, Ni and Cu) catalyzed hydrogenation of enones is presented.



Scheme 1.41 Schematic representation for the hydrogenation of α,β -unsaturated ketones.

1.4.1 Hydrogenation using Manganese

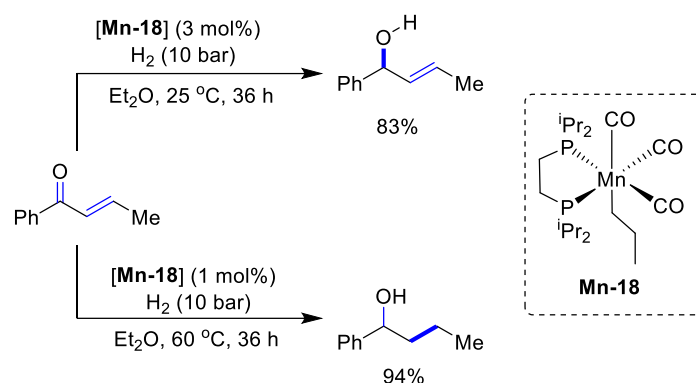
Manganese is one of the highly used metal for selective hydrogenation of α,β -unsaturated ketones. The early work on conjugated ketone reduction by Mn-catalyst demonstrated by the Sortais group in which bidentate manganese-based **Mn-16** catalyzed the selective hydrogenation of C=C of some selected chalcone derivatives with 50 bar H₂ at 25 °C in the presence of base (KHMDS or KO^tBu) (Scheme 1.42).¹⁰¹ In addition, complete hydrogenated product also obtained by changing the reaction parameters slightly. Moreover, when the ‘carvone’ molecule subjected to hydrogenation, selectively conjugated alkene hydrogenated keeping the C=C intact.



Scheme 1.42 Hydrogenation of α,β -unsaturated ketones by **Mn-16**.

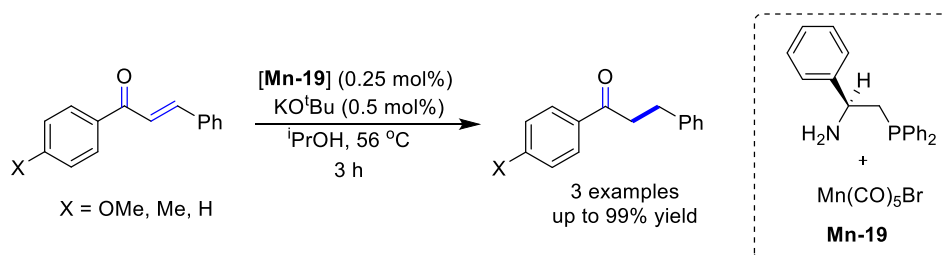
In the same line, Vielhaber and Topf shown hydrogenation of chalcone by nitrogen-based bidentate **Mn-17** complex which provides mixture of products, completely reduced alcohol (43%) and saturated ketone (55%) at 40 bar H₂ pressure and 120 °C.¹⁰² The major focus is centred on the ketone hydrogenation and selective C=C hydrogenation of α,β -unsaturated carboxylic acid derivatives (esters).

Recently, Kirchner and co-workers developed bidentate phosphine ligated manganese catalyst **Mn-18** which hydrogenates α,β -unsaturated ketones to either allylic alcohol or saturated alcohol using 10 bar H₂ pressure depending upon the temperature employed (Scheme 1.43).¹⁰³ Thus, in this base-free protocol, saturated alcohol form as a major product at 60 °C while allylic alcohol remains major one at 25 °C.



Scheme 1.43 Hydrogenation of α,β -unsaturated ketones by **Mn-18**.

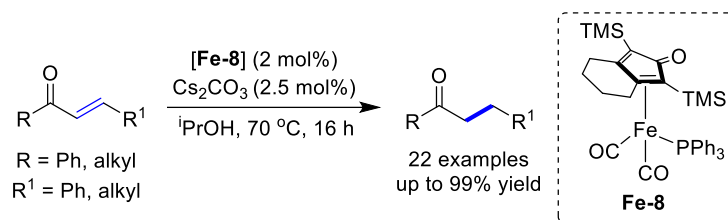
The David Lacy group developed a protocol for transfer hydrogenation of chalcone derivatives by β -amino phosphine Mn catalyst **Mn-19** using isopropanol as a hydrogen source and KO^tBu (Scheme 1.44).¹⁰⁴ This protocol is very mild which operates at 56 °C temperature using 0.25 mol% of **Mn-19** and 0.5 mol% KO^tBu. However, here also main focus is given for ketone reduction and only 3 examples of chalcone are presented.



Scheme 1.44 Transfer Hydrogenation of chalcones by **Mn-19**.

1.4.2 Hydrogenation using Iron

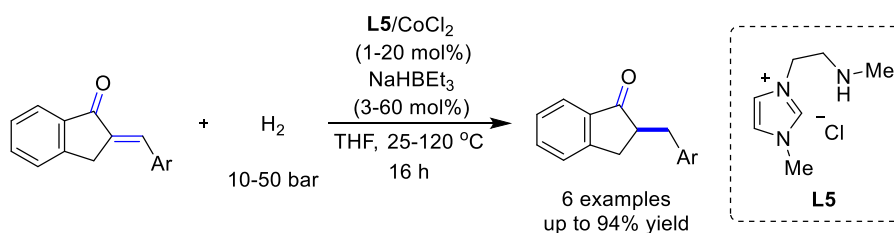
Iron is most abundant 3d-transition metal and therefore its appealing to utilize it for hydrogenation reactions. However, only known report for chalcone hydrogenation with iron based catalyst unfolded in 2018 by Poater and Renaud.¹⁰⁵ Here, the authors synthesized the iron tricarbonyl complex **Fe-8** with electron-rich cyclopentadienone backbone which performs transfer hydrogenation of α,β -unsaturated ketones to saturated ketone using isopropanol as a hydrogen sacrificial and Cs₂CO₃ as a base (Scheme 1.45). This report shows the only 3d-transition metal catalyzed protocol which completely devoted to the hydrogenation of α,β -unsaturated ketones derivatives. The number of functional group tolerated this protocol and rewarded excellent chemo-selectivity for hydrogenation of C=C bond of both aliphatic and aromatic α,β -unsaturated ketones.



Scheme 1.45 Transfer Hydrogenation of α,β -unsaturated ketones by **Fe-8**.

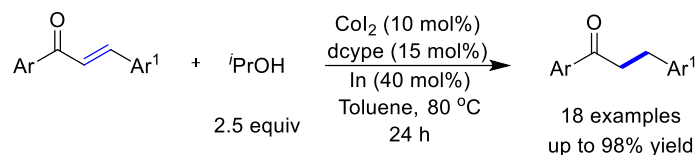
1.4.3 Hydrogenation using Cobalt

The cobalt-catalyzed hydrogenation of activated C=C double bond with molecular hydrogen reported by Liu group which describes use of CoCl_2 salt with carbene-based ligand (**L5**) catalyzed the hydrogenation of activated alkenes at 10-50 hydrogen pressure and 25-120 $^\circ\text{C}$ (Scheme 1.46).¹⁰⁶ A range of tri- and tetra-substituted alkenes of α,β -unsaturated carbonyl compounds (particularly ketones) hydrogenated successfully to provide respective saturated carbonyl products. Particularly, a cyclic α,β -unsaturated ketones have been hydrogenated to great extent providing up to 94% of saturated cyclic ketones. This $\text{CoCl}_2/\mathbf{L5}$ catalytic system is so efficient that it recorded the TON upto 760.



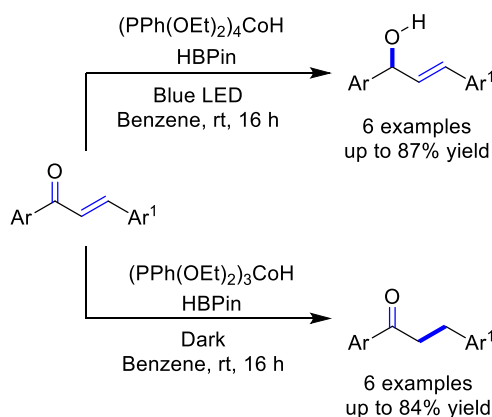
Scheme 1.46 Hydrogenation of α,β -unsaturated ketones by carbene/ CoCl_2 system.

A CoI_2 catalyzed transfer hydrogenation of chalcone derivatives reported in 2019. Thus, 10 mol% CoI_2 and phosphine-based dcppe (1,2-Bis(dicyclohexylphosphino)ethane) ligand (20 mol%) and indium (In) (40 mol%) as an additive catalyzed the transfer hydrogenation of C=C of chalcone using $i\text{PrOH}$ as a hydrogen source at 80 $^\circ\text{C}$ (Scheme 1.47).¹⁰⁷ Chalcones with different functionalities like, $-\text{OMe}$, $-\text{Cl}$, $-\text{CF}_3$ are survived under the optimized reaction condition and transformed into respective ketones with high yields. The authors have proposed the formation of low-valent active cobalt species with the help of indium during the reaction.



Scheme 1.47 Hydrogenation of chalcones by dcype/CoI₂ system.

Photo-controlled cobalt catalyst synthesized by the Teskey group and applied for the reduction of α,β -unsaturated ketones. This photo-catalyst provided different selectivity for product in the presence and absence of light as carbonyl reduced product forms in former case while C=C reduces in the dark (Scheme 1.48).¹⁰⁸ The pinacol-borane was used as a hydrogenating agent. The reaction goes through the formation of hydroboration intermediate which is then subjected to aqueous work-up to get hydrogenated product. In the presence of light (PPh(OEt)₂)₃CoH is an active catalyst and (PPh(OEt)₂)₄CoH is active catalyst in the dark which govern the selectivity for the product. Apart from pinacolborane, tertiarybutyl amine also has been used as hydrogen source in transfer hydrogenation β -trifluoromethylated α,β -unsaturated ketones catalyzed by Co(ClO₄)₂·6H₂O.¹⁰⁹



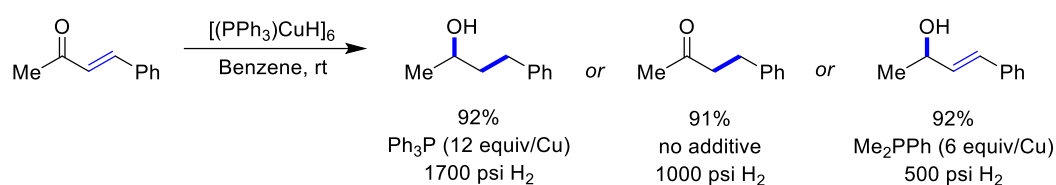
Scheme 1.48 Transfer hydrogenation of chalcones using HBPIn.

1.4.4 Hydrogenation using Nickel and Copper

Yus and co-workers proposed a NiCl₂ catalyzed transfer hydrogenation of α,β -unsaturated ketones using ethanol as a hydrogen source.¹¹⁰ This protocol involved formation of the nickel nanoparticles by the reaction of NiCl₂ with lithium which reduces Ni(II) to Ni(0). In addition, lithium also helps in dehydrogenation of EtOH to provide molecular hydrogen. The polymer supported arene helped in transfer of electron from lithium to NiCl₂

to reduce it to Ni(0). Different aliphatic and aromatic α,β -unsaturated ketones reduced to respective saturated ketone with excellent yield.

The copper as a catalyst mainly explored by the Stryker group for the hydrogenation of enones. In 1989, Stryker and co-workers made a phosphine based $[(PPh_3)CuH]_6$ catalyst which used to hydrogenate enones.¹¹¹ However, the selectivity obtained for product was poor as both saturated ketone and saturated alcohol formed in significant amount. Later on, in 2000, the same group explored the $[(PPh_3)CuH]_6$ catalyst for the hydrogenation of enones to get selectively enol as a product when PPh_3 was used as an additive, while saturated alcohol found to be major product if Me_2PPh added as an additive. Moreover, the absence of phosphine additive gave exclusively saturated ketone (Scheme 1.49).¹¹²



Scheme 1.49 Selective hydrogenation of chalcone by $[(PPh_3)CuH]_6$.

1.5 OBJECTIVE OF THE PRESENT STUDY

Catalytic hydrogenation of unsaturated bonds is a crucial synthetic path for achieving saturated bonds. Traditionally, two pathways are involved in this process, i) catalytic hydrogenation with molecular hydrogen and ii) transfer hydrogenation. Over the past few decades, there has been significant advancement perceived in both methods. However, this growth was primarily accomplished using noble transition metal catalysts, i.e., 4d/5d transition metals. These rare metals are very high in cost and are naturally limited, which affect their usage in more practical and sustainable hydrogenative transformation. To cope with the challenges related to the use of 4d/5d transition metals, researchers are focusing on the naturally abundant and cost-effective 3d transition metals for catalytic hydrogenations. Though the use of 3d transition metals address the issue of high cost, the harsh reaction conditions and use of highly reactive reagents restrict their applicability. Also, this eventually influences the selective synthesis of a product. Similarly, the hydrogenative transformation of unsaturated bonds, particularly alkynes, nitriles, and chalcones, is restricted by either the utilization of noble metals or limited to harsh reaction conditions and the use of sensitive reagents. In addition, the stereo-selective synthesis of desired reduced product from (conjugated) unsaturated bonds is disturbed by the extreme reaction parameters. Hence, there

is an urgent need to design concise, practical, sustainable synthetic approach using 3d transition metal catalysts through which one can perform the hydrogenative transformations of such multiple unsaturated bonds at milder reaction conditions in a stereo-selective manner. Thus, the objectives of work presented here were to look into the problem related to harsh reaction conditions and attempt to resolve those by designing easy-to-use catalytic systems, particularly by cobalt and manganese. Moreover, the direct application of these user-friendly catalytic systems for the chemo- and stereo-selective hydrogenation of nitriles, alkynes and chalcones using milder reaction conditions was another aspect of the present work.

The results obtained from the study are discussed in this thesis. In chapter 2, the synthesis of hemi-labile and phosphine-free quinolonyl-based (*NNN*)-type pincer and non-pincer cobalt complexes is described. These well-defined anionic non-pincer cobalt complexes $\kappa^2\text{-}(\text{Q}^{\text{NN}})\text{CoX}_2(\text{N}^{\text{C}(\text{O})\text{HNEt}_2})$ ($\text{X} = \text{Cl}, \text{Br}$) efficiently catalyzed the semi-hydrogenation of diverse alkynes to deliver highly chemo-selective and stereo-divergent (*Z*)-alkenes at room temperature. This hydrogenation exhibited broad substrate scope with the tolerance of sensitive functional groups, such as $-\text{Cl}$, $-\text{Br}$, $-\text{I}$, $-\text{OH}$, $-\text{NH}_2$, $-\text{COOMe}$, and pyridinyl, employing a stable and user-friendly ammonia borane hydrogen source. The anionic non-pincer cobalt complex found to be active for isomerization of (*Z*)- to (*E*)- alkene at 60 °C. Furthermore, the mechanistic studies put forward the crucial role of amide N–H of ligand backbone at room temperature activation of non-pincer cobalt catalyst.

In Chapter 3, the room temperature transfer hydrogenation of nitriles to symmetrical secondary amines using $\text{H}_3\text{N-BH}_3$ as a hydrogen source and a ‘User-Friendly’ (xantphos) CoCl_2 catalyst has been discussed. The optimized mild reaction parameters were reliable with different functional groups like $-\text{F}$, $-\text{Cl}$, $-\text{Br}$, $-\text{I}$, $-\text{CH}_2\text{OH}$, $-\text{COOMe}$, and thiophenyl. Similarly, the unsymmetrical secondary amines were obtained by adding an external amine source using cheaper, i. e., $\text{Me}_2\text{NH-BH}_3$. An excellent substrate scope with various functional group tolerance has been observed under the optimized reaction protocol. The synthetic utility is shown by carrying out the reaction at a gram scale with 82% isolated yield. At the same line, Chapter 4 describes the catalytic hydrogenation of nitrile to secondary amines and imines. In this context, the CoBr_2 (5 mol%) and 15 mol% ammonia-borane as an additive catalyzes the hydrogenation of nitriles into secondary imines. This reaction needs 15 bar hydrogen pressure for the transformation mentioned above. In contrast, when CoCl_2 was replaced with CoBr_2 , a change in product selectivity was observed and the secondary amines

formed as significant product. Thus, the catalytic amount of CoCl_2 with ammonia-borane (12 mol%) carries out the hydrogenation of nitriles to secondary amines at 20 bar hydrogen pressure. The reaction protocol seems tolerable with distinct functional groups like synthetically important $-\text{F}$, $-\text{Cl}$, $-\text{Br}$, $-\text{CF}_3$, $-\text{OMe}$ and gave moderate to good yield for the respective secondary amine. Interestingly, an ester moiety remained intact during the course of reaction and regio-selectively nitrile hydrogenation was observed.

In chapter 5, the chemo-selective transfer hydrogenation of $\text{C}=\text{C}$ of chalcones is presented. The phosphine-based $\text{Mn}(\text{I})$ and $\text{Mn}(\text{II})$ pincer complexes are synthesized to carry out this transformation. The newly synthesized complexes were characterized by elemental analysis as well as X-ray crystallography. These complexes have an acidic $\text{N}-\text{H}$ at the ligand backbone, which may help in metal-ligand cooperation (MLC) for catalysis. Among the newly synthesized complexes, $\text{Mn}(\text{II})$ complex are found to be catalytically inactive, whereas $\text{Mn}(\text{I})$ catalyse the transfer hydrogenation of chalcones under mild conditions. Thus, $\text{Mn}(\text{I})$ selectively hydrogenates $\text{C}=\text{C}$ bond of chalcone at room temperature using ammonia-borane as a hydrogen source. Interestingly, the reaction works with the only half equivalent of ammonia-borane. A range of functional groups such as $-\text{F}$, $-\text{Cl}$, $-\text{Br}$, $-\text{CF}_3$, $-\text{NO}_2$, $-\text{OMe}$, alkyl, and heterocycles like thiophene, pyrrole, furan, indoles endure the reaction condition and provided respective reduced saturated ketones in high yields. Surprisingly, the trisubstituted $\text{C}=\text{C}$ of chalcone didn't show any conversion into a reduced product. In addition, the isolated alkenes and alkynes also remained unaffected under the optimized reaction condition.

1.6 REFERENCES

- (1) L. Cervený, Catalytic Hydrogenation; *Elsevier: Amsterdam* **1986**.
- (2) K. Weissermel, H. J. A., Industrial Organic Chemistry, *Wiley-VCH,; Weinheim*. **2003**.
- (3) J. G. de Vries, E., C. J., Eds. *Wiley-VCH: Weinheim* **2007**.
- (4) P. G. Andersson, I. J. M. *Wiley-VCH Verlag GmbH & Co. KGaA: 2008*.
- (5) Ram, S.; Ehrenkaufner, R. E. *Tetrahed. Lett.* **1984**, *25*, 3415-3418.
- (6) Dubuis, H. L. a. R. *Org. Synth.* **1966**, *46*, 89.
- (7) Johnstone, R. A. W.; Wilby, A. H.; Entwistle, I. D. *Chem. Rev.* **1985**, *85*, 129-170.
- (8) Widegren, J. A.; Finke, R. G. *Journal of Molecular Catalysis A: Chemical* **2003**, *198*, 317-341.
- (9) E. Farnetti, R. D. M., J. Kašpar *Vol II: Homogeneous and Heterogeneous Catalysis*, 50–86.
- (10) Harmon, R. E.; Gupta, S. K.; Brown, D. J. *Chemical Reviews* **1973**, *73*, 21-52.
- (11) Filonenko, G. A.; van Putten, R.; Hensen, E. J. M.; Pidko, E. A. *Chem. Soc. Rev.* **2018**, *47*, 1459-1483.
- (12) Wang, D.; Astruc, D. *Chem. Rev.* **2015**, *115*, 6621-6686.
- (13) McPartlin, M.; Mason, R. *Chem. Commun.* **1967**, 545-546.
- (14) Trocha-Grimshaw, J.; Henbest, H. B. *Chem. Commun.* **1967**, 544-544.
- (15) Ananikov, V. P. *ACS Catal.* **2015**, *5*, 1964-1971.
- (16) Allen, S. E.; Walvoord, R. R.; Padilla-Salinas, R.; Kozłowski, M. C. *Chem. Rev.* **2013**, *113*, 6234-6458.
- (17) Werkmeister, S.; Junge, K.; Beller, M. *Org. Process Res. Dev.* **2014**, *18*, 289-302.
- (18) Alig, L.; Fritz, M.; Schneider, S. *Chem. Rev.* **2019**, *119*, 2681-2751.
- (19) Liu, W.; Sahoo, B.; Junge, K.; Beller, M. *Acc. Chem. Res.* **2018**, *51*, 1858-1869.
- (20) Fouche, M.; Rooney, L.; Barrett, A. G. M. *J. Org. Chem.* **2012**, *77*, 3060-3070.
- (21) Adams, J. P. *J. Chem. Soc., Perkin Trans.* **2000**, *1*, 125-139.
- (22) A. Haskel, E. K. *Handbook of Organopalladium Chemistry (Eds.: E.-i. Negishi, A. de Meijere)*, Wiley, New York **2002**, 2.
- (23) Dupau, P. (Eds: M. Beller, H.-U. Blaser), Springer, Heidelberg **2012**, 47.
- (24) L. Mathiesen, K. E. M., M. S. Nenseter, R. B. Sund *Pharmacol. Toxicol* **1996**, *78*, 143.
- (25) T. Langer, M. E., R. D. Hoffmann, P. Chiba, G. F. Ecker *Arch. Pharm* **2004**, 337.

-
- (26) S. Cheenpracha, C. K., C. Ponglimanont, S. Subhadhir-asakul, S. Tewtrakul *Bioorg. Med. Chem.* **2006**, *14*, 1710.
- (27) D. J. Lowes, W. A. G., M. C. Connelly, F. Zhu, M. S. Sigal, J. A. Clark, A. S. Lemoff, J. L. Derisi, E. B. Wilson, R. K. Guy *J. Med. Chem.* **2011**, *54*, 7477.
- (28) Oger, C.; Balas, L.; Durand, T.; Galano, J.-M. *Chem. Rev.* **2013**, *113*, 1313-1350.
- (29) Semenov, V. V.; Kiselyov, A. S.; Titov, I. Y.; Sagamanova, I. K.; Ikizalp, N. N.; Chernysheva, N. B.; Tsyganov, D. V.; Konyushkin, L. D.; Firgang, S. I.; Semenov, R. V.; Karmanova, I. B.; Raihstat, M. M.; Semenova, M. N. *J. Nat. Prod.* **2010**, *73*, 1796-1802.
- (30) Tron, G. C.; Pirali, T.; Sorba, G.; Pagliai, F.; Busacca, S.; Genazzani, A. A. *J. Med. Chem.* **2006**, *49*, 3033-3044.
- (31) Nicolaou, K. C.; Daines, R. A.; Chakraborty, T. K.; Ogawa, Y. *J. Am. Chem. Soc.* **1987**, *109*, 2821-2822.
- (32) Odinkov, V. N. *Chem. Nat. Compd.* **2000**, *36*, 11-39.
- (33) Leutzsch, M.; Wolf, L. M.; Gupta, P.; Fuchs, M.; Thiel, W.; Farès, C.; Fürstner, A. *Angew. Chem. Int. Ed.* **2015**, *54*, 12431-12436.
- (34) Yang, J.; Wang, C.; Sun, Y.; Man, X.; Li, J.; Sun, F. *Chem. Commun.* **2019**, *55*, 1903-1906.
- (35) Tani, K. e.; Iseki, A.; Yamagata, T. *Chem. Commun.* **1999**, 1821-1822.
- (36) Vasilikogiannaki, E.; Titilas, I.; Vassilikogiannakis, G.; Stratakis, M. *Chem. Commun.* **2015**, *51*, 2384-2387.
- (37) Karunananda, M. K.; Mankad, N. P. *J. Am. Chem. Soc.* **2015**, *137*, 14598-14601.
- (38) Maji, B.; Barman, M. K. *Synthesis* **2017**, *49*, 3377-3393.
- (39) Garbe, M.; Budweg, S.; Papa, V.; Wei, Z.; Hornke, H.; Bachmann, S.; Scalone, M.; Spannenberg, A.; Jiao, H.; Junge, K.; Beller, M. *Catal. Sci. Technol.* **2020**, *10*, 3994-4001.
- (40) Zubar, V.; Sklyaruk, J.; Brzozowska, A.; Rueping, M. *Org. Lett.* **2020**, *22*, 5423-5428.
- (41) Farrar-Tobar, R. A.; Weber, S.; Csendes, Z.; Ammaturo, A.; Fleissner, S.; Hoffmann, H.; Veiros, L. F.; Kirchner, K. *ACS Catal.* **2022**, *12*, 2253-2260.
- (42) Brzozowska, A.; Azofra, L. M.; Zubar, V.; Atodiresei, I.; Cavallo, L.; Rueping, M.; El-Sepelgy, O. *ACS Catal.* **2018**, *8*, 4103-4109.
- (43) Zhou, Y.-P.; Mo, Z.; Luecke, M.-P.; Driess, M. *Chem. Eur. J.* **2018**, *24*, 4780-4784.
-

-
- (44) Sklyaruk, J.; Zubar, V.; Borghs, J. C.; Rueping, M. *Org. Lett.* **2020**, *22*, 6067-6071.
- (45) Torres-Calis, A.; Garcia, J. J. *Catal. Sci. Technol.* **2022**, *12*, 3004-3015.
- (46) Bianchini, C.; Meli, A.; Peruzzini, M.; Vizza, F.; Zanobini, F.; Frediani, P. *Organometallics* **1989**, *8*, 2080-2082.
- (47) Enthaler, S.; Haberberger, M.; Irran, E. *Chem. Asian. J.* **2011**, *6*, 1613-1623.
- (48) Haberberger, M.; Irran, E.; Enthaler, S. *Eur. J. Inorg. Chem.* **2011**, *2011*, 2797-2802.
- (49) Belger, C.; Plietker, B. *Chem. Commun.* **2012**, *48*, 5419-5421.
- (50) Johnson, C.; Albrecht, M. *Catal. Sci. Technol.* **2018**, *8*, 2779-2783.
- (51) Srimani, D.; Diskin-Posner, Y.; Ben-David, Y.; Milstein, D. *Angew. Chem. Int. Ed.* **2013**, *52*, 14131-14134.
- (52) Gorgas, N.; Brünig, J.; Stöger, B.; Vanicek, S.; Tilset, M.; Veiros, L. F.; Kirchner, K. *J. Am. Chem. Soc.* **2019**, *141*, 17452-17458.
- (53) Tokmic, K.; Fout, A. R. *J. Am. Chem. Soc.* **2016**, *138*, 13700-13705.
- (54) Chen, C.; Huang, Y.; Zhang, Z.; Dong, X.-Q.; Zhang, X. *Chem. Commun.* **2017**, *53*, 4612-4615.
- (55) Fu, S.; Chen, N.-Y.; Liu, X.; Shao, Z.; Luo, S.-P.; Liu, Q. *J. Am. Chem. Soc.* **2016**, *138*, 8588-8594.
- (56) Landge, V. G.; Pitchaimani, J.; Midya, S. P.; Subaramanian, M.; Madhu, V.; Balaraman, E. *Catal. Sci. Technol.* **2018**, *8*, 428-433.
- (57) Chen, K.; Zhu, H. n.; Li, Y.; Peng, Q.; Guo, Y.; Wang, X. *ACS Catal.* **2021**, *11*, 13696-13705.
- (58) Decker, D.; Wei, Z.; Rabeah, J.; Drexler, H.-J.; Bruckner, A.; Jiao, H.; Beweries, T. *Inorg. Chem. Front.* **2022**, *9*, 761-770.
- (59) Brown, C. A.; Ahuja, V. K. *J. Chem. Soc., Chem. Commun.* **1973**, 553-554.
- (60) Barrios-Francisco, R.; Garcia, J. J. *Appl. Catal. A* **2010**, *385*, 108-113.
- (61) Richmond, E.; Moran, J. *J. Org. Chem.* **2015**, *80*, 6922-6929.
- (62) Thiel, N. O.; Kaewmee, B.; Tran Ngoc, T.; Teichert, J. F. *Chem. Eur. J.* **2020**, *26*, 1597-1603.
- (63) Ramirez, B. L.; Lu, C. C. *J. Am. Chem. Soc.* **2020**, *142*, 5396-5407.
- (64) Hale, D. J.; Ferguson, M. J.; Turculet, L. *ACS Catal.* **2022**, *12*, 146-155.
- (65) Semba, K.; Kameyama, R.; Nakao, Y. *Synlett* **2015**, *26*, 318-322.
- (66) Pape, F.; Thiel, N. O.; Teichert, J. F. *Chem. Eur. J.* **2015**, *21*, 15934-15938.
-

-
- (67) Thiel, N. O.; Teichert, J. F. *Org. Biomol. Chem.* **2016**, *14*, 10660-10666.
- (68) Wakamatsu, T.; Nagao, K.; Ohmiya, H.; Sawamura, M. *Organometallics* **2016**, *35*, 1354-1357.
- (69) Korytiakova, E.; Thiel, N. O.; Pape, F.; Teichert, J. F. *Chem. Commun.* **2017**, *53*, 732-735.
- (70) Kusy, R.; Grela, K. *Green Chem.* **2021**, *23*, 5494-5502.
- (71) Buchwald, S.; Mauger, C.; Mignani, G.; Scholz, U. *Adv. Synth. Catal.* **2006**, *348*, 23-39.
- (72) Rossi, A.; Barraco, A.; Donda, P. *Ann. Gen. Hosp. Psychiatry* **2004**, *3*, 2.
- (73) Lavorini, F.; Geri, P.; Mariani, L.; Marmai, C.; Maluccio, N. M.; Pistolesi, M.; Fontana, G. A. *Br. J. Clin. Pharmacol.* **2006**, *62*, 403-411.
- (74) Subedi, M.; Bajaj, S.; Kumar, M. S.; Yc, M. *Biomed. Pharmacother.* **2019**, *111*, 443-451.
- (75) Radosevich, A. T.; Melnick, J. G.; Stoian, S. A.; Bacciu, D.; Chen, C.-H.; Foxman, B. M.; Ozerov, O. V.; Nocera, D. G. *Inorg. Chem.* **2009**, *48*, 9214-9221.
- (76) Tondreau, A. M.; Boncella, J. M. *Polyhedron* **2016**, *116*, 96-104.
- (77) Elangovan, S.; Topf, C.; Fischer, S.; Jiao, H.; Spannenberg, A.; Baumann, W.; Ludwig, R.; Junge, K.; Beller, M. *J. Am. Chem. Soc.* **2016**, *138*, 8809-8814.
- (78) Weber, S.; Stoger, B.; Kirchner, K. *Org. Lett.* **2018**, *20*, 7212-7215.
- (79) Weber, S.; Veiros, L. F.; Kirchner, K. *Adv. Synth. Catal.* **2019**, *361*, 5412-5420.
- (80) Garduño, J. A.; García, J. J. *ACS Catal.* **2019**, *9*, 392-401.
- (81) Garduño, J. A.; Flores-Alamo, M.; García, J. J. *ChemCatChem* **2019**, *11*, 5330-5338.
- (82) Sarkar, K.; Das, K.; Kundu, A.; Adhikari, D.; Maji, B. *ACS Catal.* **2021**, *11*, 2786-2794.
- (83) Bornschein, C.; Werkmeister, S.; Wendt, B.; Jiao, H.; Alberico, E.; Baumann, W.; Junge, H.; Junge, K.; Beller, M. *Nat. Comm.* **2014**, *5*, 4111-4121.
- (84) Langer, R.; Iron, M. A.; Konstantinovski, L.; Diskin-Posner, Y.; Leitus, G.; Ben-David, Y.; Milstein, D. *Chem. Eur. J.* **2012**, *18*, 7196-7209.
- (85) Chakraborty, S.; Leitus, G.; Milstein, D. *Chem. Commun.* **2016**, *52*, 1812-1815.
- (86) Chakraborty, S.; Leitus, G.; Milstein, D. *Angew. Chem. Int. Ed* **2017**, *56*, 2074-2078.
- (87) Chakraborty, S.; Milstein, D. *ACS Catal.* **2017**, *7*, 3968-3972.
-

-
- (88) Mukherjee, A.; Srimani, D.; Chakraborty, S.; Ben-David, Y.; Milstein, D. *J. Am. Chem. Soc.* **2016**, *137*, 8888-8891.
- (89) Adam, R.; Bheeter, C. B.; Cabrero-Antonino, J. R.; Junge, K.; Jackstell, R.; Beller, M. *ChemSusChem* **2017**, *10*, 842-846.
- (90) Tokmic, K.; Jackson, B. J.; Salazar, A.; Woods, T. J.; Fout, A. R. *J. Am. Chem. Soc.* **2017**, *139*, 13554-13561.
- (91) Dai, H.; Guan, H. *ACS Catal.* **2018**, *8*, 9125-9130.
- (92) Schneekonig, J.; Tannert, B.; Hornke, H.; Beller, M.; Junge, K. *Catal. Sci. Technol.* **2019**, *9*, 1779-1783.
- (93) Benito-Garagorri, D.; Becker, E.; Wiedermann, J.; Lackner, W.; Pollak, M.; Mereiter, K.; Kisala, J.; Kirchner, K. *Organometallics* **2006**, *25*, 1900-1913.
- (94) Li, H.; Al-Dakhil, A.; Lupp, D.; Gholap, S. S.; Lai, Z.; Liang, L.; Huang, K.-W. *Org. Lett.* **2018**, *20*, 6430-6435.
- (95) Shao, Z.; Fu, S.; Wei, M.; Zhou, S.; Liu, Q. *Angew. Chem. Int. Ed.* **2016**, *55*, 14653-14657.
- (96) Zerecero-Silva, P.; Jimenez-Solar, I.; Crestani, M. G.; Arevalo, A.; Barrios-Francisco, R.; Garcia, J. J. *Appl. Catal. A* **2009**, *363*, 230-234.
- (97) Garduño, J. A.; García, J. J. *ACS Omega* **2017**, *2*, 2337-2343.
- (98) Vermaak, V.; Vosloo, H. C. M.; Swarts, A. J. *Mol. Catal.* **2021**, *511*, 111738.
- (99) van der Waals, D.; Pettman, A.; Williams, J. M. J. *RSC Adv.* **2014**, *4*, 51845-51849.
- (100) Song, H.; Xiao, Y.; Zhang, Z.; Xiong, W.; Wang, R.; Guo, L.; Zhou, T. *J. Org. Chem.* **2022**, *87*, 790-800.
- (101) Wei, D.; Bruneau-Voisine, A.; Chauvin, T.; Dorcet, V.; Roisnel, T.; Valyaev, D. A.; Lugan, N.; Sortais, J.-B. *Adv. Synth. Catal.* **2017**, *360*, 676-681.
- (102) Vielhaber, T.; Topf, C. *Appl. Catal. A-Gen.* **2021**, *623*, 118280.
- (103) Weber, S.; Brünig, J.; Veiros, L. F.; Kirchner, K. *Organometallics* **2021**, *40*, 1388-1394.
- (104) Vigneswaran, V.; MacMillan, S. N.; Lacy, D. C. *Organometallics* **2019**, *38*, 4387-4391.
- (105) Lator, A.; Gaillard, S.; Poater, A.; Renaud, J.-L. *Chem. Eur. J.* **2018**, *24*, 5770-5774.
- (106) Wei, Z.; Wang, Y.; Li, Y.; Ferraccioli, R.; Liu, Q. *Organometallics* **2020**, *39*, 3082-3087.

- (107) Jiang, B.-L.; Ma, S.-S.; Wang, M.-L.; Liu, D.-S.; Xu, B.-H.; Zhang, S.-J. *ChemCatChem* **2019**, *11*, 1701-1706.
- (108) Beltran, F.; Bergamaschi, E.; Funes-Ardoiz, I.; Teskey, C. J. *Angew. Chem. Int. Ed.* **2020**, *59*, 21176-21182.
- (109) Li, X.; Wu, X.; Tang, L.; Xie, F.; Zhang, W. *Chem. Asian J.* **2019**, *14*, 3835-3839.
- (110) Alonso, F.; Osante, I.; Yus, M. *ChemInform* **2007**, *38*.
- (111) Mahoney, W. S.; Stryker, J. M. *J. Am. Chem. Soc.* **1989**, *111*, 8818-8823.
- (112) Chen, J.-X.; Daeuble, J. F.; Brestensky, D. M.; Stryker, J. M. *Tetrahedron* **2000**, *56*, 2153-2166.

Chapter 2

Room Temperature (Z)-Selective Transfer Hydrogenation of Alkynes by NNN-Cobalt Catalyst

This chapter has been partly adapted from the publication "Room temperature (Z)-selective hydrogenation of alkynes by hemilabile and non-innocent (NNN)Co(II) catalyst" **Sharma, D. M.**; Gouda, C.; Gonnade, R.; and Punji, B. *Catal. Sci. Technol.*, **2022**, *12*, 1843–1849.

2.1 INTRODUCTION

Stereo-defined alkenes represent a dominant functionality in various synthetic transformations and polyfunctionalized bioactive compounds.¹ Such stereo-selective alkenes play a pivotal role in governing the peculiar characteristics of certain drugs and biomolecules, like in Combretastatin A4,^{2,3} Cruentaren B,⁴ Amphotericin,⁵ and *Lepidoptera* pheromones.⁶ Among the various routes of alkene synthesis,^{7,8} the selective hydrogenation of alkynes is considered the finest approach to achieve the olefins of interest.^{9,10} However, controlling the stereo-selectivity of resulting olefin and over-hydrogenation to alkane are the major concerns in regards to alkyne hydrogenation. Overcoming these challenges, in the last few decades, various noble metal catalysts based on ruthenium,¹¹⁻¹³ palladium,¹⁴⁻¹⁶ and iridium,¹⁷⁻¹⁹ are exploited for the catalytic hydrogenation of alkynes to get desired reduced olefins with specific stereochemistry.²⁰ Particularly, in recent years, naturally abundant and less bio-toxic 3d late transition metal complexes of Mn,²¹⁻²⁴ Fe,²⁵ Ni,^{26,27} and Cu²⁸⁻³² are substantially investigated as catalysts for the hydrogenation of alkynes with promising activity and selectivity.³³

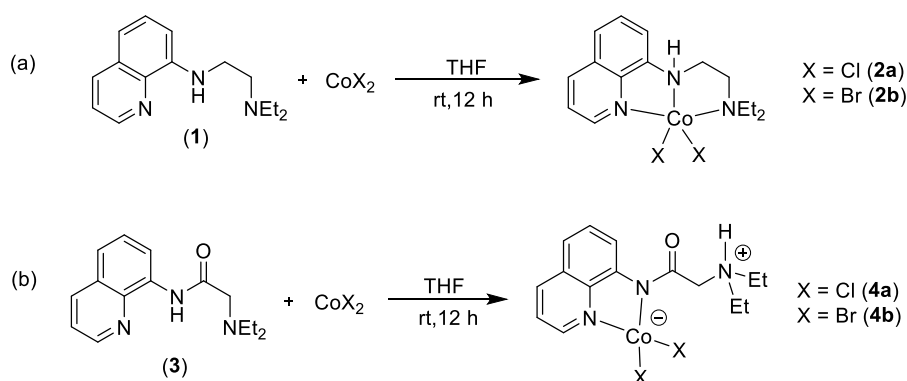
Cobalt, being one of the earth-abundant transition metals with biological significance, has substantially been explored for the hydrogenation of various unsaturated functional groups.³⁴⁻³⁶ In particular, the cobalt-catalyzed semi-hydrogenation of internal alkynes to (*E*) or (*Z*)-selective alkenes using molecular hydrogen is independently demonstrated by Fout, Zhang and Dong.³⁷⁻⁴⁰ Considering the ease of transfer hydrogenation - without being requirement of a special experimental setup, Luo and Liu demonstrated (PNP)Co(II) complexes for the semi-hydrogenation of alkynes to (*Z*)- or (*E*)-alkenes using NH₃-BH₃ as hydrogen source.^{41,42} Similarly, Balaraman, Zhou and Fan reported cobalt-catalyzed selective hydrogenation of alkynes to (*Z*)-alkenes using NH₃-BH₃ and H₂O as a hydrogen source, respectively.^{43,44} Though all these protocols efficiently provided the (*Z*)-selective alkenes from alkynes, an elevated temperature of 60-80 °C is essential and/or uses a phosphine-based ligand, whose synthesis involves a tedious multi-step process and an inert atmosphere. Therefore, developing a phosphine-free, nitrogen-ligated cobalt complex that can perform stereo-selective hydrogenation at room temperature without requiring a special experimental setup would be an ideal and user-friendly approach. With this intention, we hypothesized to develop nitrogen-based ligand with a dangling arm and acidic apical N-H that can show hemi-labile and non-innocent behaviour during the catalysis. Such a metal-bound ligand can provide suitable electronic features and vacant coordination sites for the incoming substrate

and could activate the same *via* a unified mode of action. Thus, towards our goal to explore sustainable 3d metal catalysis for hydrogenation, in this chapter, we demonstrate the development of a set of phosphine-free and air-stable, 8-aminoquinoliny-based (NNN) ligands and their coordination behaviour. Depending on the ligand backbones, both the pincer and non-pincer cobalt(II) complexes were obtained, and the non-pincer complex was found to be an efficient catalyst for the selective hydrogenation of alkyne derivatives at room temperature.

2.2 RESULTS AND DISCUSSION

2.2.1 Synthesis and Characterization of Cobalt Catalysts

We have prepared a quinoliny-amine ligand ($C_9H_6N(NH)CH_2CH_2NEt_2$) [${}^QNNN^{CH_2NEt_2}-H$; **1**] and quinoliny-amide ligand, 2-(diethylamino)-*N*-(quinolin-8-yl)acetamide, (${}^QNNN^{C(O)NEt_2}-H$) (**3**) following the previously described protocol.⁴⁵⁻⁴⁷ We intended to investigate the reactivity of ligands **1** and **3** with cobalt to understand the coordinating reactivity and catalytic activity for hydrogenation reaction. Thus, the reaction of ligand **1** with $CoCl_2$ and $CoBr_2$ at room temperature afforded the expected pincer complexes (${}^QNNN^{CH_2NEt_2}$) $CoCl_2$ (**2a**) and (${}^QNNN^{CH_2NEt_2}$) $CoBr_2$ (**2b**), respectively as purple compounds (Scheme 2.1a). Both the compounds are NMR inactive, and thus, the chemical composition is determined by elemental analysis. Moreover, the molecular structure of complex **2a** was determined by X-ray analysis, wherein the *NNN*-ligand coordinated in a tridentate fashion resulting in the distorted trigonal bipyramidal (TBP) geometry around the Co(II) center (Figure 2.1). In the structure of **2a**, the quinoliny *N2*, amine *N3* and one Cl(1) ligands are in planner position with the average bond angle between them is 118.01° , whereas the central N1 and Cl(2) are in axial position with the N(1)–Co(1)–Cl(2) bond angle close to straight angle ($172.55(8)^\circ$) (Table 2.1).



Scheme 2.1 Synthesis of cobalt complexes.

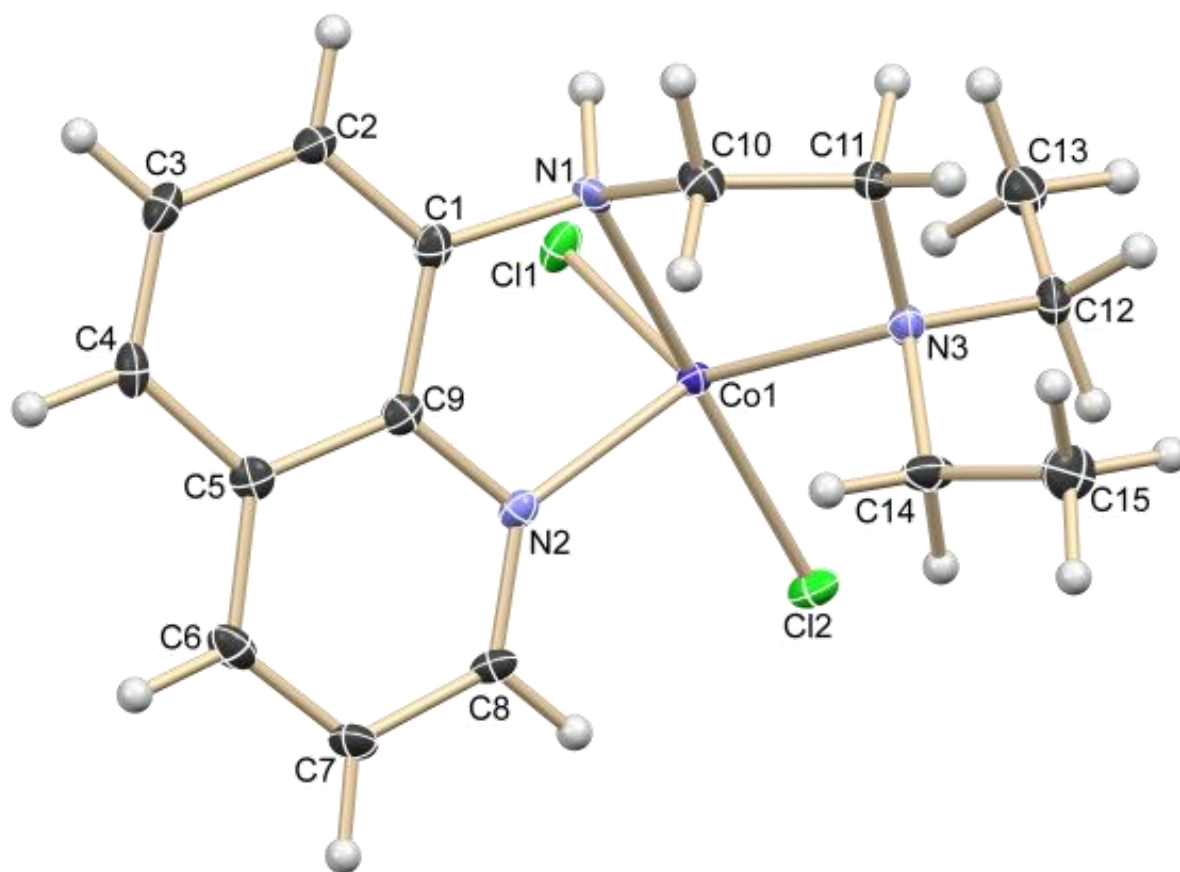


Figure 2.1 Thermal ellipsoid plot of **2a**.

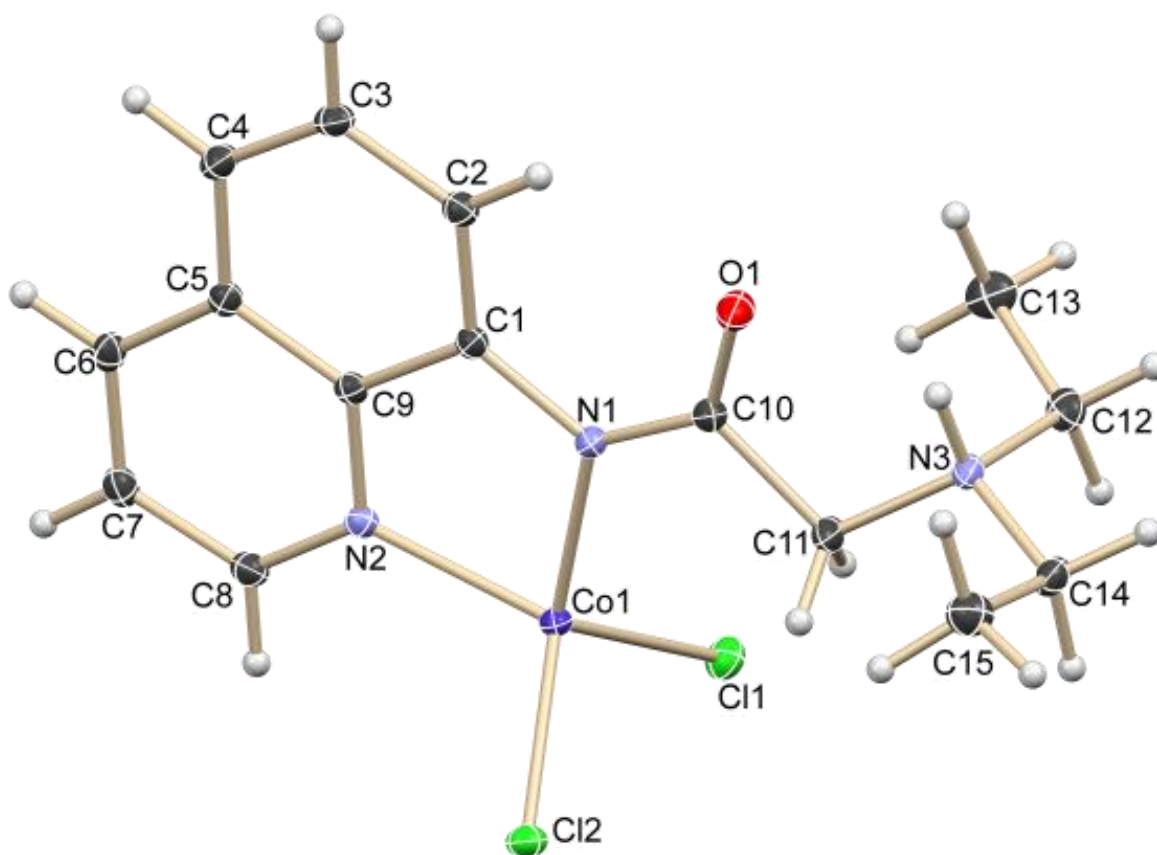


Figure 2.2. Thermal ellipsoid plot of **4a**.

Interestingly, the reaction of ligand (QNNNC(O)NEt₂)–H (**3**)⁴⁵ with CoCl₂ and CoBr₂ provided (QNN)-chelate complexes **4a** and **4b** in 94% and 95% yields, respectively (Scheme 2.1b). Both the complexes are air-stable and can be stored at room temperature for months. The chemical composition of both the complexes was verified by elemental analysis. The X-ray structural analysis of complex **4a** revealed the bidentate chelate coordination of ligand **3** to CoCl₂ with the amine nitrogen (N3) remained uncoordinated (Figure 2.2). Interestingly, the hydrogen atom of N(1)–H migrated to N(3), thus making it an anionic Co(II) complex with the N(1)–Co(1) bond length 1.9982(10) Å. The geometry around the cobalt is distorted tetrahedral, and that of the N(1) center is almost planar. We assume that the ligand **3** might initially form a tri-coordinated pincer complex (similar to that found with **1**), and later the hemi-labile arm –NEt₂ de-coordinates from cobalt upon abstracting an acidic N(1)–H. One can expect more hemi-lability with ligand **3** (for complex **4a**) than with ligand **1** (for complex **2a**) because of the more flexible and wider N(1)–C(10)–C(11) bond angle (planar) in the former. The covalent bonding character of N(1)–Co(1) in complex **4a** could make it more

electron-rich, whereas the tetra-ligation would give significant unsaturation for further reactivity.

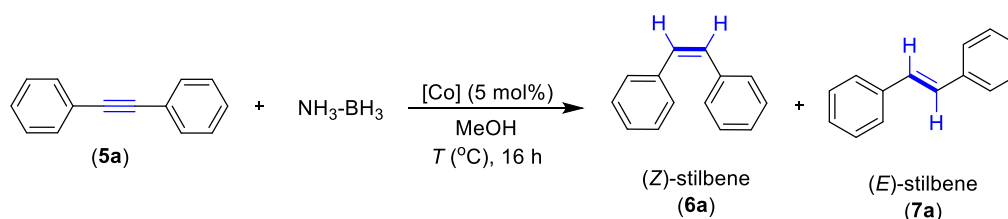
Table 2.1 Selected bond lengths (Å) and bond angles (°) for **2a** and **4a**

Bond length (Å)		Bond angles (°)	
Complex 2a			
Co(1)–N(1)	2.201(3)	N(1)–Co(1)–N(2)	77.49(11)
Co(1)–N(2)	2.099(3)	N(3)–Co(1)–N(1)	80.67(11)
Co(1)–N(3)	2.163(3)	N(1)–Co(1)–Cl(1)	86.91(8)
Co(1)–Cl(1)	2.3922(6)	N(1)–Co(1)–Cl(2)	172.55(8)
Co(1)–Cl(2)	2.3103(10)	C(1)–N(1)–C(10)	112.1(3)
N(1)–H(1)	1.0	C(10)–N(1)–Co(1)	107.6(2)
		N(1)–C(10)–Cl(1)	108.1(3)
Complex 4a			
Co(1)–N(1)	1.9982(10)	N(1)–Co(1)–N(2)	83.09(4)
Co(1)–N(2)	2.0269(10)	N(1)–Co(1)–Cl(1)	113.99(3)
Co(1)–Cl(1)	2.2658(3)	N(1)–Co(1)–Cl(2)	120.46(3)
O(1)–C(10)	1.2384(14)	Cl(2)–Co(1)–Cl(1)	105.331(12)
N(3)–H(1)	0.896(18)	C(1)–N(1)–C(10)	121.29(9)
		C(10)–N(1)–Co(1)	126.01(8)
		N(1)–C(10)–Cl(1)	113.68(10)

2.2.2 Optimization of Reaction Condition for Hydrogenation of Alkynes

After the synthesis and characterization of the pincer complexes **2a,b** and non-pincer complexes **4a,b**; we investigated their catalytic activity for the selective transfer hydrogenation of internal alkyne to an alkene. Thus, in a typical reaction, diphenyl acetylene (**5a**; 1.0 equiv) was chosen as a model substrate with ammonia-borane as hydrogen source (1.0 equiv), and cobalt catalyst (5 mol%) was used in MeOH (Table 2.2). At first, the use of both the pincer catalysts **2a,b** and non-pincer catalysts **4a,b** showed comparable activity at 65 °C with around 85% selectivity for the (*Z*)-stilbene **6a** (entries 1-4). The employment of less expensive dimethylammonia-borane (Me₂NH-BH₃) as a hydrogen source is less effective with **2a**, whereas quantitative hydrogenation was achieved in the presence of catalyst **4a** (entries 5 & 6). Interestingly, the hydrogenation at 27 °C employing catalyst **2a** or **2b** led to low conversion; however, the reaction with non-pincer catalyst **4a** retained the reactivity and provided 87% yield of (*Z*)-alkene **6a** (entries 7-9). The employment of analogous catalyst **4b**

showed slightly more selectivity for (*Z*)-alkene (91%) with complete hydrogenation (entry 10). Notably, the reduction in loading of catalyst **4b** from 5 mol% to 2 mol% provided gratifyingly more selectivity for (*Z*)-stilbene with up to 94% conversion (89% yield) (entry 11). Further lowering in catalyst loading led to a decrease in overall conversion (entry 12). The use of other protic (EtOH, ⁱPrOH) or aprotic (THF, toluene) solvents in place of MeOH led to a drastic reduction in hydrogenation (entries 14-17). The employment of simple CoCl₂, CoBr₂ or Co(OAc)₂ salts or the pincer complexes **2a** and **2b** as catalysts at 27 °C provided low to the moderate yield of hydrogenated product **6a** (entries 18-22). All these studies suggest the importance of ligand backbone in non-pincer complexes **4a,b** with regards to the flexibility and hemi-lability of dangling *N*-arm that might provide a vacant coordination sphere to the incoming substrate and stabilize the active cobalt species.

Table 2.2 Optimization of the reaction conditions for hydrogenation of alkyne^a

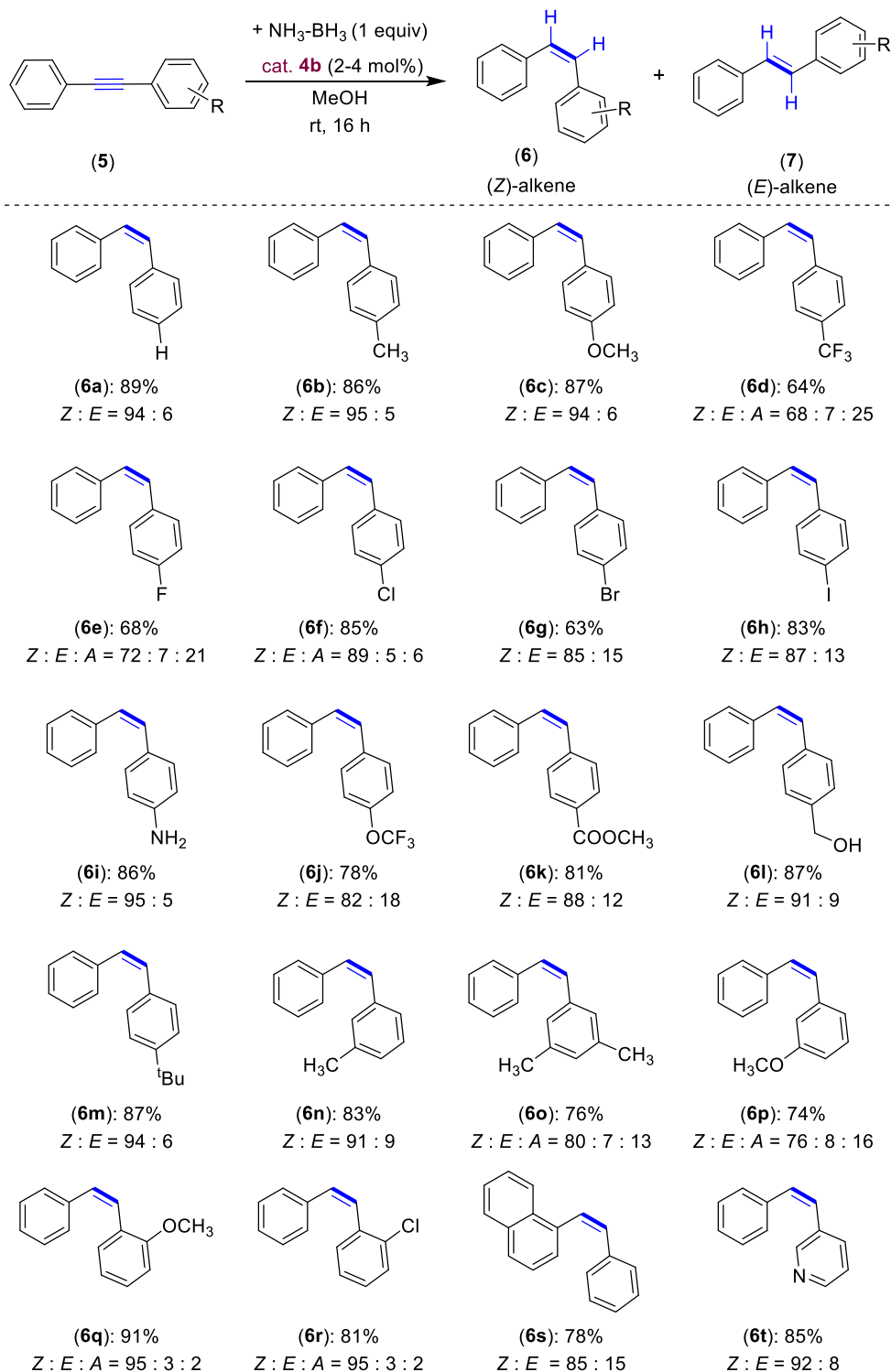
Entry	[Co]	T ($^\circ\text{C}$)	GC Conv	6a (%)	7a (%)
1	2a	65	100	85	14
2	2b	65	100	88	12
3	4a	65	100	87	13
4	4b	65	100	84	16
5 ^b	2a	65	75	61	14
6 ^b	4a	65	100	81	19
7	2a	27	55	48	7
8	2b	27	61	45	16
9	4a	27	100	87	7
10	4b	27	100	91	8
11^c	4b	27	100	94 (89%)^d	6
12 ^e	4b	27	81	73	7
13 ^{b,c}	4b	27	35	24	11
14 ^{c,f}	4b	27	24	18	6
15 ^{c,g}	4b	27	54	50	4
16 ^{c,h}	4b	27	38	31	7
17 ^{c,i}	4b	27	65	42	8
18 ^c	CoCl_2	27	15	12	3
19 ^c	CoBr_2	27	56	47	9
20	Co(OAc)_2	27	52	45	5
21 ^c	2a	27	23	18	4
22 ^c	2b	27	21	17	4

^aReaction conditions: Diphenyl acetylene (**5a**) (0.051 g, 0.50 mmol), $[\text{H}_2]$ -source (0.50 mmol), solvent (1.5 mL). ^b $\text{Me}_2\text{NH-BH}_3$ was used as a hydrogen source. ^c2 mol% loading of catalyst. ^dIsolated yield. ^e1 mol% loading of **4b**. ^fEtOH as solvent. ^giPrOH as solvent. ^hTHF as solvent. ⁱToluene as solvent.

2.2.3 Scope for Synthesis of (Z)-Alkenes

With the optimized reaction conditions in hand, we investigated substrate scope to synthesize (Z)-alkenes using 2 - 4 mol% of catalyst **4b**, ammonia-borane (1 equiv) at room temperature (Scheme 2.2). The biaryl alkynes with various substitutions at the *para*-position tolerated the reaction conditions to give respective (Z)-alkenes with high selectivity. The electron-donating groups on alkynes like methyl and methoxy showed very good selectivity for (Z)-alkene and yielded the respective compounds in 86% and 87% yields. The selectivity for (Z)-alkene was reduced when an electron-withdrawing group was attached to the *para*-position of the aryl-alkyne, i.e. $-\text{CF}_3$ and $-\text{F}$ groups (**6d,e**). Notably, a substantial amount of complete hydrogenation of alkynes to alkanes was observed for these substrates. The hydrogenation reaction could tolerate various halide substituents, i.e. chloro, bromo and iodo, affording the desired (Z)-alkenes **6f-h** in excellent yields. The tolerability of such functionalities is very important from the synthetic perspective as they can be used for further derivatization. The free amine and ester functional groups remained unaffected during the reaction and provided semi-hydrogenated (Z)-alkenes **6i** and **6k** in 86% and 81% yields, respectively. The chemo-selectivity of the catalyst for the alkyne hydrogenation over the ester group is noteworthy. Moreover, the benzylic alcohol functionality was tolerated well and gave 87% of **6l**. The alkynes with a $-\text{OCF}_3$ group or a bulky $-\text{tBu}$ moiety hydrogenated well under the reaction condition to give **6j** and **6m** in quantitative yields.

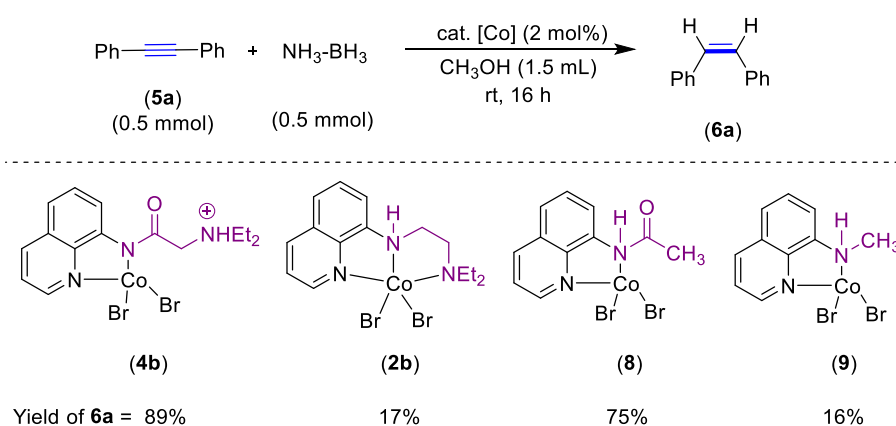
In addition to the *para*-substituted aryl-alkynes, both the *ortho*- and *meta*-substituted aryl-alkynes hydrogenated smoothly to achieve selective (Z)-alkenes **6n-6r** in good yields. Similarly, the heterocycle, 3-pyridinyl alkyne-arene reacted efficiently to provide highly selective (Z)-alkene **6t** in 85% yield. The significance of this chemo- and stereo-selective hydrogenation protocol can be highlighted for its facile reaction at room temperature and tolerance of diverse and valuable functionalities. Notably, the aryl-alkyne substrates containing $-\text{NO}_2$, $-\text{CN}$, $-\text{COCH}_3$, $-\text{OH}$, and $-\text{SH}$ functionalities were either decomposed under the reaction conditions or failed to undergo desired hydrogenation. Similarly, the alkylated alkynes remained unreactive under the optimized reaction conditions at room temperature. The protocol extended further to perform a gram scale synthesis of (Z)-stilbene which worked nicely and provided 84% yield.



Scheme 2.2 Scope of semi-hydrogenation of diarylalkyne to (Z)-Alkene. Yields (%) shown are for the isolated (Z)-alkenes. The Z : E ratio of alkenes are from the crude reaction mixture. A = alkane.

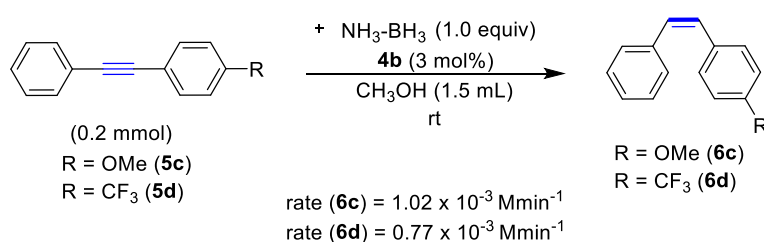
2.2.4 Mechanistic Study

2.2.4.1 Significance of N–H proton of ligands: We initiated the mechanistic investigation to understand the operational mode of cobalt catalyst and the reaction pathway. The significance of N–H proton on ligands **1** and **3** in complexes **2b** and **4b** was analyzed (Scheme 2.3). The high activity of complex **4b** compared to **2b** in the hydrogenation of alkynes suggests that the acidity or lability of N–H proton plays a crucial role in desired intermediate formation. Moreover, the developed quinolinamide complex **8** showed good catalytic activity, whereas the quinolinamine cobalt complex **9** was very poor (Scheme 2.3). This finding confirms that the acidity of N–H present in the ligand backbone plays a crucial role. Comparing the activity of complexes **4b** and **8** highlights the hemi-lability of dangling –NEt₂ arm in complex **4b** may have little role in stabilizing active catalyst species.



Scheme 2.3 Significance of N–H proton of ligands.

2.2.4.2 Rate of Reaction (Electronic Effect): The rate of the transfer hydrogenation of electronically distinct substrate was measured to inspect the electronic effect on the reaction. The rate calculated for the hydrogenation of **5c** is $1.02 \times 10^{-3} \text{ Mmin}^{-1}$ while, the same for the **5d** found to be $0.77 \times 10^{-3} \text{ Mmin}^{-1}$ which suggests that the electron-rich alkyne is slightly more reactive than the electron-deficient alkyne (Figure 2.3), which could be due to the better coordination of the former.



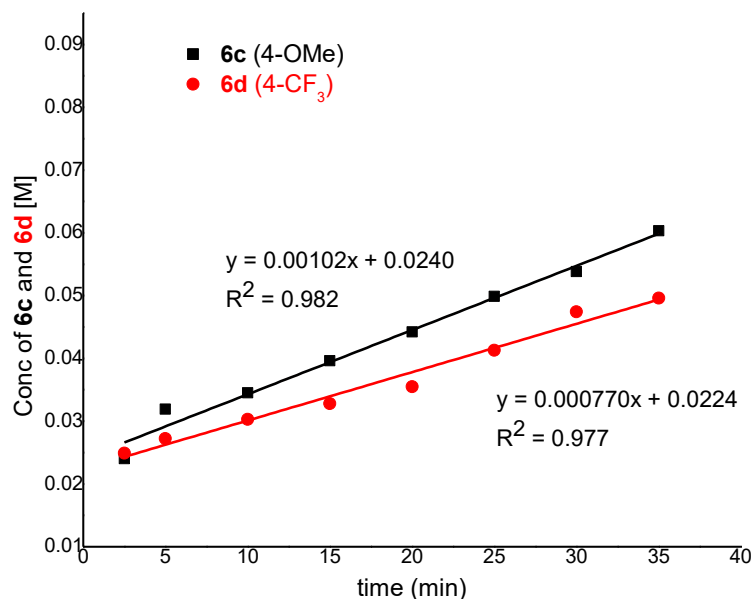
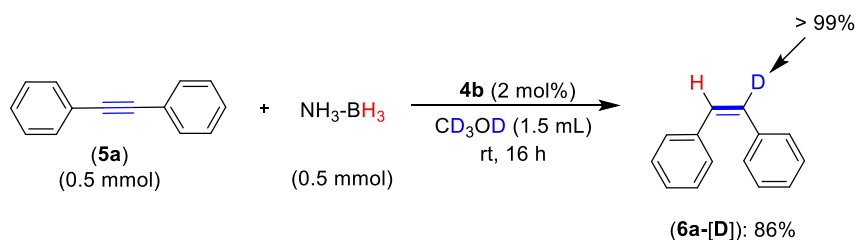


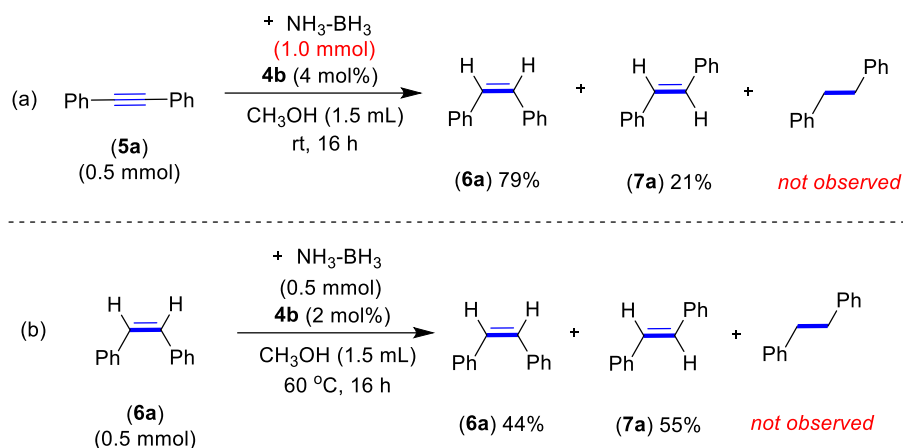
Figure 2.3 Effect of electronics on the reaction rate.

2.2.4.3 Deuterium labelling experiments: The standard hydrogenation reaction in CD₃OD solvent provided the product **6a**-[D] with >99% deuterium incorporation at one of the alkenyl carbon (Scheme 2.4), which highlights that the proton in the product arises from methanol, and the hydridic-H comes from NH₃-BH₃. However, the NH₃-BH₃ would provide both the hydrogen to product when the reaction is performed without methanol.



Scheme 2.4 Deuterium labelling experiments

2.2.4.4 Over-reduction and isomerization experiments: We treated the alkyne **5a** with two equivalents of NH₃-BH₃ at room temperature, which led to its complete conversion into stilbene isomers (*Z/E*: 79/21) without forming any alkane product (Scheme 2.5a). This result highlights the greater reactivity of catalyst **4b** for the semi-reduction of alkyne to alkene than the complete reduction to the alkane. However, the formation of 21% of (*E*)-stilbene indicated the effectiveness of catalyst **4b** for the isomerization of alkene. Moreover, the attempted hydrogenation of (*Z*)-stilbene using catalyst **4b** and NH₃-BH₃ provided isomerized product (*E*)-stilbene **7a** and did not afford alkane even at elevated temperature (Scheme 2.5b). These findings suggest that catalyst **4b** can be used for isomerization of alkenes and the catalyst is highly selective for alkyne to alkene hydrogenation.^{41,42}



Scheme 2.5 Over-reduction and isomerization experiments.

2.2.5 Probable Catalytic Cycle

Based on the preliminary investigation and literature precedents,^{37,41,42} we have proposed a tentative catalytic cycle for the **4b**-catalyzed semi-hydrogenation of alkynes (Figure 2.4). It is hypothesized that the initially formed pincer complex (NNN)CoX₂ would undergo rearrangement to non-pincer complex **4**. Complex **4** will be reduced by NH₃-BH₃ to an active Co(I) hydride complex **A**. The formation of cobalt hydride complexes from Co(II) complexes is well-documented.^{48,49} The de-coordination of flexible nitrogen-arm followed by alkyne coordination would give intermediate **C**. Insertion of an alkyne into the Co–H bond will lead to pincer alkenyl-cobalt complex **D**, which will be followed by the protonation of Co–alkenyl bond to afford product **6**.^{41,42} The methoxy-cobalt intermediate **E** would react with NH₃-BH₃ to regenerate active catalyst **A**. We assume that ligand's hemi-lability and non-innocent behaviour leads to the co-ordination and de-coordination of nitrogen-arm that provides desired stability and vacant-coordination sphere, respectively, around the cobalt center. This might assist the catalyst to facilitate hydrogenation at room temperature.

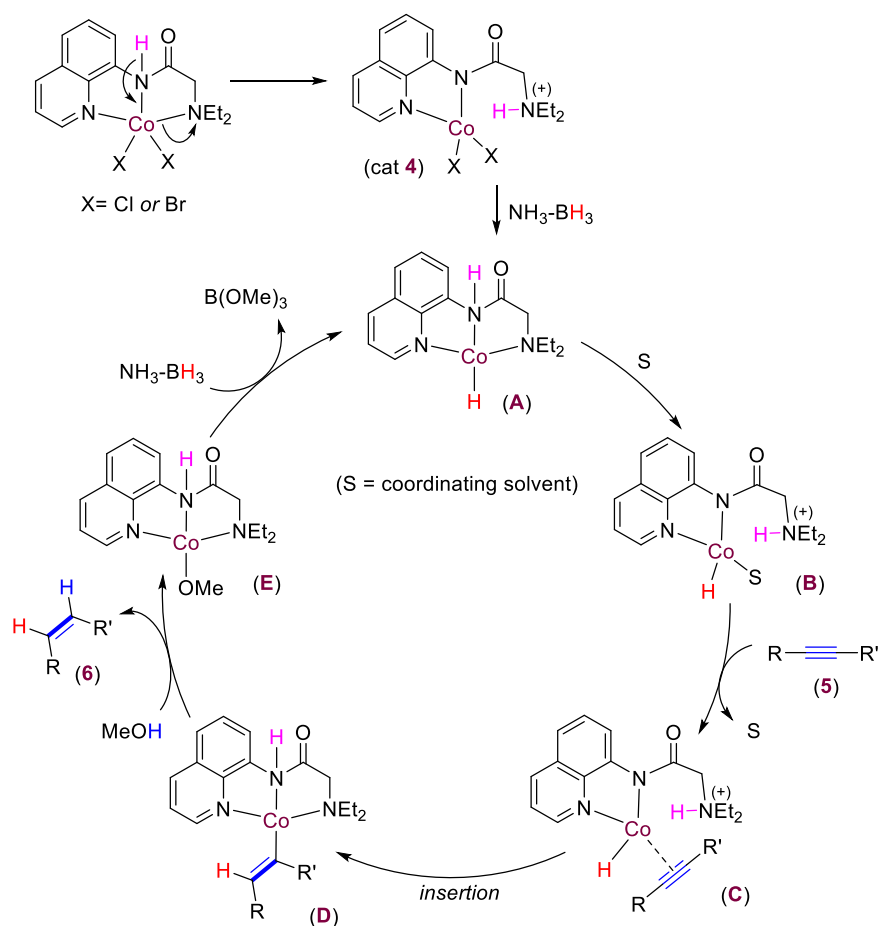


Figure 2.4 Proposed mechanism

2.3 CONCLUSION

In summary, in this chapter, we have demonstrated the room temperature chemo-selective and stereo-divergent catalytic transfer semi-hydrogenation of alkynes to (*Z*)-alkenes using phosphine-free, hemi-labile cobalt catalysts. The nitrogen ligated pincer and non-pincer Co(II) complexes were synthesized and isolated in quantitative amount and were characterized by determination of the chemical composition. The single crystal XRD study of the complex $\kappa^3\text{-(QNNN}^{\text{CH}_2\text{NEt}_2})\text{CoX}_2$ (**2a**) showed the expected pincer co-ordination of the quinolinyl-amine ligand to the Co(II) centre with distorted trigonal bipyramidal (TBP) geometry, whereas the reaction of CoX_2 with quinolinyl-amide ligand provided hemi-labile, chelate anionic complexes $\kappa^2\text{-(QNN)CoX}_2(\text{N}^{\text{C(O)HNEt}_2})$ (**4a**) which possesses tetrahedral geometry. The anionic non-pincer cobalt complexes were very effective catalysts for the semi-hydrogenation of alkynes at room temperature using an air-stable and user-friendly ammonia-borane hydrogen source. The protocol is accessible with variety of disubstituted aromatic alkynes with functional groups like, $-\text{OMe}$, $-\text{CF}_3$, $-\text{F}$, $-\text{Cl}$, $-\text{Br}$, and $-\text{OCF}_3$ at

different position. The chemo-selective reduction of alkyne in the presence of carboxylic ester was demonstrated using the optimized catalytic system. The catalyst **4b** remained highly selective towards (*Z*)-alkene as the complete reduction of alkynes to alkane in the presence of excess of ammonia-borane was not feasible. The mechanistic investigation revealed a huge contribution of hemi-lability of the nitrogen side-arm in the catalysts **4a,b** in this protocol. Also, an acidity of amidic *N-H* plays crucial role in room temperature hydrogenation of alkynes to (*Z*)-alkenes. The transfer hydrogenation in the MeOH-*d*₄ disclosed that the ammonia-borane provides hydride while proton was provided by MeOH. Overall, this system operates under extremely mild conditions and allows semi-hydrogenation of alkynes to (*Z*)-alkene with excellent yields and selectivity.

2.4 EXPERIMENTAL SECTION

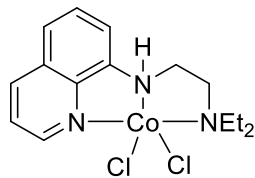
2.4.1 General Experimental

All manipulations were conducted under an argon atmosphere either in a glove box or by using standard Schlenk techniques in pre-dried glassware. The catalytic reactions were performed in oven-dried reaction vessels with Teflon screw caps. Methanol was dried and distilled from Mg-cake. All other liquid reagents were flushed with argon prior to use. The ligands *N,N*-diethyl-*N*-(2-(quinolin-8-yl)ethane-1,2-diamine) (**1**),⁴⁷ 2-(diethylamino)-*N*-(quinolin-8-yl)acetamide (**3**),⁴⁵ *N*-methyl-8-aminoquinoline,⁵⁰ *N*-acetyl-8-aminoquinoline⁵¹ were prepared according to the literature described procedures. All other chemicals were obtained from commercial sources and were used without further purification. Yields refer to the isolated compounds, estimated to be >95% pure as determined by ¹H-NMR. High resolution mass spectrometry (HRMS) mass spectra were recorded with a Thermo ScientificQ-Exactive, Accela 1250 pump. ¹H and ¹³C NMR spectra were recorded at 400 or 500 MHz (¹H), 100 or 125 MHz, (¹³C, DEPT) and 377 MHz (¹⁹F) with Bruker AV 400 and AV 500 spectrometers in CDCl₃ solutions unless otherwise specified. The ¹H and ¹³C NMR spectra were referenced to residual solvent signals (CDCl₃: δ_H = 7.26 ppm, δ_C = 77.2 ppm). Virtual triplets are denoted as “vt”.

GC Method. Gas Chromatography analyses were performed using a Shimadzu GC2010 gas chromatograph equipped with a Shimadzu AOC-20s auto sampler and a Restek RTX-5 capillary column (30 m x 25 mm x 25 μm). The instrument was set to an injection volume of 1 μL, an inlet split ratio of 10:1, and inlet and detector temperatures of 250 and 320 °C, respectively. UHP-grade argon was used as carrier gas with a flow rate of 30

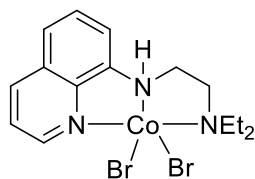
mL/min. The temperature program used for all the analyses is as follows: 80 °C, 1 min; 30 °C/min to 200°C, 2 min; 30 °C/min to 260 °C, 3 min; 30 °C/min to 300 °C, 3 min.

2.4.2 Procedure for Synthesis of Cobalt Complexes



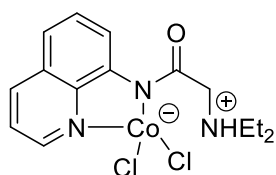
(2a)

A solution of ligand **1** (0.243 g, 1.0 mmol) in THF (10 mL) was added dropwise to the anhydrous CoCl_2 (0.130 g, 1.0 mmol) in THF (10 mL) and the reaction mixture was stirred at room temperature for 12 h. The light pink coloured precipitate obtained was filtered and washed with Et_2O (5 mL x 3). Upon drying under vacuum, the light pink complex **2a** was obtained. Yield: 0.339 g, 91%. The crystal suitable for a single-crystal X-ray diffraction was obtained from saturated solution of complex **2a** in acetonitrile at -15 °C. Elemental Analysis Calcd (%) for C, 48.28; H, 5.67; N, 11.26; Found: C, 48.36; H, 5.34; N, 10.95.



(2b)

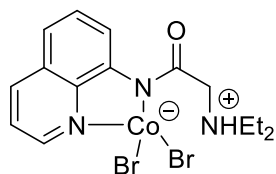
A solution of ligand **1** (0.243 g, 1.0 mmol) in THF (10 mL) was added dropwise to the anhydrous CoBr_2 (0.219 g, 1.0 mmol) in THF (10 mL) and the reaction mixture was stirred at room temperature for 12 h. The light pink coloured precipitate obtained was filtered and washed with Et_2O (5 mL x 3). Upon drying under vacuum, the light pink complex **2b** was obtained. Yield: 0.430 g, 93%. Elemental Analysis Calcd (%) for C, 38.99; H, 4.58; N, 9.09; Found: C, 38.56; H, 4.78; N, 9.47.



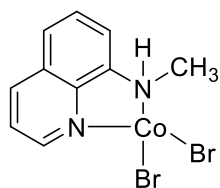
(4a)

A solution of ligand **3** (0.257 g, 1.0 mmol) in THF (10 mL) was added dropwise to the anhydrous CoCl_2 (0.130 g, 1.0 mmol) in THF (10 mL) and the reaction mixture was stirred at

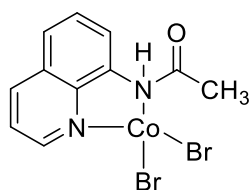
room temperature for 12 h. The dark blue coloured precipitate obtained was filtered and washed with Et₂O (5 mL x 3). Upon drying under vacuum, the dark blue complex **4a** was obtained. Yield: 0.364 g, 94%. The crystal suitable for a single-crystal X-ray diffraction was obtained from saturated solution of complex **4a** in acetonitrile at -15 °C. Elemental Analysis Calcd (%) for C, 46.53; H, 4.95; N, 10.85. Found: C, 46.24; H, 4.74; N, 10.63.

**(4b)**

A solution of ligand **3** (0.257 g, 1.0 mmol) in THF (10 mL) was added dropwise to the anhydrous CoBr₂ (0.219 g, 1.0 mmol) in THF (10 mL) and the reaction mixture was stirred at room temperature for 12 h. The dark green coloured precipitate obtained was filtered and washed with Et₂O (5 mL x 3). Upon drying under vacuum, the dark green complex **4b** was obtained. Yield: 0.452 g, 95%. Elemental Analysis Calcd (%) for C, 37.84; H, 4.02; N, 8.83. Found: C, 37.52; H, 3.95; N, 9.09.

**(8)**

A solution of *N*-acetyl-8-aminoquinoline (0.186 g, 1.0 mmol) in THF (10 mL) was added dropwise to the anhydrous CoBr₂ (0.219 g, 1.0 mmol) in THF (10 mL) and the reaction mixture was stirred at room temperature for 12 h. The greenish blue solution formed was concentrated under vacuum and Et₂O was added to the concentrated solution to obtain greenish blue precipitate. The decantation of the resulting solution followed by drying under vacuum yielded the greenish blue complex (**8**). Yield: 0.296 g, 73%. Elemental Analysis Calcd (%) for C, 32.63; H, 2.49; N, 6.92. Found: C, 32.69; H, 2.97; N, 6.46

**(9)**

A solution of *N*-methyl-8-aminoquinoline (0.158 g, 1.0 mmol) in THF (10 mL) was added dropwise to the anhydrous CoBr₂ (0.219 g, 1.0 mmol) in THF (10 mL). The reaction mixture was stirred at room temperature for 12 h. The dark purple solution obtained was concentrated under vacuum and Et₂O was added to precipitate the compound. Filtration of compound followed by washing with Et₂O and drying yielded the dark purple complex (**9**). Yield: 0.294 g, 78%. Elemental Analysis Calcd (%) for C, 31.86; H, 2.67; N, 7.43. Found: C, 32.05; H, 2.89; N, 7.58.

2.4.3 Crystallographic Data

X-ray intensity data measurements of compounds **2a** and **4a** were carried out on a Bruker D8 VENTURE Kappa Duo PHOTON II CPAD diffractometer equipped with Incoatech multilayer mirrors optics. The intensity measurements were carried out with Mo micro-focus sealed tube diffraction source (MoK_α = 0.71073 Å) at 100(2) K temperature. The X-ray generator was operated at 50 kV and 1.4 mA. A preliminary set of cell constants and an orientation matrix were calculated from three matrix sets of 36 frames (each matrix run consists of 12 frames). Data were collected with ω scan width of 0.5° at different settings of φ and 2θ with a frame time of 40 secs keeping the sample-to-detector distance fixed at 5.00 cm. The X-ray data collection was monitored by APEX3 program (Bruker, 2016).^[10] All the data were corrected for Lorentzian, polarization and absorption effects using SAINT and SADABS programs (Bruker, 2016). Using the APEX3 (Bruker) program suite, the structure was solved with the ShelXS-97(Sheldrick, 2008)^[11] structure solution program, using direct methods. The model was refined with a version of ShelXL-2018/3 (Sheldrick, 2015)^[12] using Least Squares minimization. All the hydrogen atoms were placed in a geometrically idealized position and constrained to ride on its parent atoms. The ORTEP III^[13] view of the compounds were drawn with 50% probability displacement ellipsoids, and H atoms are shown as small spheres of arbitrary radii.

Table 2.3 Crystal data of compounds **2a** and **4a**.

Crystal Data	Complex 2a	Complex 4a
Formula	C ₁₅ H ₂₁ Cl ₂ CoN ₃	C ₁₅ H ₁₉ Cl ₂ CoN ₃ O
Molecular weight	373.18 g/mol	387.16 g/mol
Crystal Size, mm	0.060 x 0.110 x 0.230	0.28 x 0.18 x 0.10
Temp. (K)	100(2)	100(2)
Wavelength (Å)	0.71073	0.71073
Crystal Syst.	monoclinic	tetragonal
Space Group	<i>P</i> ₂ ₁ / <i>c</i>	<i>P</i> -1
<i>a</i> /Å	16.6500(9)	7.3409(3)
<i>b</i> /Å	24.8705(12)	8.2378(3)
<i>c</i> /Å	7.9667(5)	14.1911(6)
α°	90	77.2420(10)
β°	90.490(2)	85.133(2)
γ°	90	77.2610(10)
<i>V</i> /Å ³	3298.8(3)	815.80(6)
<i>Z</i>	8	2
<i>D</i> _{calc} /g cm ⁻³	1.503	1.576
μ /mm ⁻¹	1.361	1.383
<i>F</i> (000)	1544	398
<i>Ab. Correct.</i>	multi-scan	multi-scan
<i>T</i> _{min} / <i>T</i> _{max}	0.745/0.9230	0.698/0.874
2 θ _{max}	56.00	56.00
Total reflns.	49368	20029
Unique reflns.	6459	3915
Obs. reflns.	5975	3761
<i>h, k, l</i> (min, max)	(-20, 20), (-27, 30), (-9, 0)	(-9, 9), (-10, 10), (-18, 18)
<i>R</i> _{int} / <i>R</i> _{sig}	0.0451 / 0.0254	0.0219 / 0.0172
No. of parameters	384	206
<i>R</i> 1 [<i>I</i> > 2 σ (<i>I</i>)]	0.0439	0.0193
<i>wR</i> 2 [<i>I</i> > 2 σ (<i>I</i>)]	0.0834	0.0518
<i>R</i> 1 [all data]	0.0481	0.0526
<i>wR</i> 2 [all data]	0.0855	0.0822
goodness-of-fit	1.132	1.072
$\Delta\rho_{\max}$, $\Delta\rho_{\min}$ (eÅ ⁻³)	+0.502, -0.703	+0.355, -0.336
CCDC	2119314	2119313

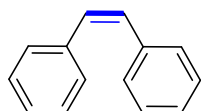
2.4.4 Representative Procedure for Hydrogenation

A Teflon screw-cap tube was introduced with catalyst **4b** (0.0048 g, 0.01 mmol), ammonia borane (0.0155 g, 0.5 mmol) and diphenylacetylene (0.089 g, 0.5 mmol) inside the glove box. The solvent MeOH (1.5 mL) was added to the reaction vessel under the argon atmosphere. The reaction mixture was then stirred at room temperature (27 °C) for 16 h. At ambient temperature, the reaction mixture was diluted with MeOH (5.0 mL) and resulting solution was concentrated under vacuum. The crude reaction mixture was purified by chromatography on silica gel using petroleum ether as eluent to obtain (Z)-stilbene **6a** (0.080 g, 89%).

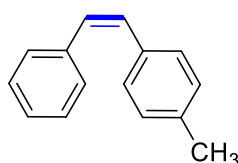
2.4.5 Gram Scale Synthesis

Representative procedure for the hydrogenation followed, using 1.069 g (6.0 mmol) of **5a**, catalyst **4b** (0.057 g, 0.12 mmol), NH₃-BH₃ (0.185 g, 6.0 mmol) and MeOH (15 mL). The reaction proceeded smoothly and gave an excellent yield of (Z)-stilbene (0.908 g, 5.04 mmol, 84%) which ensures synthetic applicability of the optimized protocol in protocol in the gram-scale production.

2.4.6 Characterization Data of (Z)-Alkenes

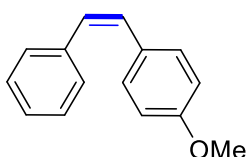


(Z)-1,2-diphenylethene (6a):⁴¹ The representative procedure was followed, using 1,2-diphenylethyne (**5a**; 0.089 g, 0.50 mmol), NH₃-BH₃ (0.0155 g, 0.5 mmol) and catalyst **4b** (0.0048 g, 0.01 mmol). Purification by column chromatography on silica gel (petroleum ether) yielded **6a** (0.080 g, 89%) as a colourless oil. ¹H-NMR (500 MHz, CDCl₃): δ 7.29-7.19(m, 10H, Ar-H), 6.63 (s, 2H, CH). ¹³C{¹H}-NMR (125 MHz, CDCl₃): δ 137.4 (2C, C_q), 130.4 (2C, CH), 129.1 (4C, CH), 128.4 (4C, CH), 127.3 (2C, CH). HRMS (ESI): m/z Calcd for C₁₄H₁₂ + H⁺ [M + H]⁺ 181.1017; Found 181.1012. The analytical data are in accordance with those reported in the literature.

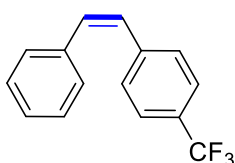


(Z)-1-methyl-4-styrylbenzene (6b):⁴¹ The representative procedure was followed, using 1-methyl-4-(phenylethynyl)benzene (**5b**; 0.096 g, 0.50 mmol), NH₃-BH₃ (0.0155 g, 0.5

mmol) and catalyst **4b** (0.0095 g, 0.02 mmol). Purification by column chromatography on silica gel (petroleum ether) yielded **6b** (0.084 g, 86%) as a colourless oil. $^1\text{H-NMR}$ (400 MHz, CDCl_3): δ 7.40 (d, $J = 7.6$ Hz, 2H, Ar-H), 7.36 (vt, $J = 6.87, 7.63$ Hz, 2H, Ar-H), 7.27-7.33 (m, 3H, Ar-H), 7.16 (d, $J = 8.0$ Hz, 2H, Ar-H), 6.69 (s, 2H, CH), 2.44 (s, 3H, CH_3). $^{13}\text{C}\{^1\text{H}\}$ -NMR (100 MHz, CDCl_3): δ 137.7 (C_q), 137 (C_q), 134.4 (C_q), 130.4 (CH), 129.7 (CH), 129.1 (2C, CH), 129 (2C, CH), 128.9 (2C, CH), 128.4 (2C, CH), 127.1 (CH), 21.4 (CH_3). HRMS (ESI): m/z Calcd for $\text{C}_{15}\text{H}_{14} + \text{H}^+$ $[\text{M} + \text{H}]^+$ 195.1174; Found 195.1168. The analytical data are in accordance with those reported in the literature.

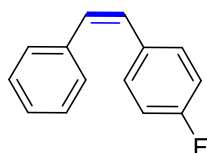


(Z)-1-methoxy-4-styrylbenzene (6c):⁴¹ The representative procedure was followed, using 1-methoxy-4-(phenylethynyl)benzene (**5c**; 0.105 g, 0.50 mmol), $\text{NH}_3\text{-BH}_3$ (0.0155 g, 0.5 mmol) and catalyst **4b** (0.0071 g, 0.015 mmol). Purification by column chromatography on silica gel (petroleum ether/EtOAc: 10/1) yielded **6c** (0.091 g, 87%) as a yellow oil. $^1\text{H-NMR}$ (500 MHz, CDCl_3): δ 7.34-7.26 (m, 4H, Ar-H), 7.25-7.21 (m, 3H, Ar-H), 6.82-6.79 (m, 2H, Ar-H), 6.59 (d, $J = 12.3$ Hz, 1H, CH), 6.56 (d, $J = 12.3$ Hz, 1H, CH), 3.83 (s, 3H, OCH_3). $^{13}\text{C}\{^1\text{H}\}$ -NMR (125 MHz, CDCl_3): δ 158.9 (C_q), 137.8 (C_q), 130.3 (3C, CH), 129.9 (CH), 129.8 (C_q), 129 (3C, CH), 128.9 (CH), 128.4 (2C, CH), 127.1 (CH), 55.4 (CH_3). HRMS (ESI): m/z Calcd for $\text{C}_{15}\text{H}_{14}\text{O} + \text{H}^+$ $[\text{M} + \text{H}]^+$ 211.1123; Found 211.1117. The analytical data are in accordance with those reported in the literature.

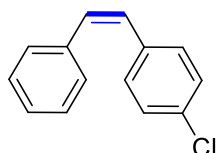


(Z)-1-styryl-4-(trifluoromethyl)benzene (6d):⁴¹ The representative procedure was followed, using 1-(phenylethynyl)-4-(trifluoromethyl)benzene (**5d**; 0.074 g, 0.3 mmol), $\text{NH}_3\text{-BH}_3$ (0.0093 g, 0.30 mmol) and catalyst **4b** (0.0043 g, 0.009 mmol). Purification by column chromatography on silica gel (petroleum ether) yielded **6d** (0.048 g, 64%) as yellow oil. $^1\text{H-NMR}$ (500 MHz, CDCl_3): δ 7.47 (d, $J = 8.4$ Hz, 2H, Ar-H), 7.34 (d, $J = 8.4$ Hz, 2H, Ar-H), 7.27-7.20 (m, 5H, Ar-H), 6.73 (d, $J = 12.9$ Hz, 1H, CH), 6.60 (d, $J = 12.3$ Hz, 1H, CH). $^{13}\text{C}\{^1\text{H}\}$ -NMR (125 MHz, CDCl_3): δ 141.1 (C_q), 136.7 (C_q), 132.5 (CH), 129.3 (2C, CH), 129.0 (2C, CH), 128.9 (CH), 128.6 (2C, CH), 128.5 (q, $^2J_{\text{C-F}} = 22.9$ Hz, C_q), 127.8

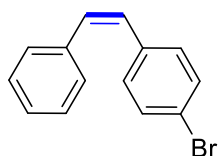
(CH), 125.3 (q, $^3J_{C-F} = 3.8$ Hz, 2C, CH), 124.4 (q, $^2J_{C-F} = 271.6$ Hz, CF₃). $^{19}\text{F-NMR}$ (377 MHz, CDCl₃): δ -62.5. The analytical data are in accordance with those reported in the literature.



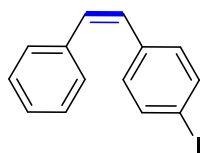
(Z)-1-fluoro-4-styrylbenzene (6e):⁴¹ The representative procedure was followed, using 1-fluoro-4-(phenylethynyl)benzene (**5e**; 0.098 g, 0.50 mmol), NH₃-BH₃ (0.0155 g, 0.5 mmol) and catalyst **4b** (0.0095 g, 0.02 mmol). Purification by column chromatography on silica gel (petroleum ether) yielded **6e** (0.067 g, 68%) as colourless oil. $^1\text{H-NMR}$ (400 MHz, CDCl₃): δ 7.29-7.24 (m, 7H, Ar-H), 6.95 (t, $J = 8.6$ Hz, 2H, Ar-H), 6.65 (d, $J = 12.3$ Hz, 1H, CH), 6.58 (d, $J = 12.3$ Hz, 1H, CH). $^{13}\text{C}\{^1\text{H}\}$ -NMR (100 MHz, CDCl₃): δ 162 (d, $^1J_{C-F} = 246.3$ Hz, CF), 137.2 (C_q), 133.4 (d, $^4J_{C-F} = 3.7$ Hz, C_q), 130.7 (d, $^3J_{C-F} = 8.0$ Hz, 2C, CH), 130.5 (d, $^5J_{C-F} = 1.5$ Hz, CH), 129.3 (CH), 129 (2C, CH), 128.5 (2C, CH), 127.4 (CH), 115.3 (d, $^2J_{C-F} = 21.1$ Hz, 2C, CH). $^{19}\text{F-NMR}$ (377 MHz, CDCl₃): δ -114.7. The analytical data are in accordance with those reported in the literature.



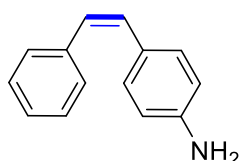
(Z)-1-chloro-4-styrylbenzene (6f):⁴¹ The representative procedure was followed, using 1-chloro-4-(phenylethynyl)benzene (**5f**; 0.106 g, 0.50 mmol), NH₃-BH₃ (0.0155 g, 0.5 mmol) and catalyst **4b** (0.0071 g, 0.015 mmol). Purification by column chromatography on silica gel (petroleum ether/EtOAc: 100/1) yielded **6f** (0.091 g, 85%) as a yellow oil. $^1\text{H-NMR}$ (500 MHz, CDCl₃): δ 7.25-7.21 (m, 5H, Ar-H), 7.20-7.16 (m, 4H, Ar-H), 6.64 (d, $J = 12.2$ Hz, 1H, CH), 6.54 (d, $J = 12.2$ Hz, 1H, CH). $^{13}\text{C}\{^1\text{H}\}$ -NMR (125 MHz, CDCl₃): δ 137 (C_q), 135.8 (C_q), 132.9 (C_q), 131.1 (CH), 130.4 (2C, CH), 129.1 (CH), 129 (2C, CH), 128.6 (2C, CH), 128.5 (2C, CH), 127.5 (CH). HRMS (ESI): m/z Calcd for C₁₄H₁₁Cl + H⁺ [M + H]⁺ 215.0628; Found 215.0622. The analytical data are in accordance with those reported in the literature.



(Z)-1-bromo-4-styrylbenzene (6g):⁴³ The representative procedure was followed, using 1-bromo-4-(phenylethynyl)benzene (**5g**; 0.077 g, 0.30 mmol), $\text{NH}_3\text{-BH}_3$ (0.0093 g, 0.3 mmol) and catalyst **4b** (0.0043 g, 0.009 mmol). Purification by column chromatography on silica gel (petroleum ether/EtOAc: 100/1) yielded **6g** (0.049 g, 63%) as yellow oil. $^1\text{H-NMR}$ (400MHz, CDCl_3): δ 7.36-7.34 (m, 2H, Ar-H), 7.28-7.22 (m, 5H, Ar-H), 7.13-7.11 (m, 2H, Ar-H), 6.65 (d, $J = 12.3$ Hz, 1H, CH), 6.52 (d, $J = 12.1$ Hz, 1H, CH). $^{13}\text{C}\{^1\text{H}\}\text{-NMR}$ (100MHz, CDCl_3): δ 137 (C_q), 136.3 (C_q), 131.5 (2C, CH), 131.2 (CH), 130.7 (2C, CH), 129.1(CH), 129 (2C, CH), 128.5 (2C, CH), 127.5 (CH), 121.1 (C_q). The analytical data are in accordance with those reported in the literature.

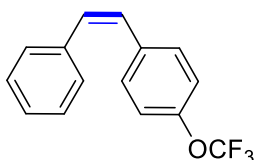


(Z)-1-iodo-4-styrylbenzene (6h):²⁹ The representative procedure was followed, using 1-iodo-4-(phenylethynyl)benzene (**5h**; 0.152 g, 0.50 mmol), $\text{NH}_3\text{-BH}_3$ (0.0155 g, 0.5 mmol) and catalyst **4b** (0.0071 g, 0.015 mmol). Purification by column chromatography on silica gel (petroleum ether/EtOAc: 100/1) yielded **6h** (0.127 g, 83%) as white powder. $^1\text{H-NMR}$ (400 MHz, CDCl_3): δ 7.59-7.56 (m, 2H, Ar-H), 7.29-7.24 (m, 5H, Ar-H), 7.02 (d, $J = 8.1$ Hz, 2H, Ar-H), 6.68 (d, $J = 12.1$ Hz, 1H, CH), 6.53 (d, $J = 12.1$ Hz, 1H, CH). $^{13}\text{C}\{^1\text{H}\}\text{-NMR}$ (100 MHz, CDCl_3): δ 137.5 (2C, CH), 137 (C_q), 136.8 (C_q), 131.3 (CH), 130.9 (2C, CH), 129.2 (CH), 128.9 (2C, CH), 128.5 (2C, CH), 127.5 (CH), 92.7 (C_q). The analytical data are in accordance with those reported in the literature.

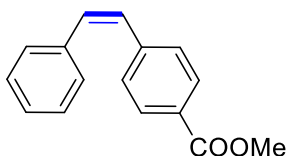


(Z)-4-styrylaniline (6i):⁴¹ The representative procedure was followed, using 4-(phenylethynyl)aniline (**5i**; 0.097 g, 0.50 mmol), $\text{NH}_3\text{-BH}_3$ (0.0155 g, 0.5 mmol) and catalyst **4b** (0.0095 g, 0.02 mmol). Purification by column chromatography on silica gel (petroleum ether/EtOAc: 5/1) yielded **6i** (0.084 g, 86%) as a brown oil. $^1\text{H-NMR}$ (500 MHz, CDCl_3): δ 7.34-7.18 (m, 5H, Ar-H), 7.09 (d, $J = 8.4$ Hz, 2H, Ar-H), 6.55 (d, $J = 8.4$ Hz, 2H, Ar-H),

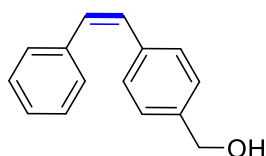
6.50 (d, $J = 12.2$ Hz, 1H, CH), 6.45 (d, $J = 12.2$ Hz, 1H, CH), 3.69 (s, 2H, NH₂). ¹³C{¹H}-NMR (125 MHz, CDCl₃): δ 145.6 (C_q), 138.1 (C_q), 130.3 (CH), 130.3 (2C, CH), 129 (2C, CH), 128.3 (2C, CH), 127.8 (CH), 127.7 (C_q), 126.9 (CH), 114.9 (2C, CH). HRMS (ESI): m/z Calcd for C₁₄H₁₃N + H⁺ [M + H]⁺ 196.1126; Found 196.1121. The analytical data are in accordance with those reported in the literature.



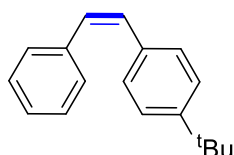
(Z)-1-styryl-4-(trifluoromethoxy)benzene (6j): The representative procedure was followed, using 1-(phenylethynyl)-4-(trifluoromethoxy)benzene (**5j**; 0.131 g, 0.50 mmol), NH₃-BH₃ (0.0155 g, 0.5 mmol) and catalyst **4b** (0.0095 g, 0.02 mmol). Purification by column chromatography on silica (petroleum ether/EtOAc: 10/1) yielded **6j** (0.103 g, 78%) as a colourless oil. ¹H-NMR (400 MHz, CDCl₃): δ 7.18-7.14 (m, 7H, Ar-H), 6.98 (d, $J = 8.4$ Hz, 2H, Ar-H), 6.58 (d, $J = 12.3$ Hz, 1H, Ar-H), 6.48 (d, $J = 12.3$ Hz, 1H, Ar-H). ¹³C{¹H}-NMR (100 MHz, CDCl₃): δ 148.3 (C_q), 137 (C_q), 136.1 (C_q), 131.4 (CH), 130.5 (2C, CH), 129 (2C, CH), 128.9 (CH), 128.6 (3C, CH), 127.6 (CH), 120.8 (CH), 120.6 (q, ¹J_{C-F} = 257.2 Hz, CF₃). ¹⁹F-NMR (377 MHz, CDCl₃): δ -57.8 (s). HRMS (ESI): m/z Calcd for C₁₅H₁₁OF₃ + H⁺ [M + H]⁺ 265.0840; Found 265.0835.



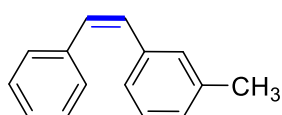
methyl (Z)-4-styrylbenzoate (6k):⁴¹ The representative procedure was followed, using methyl 4-(phenylethynyl)benzoate (**5k**; 0.118 g, 0.50 mmol), NH₃-BH₃ (0.015 g, 0.5 mmol) and catalyst **4b** (0.0071 g, 0.015 mmol). Purification by column chromatography on silica (petroleum ether/EtOAc: 10/1) yielded **6k** (0.097 g, 81%) as a yellow oil. ¹H-NMR (400 MHz, CDCl₃): δ 7.94 (d, $J = 8.4$ Hz, 2H, Ar-H), 7.36-7.35 (d, $J = 8.4$ Hz, 2H, Ar-H), 7.27 (br s, 5H, Ar-H), 6.76 (d, $J = 12.6$ Hz, 1H, CH), 6.66 (d, $J = 12.2$ Hz, 1H, CH), 3.95 (s, 3H, CH₃). ¹³C{¹H}-NMR (100 MHz, CDCl₃): δ 167.1 (C_q, CO), 142.3 (C_q), 136.8 (C_q), 132.4 (CH), 129.7 (2C, CH), 129.4 (CH), 129 (4C, CH), 128.8 (C_q), 128.5 (2C, CH), 127.7 (CH), 52.2 (CH₃). HRMS (ESI): m/z Calcd for C₁₆H₁₄O₂ + H⁺ [M + H]⁺ 239.1072; Found 239.1067. The analytical data are in accordance with those reported in the literature.



(Z)-1-(4-styrylphenyl)methanol (6l):⁵² The representative procedure was followed, using (4-(phenylethynyl)phenyl)methanol (**5l**; 0.104 g, 0.50 mmol), $\text{NH}_3\text{-BH}_3$ (0.0155 g, 0.5 mmol) and catalyst **4b** (0.0071 g, 0.015 mmol). Purification by column chromatography on silica gel (petroleum ether/EtOAc: 10/1) yielded **6l** (0.091 g, 87%) as a brown oil. $^1\text{H-NMR}$ (500 MHz, CDCl_3): δ 7.35-7.22 (m, 9H, Ar-H), 6.67 (d, $J = 12.2$ Hz, 1H, CH), 6.63 (d, $J = 12.2$ Hz, 1H, CH), 4.68 (s, 2H, CH_2), 1.88 (s, 1H, OH). $^{13}\text{C}\{^1\text{H}\}\text{-NMR}$ (125 MHz, CDCl_3): δ 139.8 (C_q), 137.4 (C_q), 136.8 (C_q), 130.5 (CH), 130 (CH), 129.2 (2C, CH), 129 (2C, CH), 128.4 (2C, CH), 127.3 (CH), 127.1 (2C, CH), 65.3 (CH_2). HRMS (ESI): m/z Calcd for $\text{C}_{15}\text{H}_{14}\text{O} + \text{H}^+$ [$\text{M} + \text{H}$] $^+$ 211.1123; Found 211.1117. The analytical data are in accordance with those reported in the literature.

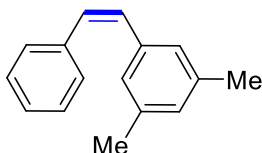


(Z)-1-(tert-butyl)-4-styrylbenzene (6m):⁵³ The representative procedure was followed, using 1-(tert-butyl)-4-(phenylethynyl)benzene (**5m**; 0.117 g, 0.50 mmol), $\text{NH}_3\text{-BH}_3$ (0.0155 g, 0.5 mmol) and catalyst **4b** (0.0048 g, 0.01 mmol). Purification by column chromatography on silica gel (petroleum ether) yielded **6m** (0.103 g, 87%) as a colourless oil. $^1\text{H-NMR}$ (500 MHz, CDCl_3): δ 7.35-7.22 (m, 9H, Ar-H), 6.60 (s, 2H, CH), 1.34 (s, 9H, CH_3). $^{13}\text{C}\{^1\text{H}\}\text{-NMR}$ (125 MHz, CDCl_3): δ 150.3 (C_q), 137.8 (C_q), 134.4 (C_q), 130.3 (CH), 129.5 (CH), 129 (2C, CH), 128.8 (2C, CH), 128.4 (2C, CH), 127.1 (CH), 125.3 (2C, CH), 34.7 (C_q), 31.5 (3C, CH_3). HRMS (ESI): m/z Calcd for $\text{C}_{18}\text{H}_{20} + \text{H}^+$ [$\text{M} + \text{H}$] $^+$ 237.1643; Found 237.1638. The analytical data are in accordance with those reported in the literature.

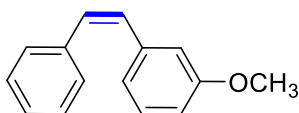


(Z)-1-methyl-3-styrylbenzene (6n):⁴¹ The representative procedure was followed, using 1-methyl-3-(phenylethynyl)benzene (**5n**; 0.096 g, 0.50 mmol), $\text{NH}_3\text{-BH}_3$ (0.0155 g, 0.5 mmol) and catalyst **4b** (0.0071 g, 0.015 mmol). Purification by column chromatography on silica gel (petroleum ether) yielded **6n** (0.081 g, 83%) as a colourless solid. $^1\text{H-NMR}$ (500 MHz, CDCl_3): δ 7.36-7.27 (m, 5H, Ar-H), 7.21-7.13 (m, 3H, Ar-H), 7.10-7.09 (d, $J = 6.9$ Hz, 1H,

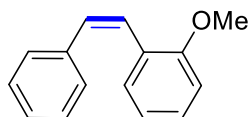
Ar-H), 6.66 (s, 2H, CH), 2.35 (s, 3H, CH₃). ¹³C{¹H}-NMR (125 MHz, CDCl₃): δ 137.9 (C_q), 137.5 (C_q), 137.3 (C_q), 130.5 (CH), 130.2 (CH), 129.8 (CH), 129 (2C, CH), 128.3 (2C, CH), 128.2 (CH), 128 (CH), 127.2 (CH), 126 (CH), 21.5 (CH₃). HRMS (ESI): *m/z* Calcd for C₁₅H₁₄ + H⁺ [M + H]⁺ 195.1174; Found 195.1168. The analytical data are in accordance with those reported in the literature.



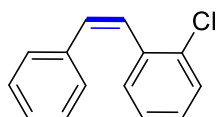
(Z)-1,3-dimethyl-5-styrylbenzene (6o): The representative procedure was followed, using 1,3-dimethyl-5-(phenylethynyl)benzene (**5o**; 0.103 g, 0.50 mmol), NH₃-BH₃ (0.0155 g, 0.5 mmol) and catalyst **4b** (0.0071 g, 0.015 mmol). Purification by column chromatography on silica gel (petroleum ether) yielded **6o** (0.079 g, 76%) as a yellow oil. ¹H-NMR (400 MHz, CDCl₃): δ 7.18 (d, *J* = 7.1 Hz, 2H, Ar-H), 7.15-7.09 (m, 3H, Ar-H), 6.80 (s, 2H, Ar-H), 6.75 (s, 1H, Ar-H), 6.46 (s, 2H, CH), 2.13 (s, 6H, CH₃). ¹³C{¹H}-NMR (100 MHz, CDCl₃): δ 137.8 (2C, C_q), 137.6 (C_q), 137.3 (C_q), 130.6 (CH), 130.1 (CH), 129.1 (2C, CH), 128.9 (CH), 128.3 (2C, CH), 127.2 (CH), 126.8 (2C, CH), 21.4 (2C, CH₃). HRMS (ESI): *m/z* Calcd for C₁₆H₁₆ + H⁺ [M + H]⁺ 209.1330; Found 209.1325.



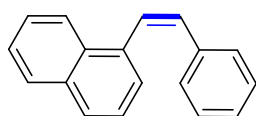
(Z)-1-methoxy-3-styrylbenzene (6p):⁵³ The representative procedure was followed, using 1-methoxy-3-(phenylethynyl)benzene (**5p**; 0.104 g, 0.50 mmol), NH₃-BH₃ (0.0155 g, 0.5 mmol) and catalyst **4b** (0.0071 g, 0.015 mmol). Purification by column chromatography on silica gel (petroleum ether/EtOAc: 5/1) yielded **6p** (0.078 g, 74%) as a colourless oil. ¹H-NMR (500 MHz, CDCl₃): δ 7.30-7.14 (m, 6H, Ar-H), 6.85 (d, *J* = 7.6 Hz, 1H, Ar-H), 6.80 (vt, *J* = 2.3 Hz, 1H, Ar-H), 6.76 (dd, *J* = 8.4, 2.3 Hz, 1H, Ar-H), 6.64 (d, *J* = 12.2 Hz, 1H, CH), 6.58 (d, *J* = 12.2 Hz, 1H, CH), 3.66 (s, 3H, CH₃). ¹³C{¹H}-NMR (125 MHz, CDCl₃): δ 159.5 (C_q), 138.7 (C_q), 137.4 (C_q), 130.7 (CH), 130.3 (CH), 129.4 (CH), 129.1 (2C, CH), 128.4 (2C, CH), 127.3 (CH), 121.7 (CH), 113.9 (CH), 113.5 (CH), 55.2 (CH₃). HRMS (ESI): *m/z* Calcd for C₁₅H₁₄O + H⁺ [M + H]⁺ 211.1123; Found 211.1117. The analytical data are in accordance with those reported in the literature.



(Z)-1-methoxy-2-styrylbenzene (6q): The representative procedure was followed, using 1-methoxy-2-(phenylethynyl)benzene (**5q**; 0.104 g, 0.50 mmol), $\text{NH}_3\text{-BH}_3$ (0.0155 g, 0.5 mmol) and catalyst **4b** (0.0071 g, 0.015 mmol). Purification by column chromatography on silica gel (petroleum ether/EtOAc: 10:1) yielded **6q** (0.096 g, 91%) as a yellow oil. $^1\text{H-NMR}$ (500 MHz, CDCl_3): δ 7.25-7.15 (m, 7H, Ar-H), 6.89 (d, $J = 8.4$ Hz, 1H, Ar-H), 6.76 (t, $J = 7.6$ Hz, 1H, Ar-H), 6.71 (d, $J = 12.2$ Hz, 1H, CH), 6.64 (d, $J = 12.2$ Hz, 1H, CH) 3.82 (s, 3H, CH_3). $^{13}\text{C}\{^1\text{H}\}\text{-NMR}$ (125 MHz, CDCl_3): δ 157.4 (C_q), 137.5 (C_q), 130.4 (CH), 130.3 (CH), 129 (2C, CH), 128.8 (CH), 128.2 (2C, CH), 127.1 (CH), 126.5 (C_q), 126 (CH), 120.8 (CH), 110.9 (CH), 55.6 (CH_3). HRMS (ESI): m/z Calcd for $\text{C}_{15}\text{H}_{14}\text{O} + \text{H}^+$ $[\text{M} + \text{H}]^+$ 211.1123; Found 211.1117.

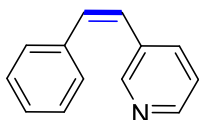


(Z)-1-chloro-2-styrylbenzene (6r): The representative procedure was followed, using 1-chloro-2-(phenylethynyl)benzene (**5r**; 0.106 g, 0.50 mmol), $\text{NH}_3\text{-BH}_3$ (0.015 g, 0.5 mmol) and catalyst **4b** (0.007 g, 0.015 mmol). Purification by column chromatography on silica gel (petroleum ether/EtOAc: 20/1) yielded **6r** (0.087 g, 81%) as a yellow oil. $^1\text{H-NMR}$ (400 MHz, CDCl_3): δ 7.42 (d, $J = 8.0$ Hz, 1H, Ar-H), 7.22-7.16 (m, 7H, Ar-H), 7.05 (t, $J = 7.5$ Hz, 1H, Ar-H), 6.74 (d, $J = 12.3$ Hz, 1H, CH), 6.69 (d, $J = 12.3$ Hz, 1H, CH). $^{13}\text{C}\{^1\text{H}\}\text{-NMR}$ (100 MHz, CDCl_3): δ 136.6 (C_q), 136.2 (C_q), 133.9 (C_q), 131.9 (CH), 130.9 (CH), 129.7 (CH), 129.2 (2C, CH), 128.7 (CH), 128.4 (2C, CH), 127.5 (CH), 127.4 (CH), 126.5 (CH). HRMS (ESI): m/z Calcd for $\text{C}_{14}\text{H}_{11}\text{Cl} + \text{H}^+$ $[\text{M} + \text{H}]^+$ 215.0628; Found 215.0622.

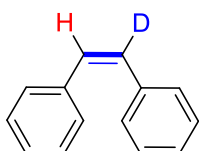


(Z)-1-styrylnaphthalene (6s):⁴³ The representative procedure was followed, using 1-(phenylethynyl)naphthalene (**5s**; 0.114 g, 0.50 mmol), $\text{NH}_3\text{-BH}_3$ (0.0155 g, 0.5 mmol) and catalyst **4b** (0.0071 g, 0.015 mmol). Purification by column chromatography on silica gel (petroleum ether) yielded **6s** (0.090 g, 78%) as a colourless solid. $^1\text{H-NMR}$ (500 MHz, CDCl_3): δ 8.11-8.09 (m, 1H, Ar-H), 7.91-7.90 (s, 1H, Ar-H), 7.81 (d, $J = 7.6$ Hz, 1H, Ar-H), 7.54-7.49 (m, 2H, Ar-H), 7.39-7.34 (m, 2H, Ar-H), 7.11 (s, 5H, Ar-H), 7.08 (d, $J =$

12.2 Hz, 1H, CH), 6.86 (d, $J = 12.2$ Hz, 1H, CH). $^{13}\text{C}\{^1\text{H}\}$ -NMR (125 MHz, CDCl_3): δ 136.9 (C_q), 135.4 (C_q), 133.8 (C_q), 132.2 (CH), 131.7 (C_q), 129.2 (2C, CH), 128.7 (CH), 128.6 (CH), 128.2 (2C, CH), 127.7 (CH), 127.3 (CH), 126.6 (CH), 126.2 (CH), 126.1 (CH), 125.8 (CH), 125.0 (CH). HRMS (ESI): m/z Calcd for $\text{C}_{18}\text{H}_{14} + \text{H}^+$ $[\text{M} + \text{H}]^+$ 231.1174; Found 231.1168. The analytical data are in accordance with those reported in the literature.



(Z)-3-styrylpyridine (6t): The representative procedure was followed, using 3-(phenylethynyl)pyridine (**5t**; 0.054 g, 0.30 mmol), $\text{NH}_3\text{-BH}_3$ (0.0093 g, 0.3 mmol) and catalyst **4b** (0.0043 g, 0.009 mmol). Purification by column chromatography on silica (petroleum ether/EtOAc: 5/1) yielded **6t** (0.046 g, 85%) as a brown oil. ^1H -NMR (500 MHz, CDCl_3): δ 8.54-8.53 (d, $J = 1.5$ Hz, 1H, Ar-H), 8.47 (dd, $J = 5.0, 4.6$ Hz, 1H, Ar-H), 7.56 (d, $J = 8.0$ Hz, 1H, Ar-H), 7.32-7.26 (m, 5H, Ar-H), 7.17 (dd, $J = 8.0, 5.0$ Hz, 1H, Ar-H), 6.80 (d, $J = 12.2$ Hz, 1H, CH), 6.60 (d, $J = 12.2$ Hz, 1H, CH). $^{13}\text{C}\{^1\text{H}\}$ -NMR (125 MHz, CDCl_3): δ 150.3 (CH), 148.2 (CH), 136.7 (C_q), 136 (CH), 133.1 (C_q), 132.9 (CH), 128.8 (2C, CH), 128.7 (2C, CH), 127.7 (CH), 126.6 (CH), 123.2 (CH). HRMS (ESI): m/z Calcd for $\text{C}_{13}\text{H}_{11}\text{N} + \text{H}^+$ $[\text{M} + \text{H}]^+$ 182.0970; Found 182.0964.



(Z)-(ethene-1,2-diyl-1-d)dibenzene (6a-[D]): The representative procedure was followed, using 1,2-diphenylethyne (**5a**; 0.089 g, 0.50 mmol), $\text{NH}_3\text{-BH}_3$ (0.0155 g, 0.5 mmol) and catalyst **4b** (0.0048 g, 0.01 mmol) in CD_3OD . Purification by column chromatography on silica gel (petroleum ether) yielded **6a-[D]** (0.078 g, 86%) as a colourless oil. ^1H -NMR (500 MHz, CDCl_3): δ 7.29-7.19(m, 10H, Ar-H), 6.63 (1H, CH). $^{13}\text{C}\{^1\text{H}\}$ -NMR (125 MHz, CDCl_3): δ 137.4 (C_q), 137.3 (C_q), 130.4 (CH), 130.3 (CH), 129.1 (CH), 128.4 (CH), 127.3 (CH).

2.4.7 Mechanistic Experiments

2.4.7.1 Procedure for Rate of Reaction (Electronic Effect)

To a flame dried screw-cap tube equipped with magnetic stir bar were introduced 1-methoxy-4-(phenylethynyl)benzene (**5c**, 0.042 g, 0.2 mmol) or 1-(phenylethynyl)-4-(trifluoromethyl)benzene (**5d**, 0.049 g, 0.2 mmol), $\text{NH}_3\text{-BH}_3$ (0.006 g, 0.2 mmol), **4b** (0.0029 g, 3 mol%), *n*-dodecane (0.025 mL, 0.11 mmol, internal standard) and MeOH (1.5 mL) inside the glove-box. The reaction mixture was then stirred at room temperature on magnetic stirrer. At regular intervals (2.5, 5, 10, 15, 20, 25, 30, 35 min), the reaction vessel was taken to glove box and an aliquot of sample was withdrawn to the GC vial (Table 2.4). The sample was diluted with MeOH and subjected to GC analysis. The concentration of product **6c** or **6d** obtained in each sample was determined with respect to the internal standard *n*-dodecane. The data of the concentration of the product **6c** or **6d** versus time (min) plot was drawn with Origin Pro 8.5, and the rate was determined by initial rate method (up to 35 min). The data were taken from the average of two independent experiments. The initial rate obtained for the transfer hydrogenation of 1-methoxy-4-(phenylethynyl)benzene (**5c**) was $1.02 \times 10^{-3} \text{ Mmin}^{-1}$. Similarly, the rate for the transfer hydrogenation of 1-(phenylethynyl)-4-(trifluoromethyl)benzene (**5d**) was $0.77 \times 10^{-3} \text{ Mmin}^{-1}$. Therefore, the $\text{rate}_{(4\text{-OMe})}/\text{rate}_{(4\text{-CF}_3)} = 1.02 \times 10^{-3}/0.77 \times 10^{-3} = 1.32$.

Table 2.4. Time-dependent formation of product **6c** or **6d** from **5c** or **5d** respectively.

Time (min)	6c [M]	6d [M]
2.5	0.0240	0.0249
5	0.0319	0.0272
10	0.0345	0.0303
15	0.0396	0.0328
20	0.0442	0.0355
25	0.0499	0.0413
30	0.0538	0.0474
35	0.0603	0.0496

2.4.7.2 Procedure for Competition Experiment (Electronic Effect)

To a flame dried screw-cap tube equipped with magnetic stir bar were introduced 1-methoxy-4-(phenylethynyl)benzene (**5c**, 0.042 g, 0.2 mmol) or 1-(phenylethynyl)-4-

(trifluoromethyl)benzene (**5d**, 0.049 g, 0.2 mmol), $\text{NH}_3\text{-BH}_3$ (0.006 g, 0.2 mmol), **4b** (0.0029 g, 3 mol%), and MeOH (1 mL) inside the glove-box. The reaction mixture was then stirred at room temperature on magnetic stirrer for 30 min. After that the reaction was quenched with MeOH and purification by column chromatography on silica gel yielded product **6c** (0.068 mmol) and **6d** (0.058 mmol).

2.4.7.3 Procedure for Deuterium Labelling Experiment

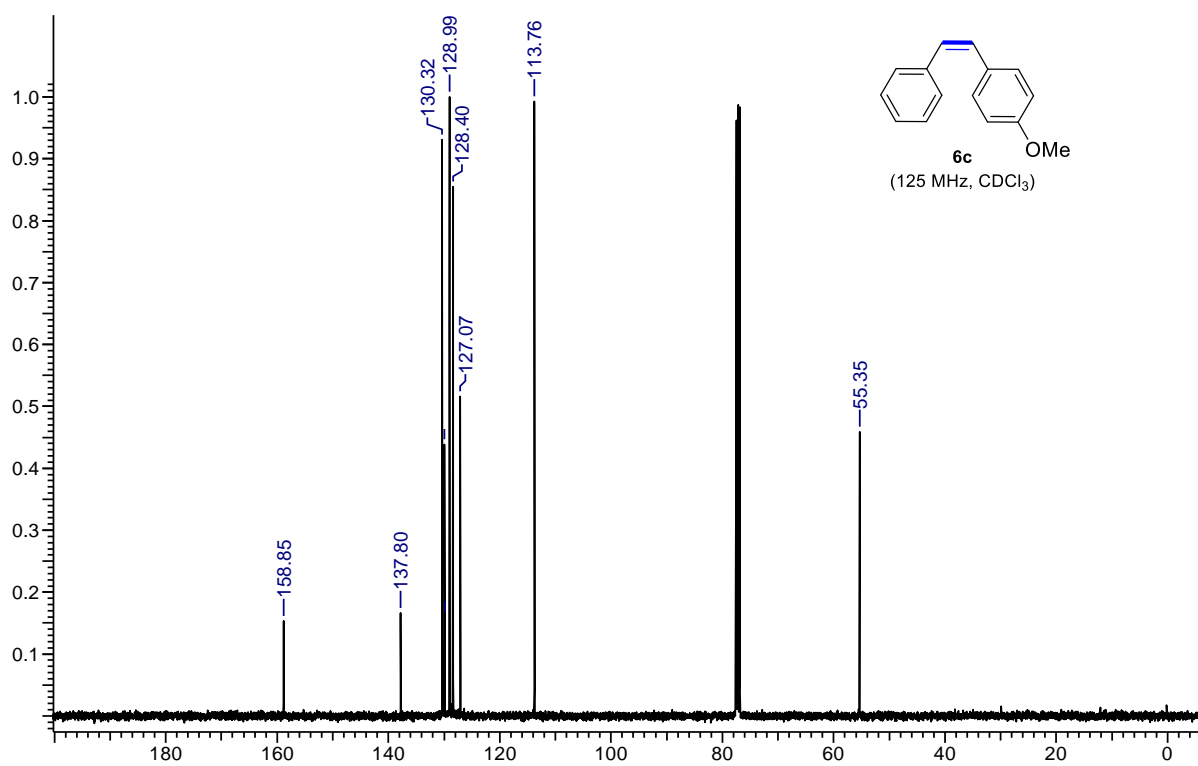
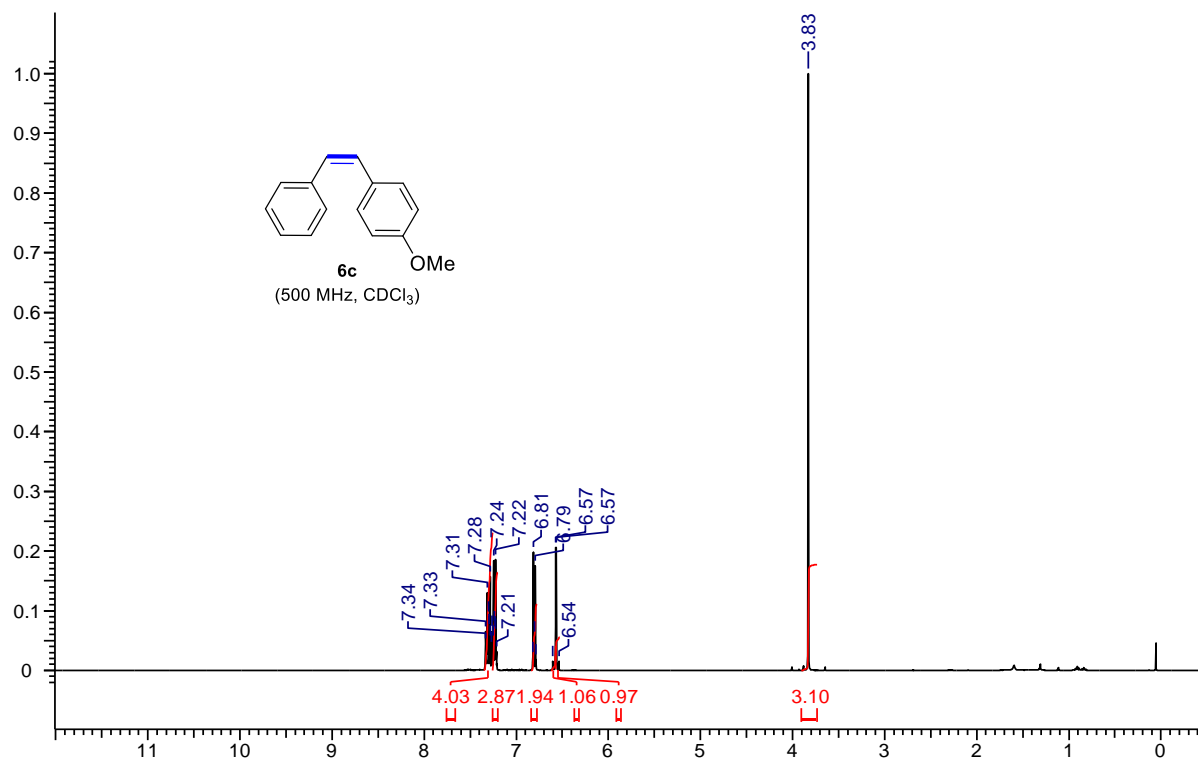
A teflon screw-cap tube equipped with magnetic bar was introduced the catalyst **4b** (0.0048 g, 0.01 mmol), ammonia-borane (0.0155 g, 0.5 mmol) and diphenylacetylene (0.089 g, 0.5 mmol) inside the glove box. The solvent CD_3OD (1.5 mL) was added to the reaction vessel under the argon atmosphere. The reaction mixture was then stirred at room temperature (27 °C) for 16 h. At ambient temperature, the reaction mixture was diluted with MeOH (5.0 mL) and resulting solution was concentrated under vacuum. The crude reaction mixture was then purified by flash chromatography using petroleum ether as eluent to obtain deuterated (*Z*)-stilbene **6a-[D]** (0.078g, 86%).

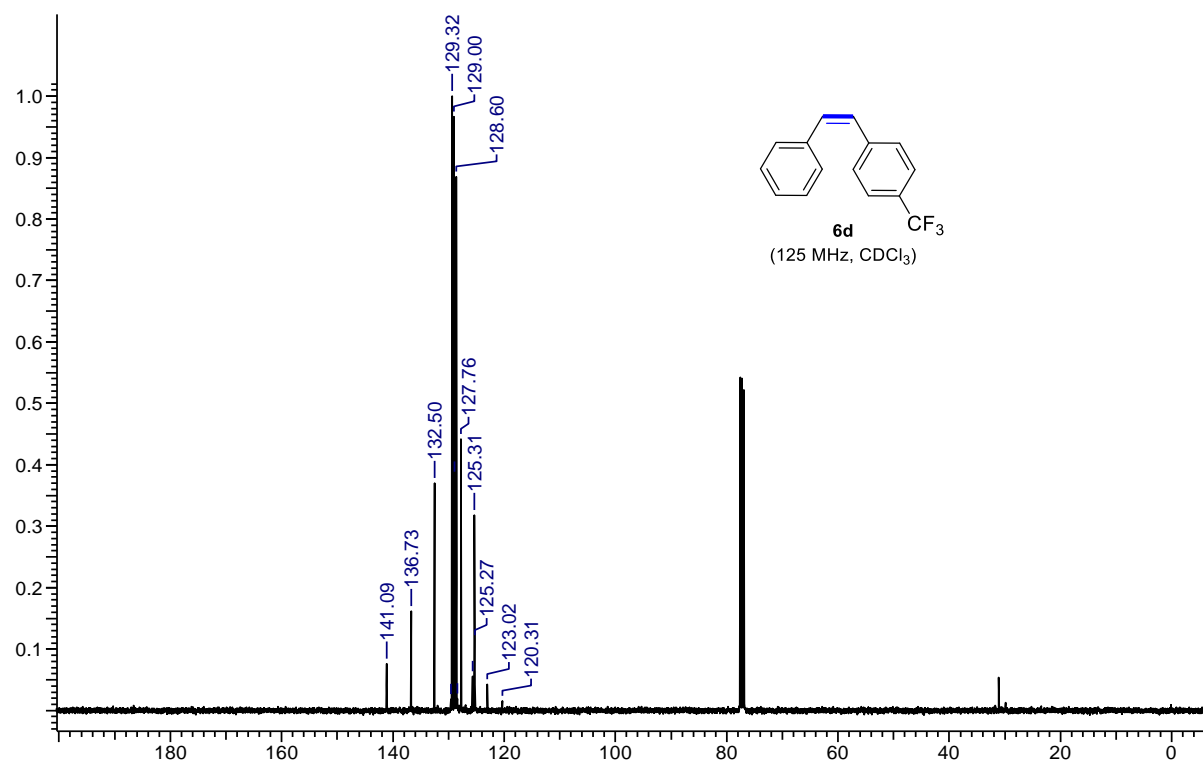
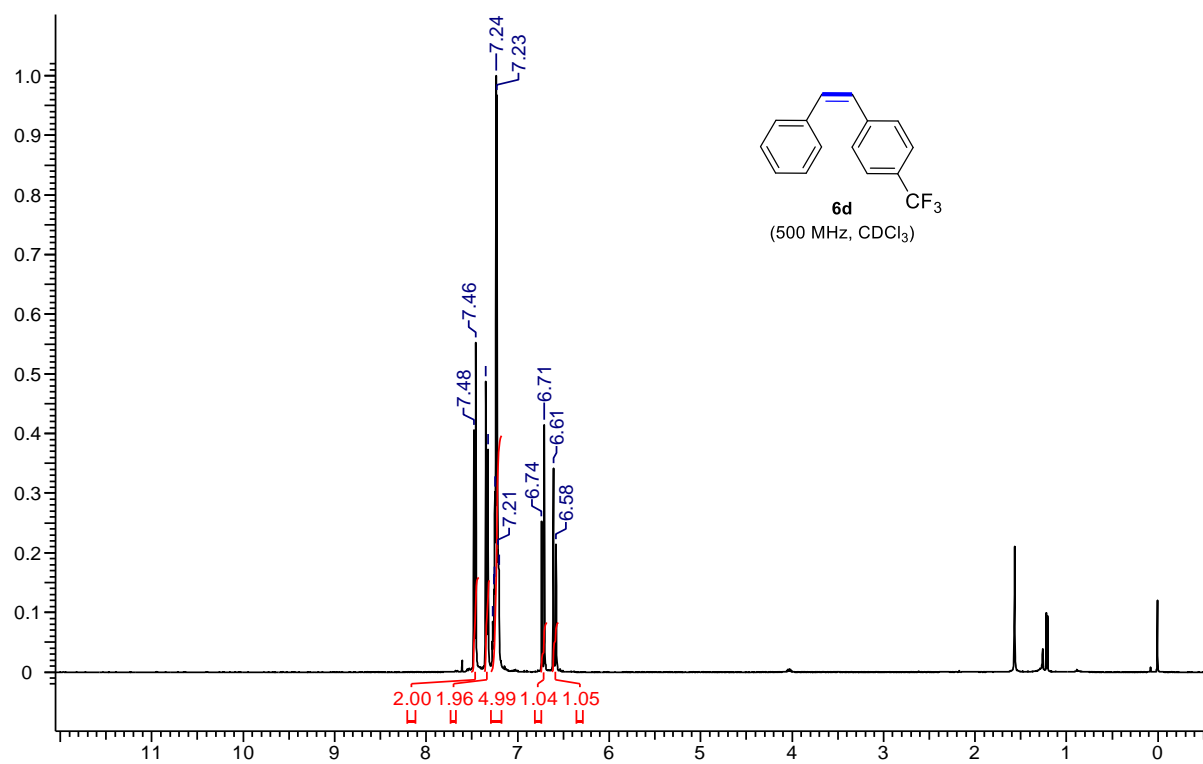
2.4.7.4 Procedure for Attempted Over-Hydrogenation with Excess of H_3NBH_3 (from **5a**)

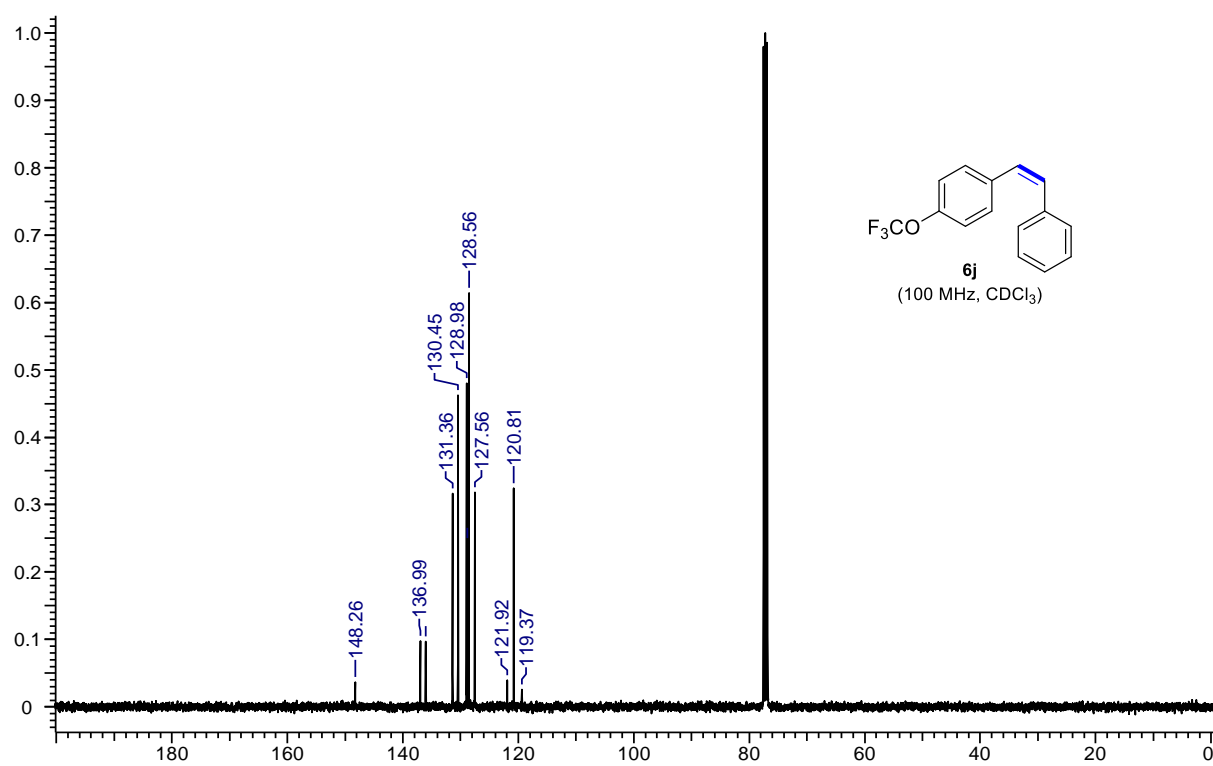
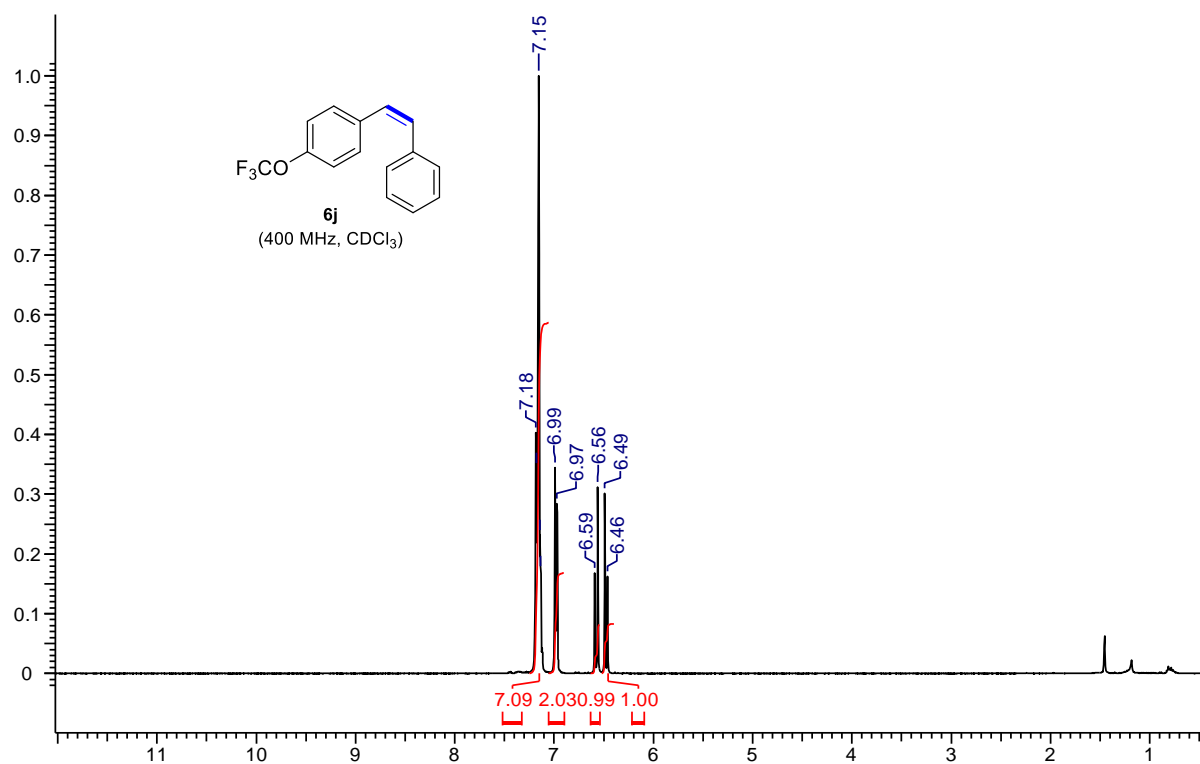
A Teflon screw-cap tube equipped with magnetic bar was introduced the catalyst **4b** (0.0048 g, 0.01 mmol), ammonia-borane (0.031 g, 1 mmol) and diphenylacetylene (0.089 g, 0.5 mmol) inside the glove box. The solvent MeOH (2 mL) was added to the reaction vessel under the argon atmosphere. The reaction mixture was then stirred at room temperature (27 °C) for 16 h. At ambient temperature, the reaction mixture was diluted with MeOH (5.0 mL) and resulting solution was concentrated under vacuum. The crude reaction mixture was then purified by flash chromatography using petroleum ether as eluent to obtain (*Z*)-stilbene **6a** (0.067 g, 74%).

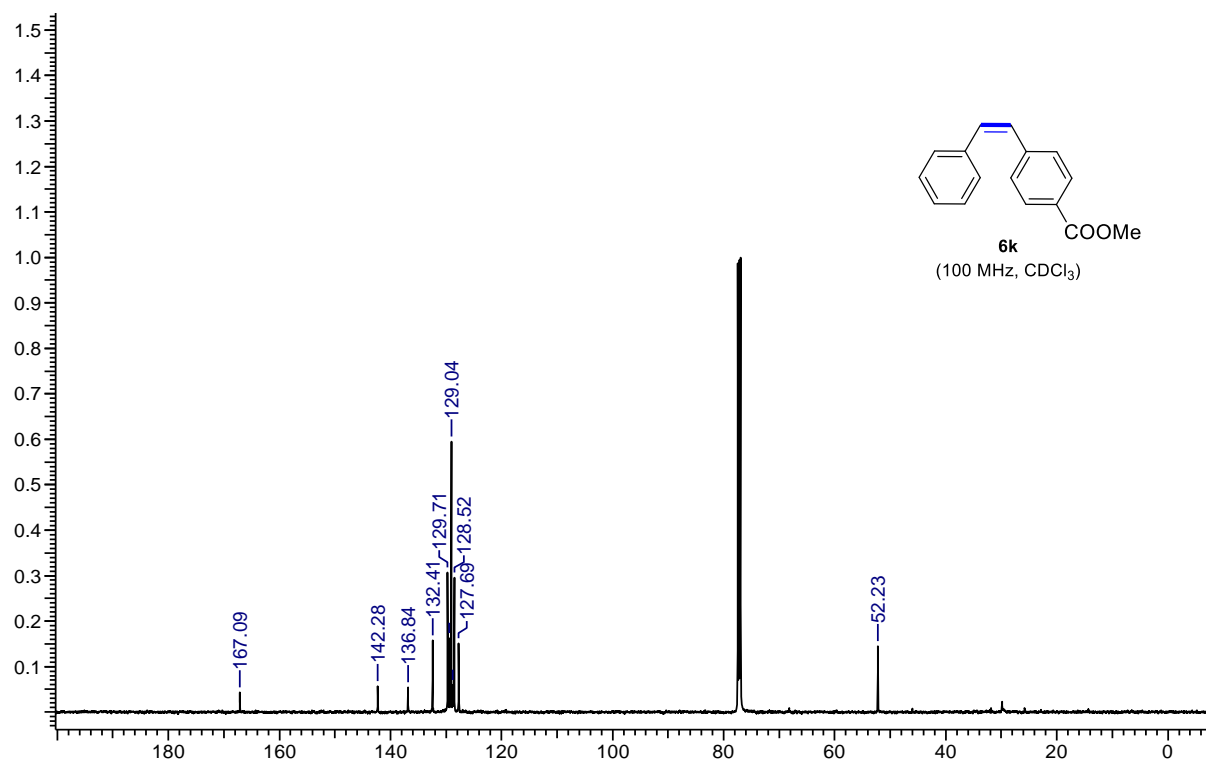
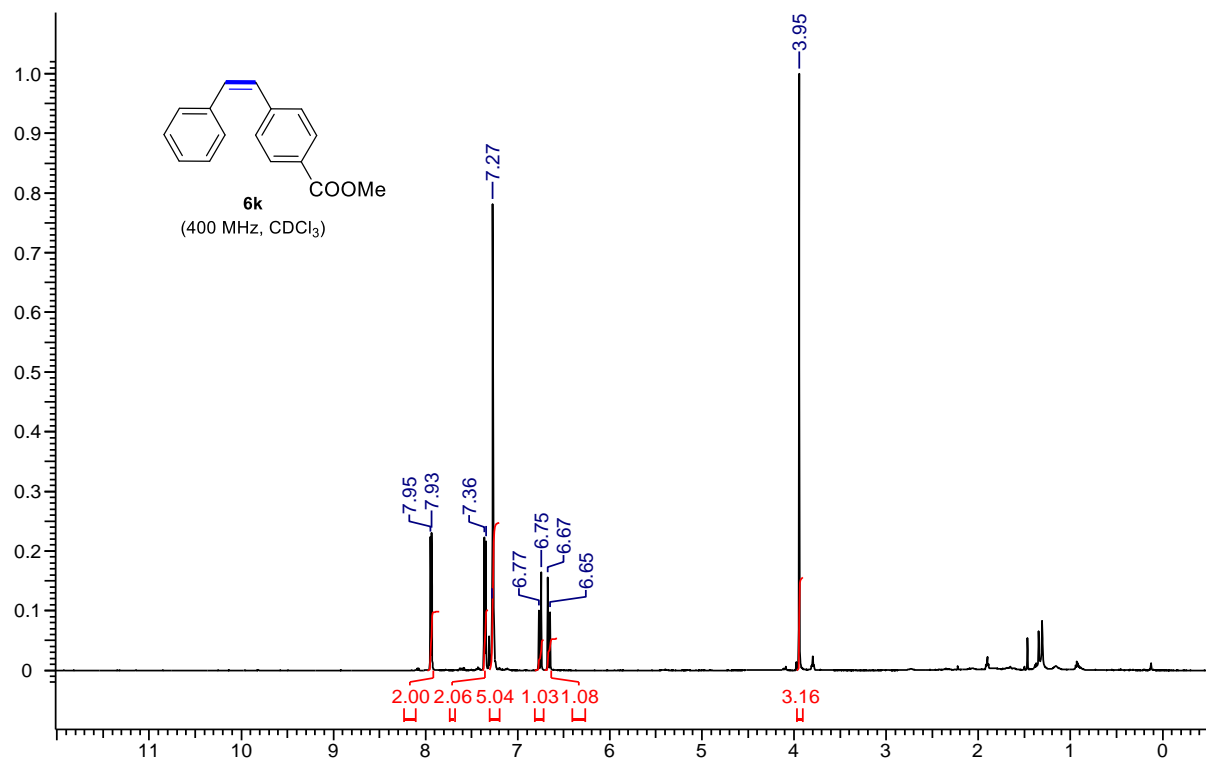
2.4.7.5 Procedure for Attempted Isomerization of (*Z*)-Stilbene

A teflon screw-cap tube equipped with magnetic bar was introduced the catalyst **4b** (0.0048 g, 0.01 mmol), ammonia-borane (0.0155 g, 0.5 mmol) and (*Z*)-stilbene (0.090 g, 0.5 mmol) inside the glove box. The solvent MeOH (1.5 mL) was added to the reaction vessel under the argon atmosphere. The reaction mixture was then stirred at 60 °C for 16 h. At ambient temperature, the reaction mixture was diluted with MeOH (5.0 mL) and resulting solution was concentrated under vacuum. The crude reaction mixture was then purified by flash chromatography using petroleum ether as eluent to obtain (*E*)-stilbene **7a** (0.050 g, 55%).









2.5 REFERENCES

- (1) Oger, C.; Balas, L.; Durand, T.; Galano, J.-M. *Chem. Rev.* **2013**, *113*, 1313-1350.
- (2) Tron, G. C.; Pirali, T.; Sorba, G.; Pagliai, F.; Busacca, S.; Genazzani, A. A. *J. Med. Chem.* **2006**, *49*, 3033-3044.
- (3) Semenov, V. V.; Kiselyov, A. S.; Titov, I. Y.; Sagamanova, I. K.; Ikizalp, N. N.; Chernysheva, N. B.; Tsyganov, D. V.; Konyushkin, L. D.; Firgang, S. I.; Semenov, R. V.; Karmanova, I. B.; Raihstat, M. M.; Semenova, M. N. *J. Nat. Prod.* **2010**, *73*, 1796-1802.
- (4) Fouché, M.; Rooney, L.; Barrett, A. G. M. *J. Org. Chem.* **2012**, *77*, 3060-3070.
- (5) Nicolaou, K. C.; Daines, R. A.; Chakraborty, T. K.; Ogawa, Y. *J. Am. Chem. Soc.* **1987**, *109*, 2821-2822.
- (6) Odinokov, V. N. *Chem. Nat. Compd.* **2000**, *36*, 11-39.
- (7) Blakemore, P. R. *J. Chem. Soc., Perkin Trans.* **2002**, 2563-2585.
- (8) Keitz, B. K.; Endo, K.; Patel, P. R.; Herbert, M. B.; Grubbs, R. H. *J. Am. Chem. Soc.* **2012**, *134*, 693-699.
- (9) Schrock, R. R.; Osborn, J. A. *J. Am. Chem. Soc.* **1976**, *98*, 2143-2147.
- (10) Crespo-Quesada, M.; Cárdenas-Lizana, F.; Dessimoz, A.-L.; Kiwi-Minsker, L. *ACS Catal.* **2012**, *2*, 1773-1786.
- (11) Trost, B. M.; Ball, Z. T.; Jöge, T. *J. Am. Chem. Soc.* **2002**, *124*, 7922-7923.
- (12) Radkowski, K.; Sundararaju, B.; Fürstner, A. *Angew. Chem. Int. Ed.* **2013**, *52*, 355-360.
- (13) Leutzsch, M.; Wolf, L. M.; Gupta, P.; Fuchs, M.; Thiel, W.; Farès, C.; Fürstner, A. *Angew. Chem. Int. Ed.* **2015**, *54*, 12431-12436.
- (14) Shen, R.; Chen, T.; Zhao, Y.; Qiu, R.; Zhou, Y.; Yin, S.; Wang, X.; Goto, M.; Han, L.-B. *J. Am. Chem. Soc.* **2011**, *133*, 17037-17044.
- (15) van Laren, M. W.; Elsevier, C. J. *Angew. Chem. Int. Ed.* **1999**, *38*, 3715-3717.
- (16) Shirakawa, E.; Otsuka, H.; Hayashi, T. *Chem. Commun.* **2005**, 5885-5886.
- (17) Tani, K. e.; Iseki, A.; Yamagata, T. *Chem. Commun.* **1999**, 1821-1822.
- (18) Yang, J.; Wang, C.; Sun, Y.; Man, X.; Li, J.; Sun, F. *Chem. Commun.* **2019**, *55*, 1903-1906.
- (19) Huang, Z.; Wang, Y.; Leng, X.; Huang, Z. *J. Am. Chem. Soc.* **2021**, *143*, 4824-4836.
- (20) Wang, D.; Astruc, D. *Chem. Rev.* **2015**, *115*, 6621-6686.

-
- (21) Brzozowska, A.; Azofra, L. M.; Zubar, V.; Atodiresei, I.; Cavallo, L.; Rueping, M.; El-Sepelgy, O. *ACS Catal.* **2018**, *8*, 4103-4109.
- (22) Garbe, M.; Budweg, S.; Papa, V.; Wei, Z.; Hornke, H.; Bachmann, S.; Scalone, M.; Spannenberg, A.; Jiao, H.; Junge, K.; Beller, M. *Catal. Sci. Technol.* **2020**, *10*, 3994-4001.
- (23) Zubar, V.; Sklyaruk, J.; Brzozowska, A.; Rueping, M. *Org. Lett.* **2020**, *22*, 5423-5428.
- (24) Sklyaruk, J.; Zubar, V.; Borghs, J. C.; Rueping, M. *Org. Lett.* **2020**, *22*, 6067-6071.
- (25) Srimani, D.; Diskin-Posner, Y.; Ben-David, Y.; Milstein, D. *Angew. Chem. Int. Ed.* **2013**, *52*, 14131-14134.
- (26) Richmond, E.; Moran, J. *J. Org. Chem.* **2015**, *80*, 6922-6929.
- (27) Barrios-Francisco, R.; Garcia, J. *J. Appl. Catal. A* **2010**, *385*, 108-113.
- (28) Thiel, N. O.; Teichert, J. F. *Org. Biomol. Chem.* **2016**, *14*, 10660-10666.
- (29) Semba, K.; Fujihara, T.; Xu, T.; Terao, J.; Tsuji, Y. *Adv. Synth. Catal.* **2012**, *354*, 1542-1550.
- (30) Wakamatsu, T.; Nagao, K.; Ohmiya, H.; Sawamura, M. *Organometallics* **2016**, *35*, 1354-1357.
- (31) Pape, F.; Thiel, N. O.; Teichert, J. F. *Chem. Eur. J.* **2015**, *21*, 15934-15938.
- (32) Korytiaková, E.; Thiel, N. O.; Pape, F.; Teichert, J. F. *Chem. Commun.* **2017**, *53*, 732-735.
- (33) Alig, L.; Fritz, M.; Schneider, S. *Chem. Rev.* **2019**, *119*, 2681-2751.
- (34) Mukherjee, A.; Milstein, D. *ACS Catal.* **2018**, *8*, 11435-11469.
- (35) Liu, W.; Sahoo, B.; Junge, K.; Beller, M. *Acc. Chem. Res.* **2018**, *51*, 1858-1869.
- (36) Ai, W.; Zhong, R.; Liu, X.; Liu, Q. *Chem. Rev.* **2019**, *119*, 2876-2953.
- (37) Tokmic, K.; Fout, A. R. *J. Am. Chem. Soc.* **2016**, *138*, 13700-13705.
- (38) Chen, J.; Shen, X.; Lu, Z. *J. Am. Chem. Soc.* **2020**, *142*, 14455-14460.
- (39) Chen, C.; Huang, Y.; Zhang, Z.; Dong, X.-Q.; Zhang, X. *Chem. Commun.* **2017**, *53*, 4612-4615.
- (40) Chen, K.; Zhu, H.; Li, Y.; Peng, Q.; Guo, Y.; Wang, X. *ACS Catal.* **2021**, *11*, 13696-13705.
- (41) Fu, S.; Chen, N.-Y.; Liu, X.; Shao, Z.; Luo, S.-P.; Liu, Q. *J. Am. Chem. Soc.* **2016**, *138*, 8588-8594.
- (42) Chen, J.; Guo, J.; Lu, Z. *Chin. J. Chem.* **2018**, *36*, 1075-1109.
- (43) Landge, V. G.; Pitchaimani, J.; Midya, S. P.; Subaramanian, M.; Madhu, V.; Balaraman, E. *Catal. Sci. Technol.* **2018**, *8*, 428-433.
-

-
- (44) Li, K.; Khan, R.; Zhang, X.; Gao, Y.; Zhou, Y.; Tan, H.; Chen, J.; Fan, B. *Chem. Commun.* **2019**, 55, 5663-5666.
- (45) Soni, V.; Jagtap, R. A.; Gonnade, R. G.; Punji, B. *ACS Catal.* **2016**, 6, 5666-5672.
- (46) Soni, V.; Khake, S. M.; Punji, B. *ACS Catal.* **2017**, 7, 4202-4208.
- (47) Yan, Q.; Fang, Y. C.; Jia, Y. X.; Duan, X. H. *New J. Chem.* **2017**, 41, 2372-2377.
- (48) Mukherjee, A.; Srimani, D.; Chakraborty, S.; Ben-David, Y.; Milstein, D. *J. Am. Chem. Soc.* **2015**, 137, 8888-8891.
- (49) Obligacion, J. V.; Semproni, S. P.; Chirik, P. J. *J. Am. Chem. Soc.* **2014**, 136, 4133.
- (50) Kim, B. S.; Jang, C.; Lee, D. J.; Youn, S. W. *Chem. Asian J.* **2010**, 5, 2336-2340.
- (51) Xu, J.; Shen, C.; Zhu, X.; Zhang, P.; Ajitha, M. J.; Huang, K.-W.; An, Z.; Liu, X. *Chem. Asian J.* **2016**, 11, 882-892.
- (52) Chen, C.; Hecht, M. B.; Kavara, A.; Brennessel, W. W.; Mercado, B. Q.; Weix, D. J.; Holland, P. L. *J. Am. Chem. Soc.* **2015**, 137, 13244-13247.
- (53) Enthaler, S.; Haberberger, M.; Irran, E. *Chem. Asian J.* **2011**, 6, 1613-1623.

Chapter 3

Selective Synthesis of Secondary Amines from Nitriles by (Xantphos)CoCl₂ Complex

This chapter has been partly adapted from the publication "Selective Synthesis of Secondary Amines from Nitriles by a User-Friendly Cobalt Catalyst" **Sharma, D. M.**; and Punji, B. *Adv. Synth. Catal.*, **2019**, *361*, 3930–3936.

3.1 INTRODUCTION

Amines are the privileged organic compounds extensively used as starting materials in the pharmaceuticals, agrochemicals, fungicides, fragrances, plastics, and dyes.¹⁻³ Thus, efficient and cost-effective synthesis of amines using a simple catalyst system is very crucial. Among the various methods developed, the synthesis of amines by the catalytic reduction of nitriles is the most common route and is among the active field of research significance.²⁻⁴ However, the catalytic reduction of nitriles suffers from critical selectivity problem leading to the formation of various amines, like primary amines, secondary amines, and tertiary amines, as well as imines. Nevertheless, notable methods are known for the selective synthesis of amines *or* imines from nitriles *via* direct hydrogenation using 4d noble metal catalysts, such as molybdenum,⁵ ruthenium,⁶⁻¹² rhodium,¹³⁻¹⁷ palladium,^{14,18} iridium,^{15,19} platinum.²⁰ Considering the sustainability and environmental benefits, recently, diverse 3d transition metal-based catalysts have been employed for the reduction of nitriles to amines and imines. For example, the groups of Beller, Milstein, and others have extensively reported on the hydrogenation of nitriles using pincer ligated manganese,²¹ iron,²²⁻²⁶ and cobalt²⁷⁻³⁴ catalysts.^{35,36} Guan has demonstrated the reduction of nitriles to primary amines in the absence of ligand, whereas the reaction led to aldimines employing ⁱPrPNP/CoX₂ catalyst.³¹ Notably, all the reported direct hydrogenation of nitriles uses a very high hydrogen pressure, which needed special reaction set-up and expertise, and could be hazardous.

The transfer hydrogenation is an alternative protocol to the direct hydrogenation of nitriles,³⁷ wherein sacrificial hydrogen source is used in place of hydrogen pressure, and simple reaction set-up is needed. In that direction, the hydrogenation of nitriles to primary- and tertiary amines has been reported by palladium catalysis using HCOOH/base as the hydrogen source.^{38,39} Similarly, the ruthenium-catalyzed reduction of nitriles to primary and secondary amines has been demonstrated.⁴⁰⁻⁴³ Considering the importance and sustainability of base metal catalysis, Li and Garcia independently demonstrated the cobalt⁴⁴ and nickel⁴⁵ catalyzed transfer hydrogenation of nitriles to primary amines and imines, wherein the selectivity remained a challenging task. Although, the selective direct hydrogenation *or* transfer hydrogenation of nitriles to primary amines and aldimines is significantly progressed, the report on the selective synthesis of secondary amines *via* reductive amination of nitriles is scarce, with one example of the (PNN)-pincer cobalt catalyzed hydrogenation of nitriles to secondary amines using ammonia-borane is demonstrated by Zhou and Liu.⁴⁶

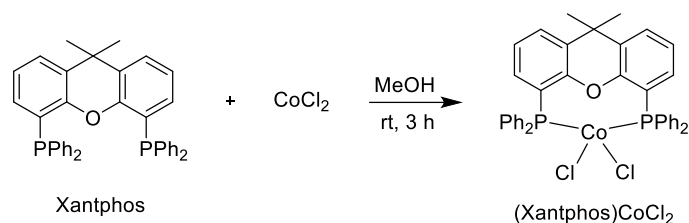
Furthermore, the developed protocols for the synthesis of amines from nitriles have certain limitations. For example, most of the approaches employ a tridentate pincer-ligated catalyst system,^{4,47,48} wherein the synthesis of pincer ligands and corresponding catalysts involves multiple steps. Besides, most of the employed ligand systems are based on the expensive and sensitive alkyl phosphines, and hence, requires specialized expertise on the ligand synthesis. Thus, a generalized protocol for the synthesis of secondary amines by using a commercially available ligand with inexpensive cobalt salt under mild hydrogen source is highly desirable. To address these limitations associated with the existing amination/reductive amination protocols, in this chapter, we discuss the development of a user-friendly (Xantphos)CoCl₂ catalyst system for the selective reductive amination of nitriles to symmetrical and unsymmetrical secondary amines under mild conditions. Thus, the cobalt catalyst selectively reduces the aromatic nitriles to symmetrical secondary amines using ammonia-borane (H₃N-BH₃) as a hydrogen source, whereas the use of external amines and dimethylamine borane (Me₂NH-BH₃) afforded unsymmetrical secondary and tertiary amines.

3.2 RESULTS AND DISCUSSION

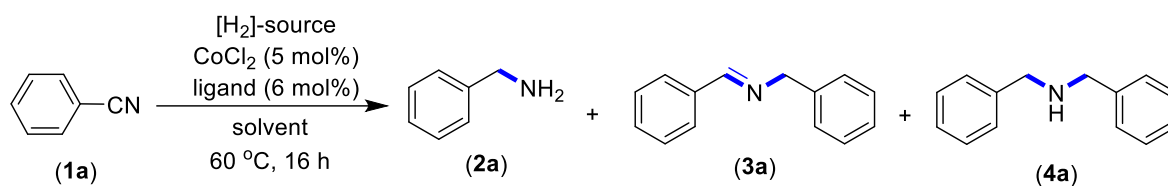
3.2.1 Optimization of Reaction Condition for the Synthesis of Symmetrical Secondary Amines

We initiated the optimization studies for the reductive amination of benzonitrile (**1a**) to afford secondary amine **4a** employing CoCl₂ and various commercially available nitrogen- and phosphine ligands (Table 3.1). Based on the literature precedents, we could quickly rationalize that the alcoholic solvents are suitable for the reductive amination. Thus, the reductive amination of benzonitrile (0.3 mmol) as a model substrate using simple CoCl₂ (5 mol%) as a catalyst and inexpensive dimethylamine borane (2.0 equiv) as the hydrogen source in methanol afforded dibenzylamine (**4a**) in addition to the trace formation of benzyl amine (**2a**) at 60 °C (entry 1). The reaction in ethanol or iso-propanol solvents did not lead to any significant improvement, and overall conversion was in the range of 15-25%. Notably, the reaction in the solvent HFIP was improved and gave 56% overall conversion with 27% of reductively aminated product **4a** (entry 4). The employment of nitrogen ligands bpy or phen has little influence on the overall amination reaction (entries 5,6). To our surprise, the use of phosphine ligands along with CoCl₂ gave quantitative conversion and good selectivity for the reductive amination product **4a** (entries 7-9). Particularly, the employment of Xantphos/CoCl₂ system provided 73% of dibenzylamine **4a** and 24% of aminated product **2a**

using $\text{Me}_2\text{NH}\cdot\text{BH}_3$ as the hydrogen source. Upon performing the same reaction using $\text{H}_3\text{N}\cdot\text{BH}_3$ as hydrogen source under Xantphos/ CoCl_2 catalyst system, the reaction afforded 87% of product **4a** (entry 10). The reaction led to the quantitative formation of product **4a** even at room temperature ($27\text{ }^\circ\text{C}$) (entry 11). Notably, the employment of 1.0 mol% of Xantphos/ CoCl_2 or (Xantphos) CoCl_2 (isolated complex) as catalyst (Scheme 3.1),⁴⁹ the reaction selectively gave reductive amination product **4a** in around 89% isolated yield (entries 12,13). When the $\text{Me}_2\text{HN}\cdot\text{BH}_3$ was employed as a hydrogen source under the optimized conditions, the reaction was slightly less effective (entry 14). Without a cobalt catalyst, the reaction failed to deliver the reductive amination or simple amination products (entry 15). The use of other cobalt precursors, such as CoBr_2 , $\text{Co}(\text{OAc})_2$, $\text{Co}(\text{OAc})_3$ along with Xantphos are slightly less effective. The catalytic reaction using *n*-hexane as solvent afforded 8% of primary amine (**2a**) and 3% of amine **4a**.



Scheme 3.1 Synthesis of (Xantphos) CoCl_2 Catalyst.

Table 1. Optimization of reaction parameters for the reductive amination of benzonitrile to dibenzylamine.^a

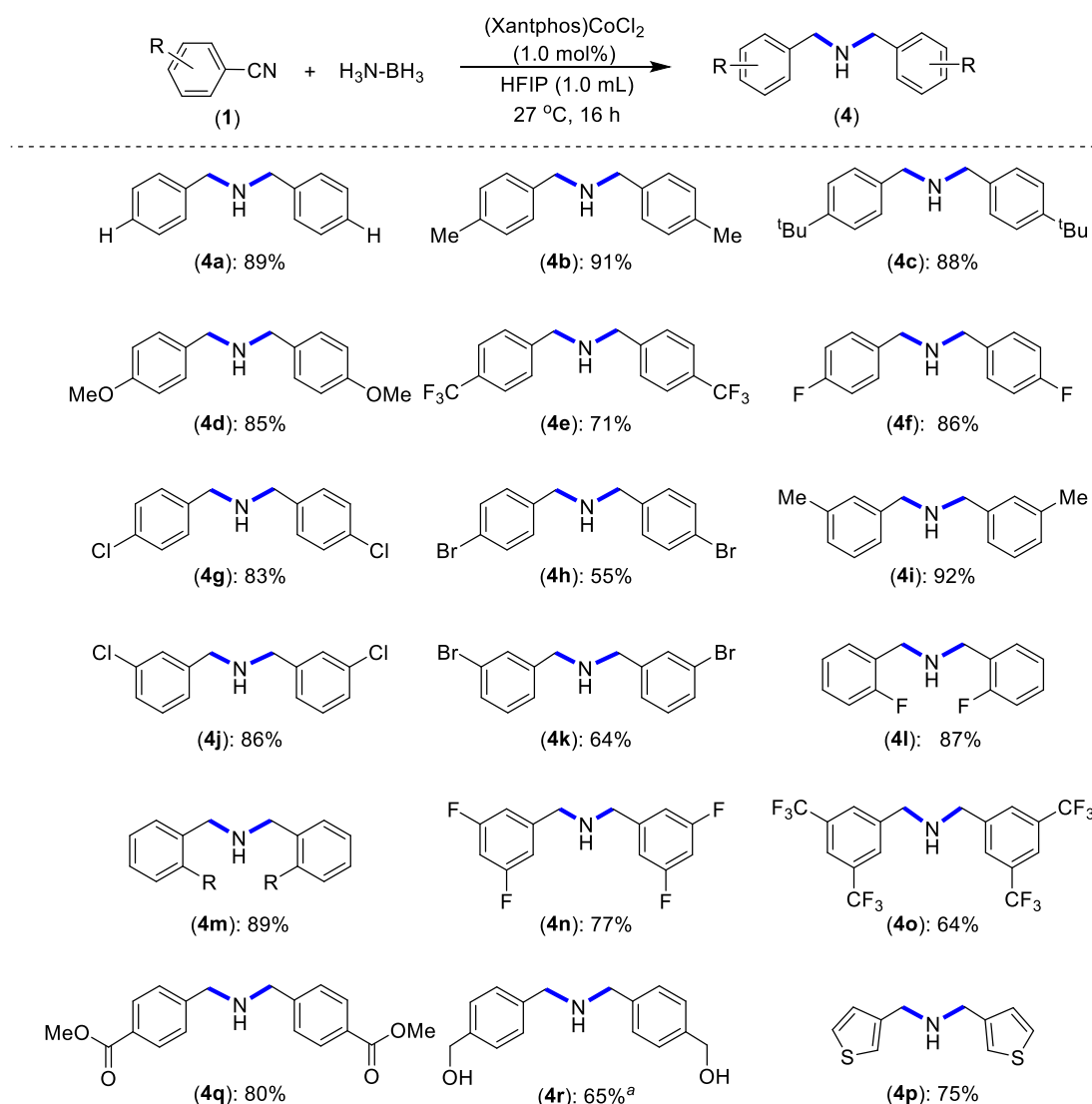
Entry	[H ₂]-Source	Ligand [or cat]	Solvent	GC conv (%) ^b	GC yield (%) ^c		
					2a	3a	4a
1	Me ₂ NH-BH ₃	-	MeOH	25	4	-	15
2	Me ₂ NH-BH ₃	-	EtOH	24	7	-	14
3	Me ₂ NH-BH ₃	-	ⁱ PrOH	15	9	-	3
4	Me ₂ NH-BH ₃	-	HFIP	56	2	3	27
5	Me ₂ NH-BH ₃	bpy	HFIP	25	14	-	7
6	Me ₂ NH-BH ₃	phen	HFIP	30	17	-	8
7 ^d	Me ₂ NH-BH ₃	PPh ₃	HFIP	100	-	16	56
8	Me ₂ NH-BH ₃	dppe	HFIP	99	3	34	61
9	Me ₂ NH-BH ₃	Xantphos	HFIP	100	24	3	73
10	NH ₃ -BH ₃	Xantphos	HFIP	100	5	2	87
11 ^e	NH ₃ -BH ₃	Xantphos	HFIP	100	4	1	90
12^{e,f}	NH₃-BH₃	Xantphos	HFIP	100	6	-	94 (88)
13^{e,f}	NH₃-BH₃	(Xantphos)CoCl₂	HFIP	100	6	-	94 (89)
14 ^e	Me ₂ NH-BH ₃	Xantphos	HFIP	75	8	12	51
15 ^e	NH ₃ -BH ₃	-	HFIP	-	-	-	-
16 ^e	NH ₃ -BH ₃	[Co]/Xantphos	HFIP	80	4	2	68
17	NH ₃ -BH ₃	(Xantphos)CoCl ₂	<i>n</i> -hexane	15	8	-	3

^aReaction conditions: Benzonitrile (0.031 g, 0.30 mmol), [H₂]-source (0.60 mmol), CoCl₂ (0.0019 g, 0.015 mmol, 5 mol%), ligand (0.018 mmol, 6 mol%), solvent (1.0 mL). ^bGC

conversion based on substrate benzonitrile. ^cYield determined using *n*-tetradecane as internal standard, isolated yield is in parenthesis. ^d12 mol% of PPh₃ was used, 25% tribenzyl amine (tertiary amine) was observed. ^eReaction carried out at 27 °C. ^fEmploying 1.0 mol% of CoCl₂/Xantphos or 1.0 mol% of (Xantphos)CoCl₂ complex. [Co] = CoBr₂, Co(OAc)₂, or Co(OAc)₃.

3.2.2 Scope for Synthesis of Symmetrical Secondary Amines

With the optimized reaction conditions in hand, we started substrate scope for the synthesis of symmetrical secondary amines using 1.0 mol% of catalyst (Xantphos)CoCl₂ and ammonia-borane (2.0 equiv) at room temperature (Scheme 3.2). Thus, the benzonitrile bearing various para-substituted functionalities, such as alkyl, alkoxy, -F, -Cl, -Br, -CF₃ smoothly underwent reductive amination to secondary benzylamines (**4a-4h**) in good to excellent yields. Both the electron-donating and electron-withdrawing functionalities favoured the reaction, thus leading to quantitative conversion. Similarly, the *meta*- and *ortho*-substituted benzonitriles participated in the reaction with excellent activity and good functional group tolerability delivering the products **4i-4m**. The tolerability of halide functionalities in the synthesis of secondary benzylamines is very crucial as these compounds can further be employed in the cross-coupling reactions. The fluoro-substituted benzonitriles, 3,5-difluorobenzonitrile and 3,5-bis(trifluoromethyl)benzonitrile underwent reductive amination under the cobalt catalysis to produce bis(3,5-difluorobenzyl)amine (**4n**) and bis(3,5-bis(trifluoromethyl)benzyl)amine (**4o**) in 77% and 64% yields, respectively. These kinds of fluoro-containing amines have extensive usage in pharmaceuticals as they significantly enhance the lipophilicity and metabolic stability of the desired drug molecule. The reductive amination reaction condition was well tolerated by aromatic nitrile with a heteroatom, i.e., 3-cyano thiophene by yielding 75% of isolated product **4p**. Furthermore, the chemo-selectivity of the methodology has been checked by using methyl-4-cyanobenzoate, wherein only the nitrile part was reduced to amine keeping the ester functionality intact (**4q**). When the 4-cyanobenzaldehyde was subjected for the reductive amination under the optimized conditions, both the carbonyl and nitrile groups were reduced to give secondary amine **4r** in 65% yield. In all the reductive amination reactions, we have selectively observed the formation of secondary amines, whereas the imines or tertiary amines were not detected. However, only traces of primary amine products were observed during the reductive amination reactions.



Scheme 3.2 Scope of reductive amination of nitriles to symmetrical secondary amines. Substrate **1** = 0.5 mmol, $\text{NH}_3\text{-BH}_3$ = 0.031 g, 1.0 mmol. ^a2.0 mmol of $\text{NH}_3\text{-BH}_3$ used.

3.2.3 Optimization of Reaction Condition and Scope for the Synthesis of Unsymmetrical Secondary Amines

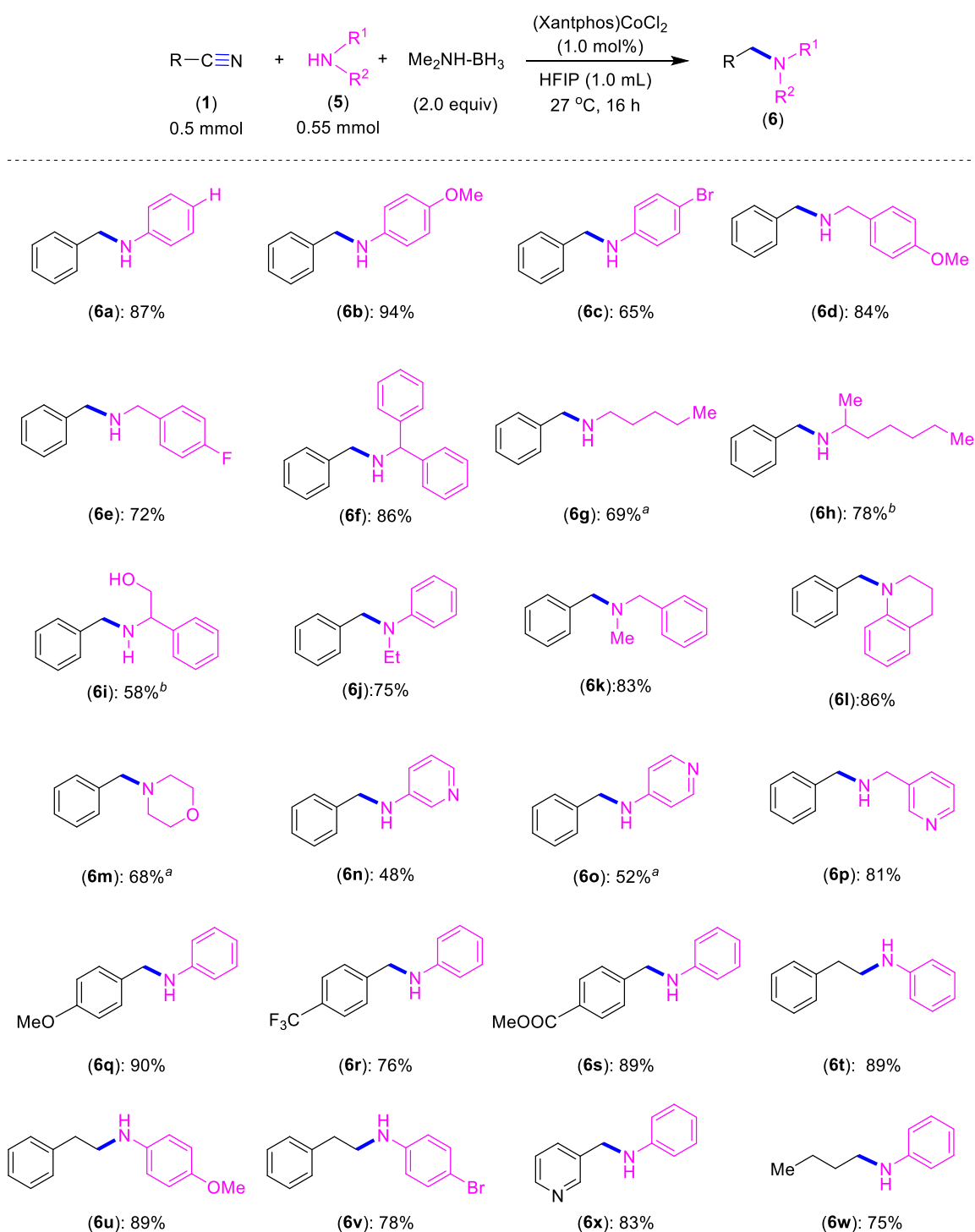
The user-friendly and inexpensive cobalt catalysis was further extended to the synthesis of unsymmetrical secondary amines and tertiary amines using diverse external amine compounds. During the reaction optimization, we have found that the use of less expensive dimethylamine-borane ($\text{Me}_2\text{NH-BH}_3$) instead of ammonia-borane as a hydrogen source was beneficial for the synthesis of unsymmetrical amines and resulted with high selectivity of the desired compound (Table 2). Thus, dimethylamine-borane was employed for the synthesis of unsymmetrical secondary amines, and tertiary amines. Initially, we have performed reductive amination of benzonitrile using diverse external amines (Scheme 3.3).

The benzonitrile underwent partial reduction and reacted smoothly with aniline derivatives to afford the desired products **6a-6c** in good to excellent yields. Similarly, benzylamines participated in the reductive amination of benzonitrile to deliver products **6d-6f** in attractive yields. In addition to the aromatics and benzylamines, the aliphatic amines can be used as external amine source for the reaction yielding **6g** and **6h** in 69% and 78%, respectively. The amine **5i** bearing –OH functionality reacted smoothly to produce the desired secondary amine (**6i**) in moderate yield. Additionally, the secondary amines as nucleophiles took part in the reductive amination of benzonitrile to give tertiary amines **6j** and **6k** in 75% and 83% yield, respectively. The secondary cyclic amines 1,2,3,4-tetrahydroquinoline and morpholine upon reaction with benzonitrile under reductive amination conditions afforded tertiary amines **6l** and **6m** in excellent yields. The reaction tolerated pyridinyl-substituted compounds and underwent reductive amination in moderate to good yields (**6n-6p**). Furthermore, electronically distinct substituents, such as –OMe, –Br, –CF₃, –COOMe were well tolerated on the benzonitrile backbone and delivered the desired products (**6q-6s**) in good to excellent yields. In addition to the aromatic nitriles, the aliphatic nitriles 2-phenylacetonitriles and butyronitrile underwent reductive amination with aniline derivatives to give secondary amines **6t-6w** in good yields. The heteroarenes nitrile, nicotinonitrile upon treatment with aniline under reductive amination conditions afforded **6x** in 83% yield. Notably, the use of 1,3-dicyanobenzene upon reductive amination with aniline produced **6y** in 74% yield, which can be employed as a tridentate *NCN*-pincer type of ligand.

Table 2. Reaction conditions for the reductive amination of benzonitrile to unsymmetrical amine.^a

entry	[H ₂]-source	GC conv. (%) ^b	GC yield (%) ^c		
			4a	6a	others
1	H ₃ N-BH ₃	100	27	68	< 4
2	Me ₂ NH-BH ₃	100	7	91 (87)	< 2

^aReaction conditions: Benzonitrile (**1a**, 0.052 g, 0.50 mmol), aniline (**5a**, 0.051 g, 0.55 mmol), [H₂]-source (1.0 mmol), (Xantphos)CoCl₂ (0.0035 g, 0.005 mmol, 1.0 mol%). ^bGC conversion based on substrate benzonitrile. ^cYield determined using *n*-tetradecane as internal standard, isolated yield is in parenthesis.

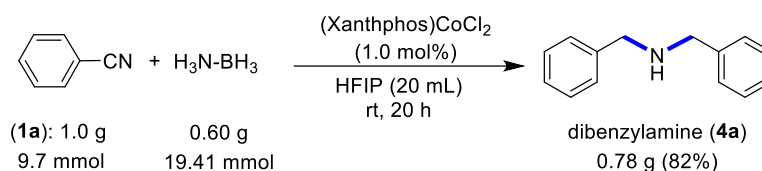


Scheme 3.3 Scope of reductive amination of nitriles to unsymmetrical secondary amines.

^a0.75 mmol of amine used. ^b1.0 mmol of amine used. ^c4.0 equiv of Me₂NH-BH₃ is used.

3.2.4 Gram Scale Synthesis of Secondary Amine

Considering the synthetic importance of secondary amines and taking advantage of simple cobalt catalyzed protocol, we have demonstrated the practical utility of the developed method for the synthesis of symmetrical secondary amine in gram scale. Thus, the reductive amination of 1.0 g benzonitrile with $\text{NH}_3\text{-BH}_3$ using $(\text{Xantphos})\text{CoCl}_2$ in HFIP gave 82% yield of product **4a** (Scheme 3.4).



Scheme 3.4 Gram scale synthesis.

3.2.5 Probable Catalytic Cycle

After studying the reaction and the literature precedents, we have proposed a probable catalytic cycle for the $(\text{Xantphos})\text{CoCl}_2$ -catalyzed transfer-hydrogenation of nitriles to secondary amines (Figure 3.1). The $(\text{Xantphos})\text{CoCl}_2$ catalyst in the presence of the ammonia-borane/dimethylammonia-borane would be converted into a Co-hydride intermediate **A**. The nitrile will then coordinate the cobalt center in **A** in an end-on fashion to give intermediate **B**. The migratory insertion of nitrile into the Co-H bond would result in the formation of intermediate **C**. The Co-imine bond in **C** would undergo protonation in the presence of HFIP, forming an imine intermediate along with species **D**. Finally, the intermediate **D** on reaction with ammonia-borane/dimethylammonia-borane provides the active catalyst (**A**) back. In the next cycle, the imine intermediate would be hydrogenated to the primary amine, following the same path described for imine formation. Finally, the condensation of the imine with primary imine will afford the secondary amine as the exclusive product.

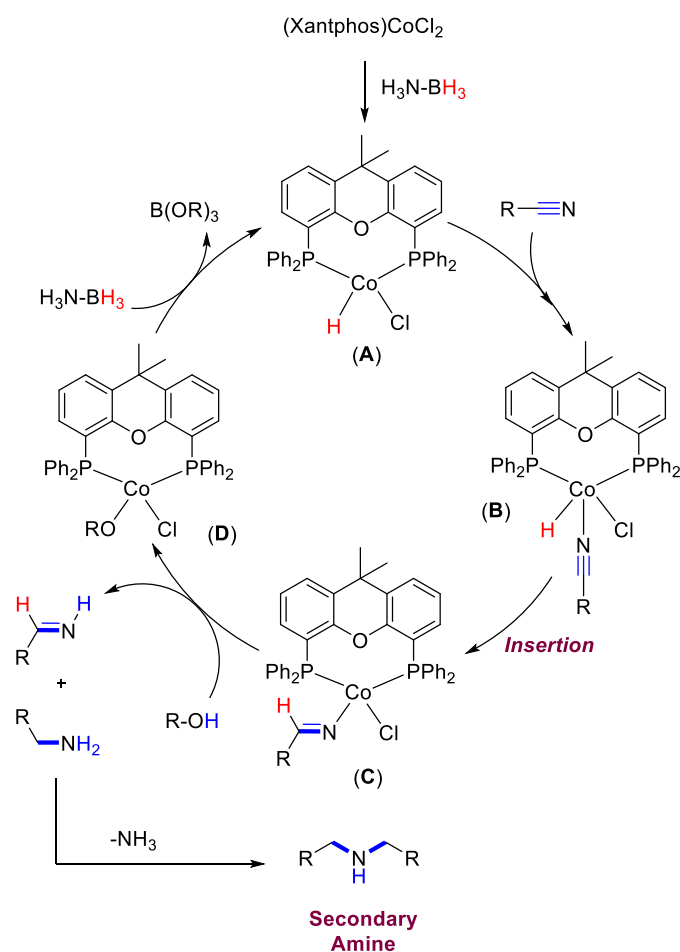


Figure 3.1 Proposed mechanism for nitrile transfer hydrogenation.

3.3 CONCLUSION

In conclusion, in this chapter, we have developed a simple, inexpensive and user-friendly cobalt-catalyzed method for the selective and practical synthesis of symmetrical and unsymmetrical secondary amines *via* reductive amination of nitriles. The employment of $(\text{Xantphos})\text{CoCl}_2$ and ammonia borane ($\text{NH}_3\text{-BH}_3$) led to the selective reduction of the nitriles to symmetrical secondary amines, whereas the use of dimethylamine borane ($\text{Me}_2\text{NH-BH}_3$) along with external amines selectively afforded unsymmetrical secondary amines, and tertiary amines. The reaction tolerated diverse functionalities, such as alkyl, alkyl ether, halides ($-\text{F}$, $-\text{Cl}$, $-\text{Br}$), $-\text{CF}_3$, $-\text{COOMe}$ and heteroarenes like pyridine and thiophene. A free alcohol group ($-\text{OH}$) which could quench the $(\text{Xantphos})\text{CoCl}_2$ catalyst, also tolerated the under the optimized reaction condition. Both the aromatic and aliphatic nitriles efficiently took part in the reaction to afford the secondary amines in excellent yields. Different external amine sources like primary and secondary amines were compatible for the reaction with nitriles and provided good to excellent yields for the respective secondary or tertiary amines.

The transfer hydrogenation of benzonitrile carried out at the gram scale which worked smoothly and afforded 82% of the dibenzylamine. The *NCN*-based pincer ligand *N,N'*-(1,3-phenylenebis(methylene))dianiline was synthesized from the reaction of aniline with 1,3-dicyanobenzene using the optimized transfer hydrogenative protocol. The developed user-friendly method is expected to be beneficial for the practical use in the synthesis of symmetrical and unsymmetrical secondary amines.

3.4 EXPERIMENTAL SECTION

3.4.1 General Experimental

All manipulations were conducted under an argon atmosphere either in a glove box or by using standard Schlenk techniques in pre-dried glassware. The catalytic reactions were performed in flame-dried reaction vessels with Teflon screw caps. The solvent, HFIP was degassed with argon before use. All other liquid reagents were flushed with argon prior to use. The complex (Xantphos)CoCl₂ was synthesized following the literature procedure.⁴⁹ All other chemicals were obtained from commercial sources and were used without further purification. Yields refer to the isolated compounds, estimated to be >95% pure as determined by ¹H-NMR. High resolution mass spectrometry (HRMS) mass spectra were recorded with a Thermo Scientific Q-Exactive, Accela 1250 pump. ¹H and ¹³C NMR spectra were recorded at 400 or 500 MHz (¹H), 100 or 125 MHz, (¹³C, DEPT) and 377 MHz (¹⁹F) with Bruker AV 400 and AV 500 spectrometers in CDCl₃ solutions unless otherwise specified. The ¹H and ¹³C NMR spectra were referenced to residual solvent signals (CDCl₃: $\delta_{\text{H}} = 7.26$ ppm, $\delta_{\text{C}} = 77.2$ ppm).

GC Method. Gas Chromatography analyses were performed using a Shimadzu GC-2010 gas chromatograph equipped with a Shimadzu AOC-20s auto sampler and a Restek RTX-5 capillary column (30 m x 25 μm). The instrument was set to an injection volume of 1 μL , an inlet split ratio of 10:1, and inlet and detector temperatures of 250 and 320 $^{\circ}\text{C}$, respectively. UHP-grade argon was used as carrier gas with a flow rate of 30 mL/min. The temperature program used for all the analyses is as follows: 80 $^{\circ}\text{C}$, 1 min; 30 $^{\circ}\text{C}/\text{min}$ to 200 $^{\circ}\text{C}$, 2 min; 30 $^{\circ}\text{C}/\text{min}$ to 260 $^{\circ}\text{C}$, 3 min; 30 $^{\circ}\text{C}/\text{min}$ to 300 $^{\circ}\text{C}$, 3 min. *n*-Tetradecane (0.01 mL, 0.038 mmol) was used as an internal standard to calculate the GC yield.

3.4.2 Representative procedure for the synthesis of symmetrical secondary amines:

Dibenzylamine. A Teflon screw-cap tube was introduced with (Xantphos)CoCl₂ (0.0035 g, 0.005 mmol), ammonia borane (0.031 g, 1.0 mmol) and benzonitrile (0.052 g, 0.50 mmol) inside the glove box. The solvent HFIP (1.0 mL) was added to the reaction vessel under the argon atmosphere. The reaction mixture was then stirred at room temperature (27 °C) for 16 h. At ambient temperature, the reaction mixture was quenched with MeOH (5.0 mL), and the resulting solution was concentrated under vacuum. The crude reaction mixture was then purified by flash chromatography using petroleum ether/EtOAc: 5/1 as eluent to obtain dibenzylamine (**4a**; 0.044 g, 89%).

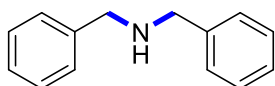
3.4.3 Representative procedure for the synthesis of unsymmetrical secondary amines:

N-Benzylaniline. A Teflon screw-cap tube was introduced with (Xantphos)CoCl₂ (0.0035 g, 0.005 mmol), dimethylamine borane (0.059 g, 1.0 mmol), benzonitrile (0.052 g, 0.50 mmol) and aniline (0.051 g, 0.55 mmol) inside the glove box. The solvent HFIP (1.0 mL) was added to the reaction vessel under the argon atmosphere. The reaction mixture was then stirred at room temperature (27 °C) for 16 h. At ambient temperature, the reaction mixture was quenched with MeOH (5.0 mL), and the resulting solution was concentrated under vacuum. The crude reaction mixture was then purified by flash chromatography using petroleum ether/EtOAc: 10/1 as eluent to obtain *N*-benzylaniline (**6a**; 0.080 g, 87%).

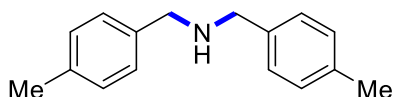
3.4.4 Procedure for gram scale synthesis of dibenzylamine (4a):

A Teflon screw-cap thick-walled pressure tube (40 mL) was introduced with (Xantphos)CoCl₂ (0.069 g, 0.097 mmol), ammonia borane (0.60 g, 19.41 mmol) and benzonitrile (1.0 g, 9.7 mmol) inside the glove box. The solvent HFIP (20.0 mL) was added to the reaction vessel under the argon atmosphere. The reaction mixture was then stirred at room temperature (27 °C) for 20 h. At ambient temperature, the reaction mixture was quenched with MeOH (30.0 mL), and the resulting solution was concentrated under vacuum. The crude reaction mixture was then purified by flash chromatography using petroleum ether/EtOAc: 5/1 as eluent to obtain dibenzylamine (**4a**; 0.78 g, 82%). *Precaution:* Reaction develops excess of ammonia pressure during the reaction, thus, the reaction vessel should be designed to hold the pressure.

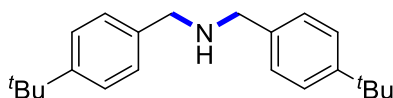
3.4.5 Characterization Data of Symmetrical Secondary Amines



dibenzylamine (4a):⁴⁶ The representative procedure was followed, using benzonitrile (**1a**; 0.052 g, 0.50 mmol) and $\text{NH}_3\text{-BH}_3$ (0.031 g, 1.0 mmol). Purification by column chromatography on silica gel (petroleum ether/EtOAc: 5/1) yielded **4a** (0.044 g, 89%) as a yellow oil. $^1\text{H-NMR}$ (400 MHz, CDCl_3): δ 7.31-7.28 (m, 8H, Ar-H), 7.24-7.19 (m, 2H, Ar-H), 3.77 (s, 4H, 2 x CH_2), 1.71 (s, 1H, NH). $^{13}\text{C}\{^1\text{H}\}\text{-NMR}$ (100 MHz, CDCl_3): δ 139.9 (2C, C_q), 128.6 (4C, CH), 128.4 (4C, CH), 127.2 (2C, CH), 53.0 (2 x CH_2). HRMS (ESI): m/z Calcd for $\text{C}_{14}\text{H}_{15}\text{N} + \text{H}^+$ [M + H]⁺ 198.1277; Found 198.1275. The analytical data are in accordance with those reported in the literature.

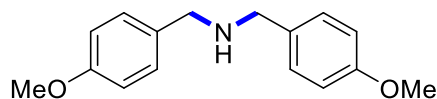


bis(4-methylbenzyl)amine (4b):⁴⁶ The representative procedure was followed, using 4-methyl benzonitrile (**1b**; 0.059 g, 0.50 mmol) and $\text{NH}_3\text{-BH}_3$ (0.031 g, 1.0 mmol). Purification by column chromatography on silica gel (petroleum ether/EtOAc: 2/1) yielded **4b** (0.051 g, 91%) as a colourless oil. $^1\text{H-NMR}$ (400 MHz, CDCl_3): δ 7.26 (d, $J = 7.9$ Hz, 4H, Ar-H), 7.17 (d, $J = 7.9$ Hz, 4H, Ar-H), 3.79 (s, 4H, 2 x CH_2), 2.37 (s, 6H, 2 x CH_3), 1.87 (s, 1H, NH). $^{13}\text{C}\{^1\text{H}\}\text{-NMR}$ (100 MHz, CDCl_3): δ 137.4 (2C, C_q), 136.6 (2C, C_q), 129.2 (4C, CH), 128.3 (4C, CH), 52.9 (2C, CH_2), 21.2 (2C, CH_3). HRMS (ESI): m/z Calcd for $\text{C}_{16}\text{H}_{19}\text{N} + \text{H}^+$ [M + H]⁺ 226.1590; Found 226.1586. The analytical data are in accordance with those reported in the literature.

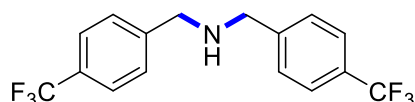


bis(4-(tert-butyl)benzyl)amine (4c):⁴⁶ The representative procedure was followed, using 4-*t*-butyl benzonitrile (**1c**; 0.079 g, 0.50 mmol) and $\text{NH}_3\text{-BH}_3$ (0.031 g, 1.0 mmol). Purification by column chromatography on silica gel (petroleum ether/EtOAc: 5/1) yielded **4c** (0.068 g, 88%) as a colourless oil. $^1\text{H-NMR}$ (500 MHz, CDCl_3): δ 7.40 (d, $J = 7.6$ Hz, 4H, Ar-H), 7.32 (d, $J = 7.6$ Hz, 4H, Ar-H), 3.83 (s, 4H, 2 x CH_2), 2.21 (s, 1H, NH), 1.36 (s, 18H, 6 x CH_3). $^{13}\text{C}\{^1\text{H}\}\text{-NMR}$ (125 MHz, CDCl_3): δ 150.1 (2C, C_q), 137.3 (2C, C_q), 128.1 (4C, CH), 125.5 (4C, CH), 52.9 (2 x CH_2), 34.6 (2C, C_q), 31.6 (6C, CH_3). HRMS (ESI): m/z Calcd for

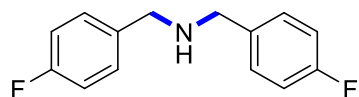
$C_{22}H_{31}N + H^+ [M + H]^+$ 310.2529; Found 310.2515. The analytical data are in accordance with those reported in the literature.



bis(4-methoxybenzyl)amine (4d):⁴⁶ The representative procedure was followed, using 4-methoxy benzonitrile (**1d**; 0.067 g, 0.50 mmol) and NH_3-BH_3 (0.031 g, 1.0 mmol). Purification by column chromatography on silica gel (petroleum ether/EtOAc: 1/1) yielded **4d** (0.055 g, 85%) as a yellow oil. 1H -NMR (500 MHz, $CDCl_3$): δ 7.25 (d, $J = 9.2$ Hz, 4H, Ar-H), 6.86 (d, $J = 8.4$ Hz, 4H, Ar-H), 3.79 (s, 6H, 2 x CH_3), 3.73 (s, 4H, 2 x CH_2), 2.06 (s, 1H, NH). $^{13}C\{^1H\}$ -NMR (125 MHz, $CDCl_3$): δ 158.8 (2C, C_q), 132.3 (2C, C_q), 129.6 (4C, CH), 114.0 (4C, CH), 55.4 (2C, CH_3), 52.5 (2C, CH_2). HRMS (ESI): m/z Calcd for $C_{16}H_{19}O_2N + H^+ [M + H]^+$ 258.1489; Found 226.1486. The analytical data are in accordance with those reported in the literature.

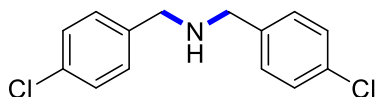


bis(4-(trifluoromethyl)benzyl)amine (4e):⁴⁶ The representative procedure was followed, using 4-trifluoromethyl benzonitrile (**1e**; 0.085 g, 0.50 mmol) and NH_3-BH_3 (0.031 g, 1.0 mmol). Purification by column chromatography on silica gel (petroleum ether/EtOAc: 1:1) yielded **4e** (0.059 g, 71%) as a colourless oil. 1H -NMR (400 MHz, $CDCl_3$): δ 7.62 (d, $J = 8.0$ Hz, 4H, Ar-H), 7.5 (d, $J = 8.0$ Hz, 4H, Ar-H), 3.88 (s, 4H, 2 x CH_2), 1.77 (s, 1H, NH). $^{13}C\{^1H\}$ -NMR (100 MHz, $CDCl_3$): δ 144.3 (2C, C_q), 129.6 (q, $^2J_{C-F} = 32.4$ Hz, 2C, C_q), 128.5 (4C, CH), 125.6 (q, $^3J_{C-F} = 3.8$ Hz, 4C, CH), 124.4 (q, $^1J_{C-F} = 271.8$ Hz, 2C, CF_3), 52.8 (2 x CH_2). ^{19}F -NMR (377 MHz, $CDCl_3$): δ -62.4. HRMS (ESI): m/z Calcd for $C_{16}H_{13}NF_6 + H^+ [M + H]^+$ 334.1025; Found 334.1017. The analytical data are in accordance with those reported in the literature.

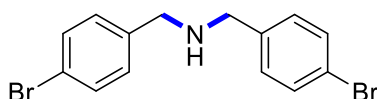


bis(4-fluorobenzyl)amine (4f):⁴⁶ The representative procedure was followed, using 4-fluoro benzonitrile (**1f**; 0.060 g, 0.50 mmol) and NH_3-BH_3 (0.031 g, 1.0 mmol). Purification by column chromatography on silica gel (petroleum ether/EtOAc: 2/1) yielded **4f** (0.050 g, 86%) as a yellow oil. 1H -NMR (500 MHz, $CDCl_3$): δ 7.31-7.27 (m, 4H, Ar-H), 7.03-6.98 (m, 4H,

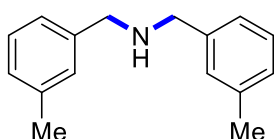
Ar-H), 3.75 (s, 4H, 2 x CH₂), 1.72 (s, 1H, NH). ¹³C{¹H}-NMR (125 MHz, CDCl₃): δ 162.7 (d, ¹J_{C-F} = 245.4 Hz, 2C, C_q), 136.0 (d, ⁴J_{C-F} = 2.9 Hz, 2C, C_q), 129.8 (d, ³J_{C-F} = 7.7 Hz, 4C, CH), 115.4 (d, ²J_{C-F} = 21.1 Hz, 4C, CH), 52.5 (2C, CH₂). ¹⁹F-NMR (377 MHz, CDCl₃): δ -115.9. HRMS (ESI): *m/z* Calcd for C₁₄H₁₃NF₂ + H⁺ [M + H]⁺ 234.1089; Found 234.1085. The analytical data are in accordance with those reported in the literature.



bis(4-chlorobenzyl)amine (4g):⁴⁶ The representative procedure was followed, using 4-chloro benzonitrile (**1g**; 0.069 g, 0.50 mmol) and NH₃-BH₃ (0.031 g, 1.0 mmol). Purification by column chromatography on silica gel (petroleum ether/EtOAc: 2/1) yielded **4g** (0.055 g, 83%) as a colourless oil. ¹H-NMR (500 MHz, CDCl₃): δ 7.34-7.29 (m, 8H, Ar-H), 3.78 (s, 4H, 2 x CH₂), 1.75 (s, 1H, NH). ¹³C{¹H}-NMR (125 MHz, CDCl₃): δ 138.8 (2C, C_q), 132.9 (2C, C_q), 129.6 (4C, CH), 128.7 (4C, CH), 52.5 (2C, CH₂). HRMS (ESI): *m/z* Calcd for C₁₄H₁₃NCl₂ + H⁺ [M + H]⁺ 266.0498; Found 266.0521. The analytical data are in accordance with those reported in the literature.

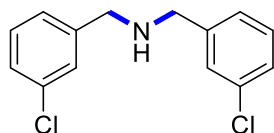


bis(4-bromobenzyl)amine (4h):⁴⁶ The representative procedure was followed, using 4-bromo benzonitrile (**1h**; 0.091 g, 0.50 mmol) and NH₃-BH₃ (0.031 g, 1.0 mmol). Purification by column chromatography on silica gel (petroleum ether/EtOAc: 1/1) yielded **4h** (0.049 g, 55%) as a yellow oil. ¹H-NMR (400 MHz, CDCl₃): δ 7.46 (d, *J* = 8.5 Hz, 4H, Ar-H), 7.22 (d, *J* = 8.5 Hz, 4H, Ar-H), 3.75 (s, 4H, 2 x CH₂), 1.75 (s, 1H, NH). ¹³C{¹H}-NMR (100 MHz, CDCl₃): δ 139.2 (2C, C_q), 131.7 (4C, CH), 130.0 (4C, CH), 121.0 (2C, C_q), 52.5 (2C, CH₂). HRMS (ESI): *m/z* Calcd for C₁₄H₁₃NBr + H⁺ [M + H]⁺ 355.9467, 357.9436; Found 355.9460, 357.9429. The analytical data are in accordance with those reported in the literature.

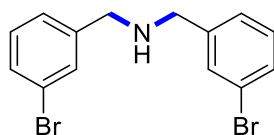


bis(3-methylbenzyl)amine (4i):²⁰ The representative procedure was followed, using 3-methyl benzonitrile (**1i**; 0.059 g, 0.50 mmol) and NH₃-BH₃ (0.031 g, 1.0 mmol). Purification by column chromatography on silica gel (petroleum ether/EtOAc: 5/1) yielded **4i** (0.052 g,

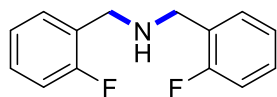
92%) as a colourless oil. $^1\text{H-NMR}$ (500 MHz, CDCl_3): δ 7.28 (vt, $J = 7.6$ Hz, 2H, Ar-H), 7.22-7.18 (m, 4H, Ar-H), 7.13 (d, $J = 7.6$ Hz, 2H, Ar-H), 3.83 (s, 4H, 2 x CH_2), 2.41 (s, 6H, 2 x CH_3), 1.90 (s, 1H, NH). $^{13}\text{C}\{^1\text{H}\}\text{-NMR}$ (125 MHz, CDCl_3): δ 140.4 (2C, C_q), 138.2 (2C, C_q), 129.1 (2C, CH), 128.5 (2C, CH), 127.9 (2C, CH), 125.4 (2C, CH), 53.4 (2C, CH_2), 21.6 (2C, CH_3). HRMS (ESI): m/z Calcd for $\text{C}_{16}\text{H}_{19}\text{N} + \text{H}^+$ $[\text{M} + \text{H}]^+$ 226.1590; Found 226.1581. The analytical data are in accordance with those reported in the literature.



bis(3-chlorobenzyl)amine (4j):⁵⁰ The representative procedure was followed, using 3-chloro benzonitrile (**1j**; 0.069 g, 0.50 mmol) and $\text{NH}_3\text{-BH}_3$ (0.031 g, 1.0 mmol). Purification by column chromatography on silica gel (petroleum ether/EtOAc: 5/1) yielded **4j** (0.057 g, 86%) as a yellow oil. $^1\text{H-NMR}$ (500 MHz, CDCl_3): δ 7.38 (s, 2H, Ar-H), 7.31-7.23 (m, 6H, Ar-H), 3.80 (s, 4H, 2 x CH_2), 1.81 (s, 1H, NH). $^{13}\text{C}\{^1\text{H}\}\text{-NMR}$ (125 MHz, CDCl_3): δ 142.3 (2C, C_q), 134.5 (2C, C_q), 129.9 (2C, CH), 128.4 (2C, CH), 127.4 (2C, CH), 126.4 (2C, CH), 52.7 (2C, CH_2). HRMS (ESI): m/z Calcd for $\text{C}_{14}\text{H}_{13}\text{NCl}_2 + \text{H}^+$ $[\text{M} + \text{H}]^+$ 266.0490; Found 226.0490. The analytical data are in accordance with those reported in the literature.



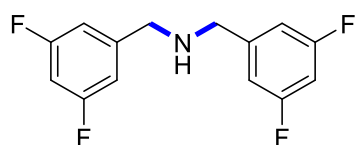
bis(3-bromobenzyl)amine (4k):⁴⁶ The representative procedure was followed, using 3-bromo benzonitrile (**1k**; 0.091 g, 0.50 mmol) and $\text{NH}_3\text{-BH}_3$ (0.031 g, 1.0 mmol). Purification by column chromatography on silica gel (petroleum ether/EtOAc: 5/1) yielded **4k** (0.057 g, 64%) as yellow oil. $^1\text{H-NMR}$ (400 MHz, CDCl_3): δ 7.51 (s, 2H, Ar-H), 7.39 (d, $J = 7.6$ Hz, 2H, Ar-H), 7.26-7.18 (m, 4H, Ar-H), 3.78 (s, 4H, 2 x CH_2), 1.68 (s, 1H, NH). $^{13}\text{C}\{^1\text{H}\}\text{-NMR}$ (100 MHz, CDCl_3): δ 142.6 (2C, C_q), 131.3 (2C, CH), 130.3 (2C, CH), 130.2 (2C, CH), 126.9 (2C, CH), 122.8 (2C, C_q), 52.7 (2C, CH_2). HRMS (ESI): m/z Calcd for $\text{C}_{14}\text{H}_{13}\text{NBr}_2 + \text{H}^+$ $[\text{M} + \text{H}]^+$ 353.9490, 355.9467, 357.9438; Found 353.9493, 355.9464, 357.9435. The analytical data are in accordance with those reported in the literature.



bis(2-fluorobenzyl)amine (4l):¹⁵ The representative procedure was followed, using 2-fluorobenzonitrile (**1l**; 0.060 g, 0.50 mmol) and $\text{NH}_3\text{-BH}_3$ (0.031 g, 1.0 mmol). Purification by column chromatography on silica (petroleum ether/EtOAc: 2/1) yielded **4l** (0.051 g, 87%) as a colourless oil. $^1\text{H-NMR}$ (500 MHz, CDCl_3): δ 7.41 (vt, $J = 7.3$ Hz, 2H, Ar-H), 7.29-7.24 (m, 2H, Ar-H), 7.14 (vt, $J = 7.3$ Hz, 2H, Ar-H), 7.06 (vt, $J = 8.5$ Hz, 2H, Ar-H), 3.90 (s, 4H, 2 x CH_2), 2.01 (s, 1H, NH). $^{13}\text{C}\{^1\text{H}\}\text{-NMR}$ (125 MHz, CDCl_3): δ 161.4 (d, $^1J_{\text{C-F}} = 245.8$ Hz, 2C, CF), 130.5 (d, $^4J_{\text{C-F}} = 4.6$ Hz, 2C, CH), 128.8 (d, $^3J_{\text{C-F}} = 8.5$ Hz, 2C, CH), 127.2 (d, $^2J_{\text{C-F}} = 15.4$ Hz, 2C, C_q), 124.2 (d, $^3J_{\text{C-F}} = 3.8$ Hz, 2C, CH), 115.4 (d, $^2J_{\text{C-F}} = 22.4$ Hz, 2C, CH), 46.8 (2C, CH_2). $^{19}\text{F-NMR}$ (377 MHz, CDCl_3): δ -119.3. HRMS (ESI): m/z Calcd for $\text{C}_{14}\text{H}_{13}\text{NF}_2 + \text{H}^+ [\text{M} + \text{H}]^+$ 234.1089; Found 234.1095. The analytical data are in accordance with those reported in the literature.

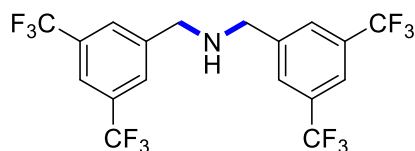


bis(2-chlorobenzyl)amine (4m):⁴⁶ The representative procedure was followed, using 2-chlorobenzonitrile (**1m**; 0.069 g, 0.50 mmol) and $\text{NH}_3\text{-BH}_3$ (0.031 g, 1.0 mmol). Purification by column chromatography on silica gel (petroleum ether/EtOAc: 5/1) yielded **4m** (0.059 g, 89%) as a colourless oil. $^1\text{H-NMR}$ (500 MHz, CDCl_3): δ 7.47 (s, 2H, Ar-H), 7.39 (s, 2H, Ar-H), 7.25-7.21 (m, 4H, Ar-H), 3.94 (s, 4H, 2 x CH_2), 2.03 (s, 1H, NH). $^{13}\text{C}\{^1\text{H}\}\text{-NMR}$ (125 MHz, CDCl_3): δ 137.6 (2C, C_q), 134.0 (2C, C_q), 130.3 (2C, CH), 129.6 (2C, CH), 128.5 (2C, CH), 127.0 (2C, CH), 50.9 (2C, CH_2). HRMS (ESI): m/z Calcd for $\text{C}_{14}\text{H}_{13}\text{NCl}_2 + \text{H}^+ [\text{M} + \text{H}]^+$ 266.0498; Found 266.0489. The analytical data are in accordance with those reported in the literature.

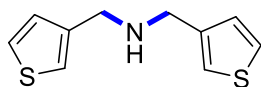


bis(3,5-difluorobenzyl)amine (4n): The representative procedure was followed, using 3,5-difluorobenzonitrile (**1n**; 0.069 g, 0.50 mmol) and $\text{NH}_3\text{-BH}_3$ (0.031 g, 1.0 mmol). Purification by column chromatography on silica gel (petroleum ether/EtOAc: 5/1) yielded **4n** (0.052 g, 77%) as a yellow oil. $^1\text{H-NMR}$ (400 MHz, CDCl_3): δ 6.91 (d, $J = 6.1$ Hz, 4H, Ar-H), 6.75-6.69 (m, 2H, Ar-H), 3.81 (s, 4H, 2 x CH_2), 1.69 (s, 1H, NH). $^{13}\text{C}\{^1\text{H}\}\text{-NMR}$

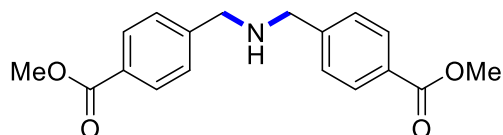
(100 MHz, CDCl₃): δ 163.3 (dd, $^1J_{C-F}$ = 248.9, $^3J_{C-F}$ = 13.1 Hz, 4C, CF), 144.3 (t, $^3J_{C-F}$ = 8.8 Hz, 2C, C_q), 110.7 (dd, J_{C-F} = 17.7, 6.2 Hz, 4C, CH), 102.6 (t, $^2J_{C-F}$ = 25.1 Hz, 2C, CH), 52.4 (2C, CH₂). ¹⁹F-NMR (377 MHz, CDCl₃): δ -62.40. HRMS (ESI): m/z Calcd for C₁₄H₁₁NF₄ + H⁺ [M + H]⁺ 270.0900; Found 270.0895.



bis(3,5-bis(trifluoromethyl)benzyl)amine (4o): The representative procedure was followed, using 3,5-bis(trifluoromethyl) benzonitrile (**1o**; 0.119 g, 0.50 mmol) and NH₃-BH₃ (0.031 g, 1.0 mmol). Purification by column chromatography on silica gel (petroleum ether/EtOAc: 2/1) yielded **4o** (0.075 g, 64%) as a pale white oil. ¹H-NMR (400 MHz, CDCl₃): δ 7.83-7.79 (br s, 6H, Ar-H), 3.98 (s, 4H, 2 x CH₂), 1.89 (s, 1H, NH). ¹³C{¹H}-NMR (100 MHz, CDCl₃): δ 142.6 (2C, C_q), 132.3 (q, $^2J_{C-F}$ = 33.1 Hz, 4C, C_q), 128.4 (4C, CH), 123.5 (q, $^1J_{C-F}$ = 272.8 Hz, 4 x CF₃), 121.5 (sept, $^3J_{C-F}$ = 3.5 Hz, 2C, CH), 52.6 (2C, CH₂). ¹⁹F-NMR (377 MHz, CDCl₃): δ -62.96. HRMS (ESI): m/z Calcd for C₁₈H₁₁NF₁₂ + H⁺ [M + H]⁺ 470.0773; Found 470.0750.

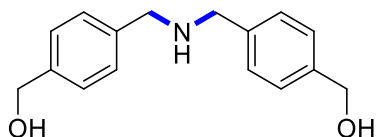


bis(thiophen-3-ylmethyl)amine (4p):⁴⁶ The representative procedure was followed, using 3-cyano thiophene (**1p**; 0.054 g, 0.50 mmol) and NH₃-BH₃ (0.031 g, 1.0 mmol). Purification by column chromatography on silica (petroleum ether/EtOAc: 1/1) yielded **4p** (0.039 g, 75%) as a yellow oil. ¹H-NMR (500 MHz, CDCl₃): δ 7.29-7.27 (m, 2H, Ar-H), 7.14 (s, 2H, Ar-H), 7.07 (d, J = 4.6 Hz, 2H, Ar-H), 3.83 (s, 4H, 2 x CH₂), 1.88 (s, 1H, NH). ¹³C{¹H}-NMR (125 MHz, CDCl₃): δ 141.3 (2C, C_q), 127.7 (2C, CH), 125.9 (2C, CH), 121.8 (2C, CH), 48.2 (2C, CH₂). HRMS (ESI): m/z Calcd for C₁₀H₁₁NS₂ + H⁺ [M + H]⁺ 210.0406; Found 210.0408. The analytical data are in accordance with those reported in the literature.



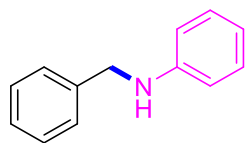
dimethyl 4,4'-(azanediylbis(methylene))dibenzoate (4q)⁴⁶: The representative procedure was followed, using methyl 4-cyanobenzoate (**1q**; 0.081 g, 0.50 mmol) and NH₃-BH₃ (0.031 g, 1.0 mmol). Purification by column chromatography on silica gel (petroleum ether/EtOAc:

1/1) yielded **4q** (0.063 g, 80%) as a colourless oil. $^1\text{H-NMR}$ (500 MHz, CDCl_3): δ 8.01 (d, $J = 8.0$ Hz, 4H, Ar-H), 7.44 (d, $J = 8.4$ Hz, 4H, Ar-H), 3.92 (s, 6H, 2 x CH_3), 3.88 (s, 4H, 2 x CH_2), 1.76 (s, 1H, NH). $^{13}\text{C}\{^1\text{H}\}$ -NMR (125 MHz, CDCl_3): δ 167.2 (2C, CO), 145.6 (2C, C_q), 130.0 (4C, CH), 129.1 (2C, C_q), 128.2 (4C, CH), 53.0 (2 x CH_3), 52.3 (2C, CH_2). HRMS (ESI): m/z Calcd for $\text{C}_{18}\text{H}_{19}\text{O}_4\text{N} + \text{H}^+$ $[\text{M} + \text{H}]^+$ 314.1387; Found 314.1381. The analytical data are in accordance with those reported in the literature.

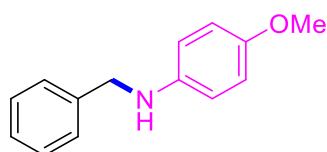


((azanediybis(methylene))bis(4,1-phenylene))dimethanol (4r): The representative procedure was followed, using 4-formyl benzonitrile (**1r**; 0.065 g, 0.50 mmol) and $\text{NH}_3\text{-BH}_3$ (0.031 g, 1.0 mmol). Purification by column chromatography on silica gel (petroleum ether/EtOAc: 2/1) yielded **4r** (0.042 g, 65%) as a white solid. $^1\text{H-NMR}$ (500 MHz, CDCl_3): δ 7.35 (s, 8H, Ar-H), 4.70 (s, 4H, 2 x CH_2), 3.81 (s, 4H, 2 x CH_2), 1.78 (s, 3H, NH/OH). $^{13}\text{C}\{^1\text{H}\}$ -NMR (125 MHz, CDCl_3): δ 139.9 (C_q), 128.6 (4C, CH), 127.4 (4C, CH), 65.3 (2 x CH_2), 53.0 (2C, CH_2). HRMS (ESI): m/z Calcd for $\text{C}_{16}\text{H}_{19}\text{O}_4\text{N} + \text{H}^+$ $[\text{M} + \text{H}]^+$ 258.1494; Found 258.1496.

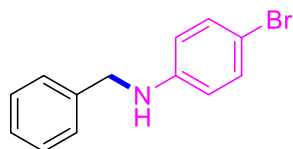
3.4.6 Characterization Data of Unsymmetrical Secondary Amine



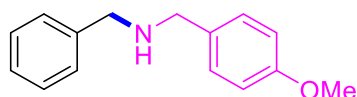
N-benzylaniline (6a):⁴⁶ The representative procedure was followed, using benzonitrile (**1a**; 0.052 g, 0.50 mmol), aniline (**5a**; 0.051 g, 0.55 mmol) and Me₂NH-BH₃ (0.059 g, 1.0 mmol). Purification by column chromatography on silica gel (petroleum ether/EtOAc: 10/1) yielded **6a** (0.080 g, 87%) as a brown oil. ¹H-NMR (400 MHz, CDCl₃): δ 7.35-7.30 (m, 4H, Ar-H), 7.27-7.25 (m, 1H, Ar-H), 7.15 (dd, *J* = 8.5, 7.3 Hz, 2H, Ar-H), 6.70 (vt, *J* = 7.3 Hz, 1H, Ar-H), 6.60 (d, *J* = 7.9 Hz, 2H, Ar-H), 4.29 (s, 2H, CH₂), 3.94 (br s, 1H, NH). ¹³C{¹H}-NMR (100 MHz, CDCl₃): δ 148.3 (C_q), 139.6 (C_q), 129.4 (2C, CH), 128.8 (2C, CH), 127.6 (2C, CH), 127.3 (CH), 117.7 (CH), 113.0 (2C, CH), 48.4 (CH₂). HRMS (ESI): *m/z* Calcd for C₁₃H₁₃N + H⁺ [M + H]⁺ 184.1121; Found 184.1113. The analytical data are in accordance with those reported in the literature.



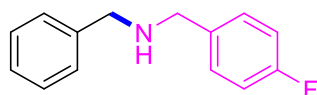
N-benzyl-4-methoxyaniline (6b):⁵¹ The representative procedure was followed, using benzonitrile (**1a**; 0.052 g, 0.50 mmol), 4-methoxy aniline (**5b**; 0.068 g, 0.55 mmol) and Me₂NH-BH₃ (0.059 g, 1.0 mmol). Purification by column chromatography on silica gel (petroleum ether/EtOAc: 10/1) yielded **6b** (0.102 g, 94%) as a colourless oil. ¹H-NMR (500 MHz, CDCl₃): δ 7.42-7.36 (m, 4H, Ar-H), 7.32-7.29 (m, 1H, Ar-H), 6.82 (d, *J* = 9.2 Hz, 2H, Ar-H), 6.65 (d, *J* = 9.2 Hz, 2H, Ar-H), 4.32 (s, CH₂), 3.78 (s, 3H, CH₃). ¹³C{¹H}-NMR (125 MHz, CDCl₃): δ 152.4 (C_q), 142.6 (C_q), 139.8 (C_q), 128.8 (2C, CH), 127.7 (2C, CH), 127.3 (CH), 115.1 (2C, CH), 114.3 (2C, CH), 56.0 (CH₂), 49.5 (CH₃). HRMS (ESI): *m/z* Calcd for C₁₄H₁₅ON + H⁺ [M + H]⁺ 214.1226; Found 214.1217. The analytical data are in accordance with those reported in the literature.



N-benzyl-4-bromoaniline (6c):⁴⁶ The representative procedure was followed, using benzonitrile (**1a**; 0.052 g, 0.50 mmol), 4-bromoaniline (**5c**; 0.086 g, 0.55 mmol) and Me₂NH-BH₃ (0.059 g, 1.0 mmol). Purification by column chromatography on silica gel (petroleum ether/EtOAc: 10/1) yielded **6c** (0.085 g, 65%) as a brown oil. ¹H-NMR (500 MHz, CDCl₃): δ 7.36-7.32 (m, 4H, Ar-H), 7.29-7.26 (m, 1H, Ar-H), 7.22 (d, *J* = 8.8 Hz, 2H, Ar-H), 6.48 (d, *J* = 8.8 Hz, 2H, Ar-H), 4.28 (s, CH₂), 4.03 (br s, 1H, NH). ¹³C{¹H}-NMR (125 MHz, CDCl₃): δ 147.2 (C_q), 139.0 (C_q), 132.1 (2C, CH), 128.9 (2C, CH), 127.6 (3C, CH), 114.6 (2C, CH), 109.3 (C_q), 48.4 (CH₂). HRMS (ESI): *m/z* Calcd for C₁₃H₁₂NBr + H⁺ [M + H]⁺ 262.0226; Found 262.0228. The analytical data are in accordance with those reported in the literature.

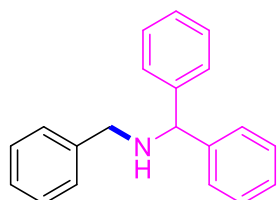


N-benzyl-1-(4-methoxyphenyl)methanamine (6d):⁴⁶ The representative procedure was followed, using benzonitrile (**1a**; 0.052 g, 0.50 mmol), 4-methoxy benzylamine (**5d**; 0.075 g, 0.55 mmol) and Me₂NH-BH₃ (0.059 g, 1.0 mmol). Purification by column chromatography on silica gel (petroleum ether/EtOAc: 10/1) yielded **6d** (0.096 g, 84%) as a yellow oil. ¹H-NMR (500 MHz, CDCl₃): δ 7.37-7.31 (m, 4H, Ar-H), 7.29-7.24 (m, 3H, Ar-H), 6.87 (d, *J* = 8.4 Hz, 2H, Ar-H), 3.80 (s, 5H, CH₂ & CH₃), 3.75 (s, 2H, CH₂), 2.04 (br s, 1H, NH). ¹³C{¹H}-NMR (125 MHz, CDCl₃): δ 158.8 (C_q), 140.3 (C_q), 132.4 (C_q), 129.5 (2C, CH), 128.6 (2C, CH), 128.3 (2C, CH), 127.1 (CH), 113.9 (2C, CH), 55.4 (CH₃), 53.1 (CH₂), 52.6 (CH₂). HRMS (ESI): *m/z* Calcd for C₁₅H₁₇NO + H⁺ [M + H]⁺ 228.1383; Found 228.1378. The analytical data are in accordance with those reported in the literature.

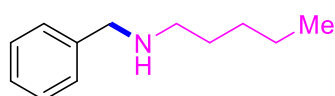


N-benzyl-1-(4-fluorophenyl)methanamine (6e):⁵² The representative procedure was followed, using benzonitrile (**1a**; 0.052 g, 0.50 mmol), 4-fluoro benzylamine (**5e**; 0.069 g, 0.55 mmol) and Me₂NH-BH₃ (0.059 g, 1.0 mmol). Purification by column chromatography on silica gel (petroleum ether/EtOAc: 5/1) yielded **6e** (0.078 g, 72%) as a yellow oil. ¹H-NMR (400 MHz, CDCl₃): δ 7.35-7.26 (m, 7H, Ar-H), 7.02 (vt, *J* = 8.8 Hz, 2H, Ar-H), 3.80

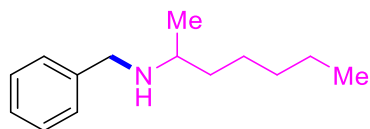
(s, 2H,CH₂), 3.78 (s, 2H,CH₂), 1.76 (br s, 1H, NH). ¹³C{¹H}-NMR (100 MHz, CDCl₃): δ 162.1 (d, ¹J_{C-F}= 244.4 Hz, C_q), 140.3 (C_q), 136.1 (d, ⁴J_{C-F}= 2.9 Hz, C_q), 129.8 (d, ³J_{C-F}= 7.7 Hz, 2C, CH), 128.6 (2C, CH), 128.3 (2C, CH), 127.2 (CH), 115.3 (d, ²J_{C-F}= 21.1 Hz, 2C, CH), 53.3 (CH₂), 52.5 (CH₂). ¹⁹F-NMR (377 MHz, CDCl₃): δ -116.0. HRMS (ESI): *m/z* Calcd for C₁₄H₁₄NF + H⁺ [M + H]⁺ 216.1183; Found 216.1174. The analytical data are in accordance with those reported in the literature.



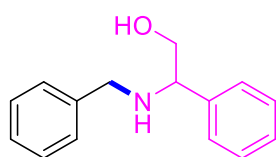
N-benzyl-1,1-diphenylmethanamine (6f):⁵³ The representative procedure was followed, using benzonitrile (**1a**; 0.052 g, 0.50 mmol), diphenyl methylamine (**5f**; 0.101 g, 0.55 mmol) and Me₂NH-BH₃ (0.059 g, 1.0 mmol). Purification by column chromatography on silica (petroleum ether/EtOAc: 10/1) yielded **6f** (0.117 g, 86%) as a yellow oil. ¹H-NMR (500 MHz, CDCl₃): δ 7.42-7.39 (m, 4H, Ar-H), 7.33-7.29 (m, 5H, Ar-H), 7.28-7.25 (m, 3H, Ar-H), 7.24-7.21 (m, 1H, Ar-H), 7.18 (vt, *J* = 7.2 Hz, 2H, Ar-H), 4.83 (s, 1H, CH), 3.72 (s, 2H, CH₂), 1.86 (s, 1H, NH). ¹³C{¹H}-NMR (125 MHz, CDCl₃): δ 144.1 (2C, C_q), 140.6 (C_q), 128.7 (4C, CH), 128.5 (2C, CH), 128.3 (2C, CH), 127.5 (4C, CH), 127.2 (2C, CH), 127.1 (CH), 66.6 (CH), 52.0 (CH₂). HRMS (ESI): *m/z* Calcd for C₂₀H₁₇N + H⁺ [M + H]⁺ 274.1590; Found 274.1582. The analytical data are in accordance with those reported in the literature.



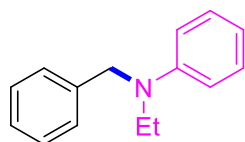
N-benzylpentan-1-amine (6g):⁴⁶ The representative procedure was followed, using benzonitrile (**1a**; 0.052 g, 0.50 mmol), 1-amino-pentane (**5g**; 0.065 g, 0.75 mmol) and Me₂NH-BH₃ (0.059 g, 1 mmol). Purification by column chromatography on silica gel (petroleum ether/EtOAc: 2/1) yielded **4g** (0.061 g, 69%) as a yellow oil. ¹H-NMR (400 MHz, CDCl₃): δ 7.30-7.24 (m, 4H, Ar-H), 7.23-7.19 (m, 1H, Ar-H), 3.75 (s, 2H, CH₂), 2.58 (t, *J* = 7.6 Hz, 2H, CH₂), 2.05 (br s, 1H, NH), 1.51-1.44 (m, 2H, CH₂), 1.29-1.23 (m, 4H, CH₂), 0.84 (t, *J* = 6.9 Hz, 3H, CH₃). ¹³C{¹H}-NMR (100 MHz, CDCl₃): δ 140.4 (C_q), 128.6 (2C, CH), 128.4 (2C, CH), 127.1 (CH), 54.1 (CH₂), 49.5 (CH₂), 29.8 (CH₂), 29.7 (CH₂), 22.8 (CH₂), 14.2 (CH₃). HRMS (ESI): *m/z* Calcd for C₁₂H₁₉N + H⁺ [M + H]⁺ 178.1590; Found 178.1587. The analytical data are in accordance with those reported in the literature.



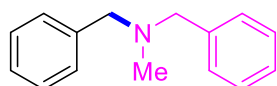
N-benzylheptan-2-amine (6h):⁵⁴ The representative procedure was followed, using benzonitrile (**1a**; 0.052 g, 0.50 mmol), 2-amino heptane (**5h**; 0.115 g, 1 mmol) and Me₂NH-BH₃ (0.059 g, 1.0 mmol). Purification by column chromatography on silica gel (petroleum ether/EtOAc: 2/1) yielded **6h** (0.080 g, 78%) as a colourless oil. ¹H-NMR (500 MHz, CDCl₃): δ 7.26-7.24 (m, 4H, Ar-H), 7.20-7.16 (m, 1H, Ar-H), 3.79-3.66 (m, 2H, CH₂), 3.03 (br s, 1H, NH), 2.65-2.59 (m, 1H, CH), 1.46-1.41 (m, 1H, CH), 1.30-1.17 (m, 7H, CH₂), 1.03 (d, *J* = 6.5 Hz, 3H, CH₃), 0.82 (t, *J* = 6.9 Hz, 3H, CH₃). ¹³C{¹H}-NMR (125 MHz, CDCl₃): δ 140.2 (C_q), 128.6 (2C, CH), 128.4 (2C, CH), 127.2 (CH), 52.6 (CH₂), 51.2 (CH), 36.8 (CH₂), 32.1 (CH₂), 26.0 (CH₂), 22.8 (CH₂), 20.1 (CH₃), 14.2 (CH₃). HRMS (ESI): *m/z* Calcd for C₁₄H₂₃N + H⁺ [M + H]⁺ 206.1903; Found 206.1900. The analytical data are in accordance with those reported in the literature.



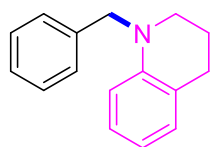
2-(benzylamino)-2-phenylethan-1-ol (6i):⁴⁶ The representative procedure was followed, using benzonitrile (**1a**; 0.052 g, 0.50 mmol), 2-amino-2-phenylethan-1-ol (**5i**; 0.137 g, 1.0 mmol) and Me₂NH-BH₃ (0.059 g, 1.0 mmol). Purification by column chromatography on silica gel (petroleum ether/EtOAc: 1/1) yielded **6i** (0.066 g, 58%) as a colourless oil. ¹H-NMR (400 MHz, CDCl₃): δ 7.40-7.36 (m, 2H, Ar-H), 7.33-7.24 (m, 8H, Ar-H), 3.83-3.80 (m, 1H, CH₂), 3.75 (d, *J* = 13.0 Hz, 1H, CH₂), 3.72-3.68 (m, 1H, CH₂), 3.59 (d, *J* = 6.1 Hz, 1H, CH₂), 3.57-3.54 (m, 1H, CH), 2.56 (br s, 1H, NH), ¹³C{¹H}-NMR (125 MHz, CDCl₃): δ 140.5 (C_q), 140.1 (C_q), 128.8 (2C, CH), 128.6 (2C, CH), 128.4 (2C, CH), 127.8 (CH), 127.5 (2C, CH), 127.3 (CH), 66.9 (CH₂), 63.9 (CH), 51.3 (CH₂). HRMS (ESI): *m/z* Calcd for C₁₅H₁₇ON + H⁺ [M + H]⁺ 228.1383; Found 228.1380. The analytical data are in accordance with those reported in the literature.



N-benzyl-N-ethylaniline (6j):⁵⁵ The representative procedure was followed, using benzonitrile (**1a**; 0.052 g, 0.50 mmol), *N*-ethyl aniline (**5j**; 0.067 g, 0.55 mmol) and Me₂NH-BH₃ (0.059 g, 1.0 mmol). Purification by column chromatography on silica gel (petroleum ether/EtOAc: 20/1) yielded **6j** (0.079 g, 75%) as a colourless oil. ¹H-NMR (400 MHz, CDCl₃): δ 7.31-7.27 (m, 2H, Ar-H), 7.24-7.21 (m, 3H, Ar-H), 7.19-7.15 (m, 2H, Ar-H), 6.69-6.63 (m, 3H, Ar-H), 4.50 (s, 2H, CH₂), 3.47 (q, *J* = 6.9 Hz, 2H, CH₂), 1.19 (t, *J* = 6.9 Hz, 3H, CH₃). ¹³C{¹H}-NMR (100 MHz, CDCl₃): δ 148.6 (C_q), 139.4 (C_q), 129.4 (2C, CH), 128.7 (2C, CH), 126.9 (CH), 126.7 (2C, CH), 116.2 (CH), 112.3 (2C, CH), 54.2 (CH₂), 45.3 (CH₂), 12.3 (CH₃). HRMS (ESI): *m/z* Calcd for C₁₅H₁₇N + H⁺ [M + H]⁺ 212.1434; Found 212.1434. The analytical data are in accordance with those reported in the literature.

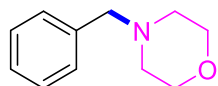


N-benzyl-N-methyl-1-phenylmethanamine (6k):⁵⁶ The representative procedure was followed, using benzonitrile (**1a**; 0.052 g, 0.50 mmol), *N*-methyl benzylamine (**5k**; 0.067 g, 0.55 mmol) and Me₂NH-BH₃ (0.059 g, 1.0 mmol). Purification by column chromatography on silica gel (petroleum ether/EtOAc: 10/1) yielded **6k** (0.088 g, 83%) as a brown oil. ¹H-NMR (400 MHz, CDCl₃): δ 7.39-7.31 (m, 8H, Ar-H), 7.27-7.24 (m, 2H, Ar-H), 3.54 (s, 4H, CH₂), 2.20 (s, 3H, CH₃). ¹³C{¹H}-NMR (100 MHz, CDCl₃): δ 139.4 (2C, C_q), 129.1 (4C, CH), 128.4 (4C, CH), 127.1 (2C, CH), 62.0 (2C, CH₂), 42.4 (CH₃). HRMS (ESI): *m/z* Calcd for C₁₅H₁₇N + H⁺ [M + H]⁺ 212.1434; Found 212.1431. The analytical data are in accordance with those reported in the literature.

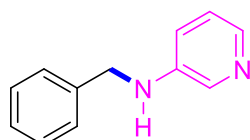


1-benzyl-1,2,3,4-tetrahydroquinoline (6l):⁵⁷ The representative procedure was followed, using benzonitrile (**1a**; 0.052 g, 0.50 mmol), 1,2,3,4-tetrahydroquinoline (**5l**; 0.073 g, 0.55 mmol) and Me₂NH-BH₃ (0.059 g, 1.0 mmol). Purification by column chromatography on silica gel (petroleum ether/EtOAc: 5/1) yielded **6l** (0.096 g, 86%) as a yellow oil. ¹H-NMR (500 MHz, CDCl₃): δ 7.43-7.40 (m, 2H, Ar-H), 7.38-7.32 (m, 3H, Ar-H), 7.09-7.06 (m, 2H,

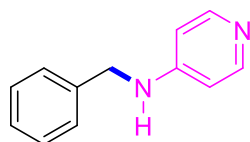
Ar-H), 6.68 (vt, $J = 7.6$ Hz, 1H, Ar-H), 6.61 (d, $J = 8.4$ Hz, 1H, Ar-H), 4.57 (s, 2H, CH₂), 3.46 (t, $J = 5.7$ Hz, 2H, CH₂), 2.93 (t, $J = 6.1$ Hz, 2H, CH₂), 2.11 (pent, 2H, $J = 6.1$ Hz, CH₂). ¹³C{¹H}-NMR (125 MHz, CDCl₃): δ 145.8 (C_q), 139.1 (C_q), 129.1 (CH), 128.7 (2C, CH), 127.3 (CH), 126.9 (CH), 126.8 (2C, CH), 122.4 (C_q), 116.0 (CH), 111.1 (CH), 55.3 (CH₂), 50.0 (CH₂), 28.4 (CH₂), 22.5 (CH₂). HRMS (ESI): m/z Calcd for C₁₆H₁₇N + H⁺ [M + H]⁺ 224.1429; Found 224.1434. The analytical data are in accordance with those reported in the literature.



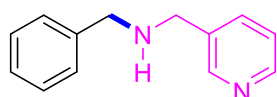
4-benzylmorpholine (6m):⁴⁶ The representative procedure was followed, using benzonitrile (**1a**; 0.052 g, 0.50 mmol), morpholine (**5m**; 0.065 g, 0.75 mmol) and Me₂NH-BH₃ (0.059 g, 1.0 mmol). Purification by column chromatography on silica gel (DCM/Methanol: 2/1) yielded **6m** (0.060 g, 68%) as a yellow oil. ¹H-NMR (400 MHz, CDCl₃): δ 7.33-7.31 (m, 4H, Ar-H), 7.28-7.24 (m, 1H, Ar-H), 3.70 (t, $J = 4.6$ Hz, 4H, 2 x CH₂), 3.49 (s, 2H, CH₂), 2.44 (t, 4H, $J = 4.6$ Hz, 2 x CH₂). ¹³C{¹H}-NMR (100 MHz, CDCl₃): δ 137.9 (C_q), 129.4 (2C, CH), 128.4 (2C, CH), 127.3 (CH), 67.2 (2 x CH₂), 63.6 (2 x CH₂), 53.8 (s, CH₂), HRMS (ESI): m/z Calcd for C₁₁H₁₅NO + H⁺ [M + H]⁺ 178.1226; Found 178.1227. The analytical data are in accordance with those reported in the literature.



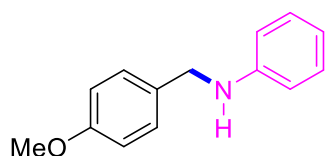
N-benzylpyridin-3-amine (6n):⁴⁶ The representative procedure was followed, using benzonitrile (**1a**; 0.052 g, 0.50 mmol), 3-amino pyridine (**5n**; 0.052 g, 0.55 mmol) and Me₂NH-BH₃ (0.059 g, 1.0 mmol). Purification by column chromatography on silica gel (petroleum ether/EtOAc: 1/10) yielded **6n** (0.044 g, 48%) as a colourless oil. ¹H-NMR (500 MHz, CDCl₃): δ 8.07 (s, 1H, Ar-H), 7.95 (s, 1H, Ar-H), 7.36-7.25 (m, 5H, Ar-H), 7.07-7.04 (dd, $J = 4.6, 3.8$ Hz, 1H, Ar-H), 6.86 (dd, $J = 8.4, 2.3$ Hz, 1H, Ar-H), 4.33 (s, 2H, CH₂), 4.21 (br s, 1H, NH). ¹³C{¹H}-NMR (125 MHz, CDCl₃): δ 144.3 (C_q), 138.9 (CH), 138.6 (CH), 136.2 (CH), 129.0 (2C, CH), 127.7 (CH), 127.6 (2C, CH), 123.9 (C_q), 118.8 (CH), 48.0 (CH₂). HRMS (ESI): m/z Calcd for C₁₂H₁₂N₂ + H⁺ [M + H]⁺ 185.1073; Found 185.1073. The analytical data are in accordance with those reported in the literature.



N-benzylpyridin-4-amine (6o):⁵⁸ The representative procedure was followed, using benzonitrile (**1a**; 0.052 g, 0.50 mmol), 4-amino pyridine (**5o**; 0.071 g, 0.75 mmol) and Me₂NH-BH₃ (0.059 g, 1.0 mmol). Purification by column chromatography on silica (petroleum ether/EtOAc: 1/10) yielded **6o** (0.048 g, 52%) as a yellow oil. ¹H NMR (500 MHz, CDCl₃): δ 8.04 (d, *J* = 3.0 Hz, 1H, Ar-H), 7.95 (d, *J* = 4.6 Hz, 1H, Ar-H), 7.33 (d, *J* = 4.2 Hz, 4H, Ar-H), 7.29-7.26 (m, 1H, Ar-H), 7.04 (dd, *J* = 4.3 Hz, 1H, Ar-H), 6.87-6.83 (m, 1H, Ar-H), 4.32 (s, CH₂), 4.23 (br s, NH). ¹³C{¹H}-NMR (125 MHz, CDCl₃): δ 144.2 (C_q), 139.0 (CH), 138.7 (C_q), 136.3 (CH), 128.9 (2C, CH), 127.6 (CH), 127.5 (2C, CH), 123.9 (CH), 118.7 (CH), 48.0 (CH₂). HRMS (ESI): *m/z* Calcd for C₁₂H₁₂N₂ + H⁺ [M + H]⁺ 185.1073; Found 185.1067. The analytical data are in accordance with those reported in the literature.

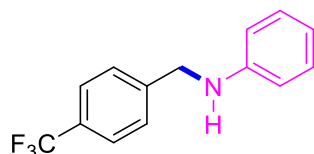


N-benzyl-1-(pyridin-3-yl)methanamine (6p):⁵⁹ The representative procedure was followed, using benzonitrile (**1a**; 0.052 g, 0.50 mmol), pyridin-3-ylmethanamine (**5p**; 0.059 g, 0.55 mmol) and Me₂NH-BH₃ (0.059 g, 1.0 mmol). Purification by column chromatography on silica gel (petroleum ether/EtOAc: 2/1) yielded **6p** (0.080 g, 81%) as a yellow oil. ¹H-NMR (400 MHz, CDCl₃): δ 8.57 (s, 1H, Ar-H), 8.45 (d, *J* = 4.3 Hz, 1H, Ar-H), 7.71 (d, *J* = 7.9 Hz, 1H, Ar-H), 7.34 (d, *J* = 4.3 Hz, 4H, Ar-H), 7.30-7.24 (m, 2H, Ar-H), 3.81 (s, CH₂), 2.32 (s, 1H, NH). ¹³C{¹H}-NMR (100 MHz, CDCl₃): δ 149.7 (CH), 148.4 (CH), 139.7 (C_q), 136.0 (CH), 135.6 (C_q), 128.5 (2C, CH), 128.2 (2C, CH), 127.2 (CH), 123.5 (CH), 53.1 (CH₂) 50.4 (CH₂). HRMS (ESI): *m/z* Calcd for C₁₃H₁₄N₂ + H⁺ [M + H]⁺ 199.1230; Found 199.1223. The analytical data are in accordance with those reported in the literature.

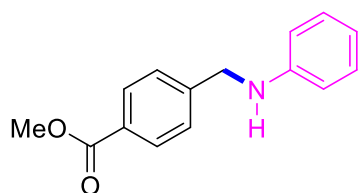


N-(4-methoxybenzyl)aniline (6q):⁶⁰ The representative procedure was followed, using 4-methoxy benzonitrile (**1b**; 0.067 g, 0.50 mmol), aniline (**5a**; 0.051 g, 0.55 mmol) and Me₂NH-BH₃ (0.059 g, 1.0 mmol). Purification by column chromatography on silica gel

(petroleum ether/EtOAc: 10/1) yielded **6q** (0.096 g, 90%) as a yellow oil. $^1\text{H-NMR}$ (500 MHz, CDCl_3): δ 7.32 (d, $J = 8.4$ Hz, 2H, Ar-H), 7.20 (vt, $J = 7.6$ Hz, 2H, Ar-H), 6.91 (d, $J = 9.2$ Hz, 2H, Ar-H), 6.74 (vt, $J = 7.6$ Hz, 1H, Ar-H), 6.66 (d, $J = 7.6$ Hz, 2H, Ar-H), 4.28 (s, 2H, CH_2), 3.83 (s, 3H, CH_3). $^{13}\text{C}\{^1\text{H}\}$ -NMR (125 MHz, CDCl_3): δ 159.0 (C_q), 148.4 (C_q), 131.6 (C_q), 129.4 (2C, CH), 129.0 (2C, CH), 117.7 (CH), 114.2 (2C, CH), 113.0 (2C, CH), 55.5 (CH_2), 48.0 (CH_3). HRMS (ESI): m/z Calcd for $\text{C}_{14}\text{H}_{13}\text{NO} + \text{H}^+$ $[\text{M} + \text{H}]^+$ 212.1070; Found 212.1069. The analytical data are in accordance with those reported in the literature.

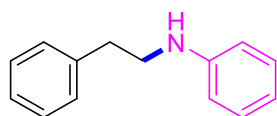


***N*-(4-(trifluoromethyl)benzyl)aniline (6r):**⁶⁰ The representative procedure was followed, using 4-trifluoromethyl benzonitrile (**1c**; 0.085 g, 0.50 mmol), aniline (**5a**; 0.051 g, 0.55 mmol) and $\text{Me}_2\text{NH-BH}_3$ (0.059 g, 1.0 mmol). Purification by column chromatography on silica (petroleum ether/EtOAc: 5/1) yielded **6r** (0.095 g, 76%) as a colourless oil. $^1\text{H-NMR}$ (400 MHz, CDCl_3): δ 7.49 (d, $J = 7.9$ Hz, 2H, Ar-H), 7.37 (d, $J = 7.9$ Hz, 2H, Ar-H), 7.08 (vt, $J = 7.9$ Hz, 2H, Ar-H), 6.64 (vt, $J = 7.3$ Hz, 1H, Ar-H), 6.50 (d, $J = 7.9$ Hz, 2H, Ar-H), 4.30 (s, 2H, CH_2), 4.03 (s, 1H, NH). $^{13}\text{C}\{^1\text{H}\}$ -NMR (100 MHz, CDCl_3): δ 147.8 (C_q), 144.0 (C_q), 129.6 ($^2J_{\text{C-F}} = 33.1$ Hz, C_q), 129.5 (2C, CH), 127.6 (2C, CH), 125.7 ($^3J_{\text{C-F}} = 3.5$ Hz, 2C, CH), 124.4 (q, $^1J = 272.8$ Hz, CF_3), 118.1 (CH), 113.1 (2C, CH), 47.9 (CH_2). $^{19}\text{F-NMR}$ (377 MHz, CDCl_3): δ -62.4. HRMS (ESI): m/z Calcd for $\text{C}_{14}\text{H}_{12}\text{NF}_3 + \text{H}^+$ $[\text{M} + \text{H}]^+$ 252.0995; Found 252.0992. The analytical data are in accordance with those reported in the literature.

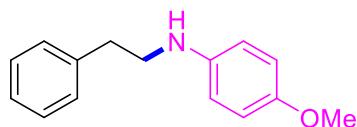


1-(4-((phenylamino)methyl)phenyl)ethan-1-one (6s):⁶¹ The representative procedure was followed, using methyl 4-cyanobenzoate (**1e**; 0.081 g, 0.50 mmol), aniline (**5a**; 0.051 g, 0.55 mmol) and $\text{Me}_2\text{NH-BH}_3$ (0.059 g, 1.0 mmol). Purification by column chromatography on silica (petroleum ether/EtOAc: 10/1) yielded **6r** (0.107 g, 89%) as a colourless oil. $^1\text{H-NMR}$ (400 MHz, CDCl_3): δ 8.05 (d, $J = 7.9$ Hz, 2H, Ar-H), 7.49 (d, $J = 7.9$ Hz, 2H, Ar-H), 7.21 (vt, $J = 7.9$ Hz, 2H, Ar-H), 6.77 (vt, $J = 7.3$ Hz, 1H, Ar-H), 6.65 (d, $J = 8.5$ Hz, 2H, Ar-H), 4.43 (s, 2H, CH_2), 4.21 (s, 1H, NH), 3.95 (s, 3H, CH_3). $^{13}\text{C}\{^1\text{H}\}$ -NMR (100 MHz, CDCl_3): δ

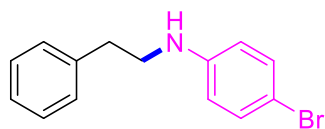
167.1 (CO), 147.9 (C_q), 145.1 (C_q), 130.0 (2C, CH), 129.4 (2C, CH), 129.1 (C_q), 127.2 (2C, CH), 117.9 (CH), 113.0 (2C, CH), 52.2 (CH₂), 48.0 (CH₃). HRMS (ESI): *m/z* Calcd for C₁₅H₁₅O₂N + H⁺ [M + H]⁺ 242.1176; Found 242.1171. The analytical data are in accordance with those reported in the literature.



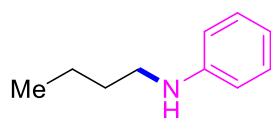
***N*-phenethylamine (6t):**⁴⁶ The representative procedure was followed, using benzylocyanide (**1f**; 0.058 g, 0.5 mmol), aniline (**5a**; 0.051 g, 0.55 mmol) and Me₂NH-BH₃ (0.059 g, 1.0 mmol). Purification by column chromatography on silica (petroleum ether/EtOAc: 10/1) yielded **6t** (0.088 g, 89%) as a colourless oil. ¹H-NMR (400 MHz, CDCl₃): δ 7.33 (vt, *J* = 7.2 Hz, 2H, Ar-H), 7.27-7.17 (m, 5H, Ar-H), 6.73 (vt, *J* = 7.6 Hz, 1H, Ar-H), 6.63 (d, *J* = 8.4 Hz, 2H, Ar-H), 3.68 (br s, 1H, NH), 3.41 (t, *J* = 7.2 Hz, 2H, CH₂), 2.93 (t, *J* = 7.2 Hz, 2H, CH₂). ¹³C{¹H}-NMR (100 MHz, CDCl₃): δ 148.2 (C_q), 139.5 (C_q), 129.5 (2C, CH), 129.0 (2C, CH), 128.8 (2C, CH), 126.6 (CH), 117.6 (CH), 113.2 (2C, CH), 45.2 (CH₂), 35.7 (CH₂). HRMS (ESI): *m/z* Calcd for C₁₄H₁₅N + H⁺ [M + H]⁺ 198.1277; Found 198.1276. The analytical data are in accordance with those reported in the literature.



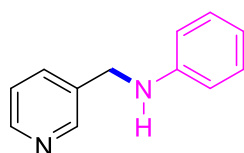
4-methoxy-*N*-phenethylamine (6u):⁶² The representative procedure was followed, using benzylocyanide (**1f**; 0.058 g, 0.5 mmol), 4-methoxy aniline (**5b**; 0.069 g, 0.55 mmol) and Me₂NH-BH₃ (0.059 g, 1.0 mmol). Purification by column chromatography on silica gel (petroleum ether/EtOAc: 20/1) yielded **6u** (0.101 g, 89%) as a yellow oil. ¹H-NMR (400 MHz, CDCl₃): δ 7.38 (vt, *J* = 7.6 Hz, 2H, Ar-H), 7.31-7.27 (m, 3H, Ar-H), 6.85 (d, *J* = 7.2 Hz, 2H, Ar-H), 6.65 (d, *J* = 8.4 Hz, 2H, Ar-H), 3.80 (s, 3H, CH₃), 3.41 (t, *J* = 6.9 Hz, 2H, CH₂), 3.23 (s, 1H, NH), 2.96 (t, *J* = 7.2 Hz, 2H, CH₂). ¹³C{¹H}-NMR (100 MHz, CDCl₃): δ 152.4 (C_q), 142.4 (C_q), 139.6 (C_q), 128.9 (2C, CH), 128.7 (2C, CH), 126.5 (CH), 115.1 (2C, CH), 114.6 (2C, CH), 55.9 (CH₃), 46.2 (CH₂), 35.7 (CH₂). HRMS (ESI): *m/z* Calcd for C₁₅H₁₇NO + H⁺ [M + H]⁺ 228.1344; Found 228.1343. The analytical data are in accordance with those reported in the literature.



4-bromo-N-phenethylamine (6v):⁶³ The representative procedure was followed, using benzyl cyanide (**1f**; 0.058 g, 0.5 mmol), 4-bromo aniline (**5c**; 0.095 g, 0.55 mmol) and Me₂NH-BH₃ (0.059 g, 1.0 mmol). Purification by column chromatography on silica (petroleum ether/EtOAc: 20/1) yielded **6v** (0.108 g, 78%) as a brown oil. ¹H-NMR (400 MHz, CDCl₃): δ 7.35 (vt, *J* = 7.2 Hz, 2H, Ar-H), 7.29-7.23 (m, 5H, Ar-H), 6.51 (d, *J* = 8.0 Hz, 2H, Ar-H), 3.72 (s, 1H, NH), 3.41 (t, *J* = 6.9 Hz, 2H, CH₂), 2.93 (t, *J* = 6.5 Hz, 2H, CH₂). ¹³C{¹H}-NMR (100 MHz, CDCl₃): δ 147.1 (C_q), 139.2 (C_q), 132.1 (2C, CH), 128.9 (2C, CH), 128.8 (2C, CH), 126.7 (CH), 114.7 (2C, CH), 109.1 (C_q), 45.1 (CH₂), 35.5 (CH₂). HRMS (ESI): *m/z* Calcd for C₁₄H₁₄NBr + H⁺ [M + H]⁺ 276.0382; Found 276.0388. The analytical data are in accordance with those reported in the literature.

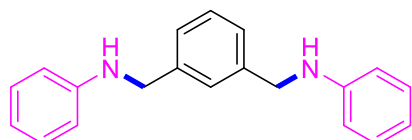


N-butylaniline (6w):⁶⁴ The representative procedure was followed, using butyronitrile (**1h**; 0.034 g, 0.5 mmol), aniline (**5a**; 0.051 g, 0.55 mmol) and Me₂NH-BH₃ (0.059 g, 1.0 mmol). Purification by column chromatography on silica gel (petroleum ether/EtOAc: 10/1) yielded **6w** (0.056 g, 75%) as a colourless oil. ¹H-NMR (500 MHz, CDCl₃): δ 7.20 (vt, *J* = 8.4 Hz, 2H, Ar-H), 6.71 (vt, *J* = 7.2 Hz, 1H, Ar-H), 6.63 (d, *J* = 7.6 Hz, 2H, Ar-H), 3.60 (br s, 1H, NH), 3.14 (t, *J* = 7.2 Hz, 2H, CH₂), 1.63 (pent, *J* = 7.3 Hz, 2H, CH₂), 1.50-1.42 (m, 2H, CH₂), 0.99 (t, *J* = 7.2 Hz, 3H, CH₃). ¹³C{¹H}-NMR (125 MHz, CDCl₃): δ 148.7 (C_q), 129.4 (2C, CH), 117.2 (CH), 112.9 (2C, CH), 43.8 (CH₂), 31.9 (CH₂), 20.5 (CH₂), 14.1 (CH₃). HRMS (ESI): *m/z* Calcd for C₁₀H₁₅N + H⁺ [M + H]⁺ 150.1277; Found 150.1271. The analytical data are in accordance with those reported in the literature.

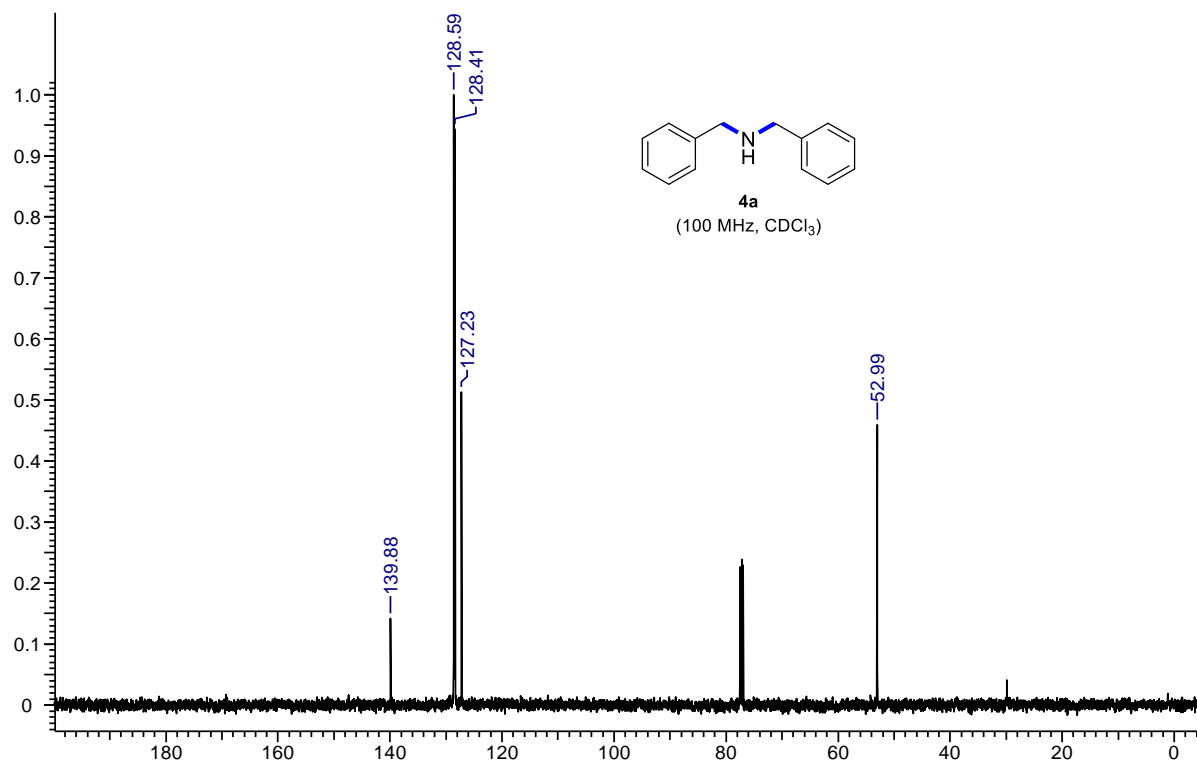
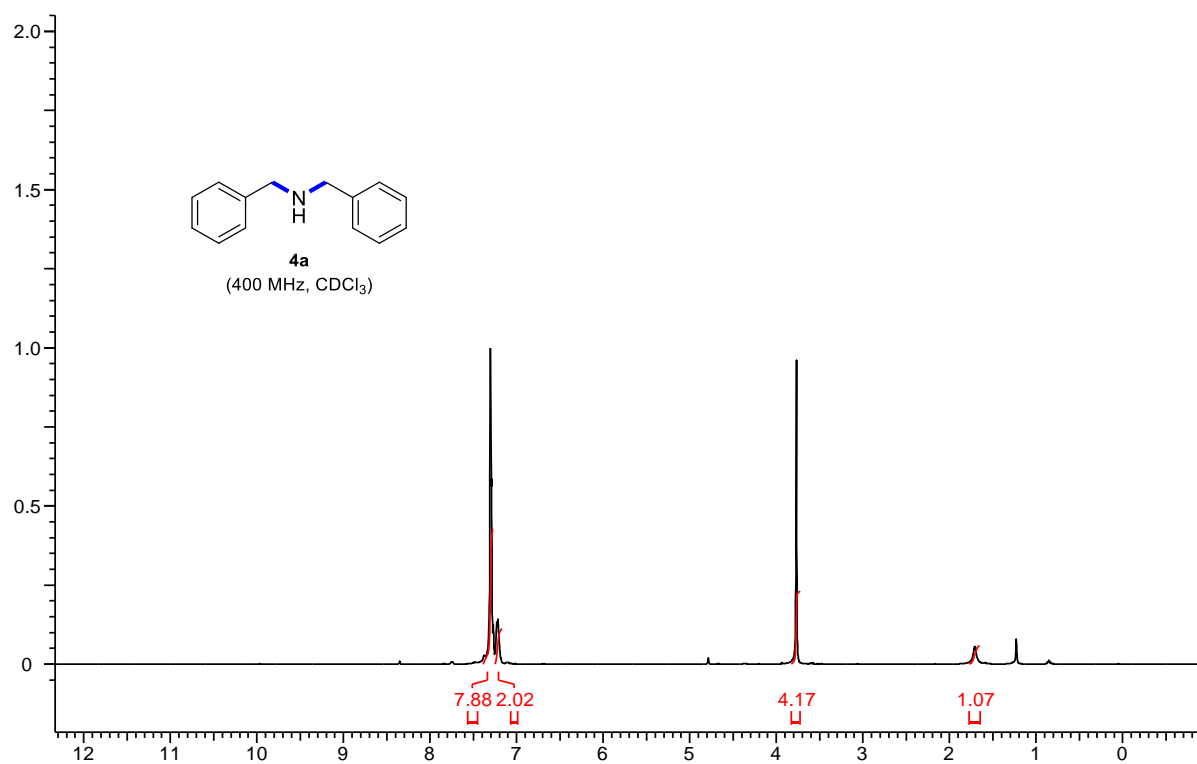


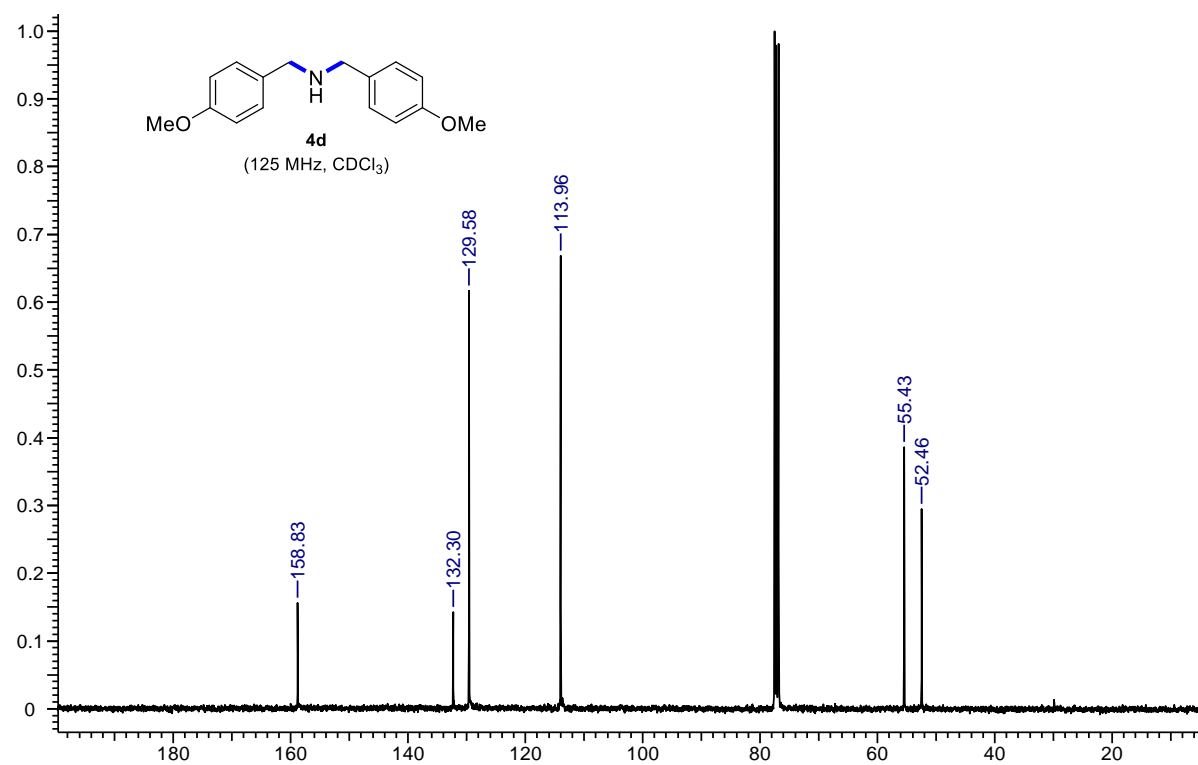
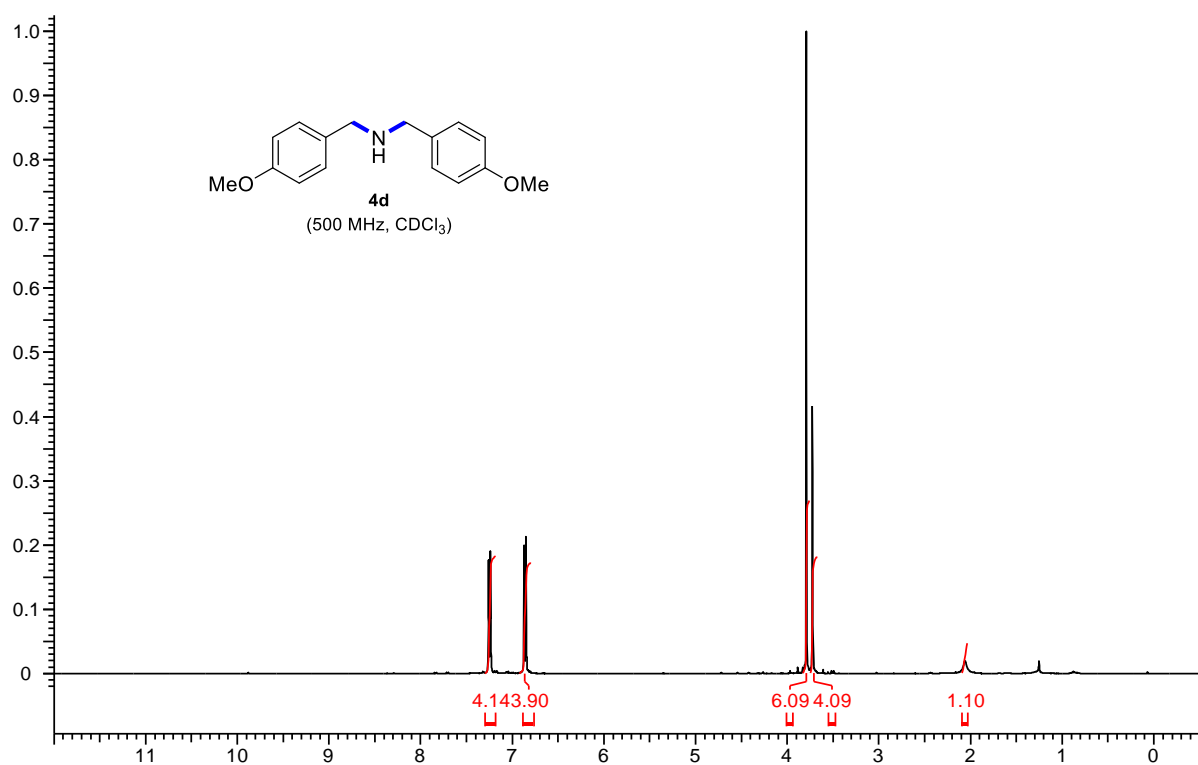
N-(pyridin-3-ylmethyl)aniline (6x):⁶⁵ The representative procedure was followed, using 3-cyano pyridine (**1d**; 0.052 g, 0.5 mmol), aniline (**5a**; 0.051 g, 0.55 mmol) and Me₂NH-BH₃ (0.059 g, 1.0 mmol). Purification by column chromatography on silica gel (petroleum ether/EtOAc: 1/1) yielded **6x** (0.076 g, 83%) as off white solid. ¹H-NMR (400 MHz, CDCl₃):

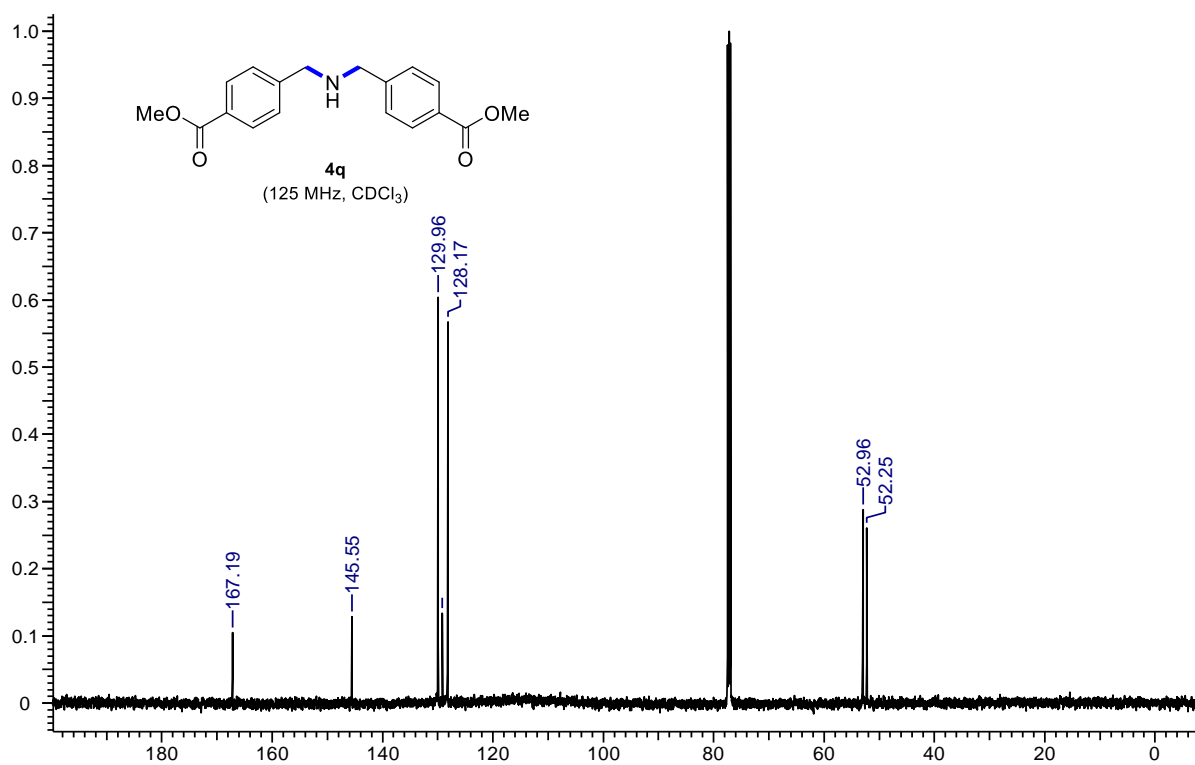
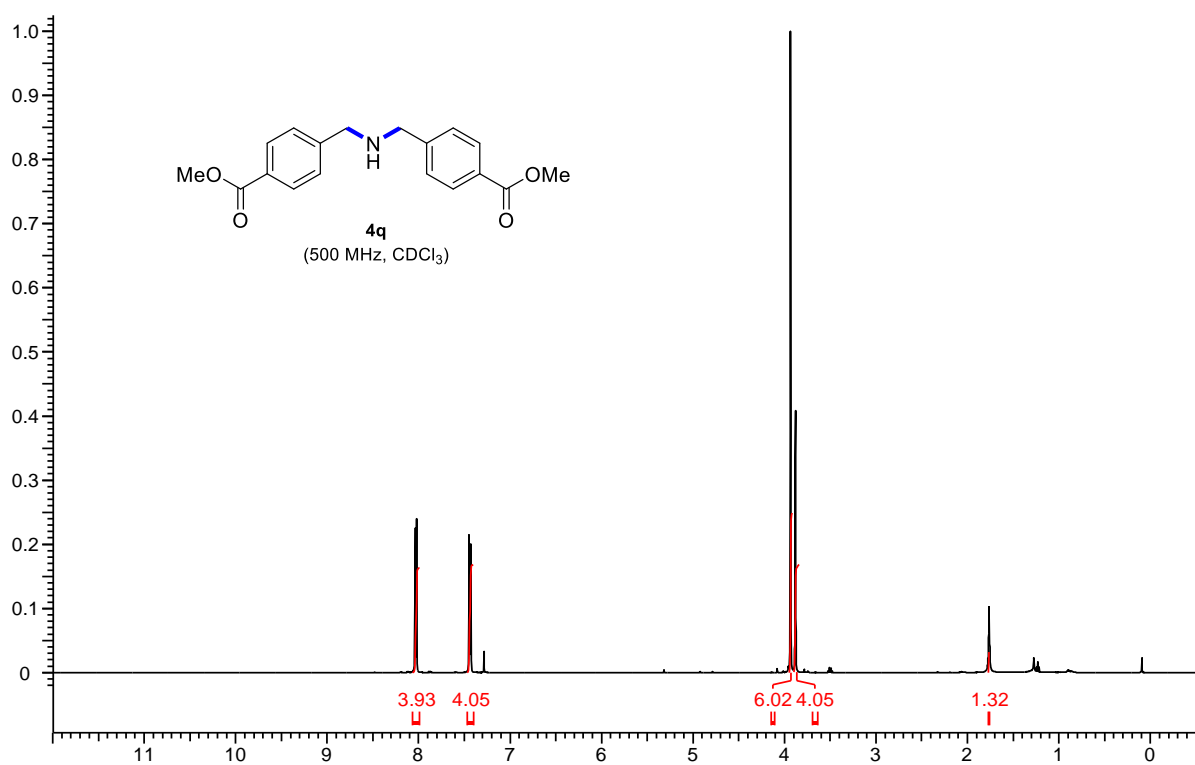
δ 8.66 (s, 1H, Ar-H), 8.56 (d, $J = 3.7$ Hz, 1H, Ar-H), 7.72 (d, $J = 7.9$ Hz, 1H, Ar-H), 7.30-7.27 (m, 1H, Ar-H), 7.20 (vt, $J = 7.9$ Hz, 2H, Ar-H), 6.77 (vt, $J = 7.3$ Hz, 1H, Ar-H), 6.65 (d, $J = 7.9$ Hz, 2H, Ar-H), 4.38 (s, CH₂), 4.10 (s, 1H, NH). ¹³C{¹H}-NMR (100 MHz, CDCl₃): δ 149.3 (CH), 148.9 (CH), 147.8 (C_q), 135.3 (CH), 135.1 (C_q), 129.5 (2C, CH), 123.7 (CH), 118.2 (CH), 113.1 (2C, CH), 46.0 (CH₂). HRMS (ESI): m/z Calcd for C₁₂H₁₂N₂ + H⁺ [M + H]⁺ 185.1073; Found 185.1073. The analytical data are in accordance with those reported in the literature.

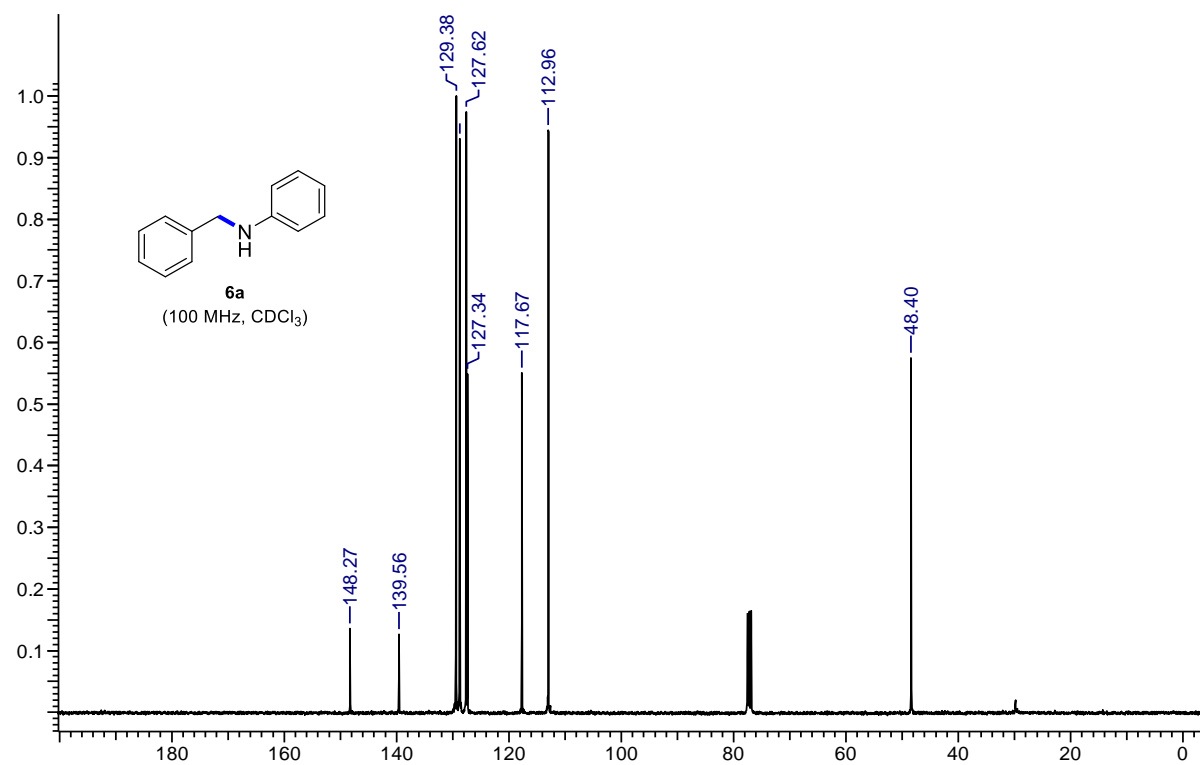
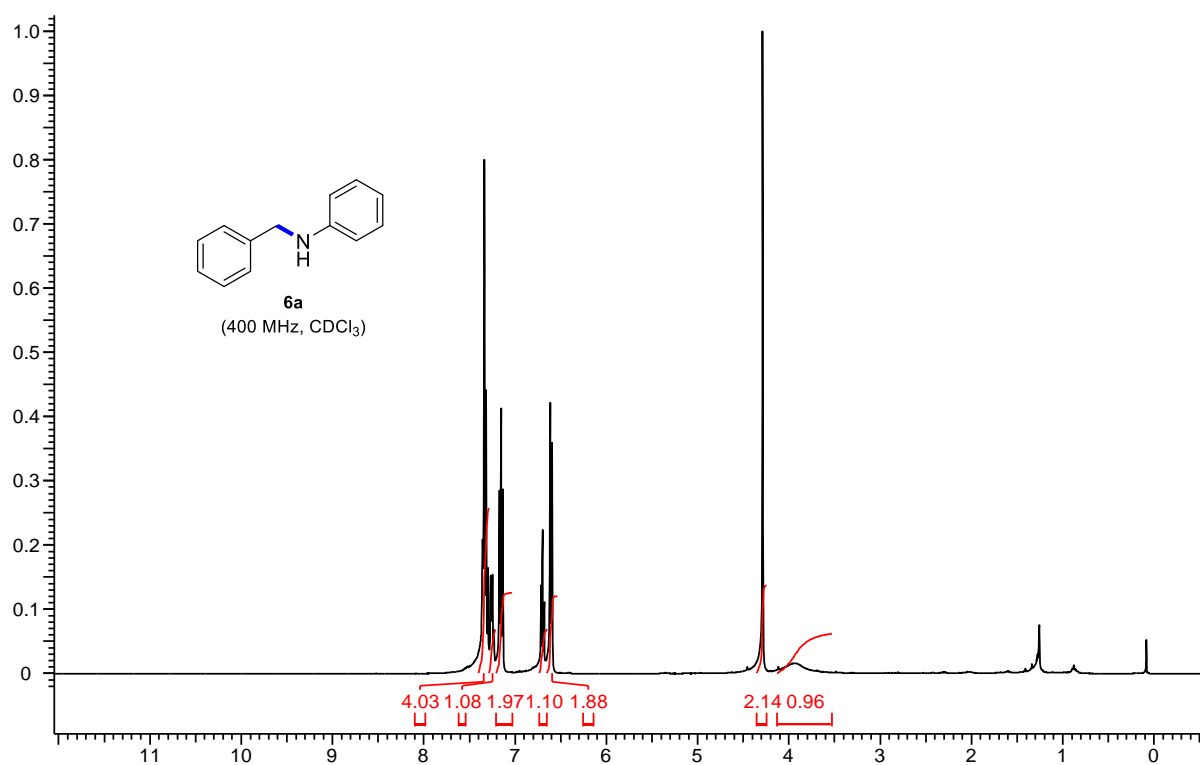


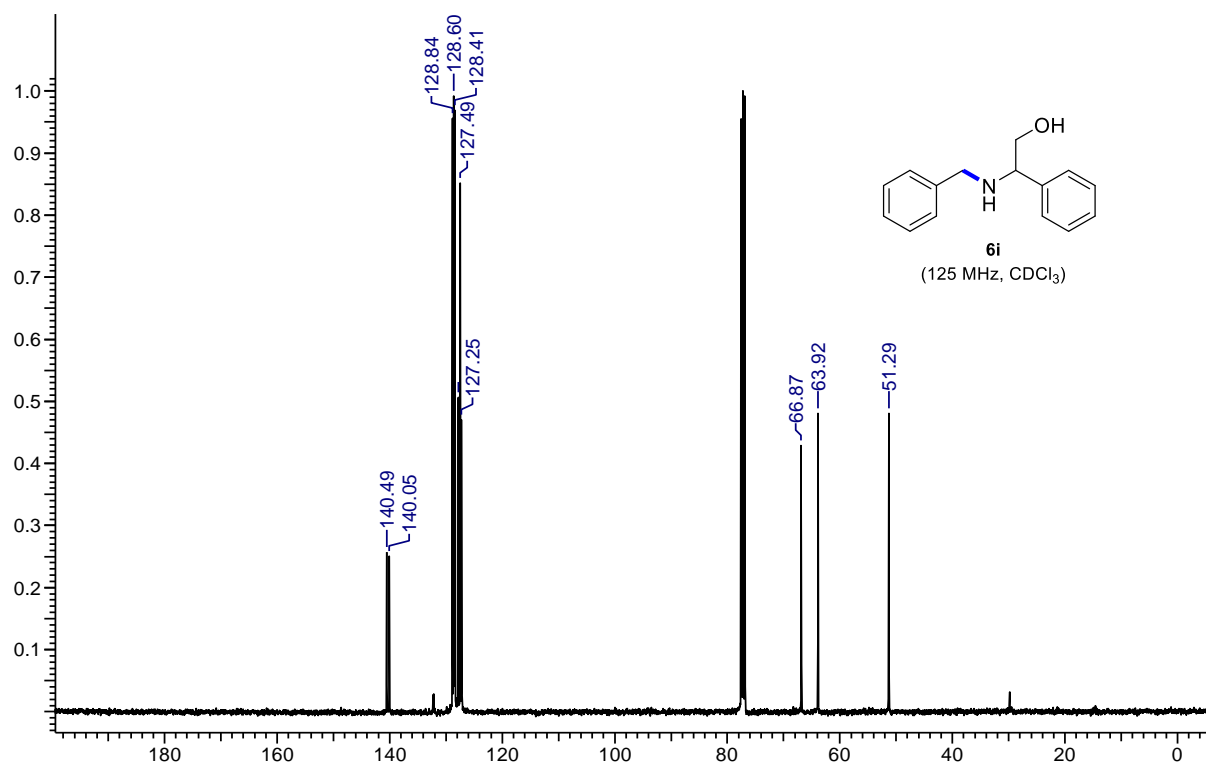
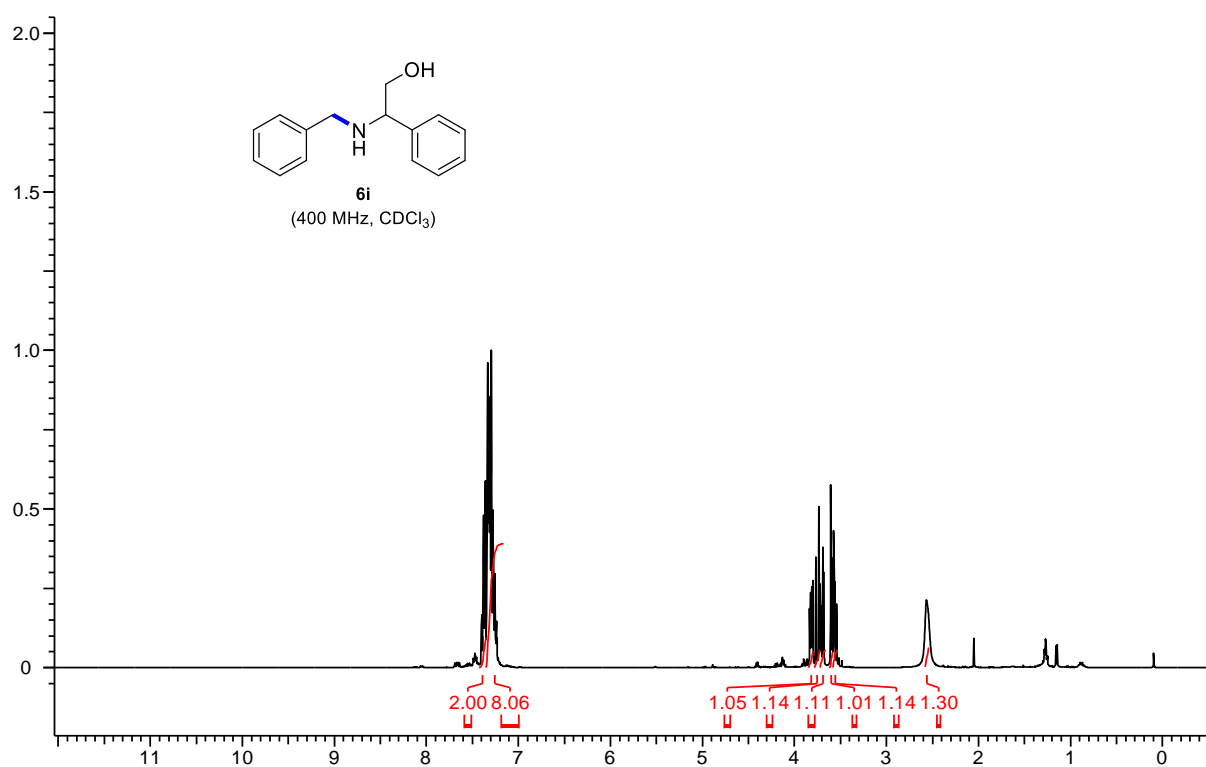
***N,N'*-(1,3-phenylenebis(methylene))dianiline (6y)**: The representative procedure was followed, using 1,3-dicyanobenzene (**1g**; 0.064 g, 0.5 mmol), aniline (**5a**; 0.102 g, 1.1 mmol) and Me₂NH-BH₃ (0.117 g, 2.0 mmol). Purification by column chromatography on silica gel (petroleum ether/EtOAc: 5/1) yielded **6y** (0.107 g, 74%) as a white oil. ¹H-NMR (500 MHz, CDCl₃): δ 7.40 (s, 1H, Ar-H), 7.35-7.29 (m, 3H, Ar-H), 7.19 (vt, $J = 7.2$ Hz, 4H, Ar-H), 6.74 (vt, $J = 7.2$ Hz, 2H, Ar-H), 6.65 (d, $J = 7.6$ Hz, 4H, Ar-H), 4.34 (s, 4H, 2 x CH₂), 4.04 (s, 2H, 2 x NH). ¹³C{¹H}-NMR (125 MHz, CDCl₃): δ 148.3 (2C, C_q), 140.1 (2C, C_q), 129.5 (4C, CH), 129.1 (2C, CH), 126.8 (2C, CH), 126.6 (CH), 117.8 (CH), 113.1 (4C, CH), 48.5 (2 x CH₂). HRMS (ESI): m/z Calcd for C₂₀H₂₀N₂ + H⁺ [M + H]⁺ 289.1699; Found 289.1691.

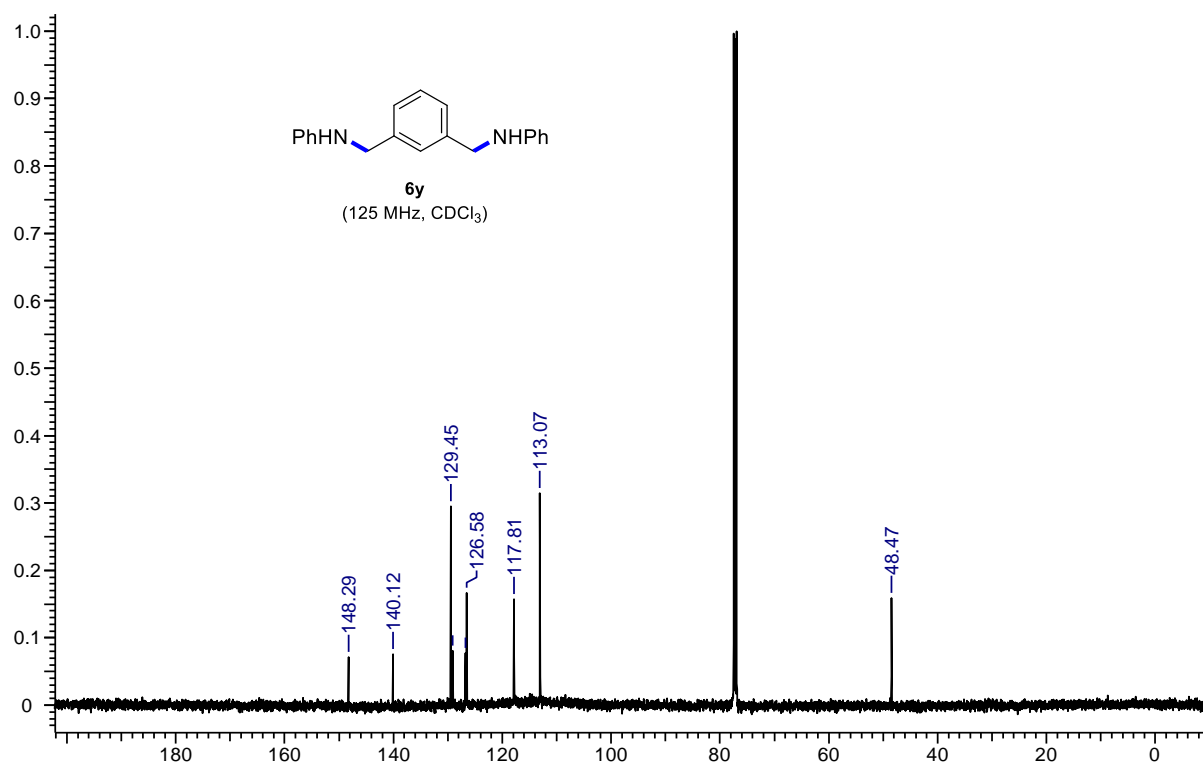
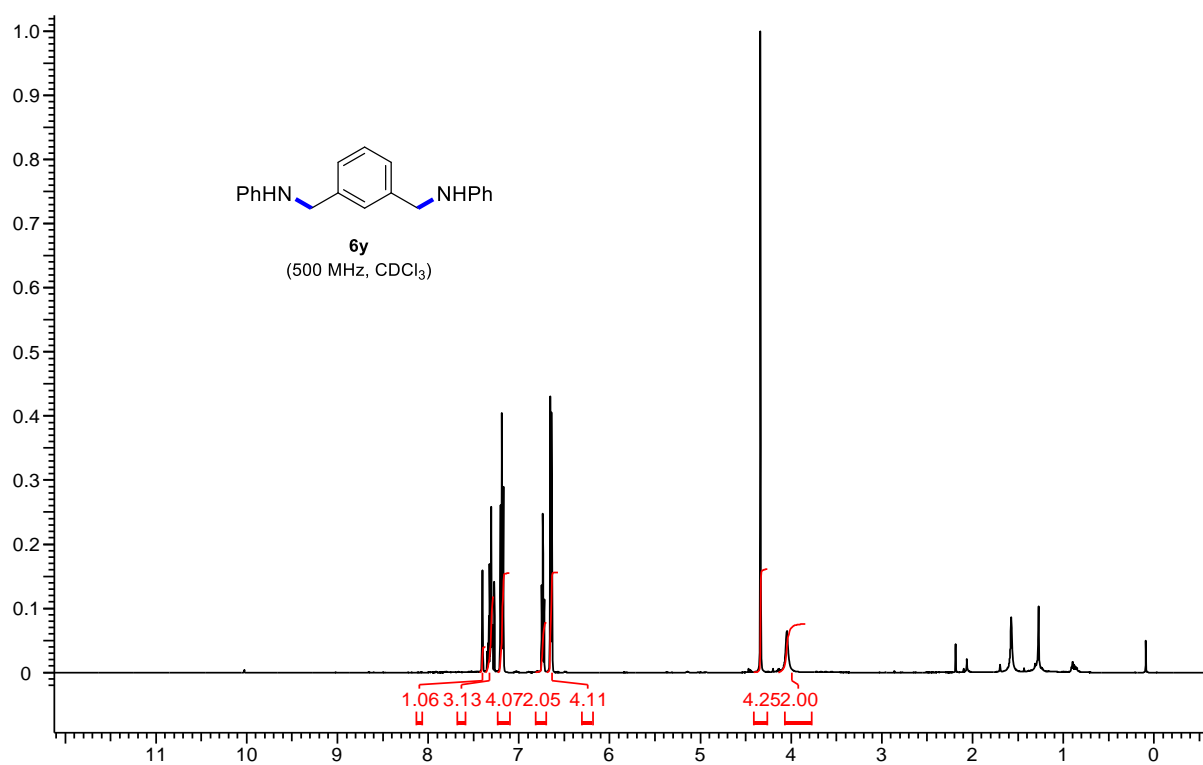
3.4.7 ^1H & ^{13}C Spectra of Selected Secondary Amines











3.5 REFERENCES

- (1) Blaser, H.-U.; Malan, C.; Pugin, B.; Spindler, F.; Steiner, H.; Studer, M. *Adv. Synth. Catal.* **2003**, *345*, 103-151.
- (2) Bagal, D. B.; Bhanage, B. M. *Adv. Synth. Catal.* **2015**, *357*, 883-900.
- (3) Werkmeister, S.; Junge, K.; Beller, M. *Org. Pro. Res. Dev.* **2014**, *18*, 289-302.
- (4) Liu, W.; Sahoo, B.; Junge, K.; Beller, M. *Acc. Chem. Res.* **2018**, *51*, 1858-1869.
- (5) Chakraborty, S.; Berke, H. *ACS Catal.* **2014**, *4*, 2191-2194.
- (6) Reguillo, R.; Grellier, M.; Vautravers, N.; Vendier, L.; Sabo-Etienne, S. *J. Am. Chem. Soc.* **2010**, *132*, 7854-7855.
- (7) Srimani, D.; Feller, M.; Ben-David, Y.; Milstein, D. *Chem. Commun.* **2012**, *48*, 11853-11855.
- (8) Miao, X.; Bidange, J.; Dixneuf, P. H.; Fischmeister, C. d.; Bruneau, C.; Dubois, J.-L.; Couturier, J.-L. *ChemCatChem* **2012**, *4*, 1911-1916.
- (9) Werkmeister, S.; Junge, K.; Wendt, B.; Spannenberg, A.; Jiao, H.; Bornschein, C.; Beller, M. *Chem. Eur. J.* **2014**, *20*, 4227-4231.
- (10) Adam, R.; Alberico, E.; Baumann, W.; Drexler, H.-J.; Jackstell, R.; Junge, H.; Beller, M. *Chem. Eur. J.* **2016**, *22*, 4991-5002.
- (11) Adam, R.; Bheeter, C. B.; Jackstell, R.; Beller, M. *ChemCatChem* **2016**, *8*, 1329-1334.
- (12) Saha, S.; Kaur, M.; Singh, K.; Bera, J. K. *J. Organomet. Chem.* **2016**, *812*, 87-94.
- (13) Galan, A.; De Mendoza, J.; Prados, P.; Rojo, J.; Echavarren, A. M. *J. Org. Chem.* **1991**, *56*, 452-454.
- (14) Monguchi, Y.; Mizuno, M.; Ichikawa, T.; Fujita, Y.; Murakami, E.; Hattori, T.; Maegawa, T.; Sawama, Y.; Sajiki, H. *J. Org. Chem.* **2017**, *82*, 10939-10944.
- (15) Sato, Y.; Kayaki, Y.; Ikariya, T. *Organometallics* **2016**, *35*, 1257-1264.
- (16) Nishida, Y.; Chaudhari, C.; Imatome, H.; Sato, K.; Nagaoka, K. *Chem. Lett.* **2018**, *47*, 938-940.
- (17) Nait Ajjou, A.; Robichaud, A. *Appl. Organometal. Chem.* **2018**, *32*, e4481.
- (18) Saito, Y.; Ishitani, H.; Ueno, M.; Kobayashi, S. *ChemistryOpen* **2017**, *6*, 211-215.
- (19) Chin, C. S.; Lee, B. *Catal. Lett.* **1992**, *14*, 135-140.
- (20) Lu, S.; Wang, J.; Cao, X.; Li, X.; Gu, H. *Chem. Commun.* **2014**, *50*, 3512-3515.
- (21) Elangovan, S.; Topf, C.; Fischer, S.; Jiao, H.; Spannenberg, A.; Baumann, W.; Ludwig, R.; Junge, K.; Beller, M. *J. Am. Chem. Soc.* **2016**, *138*, 8809-8814.

-
- (22) Bornschein, C.; Werkmeister, S.; Wendt, B.; Jiao, H.; Alberico, E.; Baumann, W.; Junge, H.; Junge, K.; Beller, M. *Nature Commun.* **2014**, *5*, 4111.
- (23) Chakraborty, S.; Leitus, G.; Milstein, D. *Chem. Commun.* **2016**, *52*, 1812-1815.
- (24) Lange, S.; Elangovan, S.; Cordes, C.; Spannenberg, A.; Jiao, H.; Junge, H.; Bachmann, S.; Scalone, M.; Topf, C.; Junge, K.; Beller, M. *Catal. Sci. Technol.* **2016**, *6*, 4768-4772.
- (25) Chakraborty, S.; Milstein, D. *ACS Catal.* **2017**, *7*, 3968-3972.
- (26) Chakraborty, S.; Leitus, G.; Milstein, D. *Angew. Chem. Int. Ed.* **2017**, *56*, 2074-2078.
- (27) Mukherjee, A.; Srimani, D.; Chakraborty, S.; Ben-David, Y.; Milstein, D. *J. Am. Chem. Soc.* **2015**, *137*, 8888-8891.
- (28) Chen, F.; Topf, C.; Radnik, J.; Kreyenschulte, C.; Lund, H.; Schneider, M.; Surkus, A.-E.; He, L.; Junge, K.; Beller, M. *J. Am. Chem. Soc.* **2016**, *138*, 8781-8788.
- (29) Tokmic, K.; Jackson, B. J.; Salazar, A.; Woods, T. J.; Fout, A. R. *J. Am. Chem. Soc.* **2017**, *139*, 13554-13561.
- (30) Adam, R.; Bheeter, C. B.; Cabrero-Antonino, J. R.; Junge, K.; Jackstell, R.; Beller, M. *ChemSusChem* **2017**, *10*, 842-846.
- (31) Dai, H.; Guan, H. *ACS Catal.* **2018**, *8*, 9125-9130.
- (32) Ferraccioli, R.; Borovika, D.; Surkus, A.-E.; Kreyenschulte, C.; Topf, C.; Beller, M. *Catal. Sci. Technol.* **2018**, *8*, 499-507.
- (33) Li, H.; Al-Dakhil, A.; Lupp, D.; Gholap, S. S.; Lai, Z.; Liang, L.-C.; Huang, K.-W. *Org. Lett.* **2018**, *20*, 6430-6435.
- (34) Schneekönig, J.; Tannert, B.; Hornke, H.; Beller, M.; Junge, K. *Catal. Sci. Technol.* **2019**, *9*, 1779-1783.
- (35) Filonenko, G. A.; van Putten, R.; Hensen, E. J. M.; Pidko, E. A. *Chem. Soc. Rev.* **2018**, *47*, 1459-1483.
- (36) Junge, K.; Papa, V.; Beller, M. *Chem. Eur. J.* **2019**, *25*, 122-143.
- (37) Wang, D.; Astruc, D. *Chem. Rev.* **2015**, *115*, 6621-6686.
- (38) Shares, J.; Yehl, J.; Kowalsick, A.; Byers, P.; Haaf, M. P. *Tet. Lett.* **2012**, *53*, 4426-4428.
- (39) Vilches-Herrera, M.; Werkmeister, S.; Junge, K.; Borner, A.; Beller, M. *Catal. Sci. Technol.* **2014**, *4*, 629-632.
- (40) Werkmeister, S.; Bornschein, C.; Junge, K.; Beller, M. *Chem. Eur. J.* **2013**, *19*, 4437-4440.
-

-
- (41) Werkmeister, S.; Bornschein, C.; Junge, K.; Beller, M. *Eur. J. Org. Chem.* **2013**, *2013*, 3671-3674.
- (42) Labes, R.; González-Calderón, D.; Battilocchio, C.; Mateos, C.; Cumming, G. R.; de Frutos, O.; Rincón, J. A.; Ley, S. V. *Synlett.* **2017**, *28*, 2855–2858.
- (43) Alshakova, I. D.; Gabidullin, B.; Nikonov, G. I. *ChemCatChem* **2018**, *10*, 4860-4869.
- (44) Long, J.; Shen, K.; Li, Y. *ACS Catal.* **2017**, *7*, 275-284.
- (45) Garduno, J. A.; Garcia, J. J. *ACS Omega* **2017**, *2*, 2337-2343.
- (46) Shao, Z.; Fu, S.; Wei, M.; Zhou, S.; Liu, Q. *Angew. Chem. Int. Ed.* **2016**, *55*, 14653-14657.
- (47) Werkmeister, S.; Neumann, J.; Junge, K.; Beller, M. *Chem. Eur. J.* **2015**, *21*, 12226-12250.
- (48) Kallmeier, F.; Kempe, R. *Angew. Chem. Int. Ed.* **2018**, *57*, 46-60.
- (49) Mondal, A. K.; Sundararajan, M.; Konar, S. *Dalton Trans.* **2018**, *47*, 3745-3754.
- (50) Arachchige, P. T. K.; Lee, H.; Yi, C. S. *J. Org. Chem.* **2018**, *83*, 4932-4947.
- (51) Patel, H. A.; Rawat, M.; Patel, A. L.; Bedekar, A. V. *Appl. Organometal. Chem.* **2019**, *33*, e4767.
- (52) Varjosaari, S. E.; Skrypai, V.; Suating, P.; Hurley, J. J. M.; Lio, A. M. D.; Gilbert, T. M.; Adler, M. J. *Adv. Synth. Catal.* **2017**, *359*, 1872-1878.
- (53) Laroche, B.; Ishitani, H.; Kobayashi, S. *Adv. Synth. Catal.* **2018**, *360*, 4699-4704.
- (54) Nguyen, H. N.; Lee, H.; Audörsch, S.; Reznichenko, A. L.; Nawara-Hultsch, A. J.; Schmidt, B.; Hultsch, K. C. *Organometallics* **2018**, *37*, 4358-4379.
- (55) Sitte, N. A.; Bursch, M.; Grimme, S.; Paradies, J. *J. Am. Chem. Soc.* **2019**, *141*, 159-162.
- (56) Li, N.; Bai, J.; Zheng, X.; Rao, H. *J. Org. Chem.* **2019**, *84*, 6928-6939.
- (57) Cosgrove, S. C.; Plane, J. M. C.; Marsden, S. P. *Chem. Sci.* **2018**, *9*, 6647-6652.
- (58) Wu, Z.; Yang, G.; Zhao, X.; Wu, J.; Wu, S. *J. Heterocyclic Chem.* **2019**, *56*, 234-238.
- (59) Singh, V.; Kumar, V.; Gupta, A. N.; Drew, M. G. B.; Singh, N. *New J. Chem.* **2014**, *38*, 3737-3748.
- (60) Elliott, D. C.; Marti, A.; Mauleón, P.; Pfaltz, A. *Chem. Eur. J.* **2019**, *25*, 1918-1922.
- (61) Ye, D.; Huang, R.; Zhu, H.; Zou, L.-H.; Wang, D. *Org. Chem. Front.* **2019**, *6*, 62-69.
- (62) Emayavaramban, B.; Chakraborty, P.; Sundararaju, B. *ChemSusChem* **2019**, *12*, 3089-3093.
- (63) Wong, C. M.; Peterson, M. B.; Pernik, I.; McBurney, R. T.; Messerle, B. A. *Inorg. Chem.* **2017**, *56*, 14682-14687.
-

- (64) Ganguli, K.; Shee, S.; Panja, D.; Kundu, S. *Dalton Trans.* **2019**, 48, 7358-7366.
- (65) Wu, Y.; Huang, Y.; Dai, X.; Shi, F. *ChemSusChem* **2019**, 12, 3185-3191.

Chapter 4

Catalytic Hydrogenation of Nitriles to Secondary Amines and Imines using Cobalt Catalyst and Molecular H₂

4.1 INTRODUCTION

Hydrogenation of nitriles is among the most performed synthetic reaction in traditional organic chemistry. The reduced products of nitriles, i.e., primary amines, secondary amines or imines are of the prime importance due to their application in pharmaceuticals, dyes, agrochemicals.¹⁻³ In that regards, the selective catalytic hydrogenation of nitriles to any of the mentioned products is significant process in academia and industries.²⁻⁴ Traditionally, the transition-metal catalyzed nitrile hydrogenation has been remained the best route to obtain the amines.⁴ However, the catalytic reduction of nitriles leads to number of reduced products as mentioned in chapter 3, thus, design and development of a catalytic system which can selectively afford the product of choice is of great importance. Mainly the noble transition metal catalysts are developed for the hydrogenation of nitriles to amine products using either hydrogen pressure or hydrogen sacrificial.⁵⁻¹⁷ Nonetheless, the low natural abundance of these 2nd and 3rd row transition metals ultimately affects their cost which is on high side and hence, they need to be substituted by their 3d counterparts.

The first-row transition metal catalysts have dominated recent decade research on hydrogenation. Particularly, the hydrogenation of nitrile is well explored with late 3d-transition metals like manganese,¹⁸ iron,¹⁹⁻²³ and cobalt.²⁴⁻³⁰ However, many first-row transition metal catalysts are designed to obtain the primary amine as a product of nitrile hydrogenation.³¹ Nonetheless, a protocol to get another product, i.e., secondary imine as a result of nitrile hydrogenation was demonstrated by the Milstein group. The phosphine-based iron hydride catalyst could convert nitriles into secondary imines at 30 bar hydrogen pressure and the addition of external amine provided an unsymmetrical secondary imine.^{21,22} Similarly, a phosphine-based $\text{PN}^3\text{P-CoBr}_2$ complex hydrogenated nitriles to secondary imine using 62 bar hydrogen pressure.²⁶ The reports on synthesizing secondary amine, an essential product of nitrile hydrogen, are minimal. Shao demonstrated the hydrogenation of nitriles to secondary amines where phosphine-based (PNN)- CoCl_2 catalyst was used with ammonia-borane as a hydrogen source. In the same report, the unsymmetrical secondary amines were synthesized by adding an external amine source.³²

Recently, a $\text{Cu}(\text{OTf})_2$ -catalyzed transfer hydrogenation protocol for converting nitriles to amines has been reported by Zhou.³³ Though the transfer hydrogenation is an excellent alternative to the hydrogenation with molecular H_2 , the issue of the generation of unwanted byproducts is always associated with it. Thus, there is a demand for a base-metal catalytic system that could perform hydrogenation of nitriles to a secondary amine by using hydrogen

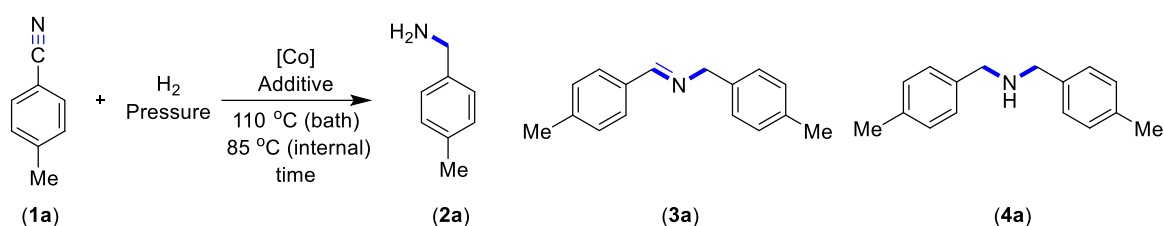
pressure. Dai and Guan, reported that the combination of Co(II) salt, i.e., CoBr₂ with NaHBEt₃, resulted in heterogeneous cobalt-boride nanoparticles formation.³⁰ These particles were capable of hydrogenating nitriles to provide primary amines. However, the same combination in the presence of PNP phosphine ligand forms a PNP-CoBr₂ complex which alters the selectivity of product to secondary imine and catalyzes the reaction homogeneously. Notably, a methodology based on a 3d-transition metal catalyst to carry out the catalytic hydrogenation of nitriles to secondary amines using hydrogen pressure is not yet disclosed. In this chapter, we disclose a catalytic system made up of a combination of Co(II) salts, i.e., CoCl₂ or CoBr₂, and ammonia-borane, which can hydrogenate nitriles to secondary amines at 20 bar hydrogen pressure. Various aromatic nitriles with functional groups like –OMe, –^tBu, –CF₃, and halides (fluoro, chloro, and bromo) hydrogenated to respective secondary amines with moderate to good yield.

4.2 RESULTS AND DISCUSSION

4.2.1 Optimization of Reaction Condition for the Hydrogenation of Nitriles to Symmetrical Secondary Amines

Dai and Guan shown that the Co-nanoparticles, obtained from Co(II) and NaBEt₃H, could catalyze the hydrogenation of nitriles to give primary amines.³⁰ The selectivity for primary amine depended on the size and structure of pores in cobalt particles. On the same verge, we thought of generating cobalt nano-particles by treating Co(II) salts with different activators to get selectively secondary amines as a product (Table 4.1). Thus, we initiated the optimization studies for the hydrogenation of nitriles to secondary amines by taking *p*-tolunitrile (**1a**) as a model substrate with CoBr₂ (10 mol%) and KO^tBu (20 mol%) in toluene and heated at 90 °C (110 °C bath temperature) using 20 bar hydrogen pressure which resulted into the complete hydrogenation of nitrile, albeit into primary amine (entry 1). The replacement of KO^tBu with NaO^tBu also led to primary amine formation in 85% (entry 2). Next, we checked other potassium bases, i.e., KHMDS and KH, which helped to get selectivity for secondary imine, but with lower conversion (entries 3, 4). Ammonia-borane as an additive to the reaction led to a drastic change in the selectivity as 64% of secondary imine (**3a**) formed with 36% secondary amine (**4a**) (entry 5). However, dimethylammonia-borane was inefficient, providing only 15% total conversion (entry 6). Next, we investigated a solvent effect in the reaction. For that, we checked solvents like dioxane, THF, 2-chlorobenzene, etc., to achieve the selectivity for the desired reductive aminated product **4a**. However, the change in solvent was not helpful for selective hydrogenation (entries 7-9).

Next, we screened the cobalt precursor to $\text{Co}(\text{OAc})_2$, which provided all three products (**2a**, **3a**, and **4a**) in almost equal amounts (entry 10). However, the CoCl_2 as a precursor provided a desired secondary amine (**4a**) as a major product with 69% conversion (entry 11). After successfully achieving the selectivity for the secondary amine, we further changed the amount of ammonia-borane to get increment for the selective **4a** formation. In that direction, we examined the different amounts of $\text{NH}_3\text{-BH}_3$, i.e., 25 mol%, 15 mol%, 10 mol%, and 12 mol%, among which 12 mol% opted for the best conversion of nitrile to secondary amine (**4a**) with 84% conversion and 79% isolated yield (entries 12-15). Thus, a mixture of CoCl_2 (10 mol%) and $\text{NH}_3\text{-BH}_3$ (12 mol%) efficiently catalyzes the selective hydrogenation of nitriles to secondary amines (**4a**) at 20 bar hydrogen pressure and 90 °C.

Table 4.1 Optimization of reaction parameters for nitrile hydrogenation.^a

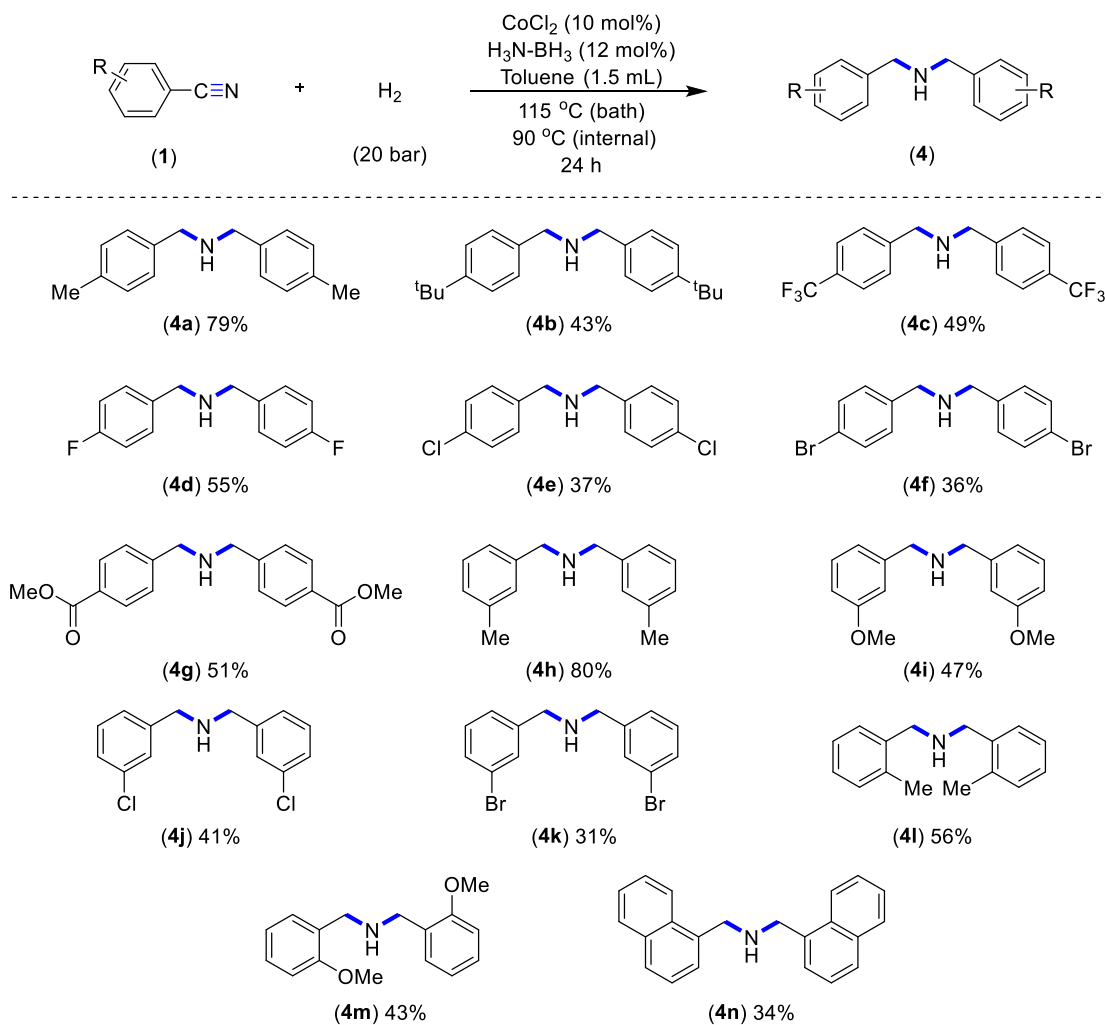
Entry	[Co]	Additive	H ₂ Pressure	Solvent	GC Conv ^b	2a ^b	3a ^b	4a ^b
1	CoBr ₂	KO ^t Bu	20 bar	Toluene	100	90	10	-
2	CoBr ₂	NaO ^t Bu	20 bar	Toluene	100	85	11	4
3	CoBr ₂	KHMDS	20 bar	Toluene	23	8	13	2
4	CoBr ₂	KH	20 bar	Toluene	41	12	21	9
5	CoBr ₂	NH ₃ -BH ₃	20 bar	Toluene	100	-	64	36
6	CoBr ₂	Me ₂ NH-BH ₃	20 bar	Toluene	15	12	3	-
7	CoBr ₂	NH ₃ -BH ₃	20 bar	Dioxane	100	87	13	-
8	CoBr ₂	NH ₃ -BH ₃	20 bar	2-chloro benzene	100	40	58	2
9	CoBr ₂	NH ₃ -BH ₃	20 bar	THF	100	71	28	1
10	Co(OAc) ₂	NH ₃ -BH ₃	20 bar	Toluene	100	34	25	41
11	CoCl ₂	NH ₃ -BH ₃	20 bar	Toluene	100	30	1	69
12 ^c	CoCl ₂	NH ₃ -BH ₃	20 bar	Toluene	100	31	4	65
13 ^d	CoCl ₂	NH ₃ -BH ₃	20 bar	Toluene	100	25	5	70
14 ^e	CoCl ₂	NH ₃ -BH ₃	20 bar	Toluene	100	18	6	76
15 ^{f,i}	CoCl₂	NH₃-BH₃	20 bar	Toluene	100	9	7	84 (79%) ^j
16	CoCl ₂	NH ₃ -BH ₃	30 bar	Toluene	100	25	7	68
17 ^{e,g}	CoBr ₂	NH ₃ -BH ₃	20 bar	Toluene	58	4	47	7
18 ^g	CoBr ₂	NH ₃ -BH ₃	20 bar	Toluene	100	-	75	25
19 ^{d,g}	CoBr ₂	NH ₃ -BH ₃	20 bar	Toluene	100	-	85	15
20 ^{g,h}	CoBr ₂	NH ₃ -BH ₃	20 bar	Toluene	30	-	16	14
21 ^{d,g}	CoBr ₂	NH ₃ -BH ₃	15 bar	Toluene	100	-	89	11
22 ^{d,g}	CoBr ₂	NH ₃ -BH ₃	10 bar	Toluene	76	12	64	-

^aReaction conditions: *p*-tolunitrile (0.0351 g, 0.30 mmol), Co(II) salt (10 mol%), Additive (20 mol%), solvent (1.5 mL). ^bGC conversion based on substrate *p*-tolunitrile. ^cNH₃-BH₃ (25 mol%), ^dNH₃-BH₃ (15 mol%), ^eNH₃-BH₃ (10 mol%), ^fNH₃-BH₃ (12 mol%), ^gCoBr₂ (5 mol%), ^hNH₃-BH₃ (5 mol%), ⁱ90 °C internal temperature. ^jisolated yield is in parenthesis.

After obtaining the best condition for secondary amine (**4a**), we optimized the parameters to get secondary imine as an exclusive product. We followed the condition at entry 5 and changed the amount of CoBr₂ (5 mol%) and ammonia-borane (10 mol%), which resulted in a lowering of total conversion (entry 17). But selectivity for imine was retained. During the study, we realized that the dependency of the product selectivity was related to the ratio of Co(II) and ammonia-borane. Thus, we investigated the effect of the different amounts of ammonia-borane, i.e., 20 mol%, 15 mol%, and 5 mol% keeping CoBr₂ constant (5 mol%) (entries 18-20). This alteration reflected that the 5 mol% CoBr₂ and 15 mol% ammonia-borane is the best combination for secondary imine. We further reduced the hydrogen pressure to 15 bar to decrease the secondary amine formation, which helped to get 89% selectivity for secondary imine (**3a**) (entry 21). Though we optimized the best condition to get secondary imine product (**3a**), we could not be able to isolate product **3a** as we observed decomposition of the same under the flash chromatography. The optimization study led us to conclude that the selectivity of the resulting nitrile hydrogenation product is mainly governed by the Co(II) salts chosen for the reaction, i.e., CoBr₂ prefers secondary imine product **3a**, while CoCl₂ converts nitrile into secondary amine **4a**. In addition, the ratio of the Co(II) salts and ammonia-borane is crucial to get a better selectivity of the desired product.

4.2.2 Scope for the Synthesis of Symmetrical Secondary Amines

After optimizing the reaction condition for the synthesis of secondary amine, we checked the scope and limitation of the protocol (Scheme 4.1). The variety of synthetically important functionalities tolerated the optimized protocol and provided moderate to good yield. The nitrile with a bulky tertiary-butyl group at the *para* position underwent hydrogenation and provided 43% of the secondary amine **4b**. The -CF₃ group, which is electron deficient, did not affect the hydrogenation of the nitrile **1c** as the product **4c** resulted in 49% yield. Synthetically useful halides like fluoro, chloro, and bromo were relevant to the reaction system as they provided moderate to a good yield of the respective reductive aminated products, **4d**, **4e**, and **4f** in 55%, 37%, and 36% yields respectively. The carboxylic ester, sensitive to hydrogenation, survived during the reaction and afforded respective secondary amine **4g** in 51% yield, highlighting the chemo-selectivity for nitrile over ester. The nitriles with substituents at the *meta* position also reacted well under the reaction condition. The electron-donating -CH₃ at the *meta* position helped to get an excellent yield of 80% for the resulting secondary amine **4h**. Similarly, nitrile with a more electron-rich methoxy group at the *meta* position also reacted well and gave 47% of **4i**.



Scheme 4.1 Scope of reductive amination of nitriles to symmetrical secondary amines. Substrate **1** = 0.5 mmol, CoCl₂ (0.0065 g, 0.05 mmol, 10 mol%), NH₃-BH₃ (0.0019 g, 0.06 mmol, 12 mol%), Toluene (1.5 mL).

Moreover, the nitriles having halides, i.e., -Cl and -Br at *meta* position yielded products **4j** and **4k** in 41% and 31% yield, respectively. The substrate with methyl or methoxy at the *ortho* position of nitrile (**3l** and **3m**) underwent hydrogenation and afforded 56% and 43% of **4l** and **4m**. The naphthalene nitrile was also hydrogenated and provided secondary amine **4n** in a 34% yield. The heterocycle containing aromatic nitriles were intolerant of the protocol as the reaction catalyzed by the cobalt-nanoparticles may be affected by the heteroatom in the heterocycle. Moreover, when aliphatic nitriles and benzyl cyanide hydrogenated under mentioned reaction condition, the complete conversion of nitrile was observed, however, in the form of primary amine. The reaction of CoX₂ with ammonia-borane leads to the generation of cobalt-boride nanoparticles whose formation during the hydrogenation is crucial and controls the reactivity and selectivity of the product. The

isolated yields of majority of secondary amines remained into moderate range which is due to the irregular formation of Co-nanoparticles during the reaction. The selectivity for the secondary amine is highly dependent of the Co-nanoparticles and uneven formation of these particles affected the yields of the secondary amines. Our attempts to afford the unsymmetrical secondary amines by adding external amine didn't led to expected outcome as the poisoning of catalyst was observed in the presence of external amine source. Similarly, our efforts towards isolation of secondary imine products were failed as the decomposition of secondary imine was observed during the flash chromatography.

4.3 CONCLUSION

In this chapter, we have demonstrated a simple nitrile hydrogenative protocol for synthesizing secondary amines from nitriles. The combination of CoCl_2 (10 mol%) and $\text{NH}_3\text{-BH}_3$ (12 mol%) selectively hydrogenates nitriles to secondary amines at 20 bar hydrogen pressure. A range of aromatic nitriles having different functionalities like methoxy, fluoro, chloro, bromo, $-\text{CF}_3$ have undergone smooth hydrogenation and afforded respective secondary amines in moderate to good yield. A nitrile with a sensitive functional group like carboxylic ester ($-\text{COOMe}$) was reduced chemo-selectively providing the secondary amine product. The selectivity for the products (secondary amine/imine) was dependent on metal precursor, i.e., CoCl_2 , while CoBr_2 has selectivity for secondary imine. The reaction between CoX_2 and ammonia-borane generates cobalt-nanoparticles which are the active catalyst for hydrogenation. The developed method shows the first 3d-transitional metal catalyzed nitrile hydrogenation process, which selectively gives secondary amine product using molecular hydrogen (H_2 pressure). The demonstrated way is expected to be helpful for the synthesis of symmetrical secondary amines.

4.4 EXPERIMENTAL SECTION

4.4.1 General Experimental

All manipulations were conducted under an argon atmosphere either in a glove box or by using standard Schlenk techniques in pre-dried glassware. The catalytic reactions were performed in flame-dried reaction vessels with Teflon screw caps. The solvent, toluene dried over Na before use. All other liquid reagents were flushed with argon prior to use. All other chemicals were obtained from commercial sources and were used without further purification. Yields refer to the isolated compounds, estimated to be >95% pure as determined by $^1\text{H-NMR}$. High resolution mass spectrometry (HRMS) mass spectra were

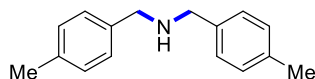
recorded with a Thermo Scientific Q-Exactiva, Accela 1250 pump. ^1H and ^{13}C NMR spectra were recorded at 400 or 500 MHz (^1H), 100 or 125 MHz, (^{13}C , DEPT) and 377 MHz (^{19}F) with Bruker AV 400 and AV 500 spectrometers in CDCl_3 solutions unless otherwise specified. The ^1H and ^{13}C NMR spectra were referenced to residual solvent signals (CDCl_3 : $\delta_{\text{H}} = 7.26$ ppm, $\delta_{\text{C}} = 77.2$ ppm).

GC Method. Gas Chromatography analyses were performed using a Shimadzu GC-2010 gas chromatograph equipped with a Shimadzu AOC-20s auto sampler and a Restek RTX-5 capillary column (30 m x 25 μm x 25 μm). The instrument was set to an injection volume of 1 μL , an inlet split ratio of 10:1, and inlet and detector temperatures of 250 and 320 $^{\circ}\text{C}$, respectively. UHP-grade argon was used as carrier gas with a flow rate of 30 mL/min. The temperature program used for all the analyses is as follows: 80 $^{\circ}\text{C}$, 1 min; 30 $^{\circ}\text{C}/\text{min}$ to 200 $^{\circ}\text{C}$, 2 min; 30 $^{\circ}\text{C}/\text{min}$ to 260 $^{\circ}\text{C}$, 3 min; 30 $^{\circ}\text{C}/\text{min}$ to 300 $^{\circ}\text{C}$, 3 min. *n*-Tetradecane (0.01 mL, 0.038 mmol) was used as an internal standard to calculate the GC yield.

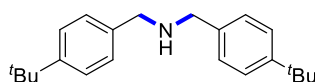
4.4.2 Representative procedure for the hydrogenation of nitriles to secondary amines:

A preheated vial introduced with CoCl_2 (0.0065 g, 0.05 mmol), ammonia-borane (0.0019 g, 0.6 mmol), nitrile (**1**, 0.052 g, 0.50 mmol), and toluene (1.5 mL) inside the glove box. The resultant reaction vial was transferred to a dry autoclave. The autoclave was flushed with H_2 (5 bar) three times in order to remove inert atmosphere. The autoclave was pressurised with 20 bar hydrogen pressure and placed into preheated oil bath. The reaction stirred for 24 h at 110 $^{\circ}\text{C}$ (oil bath temperature). After completion of reaction time the autoclave was opened by releasing the hydrogen pressure and the reaction mixture was concentrated. The crude reaction mixture was then purified by flash chromatography using petroleum ether/EtOAc: 5/1 as eluent to obtain product **4a** (0.0445 g, 79%).

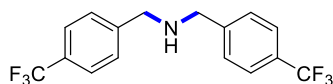
4.4.3 Characterization Data of Symmetrical Secondary Amines



Bis(4-methylbenzyl)amine (4a): The representative procedure was followed, using 4-methylbenzonitrile (**1a**; 0.059 g, 0.50 mmol), CoCl_2 (0.0065 g, 0.05 mmol), $\text{NH}_3\text{-BH}_3$ (0.0019 g, 0.615 mmol). Purification by column chromatography on silica gel (petroleum ether/EtOAc: 5/1) yielded **4a** (0.0445 g, 79%) as a colourless oil. $^1\text{H-NMR}$ (500 MHz, CDCl_3): δ 7.26 (d, $J = 7.9$ Hz, 4H, Ar-H), 7.17 (d, $J = 7.9$ Hz, 4H, Ar-H), 3.79 (s, 4H, 2 x CH_2), 2.37 (s, 6H, 2 x CH_3), 1.87 (s, 1H, NH). $^{13}\text{C}\{^1\text{H}\}\text{-NMR}$ (1125 MHz, CDCl_3): δ 137.4 (2C, C_q), 136.6 (2C, C_q), 129.2 (4C, CH), 128.3 (4C, CH), 52.9 (2C, CH_2), 21.2 (2C, CH_3). HRMS (ESI): m/z Calcd for $\text{C}_{16}\text{H}_{19}\text{N} + \text{H}^+$ $[\text{M} + \text{H}]^+$ 226.1590; Found 226.1586. The analytical data are in accordance with those reported in the literature.

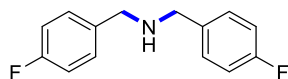


Bis(4-(tert-butyl)benzyl)amine (4b): The representative procedure was followed, using 4-*t*-butylbenzonitrile (**1b**; 0.079 g, 0.50 mmol), CoCl_2 (0.0065 g, 0.05 mmol), $\text{NH}_3\text{-BH}_3$ (0.0019 g, 0.615 mmol). Purification by column chromatography on silica gel (petroleum ether/EtOAc: 5/1) yielded **4b** (0.033 g, 43%) as a colourless oil. $^1\text{H-NMR}$ (500 MHz, CDCl_3): δ 7.40 (d, $J = 7.6$ Hz, 4H, Ar-H), 7.32 (d, $J = 7.6$ Hz, 4H, Ar-H), 3.83 (s, 4H, 2 x CH_2), 2.21 (s, 1H, NH), 1.36 (s, 18H, 6 x CH_3). $^{13}\text{C}\{^1\text{H}\}\text{-NMR}$ (125 MHz, CDCl_3): δ 150.1 (2C, C_q), 137.3 (2C, C_q), 128.1 (4C, CH), 125.5 (4C, CH), 52.9 (2 x CH_2), 34.6 (2C, C_q), 31.6 (6C, CH_3). HRMS (ESI): m/z Calcd for $\text{C}_{22}\text{H}_{31}\text{N} + \text{H}^+$ $[\text{M} + \text{H}]^+$ 310.2529; Found 310.2515. The analytical data are in accordance with those reported in the literature.

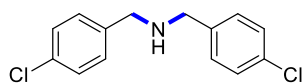


Bis(4-(trifluoromethyl)benzyl)amine (4c): The representative procedure was followed, using 4-trifluoromethyl benzonitrile (**1c**; 0.085 g, 0.50 mmol), CoCl_2 (0.0065 g, 0.05 mmol), $\text{NH}_3\text{-BH}_3$ (0.0019 g, 0.615 mmol). Purification by column chromatography on silica gel (petroleum ether/EtOAc: 1:1) yielded **4c** (0.041 g, 49%) as a colourless oil. $^1\text{H-NMR}$ (500 MHz, CDCl_3): δ 7.62 (d, $J = 8.0$ Hz, 4H, Ar-H), 7.5 (d, $J = 8.0$ Hz, 4H, Ar-H), 3.88 (s, 4H, 2 x CH_2), 1.77 (s, 1H, NH). $^{13}\text{C}\{^1\text{H}\}\text{-NMR}$ (125 MHz, CDCl_3): δ 144.3 (2C, C_q), 129.6 (q, $^2J_{\text{C-F}} = 32.4$ Hz, 2C, C_q), 128.5 (4C, CH), 125.6 (q, $^3J_{\text{C-F}} = 3.8$ Hz, 4C, CH), 124.4 (q, $^1J_{\text{C-F}} = 271.8$

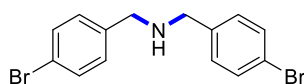
Hz, 2C, CF₃), 52.8 (2 x CH₂). ¹⁹F-NMR (377 MHz, CDCl₃): δ -62.4. HRMS (ESI): *m/z* Calcd for C₁₆H₁₃NF₆ + H⁺ [M + H]⁺ 334.1025; Found 334.1017. The analytical data are in accordance with those reported in the literature.



Bis(4-fluorobenzyl)amine (4d): The representative procedure was followed, using 4-fluorobenzonitrile (**1d**; 0.060 g, 0.50 mmol), CoCl₂ (0.0065 g, 0.05 mmol), NH₃-BH₃ (0.0019 g, 0.615 mmol). Purification by column chromatography on silica gel (petroleum ether/EtOAc: 2/1) yielded **4d** (0.032 g, 55%) as a yellow oil. ¹H-NMR (500 MHz, CDCl₃): δ 7.31-7.27 (m, 4H, Ar-H), 7.03-6.98 (m, 4H, Ar-H), 3.75 (s, 4H, 2 x CH₂), 1.72 (s, 1H, NH). ¹³C{¹H}-NMR (125 MHz, CDCl₃): δ 162.7 (d, ¹J_{C-F} = 245.4 Hz, 2C, C_q), 136.0 (d, ⁴J_{C-F} = 2.9 Hz, 2C, C_q), 129.8 (d, ³J_{C-F} = 7.7 Hz, 4C, CH), 115.4 (d, ²J_{C-F} = 21.1 Hz, 4C, CH), 52.5 (2C, CH₂). ¹⁹F-NMR (377 MHz, CDCl₃): δ -115.9. HRMS (ESI): *m/z* Calcd for C₁₄H₁₃NF₂ + H⁺ [M + H]⁺ 234.1089; Found 234.1085. The analytical data are in accordance with those reported in the literature.

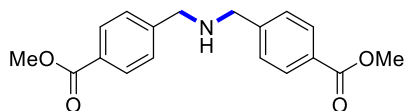


Bis(4-chlorobenzyl)amine (4e): The representative procedure was followed, using 4-chlorobenzonitrile (**1e**; 0.069 g, 0.50 mmol), CoCl₂ (0.0065 g, 0.05 mmol), NH₃-BH₃ (0.0019 g, 0.615 mmol). Purification by column chromatography on silica gel (petroleum ether/EtOAc: 2/1) yielded **4e** (0.0246 g, 37%) as a colourless oil. ¹H-NMR (500 MHz, CDCl₃): δ 7.34-7.29 (m, 8H, Ar-H), 3.78 (s, 4H, 2 x CH₂), 1.75 (s, 1H, NH). ¹³C{¹H}-NMR (125 MHz, CDCl₃): δ 138.8 (2C, C_q), 132.9 (2C, C_q), 129.6 (4C, CH), 128.7 (4C, CH), 52.5 (2C, CH₂). HRMS (ESI): *m/z* Calcd for C₁₄H₁₃NCl₂ + H⁺ [M + H]⁺ 266.0498; Found 266.0521. The analytical data are in accordance with those reported in the literature.

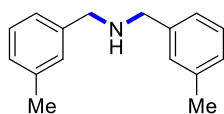


Bis(4-bromobenzyl)amine (4f): The representative procedure was followed, using 4-bromobenzonitrile (**1f**; 0.091 g, 0.50 mmol), CoCl₂ (0.0065 g, 0.05 mmol), NH₃-BH₃ (0.0019 g, 0.615 mmol). Purification by column chromatography on silica gel (petroleum ether/EtOAc: 1/1) yielded **4f** (0.032 g, 36%) as a yellow oil. ¹H-NMR (500 MHz, CDCl₃): δ 7.46 (d, *J* = 8.5 Hz, 4H, Ar-H), 7.22 (d, *J* = 8.5 Hz, 4H, Ar-H), 3.75 (s, 4H, 2 x CH₂), 1.75 (s, 1H, NH).

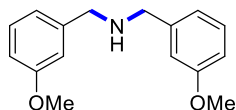
$^{13}\text{C}\{^1\text{H}\}$ -NMR (125 MHz, CDCl_3): δ 139.2 (2C, C_q), 131.7 (4C, CH), 130.0 (4C, CH), 121.0 (2C, C_q), 52.5 (2C, CH_2). HRMS (ESI): m/z Calcd for $\text{C}_{14}\text{H}_{13}\text{NBr} + \text{H}^+$ $[\text{M} + \text{H}]^+$ 355.9467, 357.9436; Found 355.9460, 357.9429. The analytical data are in accordance with those reported in the literature.



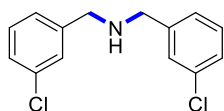
dimethyl 4,4'-(azanediylobis(methylene))dibenzoate (4g): The representative procedure was followed, using methyl 4-cyanobenzoate (**1g**; 0.081 g, 0.50 mmol), CoCl_2 (0.0065 g, 0.05 mmol), $\text{NH}_3\text{-BH}_3$ (0.0019 g, 0.615 mmol). Purification by column chromatography on silica gel (petroleum ether/EtOAc: 1/1) yielded **4g** (0.040 g, 51%) as a colourless oil. ^1H -NMR (400 MHz, CDCl_3): δ 8.01 (d, $J = 8.0$ Hz, 4H, Ar-H), 7.44 (d, $J = 8.4$ Hz, 4H, Ar-H), 3.92 (s, 6H, 2 x CH_3), 3.88 (s, 4H, 2 x CH_2), 1.76 (s, 1H, NH). $^{13}\text{C}\{^1\text{H}\}$ -NMR (100 MHz, CDCl_3): δ 167.2 (2C, CO), 145.6 (2C, C_q), 130.0 (4C, CH), 129.1 (2C, C_q), 128.2 (4C, CH), 53.0 (2 x CH_3), 52.3 (2C, CH_2). HRMS (ESI): m/z Calcd for $\text{C}_{18}\text{H}_{19}\text{O}_4\text{N} + \text{H}^+$ $[\text{M} + \text{H}]^+$ 314.1387; Found 314.1381. The analytical data are in accordance with those reported in the literature.



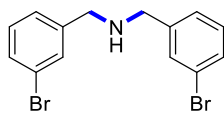
Bis(3-methylbenzyl)amine (4h): The representative procedure was followed, using 3-methyl benzonitrile (**1h**; 0.059 g, 0.50 mmol), CoCl_2 (0.0065 g, 0.05 mmol), $\text{NH}_3\text{-BH}_3$ (0.0019 g, 0.615 mmol). Purification by column chromatography on silica gel (petroleum ether/EtOAc: 5/1) yielded **4h** (0.045 g, 80%) as a colourless oil. ^1H -NMR (500 MHz, CDCl_3): δ 7.28 (vt, $J = 7.6$ Hz, 2H, Ar-H), 7.22-7.18 (m, 4H, Ar-H), 7.13 (d, $J = 7.6$ Hz, 2H, Ar-H), 3.83 (s, 4H, 2 x CH_2), 2.41 (s, 6H, 2 x CH_3), 1.90 (s, 1H, NH). $^{13}\text{C}\{^1\text{H}\}$ -NMR (125 MHz, CDCl_3): δ 140.4 (2C, C_q), 138.2 (2C, C_q), 129.1 (2C, CH), 128.5 (2C, CH), 127.9 (2C, CH), 125.4 (2C, CH), 53.4 (2C, CH_2), 21.6 (2C, CH_3). HRMS (ESI): m/z Calcd for $\text{C}_{16}\text{H}_{19}\text{N} + \text{H}^+$ $[\text{M} + \text{H}]^+$ 226.1590; Found 226.1581. The analytical data are in accordance with those reported in the literature.



Bis(3-methoxybenzyl)amine (4i): The representative procedure was followed, using 3-methoxybenzonitrile (**1i**; 0.067 g, 0.50 mmol), CoCl_2 (0.0065 g, 0.05 mmol), $\text{NH}_3\text{-BH}_3$ (0.0019 g, 0.615 mmol). Purification by column chromatography on silica gel (petroleum ether/EtOAc: 2/1) yielded **4i** (0.030 g, 47%) as a colourless oil. $^1\text{H-NMR}$ (500 MHz, CDCl_3): δ 7.22 (vt, $J = 7.6$ Hz, 2H, Ar-H), 6.90 (m, 4H, Ar-H), 6.78 (m, $J = 7.6$ Hz, 2H, Ar-H), 3.77 (s, 4H, 2 x CH_2), 3.76 (s, 6H, 2 x CH_3), 1.98 (s, 1H, NH). $^{13}\text{C}\{^1\text{H}\}\text{-NMR}$ (125 MHz, CDCl_3): δ 159.8 (2C, C_q), 142.1 (2C, C_q), 129.5 (2C, CH), 120.6 (2C, CH), 113.7 (2C, CH), 112.6 (2C, CH), 55.3 (2C, CH_2), 53.2 (2C, OCH_3). HRMS (ESI): m/z Calcd for $\text{C}_{16}\text{H}_{19}\text{O}_2\text{N} + \text{H}^+$ [$\text{M} + \text{H}$] $^+$ 258.1489; Found 258.1486. The analytical data are in accordance with those reported in the literature.

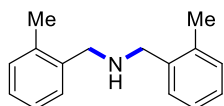


Bis(3-chlorobenzyl)amine (4j): The representative procedure was followed, using 3-chlorobenzonitrile (**1j**; 0.069 g, 0.50 mmol), CoCl_2 (0.0065 g, 0.05 mmol), $\text{NH}_3\text{-BH}_3$ (0.0019 g, 0.615 mmol). Purification by column chromatography on silica gel (petroleum ether/EtOAc: 5/1) yielded **4j** (0.027 g, 41%) as a yellow oil. $^1\text{H-NMR}$ (500 MHz, CDCl_3): δ 7.38 (s, 2H, Ar-H), 7.31-7.23 (m, 6H, Ar-H), 3.80 (s, 4H, 2 x CH_2), 1.81 (s, 1H, NH). $^{13}\text{C}\{^1\text{H}\}\text{-NMR}$ (125 MHz, CDCl_3): δ 142.3 (2C, C_q), 134.5 (2C, C_q), 129.9 (2C, CH), 128.4 (2C, CH), 127.4 (2C, CH), 126.4 (2C, CH), 52.7 (2C, CH_2). HRMS (ESI): m/z Calcd for $\text{C}_{14}\text{H}_{13}\text{NCl}_2 + \text{H}^+$ [$\text{M} + \text{H}$] $^+$ 266.0490; Found 266.0490. The analytical data are in accordance with those reported in the literature.

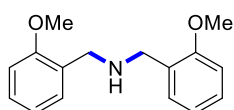


Bis(3-bromobenzyl)amine (4k): The representative procedure was followed, using 3-bromobenzonitrile (**1k**; 0.091 g, 0.50 mmol), CoCl_2 (0.0065 g, 0.05 mmol), $\text{NH}_3\text{-BH}_3$ (0.0019 g, 0.615 mmol). Purification by column chromatography on silica gel (petroleum ether/EtOAc: 5/1) yielded **4k** (0.0275 g, 31%) as yellow oil. $^1\text{H-NMR}$ (400 MHz, CDCl_3): δ 7.51 (s, 2H, Ar-H), 7.39 (d, $J = 7.6$ Hz, 2H, Ar-H), 7.26-7.18 (m, 4H, Ar-H), 3.78 (s, 4H, 2 x CH_2), 1.68 (s, 1H, NH). $^{13}\text{C}\{^1\text{H}\}\text{-NMR}$ (100 MHz, CDCl_3): δ 142.6 (2C, C_q), 131.3 (2C, CH), 130.3

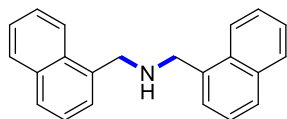
(2C, CH), 130.2 (2C, CH), 126.9 (2C, CH), 122.8 (2C, C_q), 52.7 (2C, CH₂). HRMS (ESI): *m/z* Calcd for C₁₄H₁₃NBr₂ + H⁺ [M + H]⁺ 353.9490, 355.9467, 357.9438; Found 353.9493, 355.9464, 357.9435. The analytical data are in accordance with those reported in the literature.



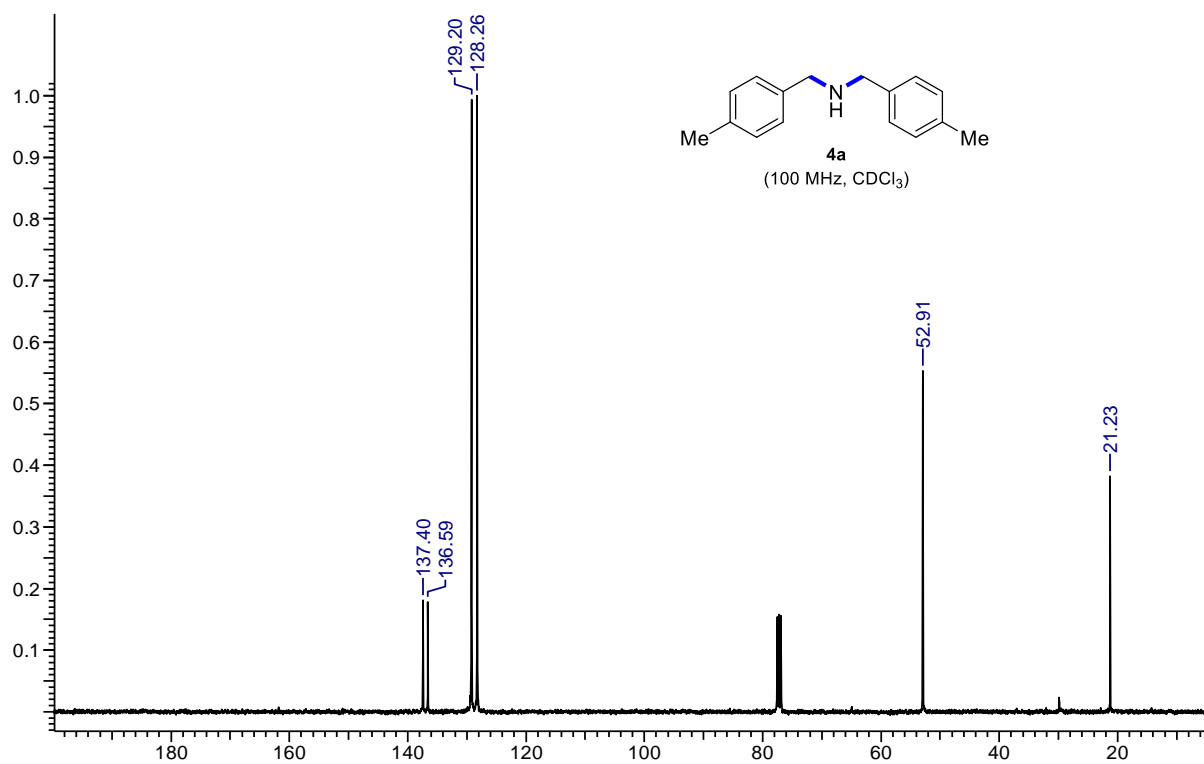
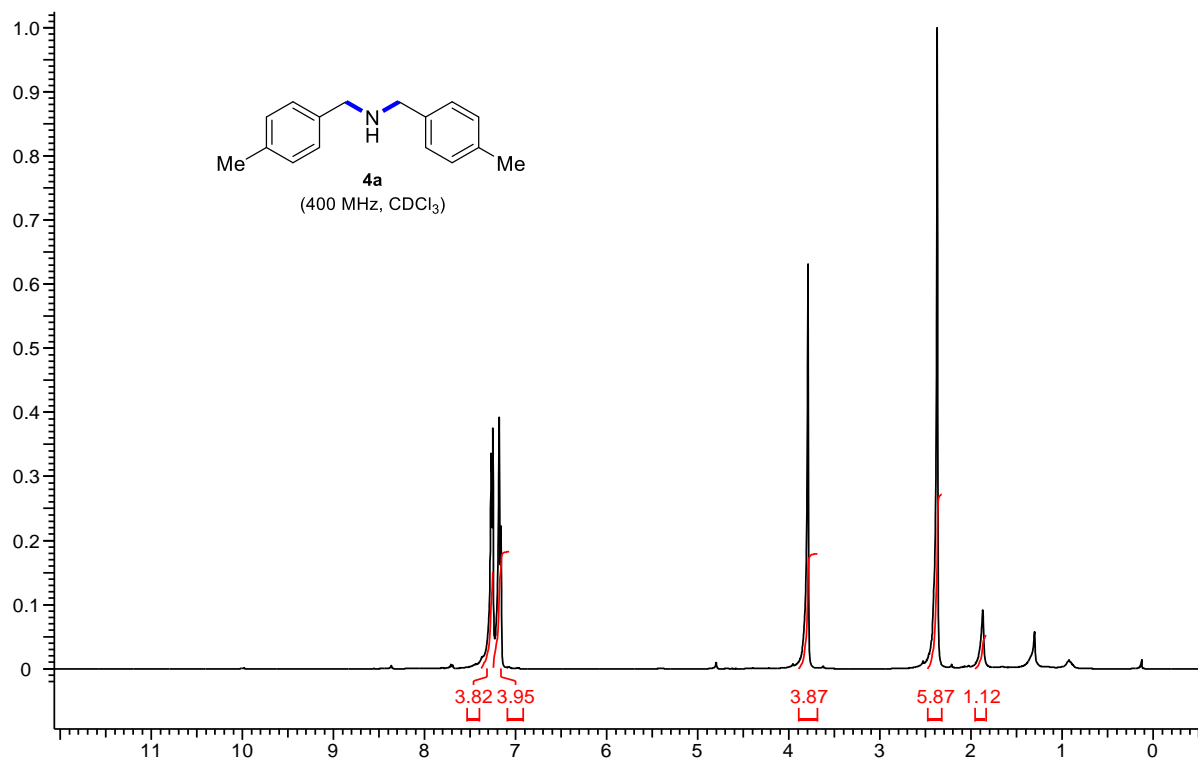
Bis(2-methylbenzyl)amine (4l): The representative procedure was followed, using 2-methylbenzonitrile (**1l**; 0.059 g, 0.50 mmol), CoCl₂ (0.0065 g, 0.05 mmol), NH₃-BH₃ (0.0019 g, 0.615 mmol). Purification by column chromatography on silica gel (petroleum ether/EtOAc: 5/1) yielded **4l** (0.032 g, 56%) as a colourless oil. ¹H-NMR (500 MHz, CDCl₃): δ 7.43-7.39 (m, 2H, Ar-H), 7.26-7.23 (m, 6H, Ar-H), 3.90 (s, 4H, 2 x CH₂), 2.41 (s, 6H, 2 x CH₃), 1.52 (s, 1H, NH). ¹³C{¹H}-NMR (125 MHz, CDCl₃): δ 138.5 (2C, C_q), 136.6 (2C, C_q), 130.4 (2C, CH), 128.6 (2C, CH), 127.2 (2C, CH), 126.1 (2C, CH), 51.6 (2C, CH₂), 19.5 (2C, CH₃). HRMS (ESI): *m/z* Calcd for C₁₆H₁₉N + H⁺ [M + H]⁺ 226.1590; Found 226.1581. The analytical data are in accordance with those reported in the literature.

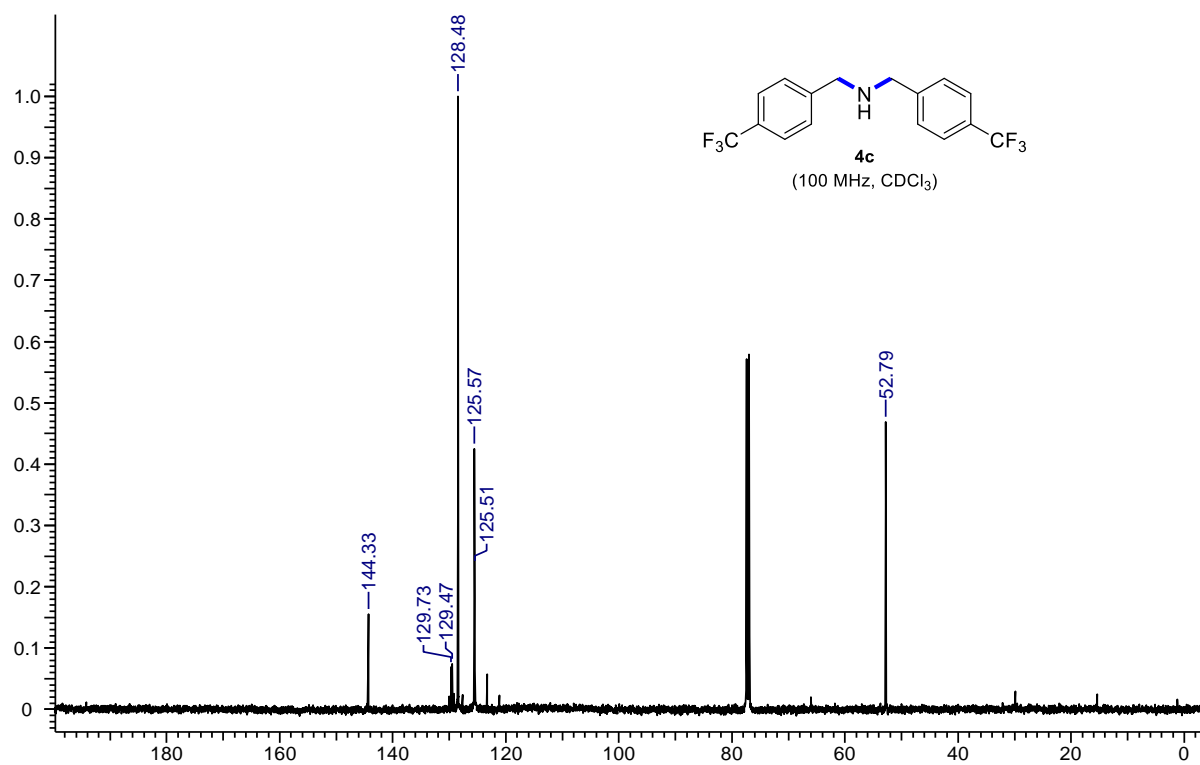
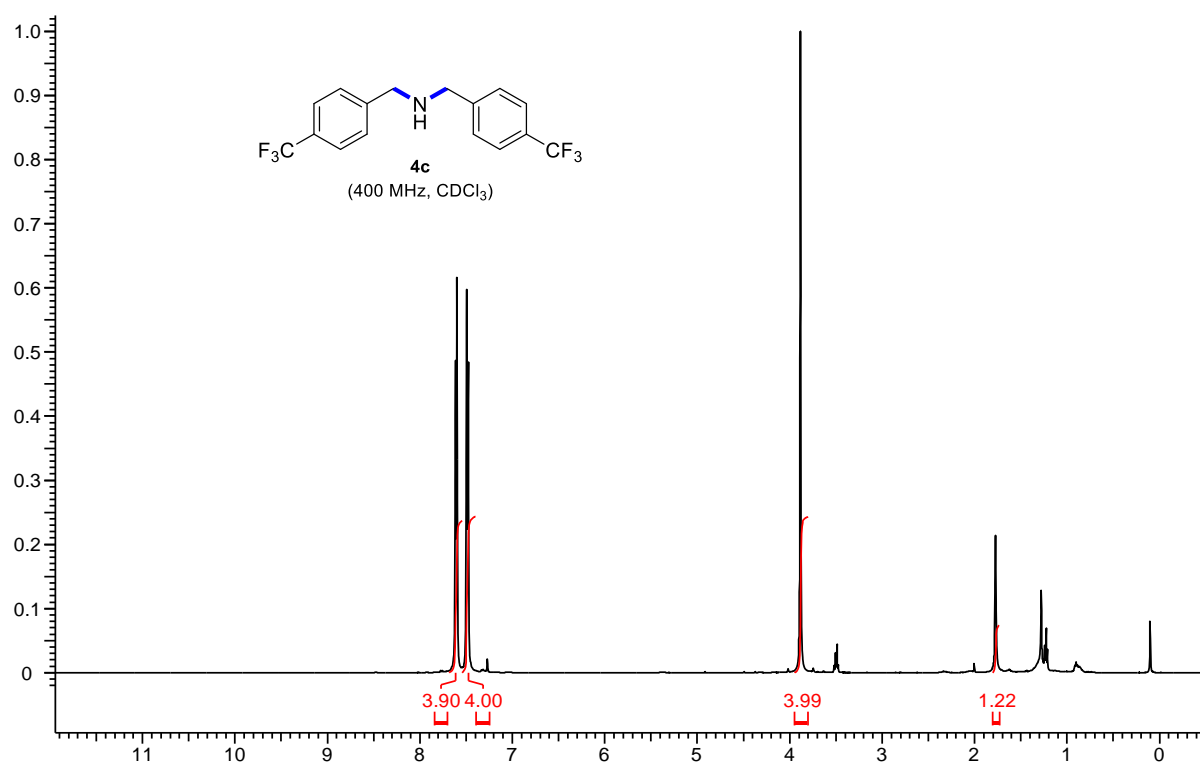


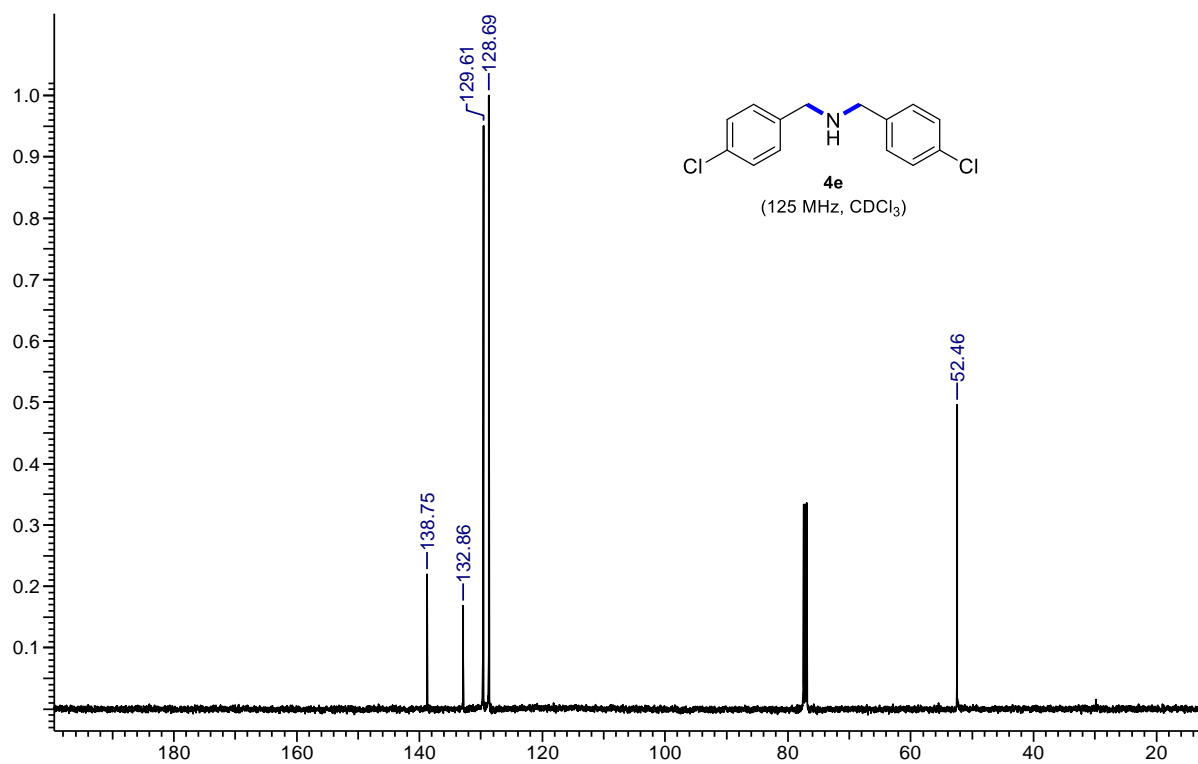
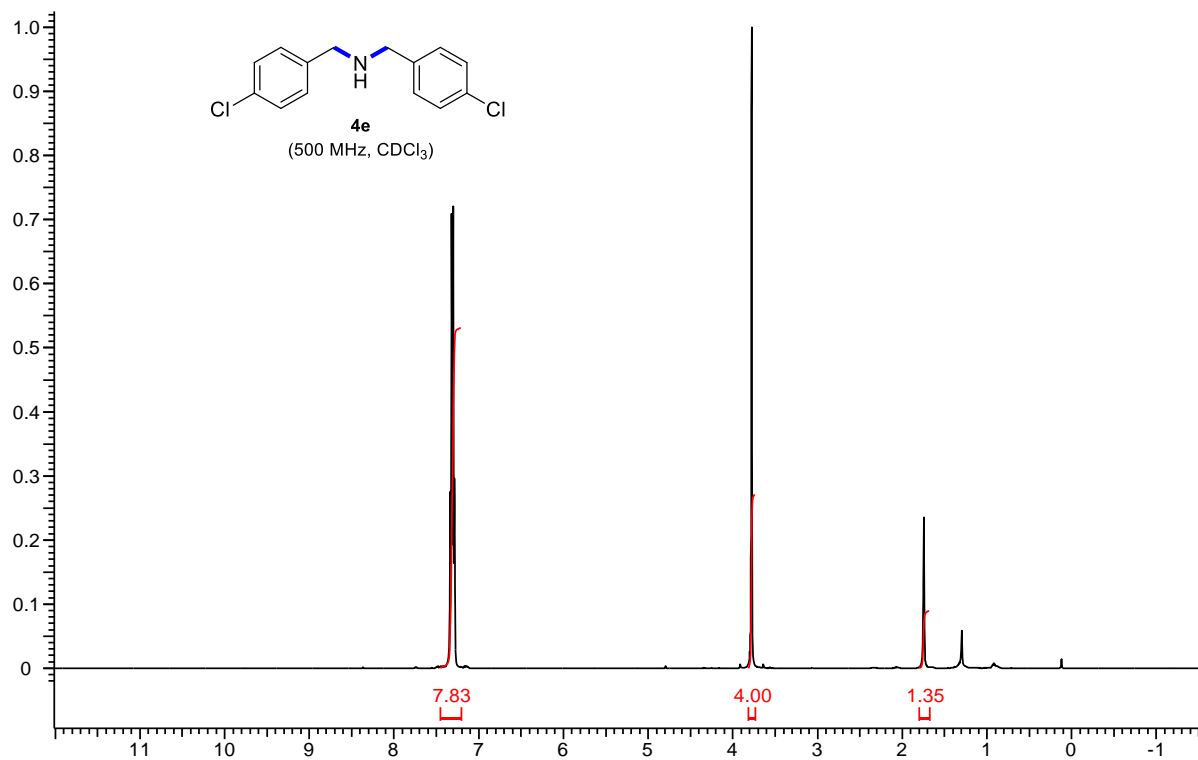
Bis(2-methoxybenzyl)amine (4m): The representative procedure was followed, using 2-methoxybenzonitrile (**1m**; 0.059 g, 0.50 mmol), CoCl₂ (0.0065 g, 0.05 mmol), NH₃-BH₃ (0.0019 g, 0.615 mmol). Purification by column chromatography on silica gel (petroleum ether/EtOAc: 3/1) yielded **4m** (0.028 g, 43%) as a colourless oil. ¹H-NMR (500 MHz, CDCl₃): δ 7.30-7.22 (m, 4H, Ar-H), 6.94-6.91 (m, 2H, Ar-H), 6.87-6.85 (m, 2H, Ar-H), 3.82 (s, 4H, 2 x CH₂), 3.81 (s, 6H, 2 x CH₃), 2.55 (s, 1H, NH). ¹³C{¹H}-NMR (125 MHz, CDCl₃): δ 157.8 (2C, C_q), 130 (2C, C_q), 128.3 (2C, CH), 126.1 (2C, CH), 120.5 (2C, CH), 110.3 (2C, CH), 55.4 (2C, OCH₃), 48.8 (2C, CH₂). HRMS (ESI): *m/z* Calcd for C₁₆H₁₉O₂N + H⁺ [M + H]⁺ 258.1489; Found 258.1486. The analytical data are in accordance with those reported in the literature.

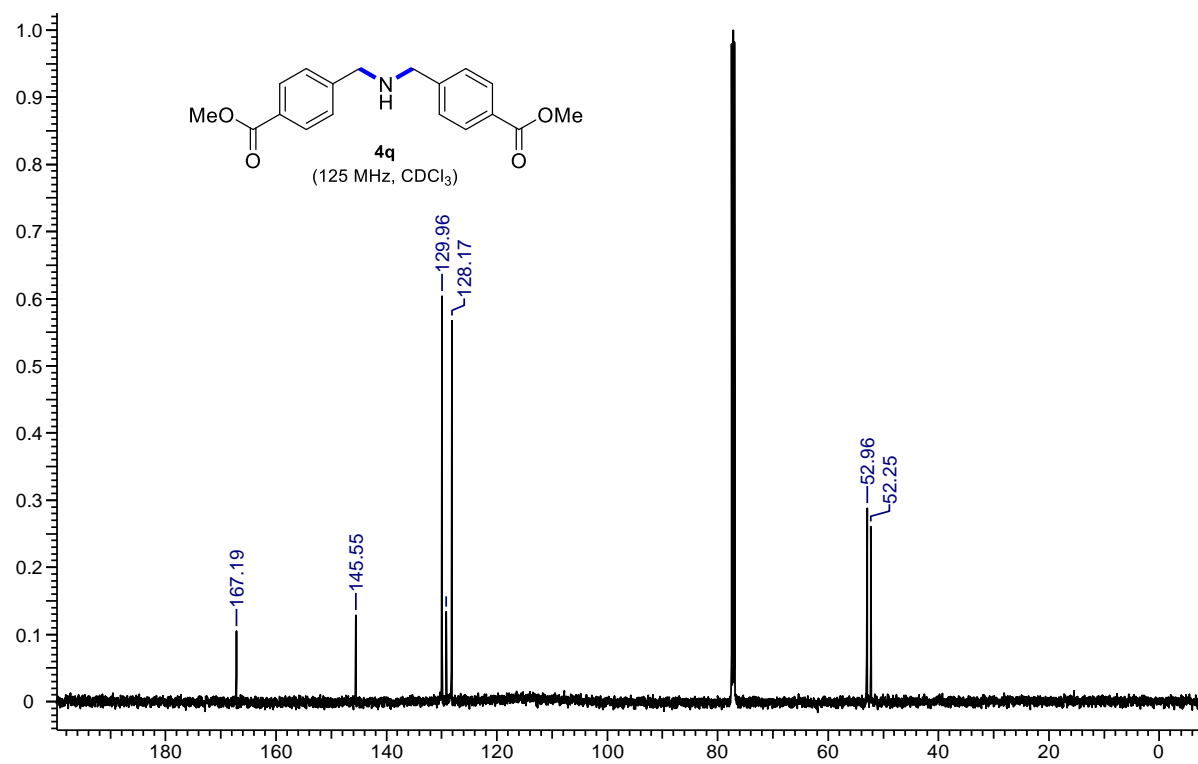
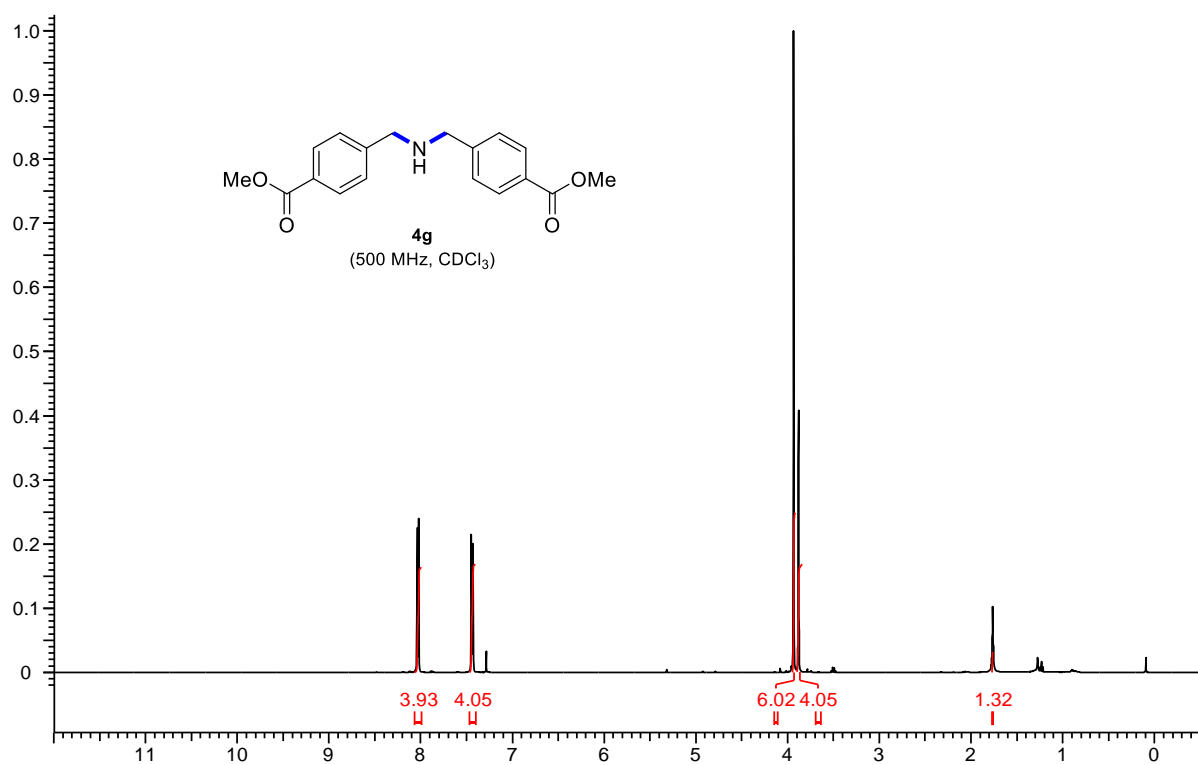


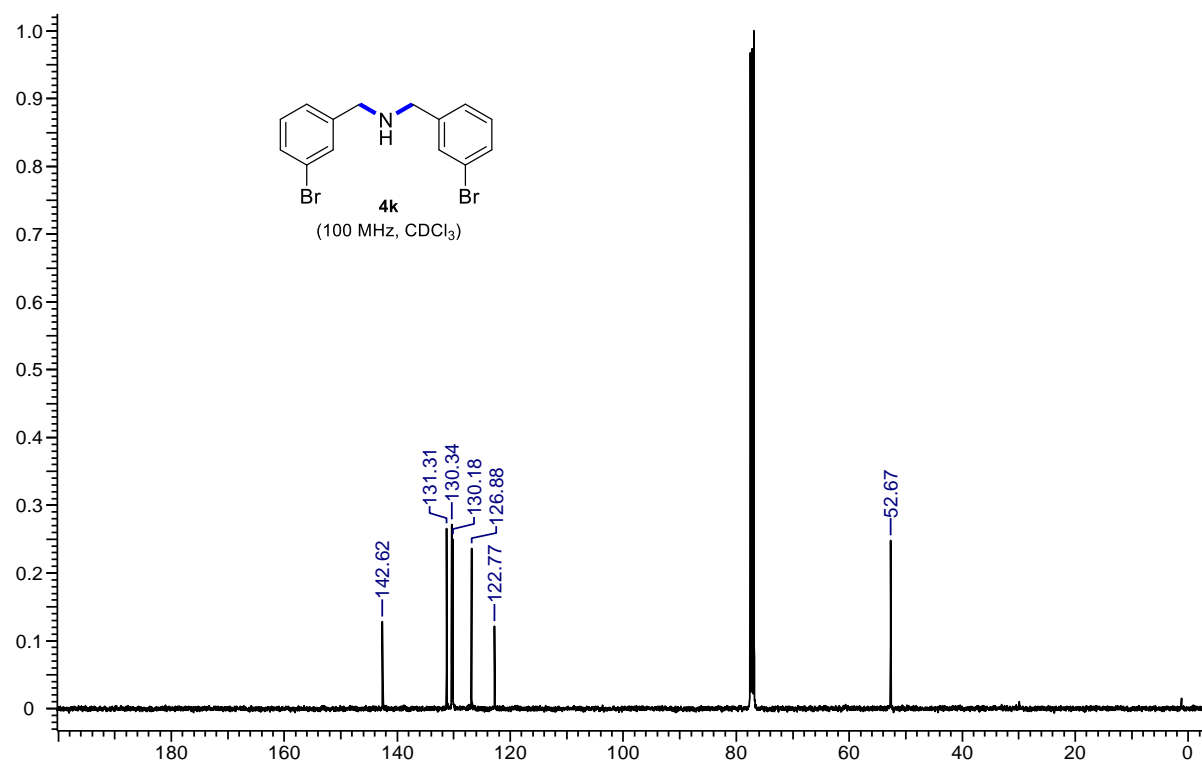
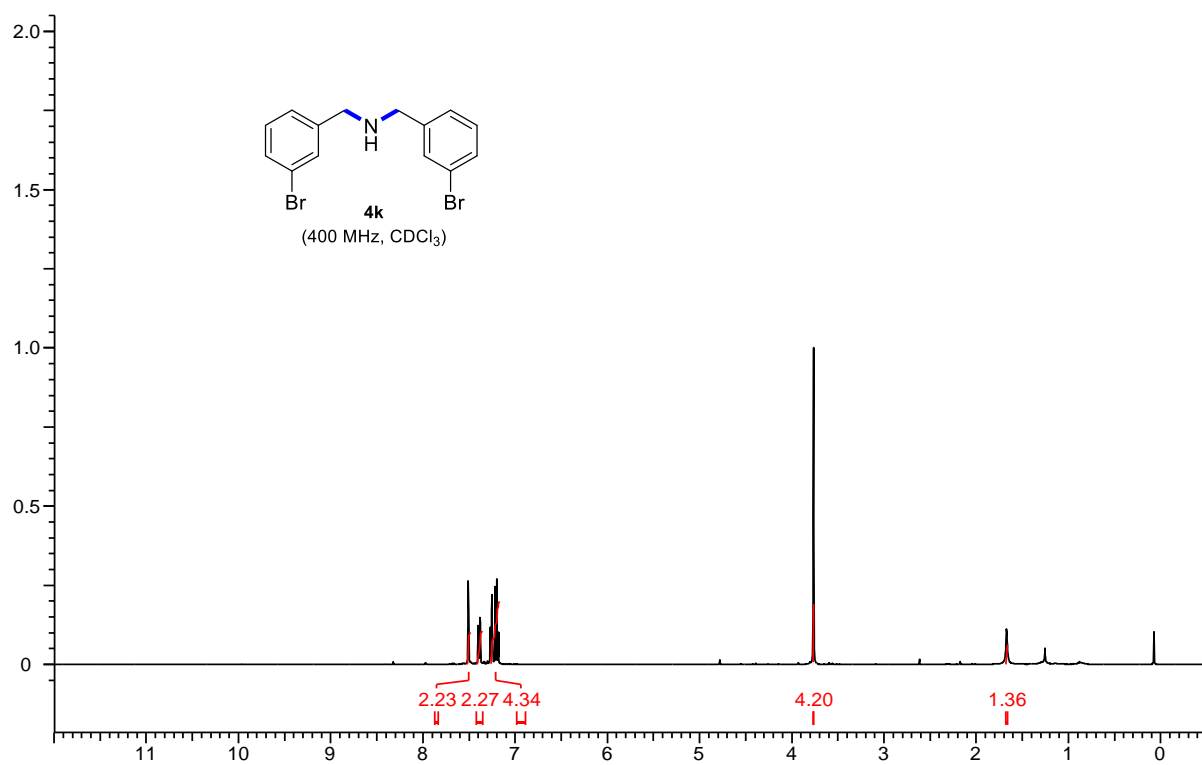
Bis(naphthalen-1-ylmethyl)amine (4n): The representative procedure was followed, using 1-naphthonitrile (**1n**; 0.077 g, 0.50 mmol), CoCl_2 (0.0065 g, 0.05 mmol), $\text{NH}_3\text{-BH}_3$ (0.0019 g, 0.615 mmol). Purification by column chromatography on silica gel (petroleum ether/EtOAc: 5/1) yielded **4n** (0.025 g, 34%) as a colourless oil. $^1\text{H-NMR}$ (500 MHz, CDCl_3): δ 8.10 (d, $J = 7.6$ Hz, 2H, Ar-H), 7.88 (s, 2H, Ar-H), 7.80 (s, 2H, Ar-H), 7.54-7.43 (m, 8H, Ar-H), 4.36 (s, 4H, 2 x CH_2), 1.77 (s, 1H, NH). $^{13}\text{C}\{^1\text{H}\}\text{-NMR}$ (125 MHz, CDCl_3): δ 135.9 (2C, C_q), 134.1 (2C, C_q), 132.1 (2C, C_q), 128.8 (2C, CH), 128.1 (2C, CH), 126.5 (2C, CH), 126.2 (2C, CH), 125.8 (2C, CH), 125.1 (2C, CH), 124.1 (2C, CH), 51.6 (2C, CH_2). The analytical data are in accordance with those reported in the literature.

4.4.4 ^1H and ^{13}C NMR Spectra of Selected Secondary Amines









4.5 REFERENCES

- (1) Blaser, H.-U.; Malan, C.; Pugin, B.; Spindler, F.; Steiner, H.; Studer, M. *Adv. Synth. Catal.* **2003**, *345*, 103-151.
- (2) Werkmeister, S.; Junge, K.; Beller, M. *Org. Pro. Res. Dev.* **2014**, *18*, 289-302.
- (3) Bagal, D. B.; Bhanage, B. M. *Adv. Synth. Catal.* **2015**, *357*, 883-900.
- (4) Liu, W.; Sahoo, B.; Junge, K.; Beller, M. *Acc. Chem. Res.* **2018**, *51*, 1858-1869.
- (5) Adam, R.; Bheeter, C. B.; Jackstell, R.; Beller, M. *ChemCatChem* **2016**, *8*, 1329-1334.
- (6) Werkmeister, S.; Junge, K.; Wendt, B.; Spannenberg, A.; Jiao, H.; Bornschein, C.; Beller, M. *Chem. Eur. J.* **2014**, *20*, 4227-4231.
- (7) Adam, R.; Alberico, E.; Baumann, W.; Drexler, H.-J.; Jackstell, R.; Junge, H.; Beller, M. *Chem. Eur. J.* **2016**, *22*, 4991-5002.
- (8) Srimani, D.; Feller, M.; Ben-David, Y.; Milstein, D. *Chem. Commun.* **2012**, *48*, 11853-11855.
- (9) Miao, X.; Bidange, J.; Dixneuf, P. H.; Fischmeister, C. d.; Bruneau, C.; Dubois, J.-L.; Couturier, J.-L. *ChemCatChem* **2012**, *4*, 1911-1916.
- (10) Reguillo, R.; Grellier, M.; Vautravers, N.; Vendier, L.; Sabo-Etienne, S. *J. Am. Chem. Soc.* **2010**, *132*, 7854-7855.
- (11) Monguchi, Y.; Mizuno, M.; Ichikawa, T.; Fujita, Y.; Murakami, E.; Hattori, T.; Maegawa, T.; Sawama, Y.; Sajiki, H. *J. Org. Chem.* **2017**, *82*, 10939-10944.
- (12) Saha, S.; Kaur, M.; Singh, K.; Bera, J. K. *J. Organomet. Chem.* **2016**, *812*, 87-94.
- (13) Galan, A.; De Mendoza, J.; Prados, P.; Rojo, J.; Echavarren, A. M. *J. Org. Chem.* **1991**, *56*, 452-454.
- (14) Saito, Y.; Ishitani, H.; Ueno, M.; Kobayashi, S. *ChemistryOpen* **2017**, *6*, 211-215.
- (15) Lu, S.; Wang, J.; Cao, X.; Li, X.; Gu, H. *Chem. Commun.* **2014**, *50*, 3512-3515.
- (16) Chin, C. S.; Lee, B. *Catal. Lett.* **1992**, *14*, 135-140.
- (17) Nait Ajjou, A.; Robichaud, A. *Appl. Organometal. Chem.* **2018**, *32*, e4481.
- (18) Elangovan, S.; Topf, C.; Fischer, S.; Jiao, H.; Spannenberg, A.; Baumann, W.; Ludwig, R.; Junge, K.; Beller, M. *J. Am. Chem. Soc.* **2016**, *138*, 8809-8814.

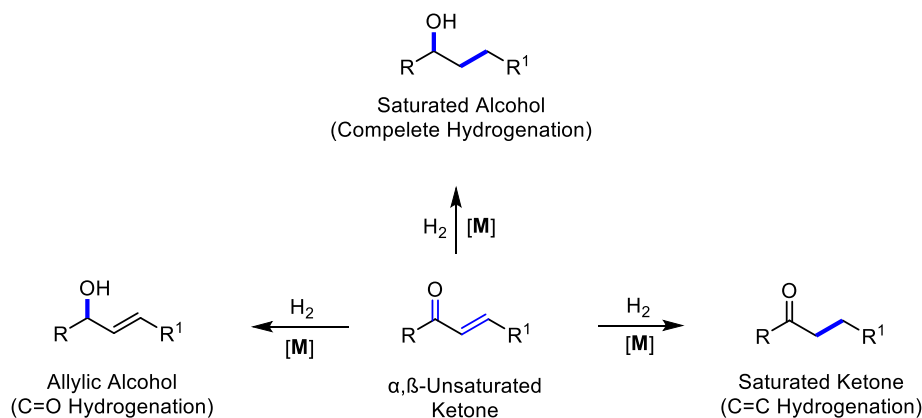
-
- (19) Bornschein, C.; Werkmeister, S.; Wendt, B.; Jiao, H.; Alberico, E.; Baumann, W.; Junge, H.; Junge, K.; Beller, M. *Nature Commun.* **2014**, *5*, 4111.
- (20) Chakraborty, S.; Leitus, G.; Milstein, D. *Chem. Commun.* **2016**, *52*, 1812-1815.
- (21) Chakraborty, S.; Leitus, G.; Milstein, D. *Angew. Chem. Int. Ed.* **2017**, *56*, 2074-2078.
- (22) Chakraborty, S.; Milstein, D. *ACS Catal.* **2017**, *7*, 3968-3972.
- (23) Lange, S.; Elangovan, S.; Cordes, C.; Spannenberg, A.; Jiao, H.; Junge, H.; Bachmann, S.; Scalone, M.; Topf, C.; Junge, K.; Beller, M. *Catal. Sci. Technol.* **2016**, *6*, 4768-4772.
- (24) Mukherjee, A.; Srimani, D.; Chakraborty, S.; Ben-David, Y.; Milstein, D. *J. Am. Chem. Soc.* **2015**, *137*, 8888-8891.
- (25) Schneekönig, J.; Tannert, B.; Hornke, H.; Beller, M.; Junge, K. *Catal. Sci. Technol.* **2019**, *9*, 1779-1783.
- (26) Li, H.; Al-Dakhil, A.; Lupp, D.; Gholap, S. S.; Lai, Z.; Liang, L.-C.; Huang, K.-W. *Org. Lett.* **2018**, *20*, 6430-6435.
- (27) Chen, F.; Topf, C.; Radnik, J.; Kreyenschulte, C.; Lund, H.; Schneider, M.; Surkus, A.-E.; He, L.; Junge, K.; Beller, M. *J. Am. Chem. Soc.* **2016**, *138*, 8781-8788.
- (28) Tokmic, K.; Jackson, B. J.; Salazar, A.; Woods, T. J.; Fout, A. R. *J. Am. Chem. Soc.* **2017**, *139*, 13554-13561.
- (29) Ferraccioli, R.; Borovika, D.; Surkus, A.-E.; Kreyenschulte, C.; Topf, C.; Beller, M. *Catal. Sci. Technol.*, **2018**, *8*, 499-507.
- (30) Dai, H.; Guan, H. *ACS Catal.* **2018**, *8*, 9125-9130.
- (31) Filonenko, G. A.; van Putten, R.; Hensen, E. J. M.; Pidko, E. A. *Chem. Soc. Rev.* **2018**, *47*, 1459-1483.
- (32) Shao, Z.; Fu, S.; Wei, M.; Zhou, S.; Liu, Q. *Angew. Chem. Int. Ed.* **2016**, *55*, 14653-14657.
- (33) Song, H.; Xiao, Y.; Zhang, Z.; Xiong, W.; Wang, R.; Guo, L.; Zhou, T. *J. Org. Chem.* **2022**, *87*, 790-800.

Chapter 5

Synthesis of PN^3N Based Mn(I) and Mn(II) Pincer Complexes and their Application in Selective Transfer Hydrogenation of Chalcones

5.1 INTRODUCTION

The catalytic hydrogenation of α,β -unsaturated carbonyl compounds, particularly ketones, is a crucial synthetic modification that leads to the generation of several products, i.e., a) allylic alcohol as a result of carbonyl hydrogenation, b) saturated ketone; a product of selective hydrogenation of alkene, as well as complete hydrogenation leading to c) saturated alcohols (Scheme 5.1). All three resulting products are of prime significance regarding their synthetic, pharmaceutical and industrial importance.¹⁻³ Hence, designing and developing a catalytic system that can carry out the selective hydrogenation of α,β -unsaturated ketones to accomplish the product of interest is a need of the hour. In that direction, the 4d and 5d-transition metals, mainly palladium,⁴ ruthenium,⁵⁻⁹ rhodium,¹⁰ and iridium¹¹ are explored as a catalyst for the selective hydrogenation of either carbonyl (C=O) or alkene (C=C) site of the α,β -unsaturated carbonyl compounds. Although a substantial advancement in the noble metal catalyzed selective hydrogenative transformation of the unsaturated carbonyls achieved over the last few decades, the high cost and limited natural availability of these rare metals demand their substitution by the first row congeners. On that line, the late 3d-transition metals such as iron,¹²⁻¹⁶ cobalt,¹⁷⁻²⁵ nickel,²⁶ and copper²⁷⁻³⁰ have recently been implemented as a catalyst to carry out the aforementioned transformation.



Scheme 5.1 Products of α,β -unsaturated ketone hydrogenation.

Researchers have practiced the synthesis of manganese-based catalytic systems to carry out the hydrogenative reaction in recent decades in the context of a plentiful availability of manganese in the earth's crust. Moreover, a range of variable oxidation states of manganese from -3 to +7 pushes it forward as a prominent contender to be used as a catalyst to perform hydrogenation reactions. In that direction, several pincer and non-pincer manganese complexes were developed by various groups to execute the hydrogenation of the

carbonyl group using molecular hydrogen or sacrificial hydrogen source.³¹⁻³⁸ However, the selective hydrogenation of α,β -unsaturated carbonyl compounds by the manganese-based catalyst is scarcely explored where, the Sortais group in 2017 exploited a PN-bidentate ligated Mn(I) complex to show the hydrogenation of two of the α,β -unsaturated ketones where both C=C reduced, and completely hydrogenated products were formed using molecular hydrogen (50 bar).³⁹ Similarly, Topf and co-workers used a picolinamine ligated Mn(I) complex to carry out the hydrogenation of chalcone to get the mixture of partially and completely hydrogenated products.⁴⁰

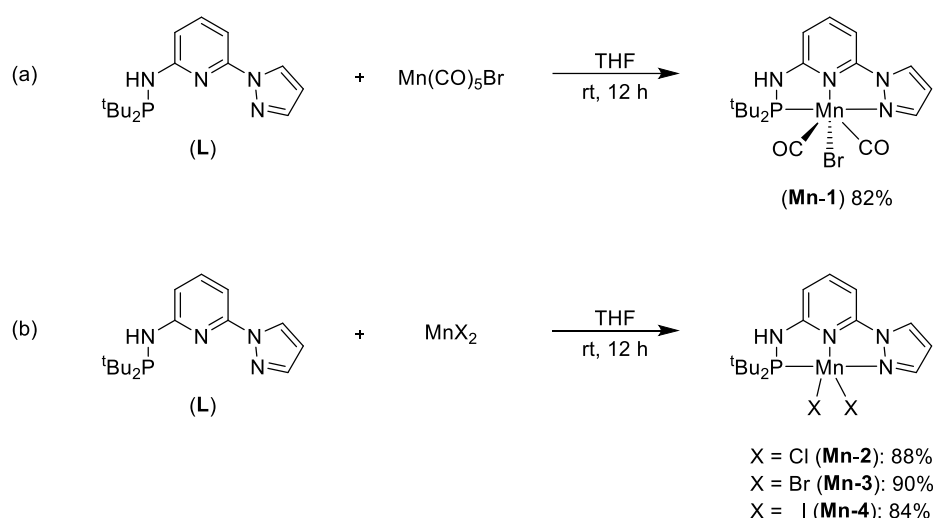
On the same line, the Kirchner group worked on the bidentate phosphine ligated Mn(I) catalyst, which either selectively hydrogenated C=O of the α,β -unsaturated aldehyde/ketone or provided fully hydrogenated products depending on the reaction temperature.⁴¹ Moreover, a β -amino phosphine ligated Mn(I) complex was utilized for the selective transfer hydrogenation of C=C of α,β -unsaturated ketones using ⁱPrOH/KO^tBu as a hydrogen source.⁴² Similarly, Huang recently developed PN³N ligated Mn(II) complexes to perform selective hydrogenation of C=O of α,β -unsaturated aldehydes at 30 bar H₂ pressure.⁴⁵ In addition, a detailed study of the reactivity of the PN³N ligand system with different metal complexes by the same group led us to synthesize a series of PN³N-based Mn(I) and Mn(II) complexes to employ them to catalyze the transfer hydrogenation of chalcones to get the selectively C=C hydrogenated saturated ketone.⁴³ All the Mn(I) catalyst-based protocols are mainly focused on the hydrogenation of simple aldehydes/ketones, whereas limited examples of α,β -unsaturated aldehyde/ketone hydrogenation are discussed. Thus, there is a need for a manganese-based catalytic system that can selectively hydrogenate a C=C double bond of α,β -unsaturated ketones under the mild condition to provide saturated ketone product. Thus, in this chapter, we displayed the synthesis of a series of Mn(I) and Mn(II) complexes with a ^tBu₂PN³N^{Pyz} ligand backbone. These complexes were thoroughly characterized and explored for the transfer hydrogenation of chalcones to saturated ketones using a half equivalent of ammonia-borane as hydrogen sacrificial at room temperature.

5.2 RESULTS AND DISCUSSION

5.2.1 Synthesis and Characterization of Manganese Complexes

The phosphine-based PN³N ligand, *N*-(di-tert-butylphosphanyl)-6-(1H-pyrazol-1-yl)pyridin-2-amine (^tBu₂PN³N^{Pyz}) (**L**) developed by the Huang group and used for synthesis of different transition metal based pincer complexes.⁵⁶ Based on the study by the same group on PN³N-based ligand systems and their pincer complexes with different transition metals,⁴³ we

considered to synthesize the manganese based pincer complexes to understand the coordinating pattern of PN^3N ligand to the Mn(I) and Mn(II) metal centre and their reactivity towards catalytic hydrogenation. Thus, we began with the treatment of ligand (**L**) with $\text{Mn}(\text{CO})_5\text{Br}$ in THF at the room temperature which resulted into light saffron coloured precipitation of the anticipated PN^3N -Mn(I) (**Mn-1**) complex in very good yield (Scheme 5.2a). The elemental analysis of Mn-(I) complex (**Mn-1**) matched with the expected chemical composition. Unfortunately, our attempts to get the suitable crystal of PN^3N -Mn(I) (**Mn-1**) complex for the single crystal XRD analysis turned out to be unsuccessful as we observed the leaching out of metal (Mn) from the core complex.



Scheme 5.2 Synthesis of series of manganese complexes.

Next, we synthesized a series of Mn(II) complexes by the reaction of phosphine ligand (**L**) with Mn(II) salts, i.e., MnCl_2 , MnBr_2 , and MnI_2 in THF at room temperature, which yielded light yellow coloured $(^t\text{Bu}_2\text{PN}^3\text{N}^{\text{Pyz}})\text{-MnX}_2$ ($\text{X} = \text{Cl}$, Br , and I for **Mn-2**, **Mn-3**, and **Mn-4** respectively) complexes in excellent amount in the form of precipitation (Scheme 5.2b). Similar to $(^t\text{Bu}_2\text{PN}^3\text{N}^{\text{Pyz}})\text{-Mn(I)}$ (**Mn-1**) complex, the chemical composition of $(^t\text{Bu}_2\text{PN}^3\text{N}^{\text{Pyz}})\text{-MnX}_2$ complexes was determined by the elemental analysis. In addition, the suitable crystal of complex **Mn-4** obtained from the saturated CH_2Cl_2 solution on slow evaporation of dichloromethane (DCM) solvent. The molecular structure determination revealed an expected tridentate coordination of $(^t\text{Bu}_2\text{PN}^3\text{N}^{\text{Pyz}})$ ligand (**L**) to the Mn(II) centre in pincer fashion (Figure 5.1). Furthermore, the study of the complex **Mn-4** revealed that; the ligand co-ordinates *NI*, *N3*, *PI* and *II* lies almost in the same plane. The same can be understood from the various bond angles like $\text{N}(3)\text{-Mn}(1)\text{-I}(1)$ is $147.42(5^\circ)$ while $\text{N}(3)\text{-Mn}(1)\text{-I}(2)$ has bond angle $102.14(5^\circ)$. This difference in bond angles conveys that the

geometry around the Mn centre is more like of distorted square pyramidal than that of trigonal bipyramidal where the difference between the above mentioned angles should have been minimal. Moreover, the angle between the I(2)–Mn(1)–I(1) bond is 109.889(15) which shows that both Iodine ligands (*I1* and *I2*) are almost perpendicular to each other rather than being trans to each other. This showed a distorted square pyramidal geometry of the catalyst **4**. Similarly, The bond angles around manganese, i.e., I(2)–Mn(1)–N(1), I(2)–Mn(1)–N(3), I(2)–Mn(1)–P(1) are 100.14(6)°, 102.14(5)°, 106.643(19)°, respectively. This suggests that the *I2* coordinate is almost perpendicular to all other coordinates of the manganese which strongly supports distorted square pyramidal geometry of the complex **Mn-4**.

Table 5.1 Selected bond lengths (Å) and bond angles (°) for **Mn-4**.

Bond length (Å)		Bond angles (°)	
Complex Mn-4			
Mn(1)–N(1)	2.187(2)	N(3)–Mn(1)–I(1)	147.42(5)
Mn(1)–N(3)	2.2777(19)	N(3)–Mn(1)–I(2)	102.14(5)
Mn(1)–P(1)	2.6271(7)	I(2)–Mn(1)–I(1)	109.889(15)
Mn(1)–I(1)	2.7322(5)	I(2)–Mn(1)–N(1)	100.14(6),
Mn(1)–I(2)	2.7275(4)	I(2)–Mn(1)–N(3)	102.14(5)
		I(2)–Mn(1)–P(1)	106.643(19)

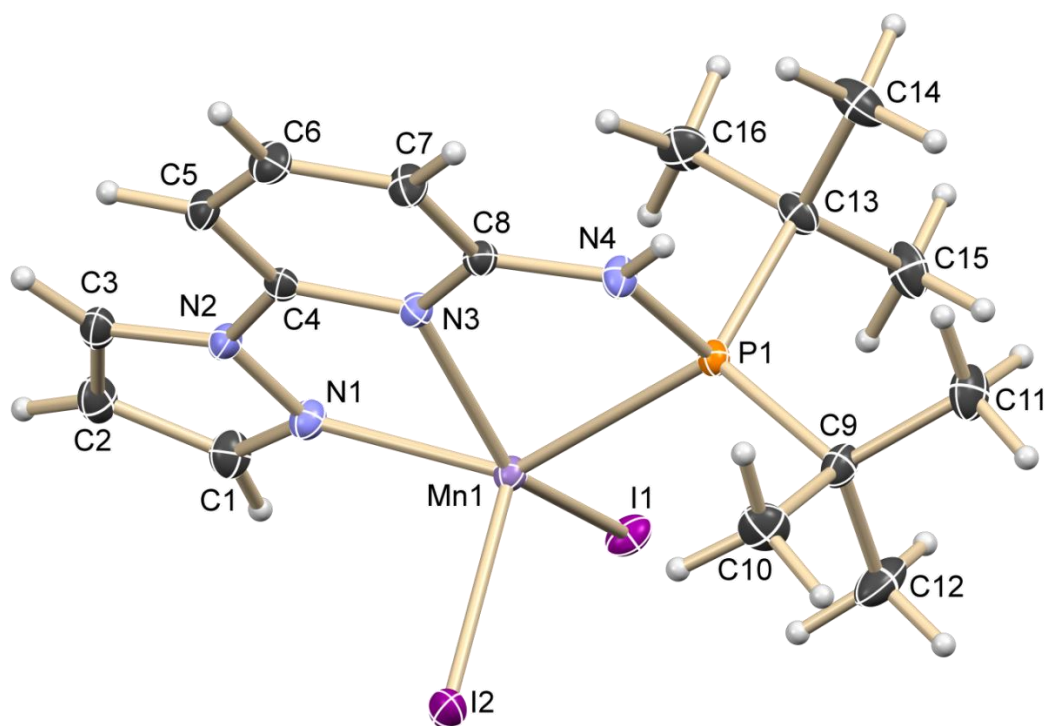
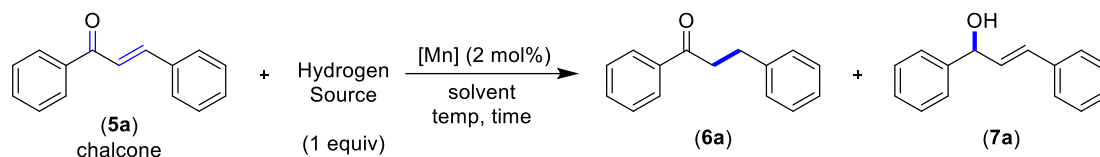


Figure 5.1 Thermal ellipsoid plot of the complex **Mn-4**.

5.2.2 Optimization of Reaction Condition

After having the series of manganese-based pincer complexes (**1-4**) in hand, we investigated their catalytic activity for the transfer hydrogenation of chalcone. Thus, in a representative reaction, (*E*)-Chalcone was taken as a standard substrate and treated with an equivalent amount of ammonia-borane in THF solution at 60 °C for 6 hours using Mn-complexes (**Mn-1** to **Mn-4**) (2 mol%) independently (entries 1-4, Table 5.1). Among all the Mn-complexes, the catalyst **Mn-1** was found to be active for the selective hydrogenation of the C=C double bond of chalcone and provided 90% of saturated ketone as exclusive product (**6a**) (entry 1). However, all other Mn(II) complexes (**Mn-2** to **Mn-4**) were identified to be inactive for the transfer hydrogenation of the C=C double bond and they produced carbonyl reduced product **7a** (entries 2-4). In fact, the product **7a** formed in the absence of Mn catalyst (entry 5). Therefore, we focused our attention on chemo-selective C=C hydrogenation with catalyst **Mn-1**. Next, we investigated the effect of reaction solvents such as 2-MeTHF, toluene, dioxane, hexane, and alcohols (entries 5-11). Among all the solvents screened, dioxane remained the best, with 95% conversion into the desired saturated ketone formation (entry 7).

Considering dioxane as a solvent of choice, next, we employed dimethylammonia-borane (a cost-effective alternative to ammonia-borane) as a hydrogen donor, which exhibited a slightly lower selectivity for the product **6a** (entry 12). Interestingly, the hydrogenation also proceeded at room temperature with excellent selectivity and provided 95% of saturated ketone **6a** (entry 13). Similarly, a decrease in the reaction time from 6 h to 2 h led to similar reactivity and selectivity for the product **6a** (entry 14). Further, we moved on to decrease the equivalents of ammonia-borane to 0.5 equivalents to the chalcone, which, to our surprise, remained effective for the reaction and provided a 94% isolated yield of saturated ketone (**6a**) (entry 15). The reduction in the catalyst loading to 1 mol% decreases the overall product selectivity to 76% (entry 16). The reaction with simple Mn(CO)₅Br (2 mol%) gave only 3% of the desired product (**6a**), which ensures the importance of the PN³N ligand backbone in the catalytic system (entry 17). Similarly, the reaction without catalyst (**Mn-1**) or ammonia-borane doesn't lead to the expected ketone product (entries 18 & 19). All these studies highlight the importance of PN³N ligand backbone as well as manganese with +1 oxidation state [Mn(I)] for the selective hydrogenation of C=C double bond in α,β -unsaturated ketones (chalcone) at the milder reaction condition.

Table 5.1. Optimization of the reaction conditions^a

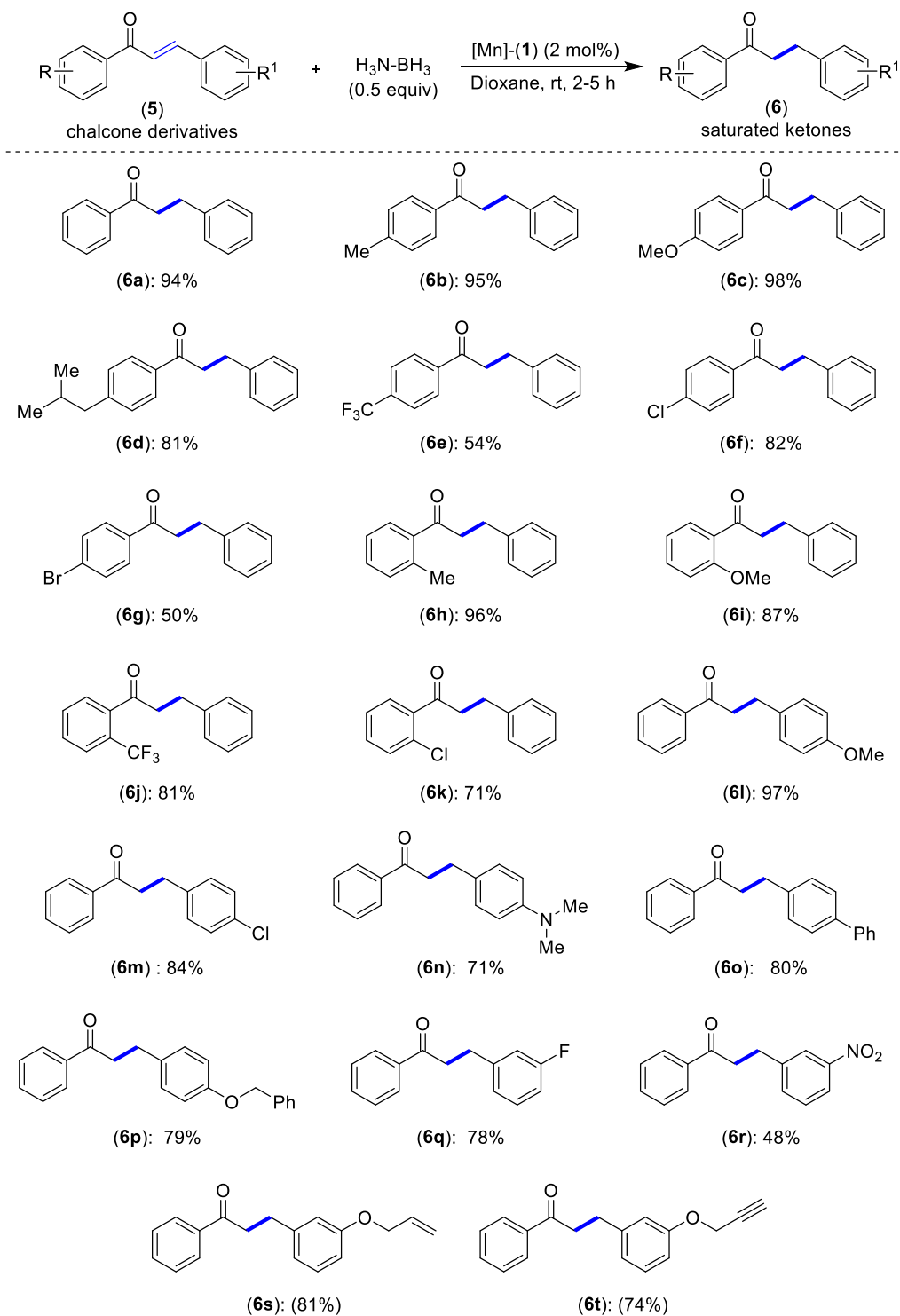
Entry	Hydrogen Source	[Mn]	Solvent	T (°C)/ t (h)	(6a) (%) ^b	(7a) (%) ^b
1	H ₃ N-BH ₃	Mn-1	THF	60 / 6	89	11
2	H ₃ N-BH ₃	Mn-2	THF	60 / 6	-	100
3	H ₃ N-BH ₃	Mn-3	THF	60 / 6	-	100
4	H ₃ N-BH ₃	Mn-4	THF	60 / 6	-	100
5	H ₃ N-BH ₃	Mn-1	2-MeTHF	60 / 6	90	10
6	H ₃ N-BH ₃	Mn-1	toluene	60 / 6	89	11
7	H ₃ N-BH ₃	Mn-1	dioxane	60 / 6	95	5
8	H ₃ N-BH ₃	Mn-1	hexane	60 / 6	24	76
9	H ₃ N-BH ₃	Mn-1	MeOH	60 / 6	43	57
10	H ₃ N-BH ₃	Mn-1	EtOH	60 / 6	39	61
11	H ₃ N-BH ₃	Mn-1	ⁱ PrOH	60 / 6	23	77
12	Me ₂ NH-BH ₃	Mn-1	dioxane	60 / 6	80	20
13	H ₃ N-BH ₃	Mn-1	dioxane	rt / 6	95	5
14	H ₃ N-BH ₃	Mn-1	dioxane	rt / 2	95	5
15^c	H₃N-BH₃	Mn-1	dioxane	rt / 2	95 (94%)	5
16 ^{c,d}	H ₃ N-BH ₃	Mn-1	dioxane	rt / 2	76	24
17 ^e	H ₃ N-BH ₃	[Mn]	dioxane	rt / 2	3	97
18	H ₃ N-BH ₃	-	dioxane	rt / 2	-	100
19	-	Mn-1	dioxane	rt / 2	-	-

^aReaction Conditions: (*E*)-chalcone (**5a**, 0.042 g, 0.20 mmol), NH₃-BH₃ (0.006 g, 0.20 mmol), [Mn] catalyst (0.004 mmol, 2 mol%), solvent (1.0 mL). ^bGC conversion, isolated yields are given in parentheses. ^c0.5 equivalent of NH₃-BH₃ used. ^d1 mol% of catalyst **1** used. ^e[Mn] = Mn(CO)₅Br.

5.2.3 Scope for Synthesis of Saturated Ketones

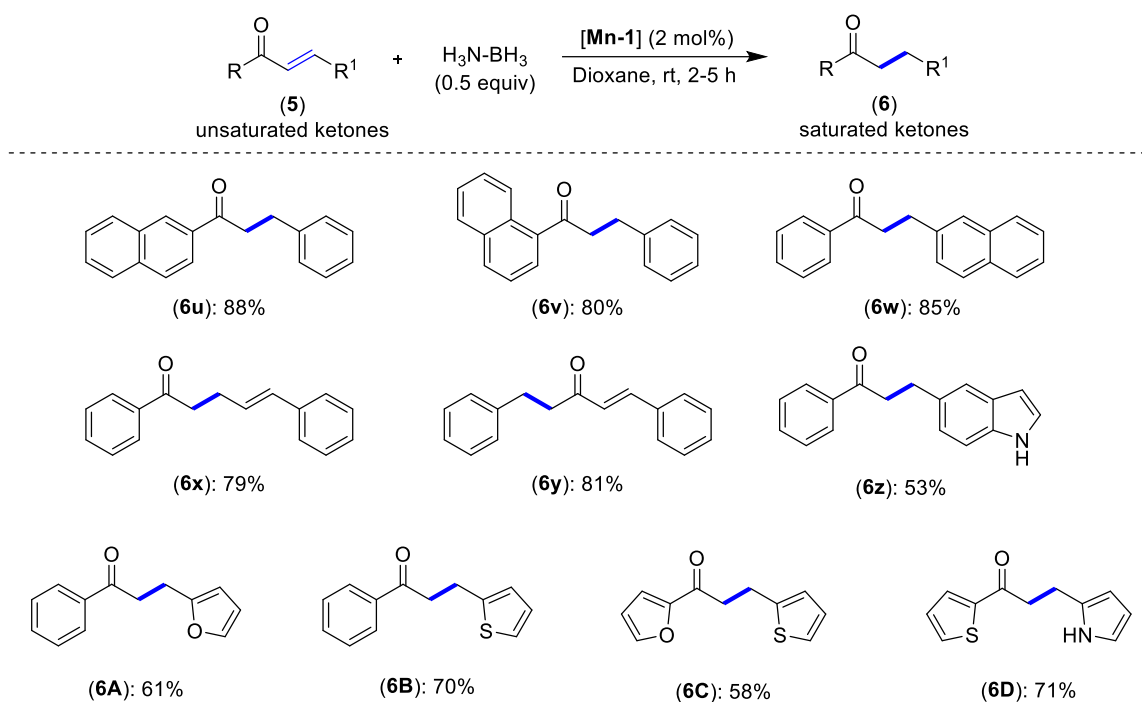
After optimizing the reaction condition, we checked the substrate scope for synthesizing the saturated ketones using 2 mol% of catalyst **Mn-1** and 0.5 equivalent of ammonia-borane in dioxane at room temperature (Scheme 5.3). The chalcone derivatives with electron-donating groups, like –Me, –OMe, at the *para*-position to the carbonyl group tolerated well under the reaction condition and provided 95% and 98% of compounds **6b** and **6c**. In addition, an isobutyl group *para* to the carbonyl also remained unaffected during the reaction and gave 81% of product **6d**. However, the electron-withdrawing –CF₃ group that is *para* to the carbonyl provided a moderate yield (54%) of respective saturated ketone **6e**, and significant formation of carbonyl reduced product **7e** was observed. The halides such as –Cl and –Br substituted ketones worked effectively to provide 76% and 50% of **6f** and **6g** products, respectively. The electron-rich groups like –Me and –OMe *ortho* to carbonyl were fine during the catalysis and gave 96% and 87% of respective **6h** and **6i**. Similarly, electron-deficient groups like –CF₃ and –Cl also provided a very good yield of the saturated ketones **6j** and **6k** (81% and 71%), respectively.

After checking the substrate scope with various substituents on the carbonyl side, next, we explored the effect of different substituents on *para* to the alkenyl carbon. The –OMe and –Cl groups tolerated well under the optimized reaction parameters and furnished the desired product **6l** and **6m** in excellent yield, i.e., 97% and 84%, respectively. Further, the chalcone with an amine (–NMe₂) and phenyl (–Ph) functionalities gave 71% and 80% yield of the hydrogenated products **6n** and **6o**. A highly sensitive benzyloxy group remained unaffected under the optimized protocol and yielded 79% of anticipated product **6p**. Similarly, electron-deficient –F and –NO₂ groups at *meta* to alkenyl group gave good to moderate yield, i.e., 78% and 48% for the respective hydrogenated products **6q** and **6r**. The mild optimized reaction parameters seemed compatible with the chalcones having sensitive functionalities such as non-conjugated alkenyl and alkynyl groups as they provided an excellent yield of the corresponding hydrogenated product **6s** and **6t**.



Scheme 5.3 Scope of semi-hydrogenation of (*E*)-chalcones to saturated ketones. Yields (%) shown are for the isolated saturated ketones.

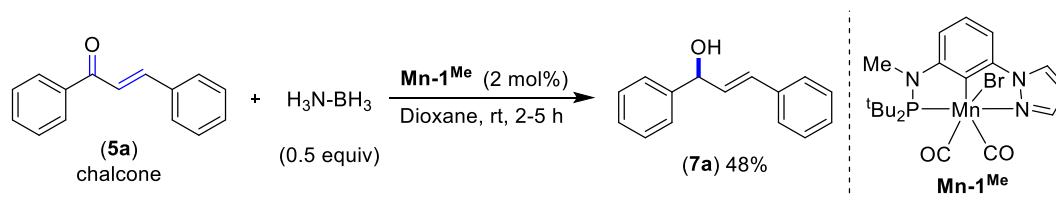
We extended the hydrogenation scope for the naphthalene substituted α,β -unsaturated ketones (Scheme 5.4). A replacement of phenyl ring with naphthalene on each side of the enones in individual examples (**6u**, **6v**, and **6w**) didn't alter the outcome of the reaction and endured relative C=C hydrogenated products in excellent yield, i.e., 88%, 79%, and 84%, respectively. Surprisingly, the C=C bond at α,β position only got hydrogenated, keeping the C=C of γ,δ position intact, when $\alpha,\beta,\gamma,\delta$ -unsaturated ketone was subjected for the transfer hydrogenation (**6x**). Similarly, when enone with alkene on both sides of the carbonyl group was treated under the optimized transfer hydrogenation condition, only one of the two C=C double bonds got reduced, giving compound **6y** in 81% yield. In addition to the simple α,β -unsaturated ketones, synthetically important heterocycles like pyrrole, thiophene, furan, and indole-containing enones were compatible with the optimized reaction condition and provided 53-71% yield for the respective selective hydrogenated products (**6z** and **6A-6D**). Additionally, the gram-scale synthesis of saturated ketone from chalcone was successfully carried out at the optimized reaction condition which shows practical applicability of the described method. The compatibility of diverse functional groups under this chemo-selective mild transfer hydrogenative method displays the significance of the optimized protocol. Notably, alkyl substituted enones were unreactive under the optimized reaction conditions, highlighting the chemo-selectivity of the protocol for the diarylenones.



Scheme 5.4 Scope of semi-hydrogenation of α,β -unsaturated ketones to saturated ketones. Yields (%) shown are for the isolated saturated ketones.

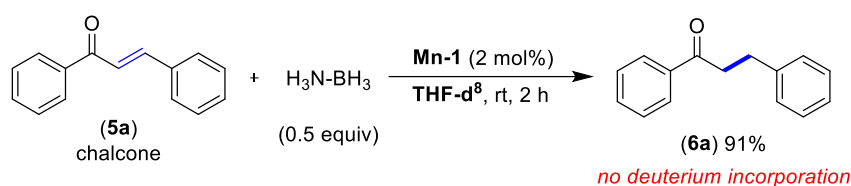
5.2.4 Mechanistic Study

5.2.4.1 Significance of N–H proton of PN^3N ligand: We intended to know the role of NH in the ligand backbone with regards to non-innocent behavior. Thus, we synthesized an analogous manganese complex Mn-1^{Me} using ligand **L1** where amine proton (*NH*) replaced with a methyl group. This newly synthesized manganese complex Mn-1^{Me} was then used to catalyze the transfer hydrogenation of the chalcone under the otherwise optimized condition which afforded only carbonyl reduced product (**7a**) in 48% yield (Scheme 5.5). This result ultimately highlights the importance of *NH* proton of PN^3N in transfer hydrogenation of chalcones using catalyst **Mn-1**. Most likely the *NH* proton involved in dearomatization/aromatization protocol.



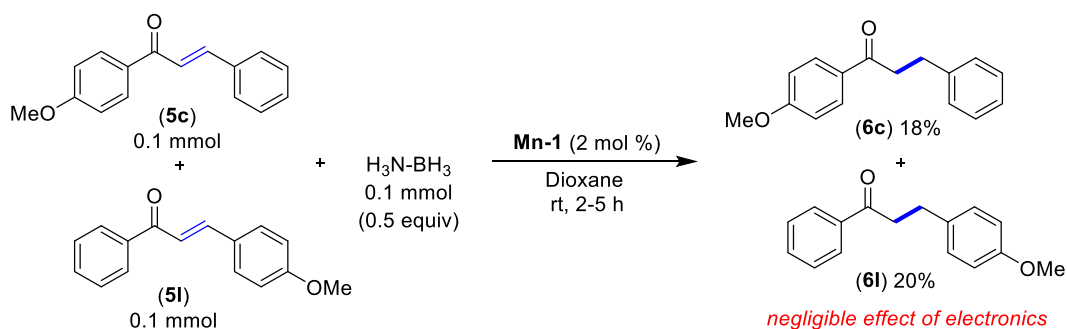
Scheme 5.5 Significance of N–H proton of the PN^3N ligand backbone.

5.2.4.2 Source of hydrogen: The optimized reaction conditions for the transfer hydrogenation showcased that; only half equivalent of ammonia-borane needed for the reaction. This led us to investigate the probability of role of the solvent as a hydrogen donor. To find this out, we performed a transfer hydrogenation of chalcone in the presence of deuteriated THF (*d*8) expecting a deuteration in the saturated ketone product (**6a**) (Scheme 5.6). However the isolated product (**6a**) does not show any deuterium incorporation which conveys that both pair of hydrogen is provided by the ammonia-borane.



Scheme 5.6 Deuterium labelling experiment.

5.2.4.3 Competition experiment (Electronic effect): The effect of electronics on the transfer hydrogenation was checked by performing a competition experiment between the chalcone substrates with electron donating –OMe group at *para* to carbonyl (**5c**) and *para* to alkenyl carbon (**5l**) where both respective products (**6c**) and (**6l**) formed in 18% and 20% yield (Scheme 5.7). This reflects negligible effect of electronics of substituents on both aromatic rings of the chalcone derivatives.



Scheme 5.7 Study of electronic effects (Competition experiment).

5.2.5 Plausible Catalytic Cycle

After conducting the preliminary mechanistic study and following the literature precedents, we have proposed a probable catalytic cycle for the [Mn-1]-catalyzed selective C=C bond hydrogenation of chalcones (Figure 5.2). At first, the Mn-1 catalyst reacts with $\text{NH}_3\text{-BH}_3$ and gets converted into the manganese-hydride [Mn-1a] intermediate, which is an active catalyst. Next, the chalcone coordinates Mn of the Mn-1a, followed by an attack of hydride at the β -position of the chalcone, giving intermediate Mn-1b via the transition state [Mn-1a']. Next, the enolate formed after the breaking of Mn-enol bond of Mn-1c, abstracts NH proton of the ligand leading to dearomatized intermediate Mn-1d along with the enol product, which is then tautomerizes into saturated ketone (6a). Finally, the dearomatized intermediate Mn-1d on reaction with $\text{NH}_3\text{-BH}_3$ provides the active catalyst [Mn-1a] back. The optimized reaction condition showed the involvement of a half equivalent of $\text{NH}_3\text{-BH}_3$, which states that a molecule of $\text{NH}_3\text{-BH}_3$ involved into two catalytic cycles ($\text{NH}_3\text{-BH}_3$ provides two molecules of hydrogen).

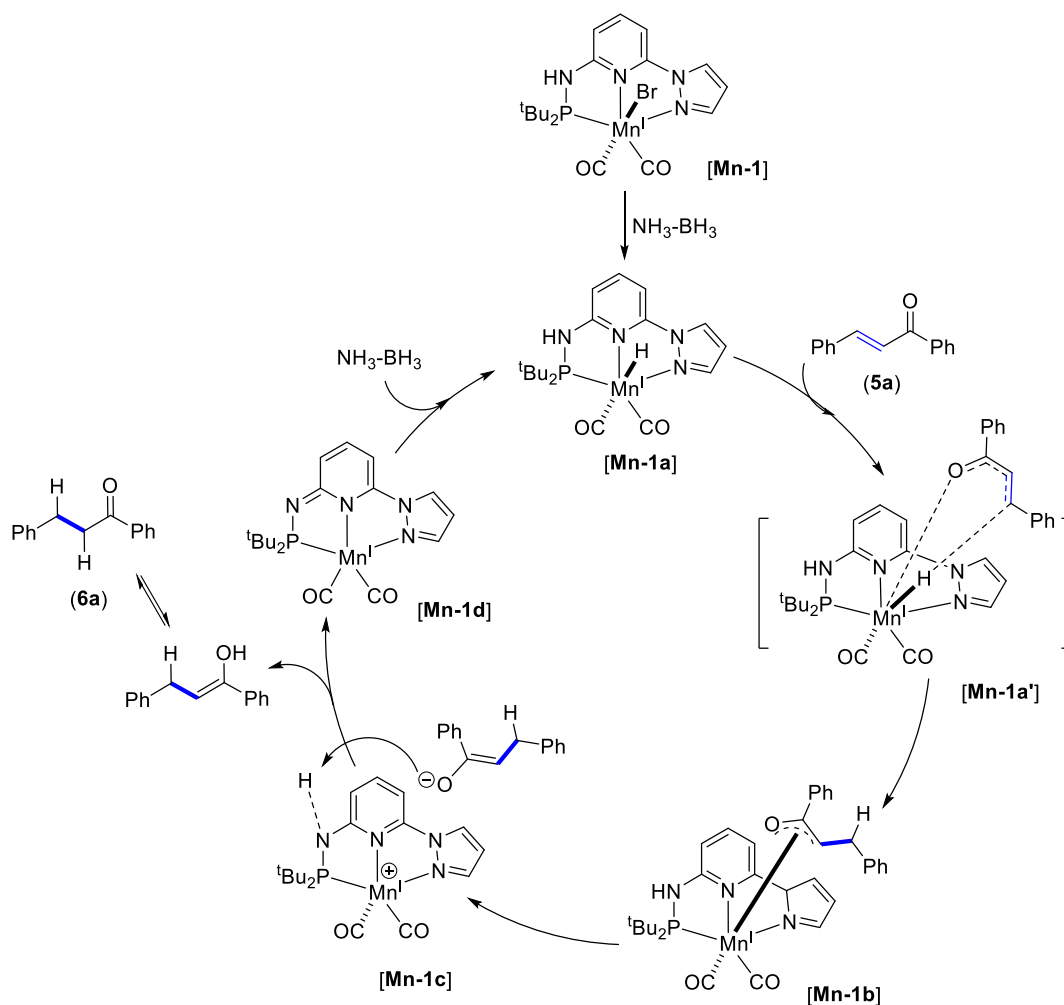


Figure 5.2 Plausible Catalytic Cycle for the transfer hydrogenation of chalcones by Mn-1.

5.3 CONCLUSION

In this chapter, we have discussed the synthesis of a series of PN^3N -based manganese Mn(I) and Mn(II) complexes and explored them for the transfer hydrogenation of α,β -unsaturated ketones. Both the catalysts Mn(I) and Mn(II) were characterized by checking their chemical composition as well as the single crystal XRD study of the complex **Mn-4**. The co-ordination of PN^3N ligand (**L**) to Mn(II) is in a pincer fashion, which revealed a distorted square pyramidal geometry of the complex **Mn-4**. All the complexes were screened for transfer hydrogenation of α,β -unsaturated ketones. Under the optimized reaction conditions, Mn-catalyst (**1**) needed just a half equivalent ammonia-borane to hydrogenate the C=C double bond (alkene) of α,β -unsaturated ketones to afford saturated ketone products. The reaction worked at very mild conditions, i.e., at room temperature, without needing an additional activator. The optimized reaction parameters were compatible with various electronically rich and deficient functional groups, including –OMe, –CF₃, halides, amine, nitro, etc., and yielded an excellent yield of the resulting products.

Moreover, the sensitive functional groups like –OBz or isolated alkene and alkyne were tolerant of the optimized protocol. Synthetically crucial heterocycles like thiophene, pyrrole, indole, furan survived during the transfer hydrogenation and provided a good yield of the resulting saturated ketones. The mechanistic study ruled out the possibility of solvent as a hydrogen donor and the hydrogen pair was donated by ammonia-borane. Further, the need for NH proton in the PN^3N -Mn(I) catalyst (**1**) is understood by conducting a reaction with a –Me substituted Mn-catalyst (**1a**), which was found to be inactive for the reaction. The mechanistic cycle was proposed by studying the mechanistic aspects and the literature precedents. Overall, here we have developed a mild transfer hydrogenation protocol for the conversion of α,β -unsaturated ketones to saturated ketones with excellent yield.

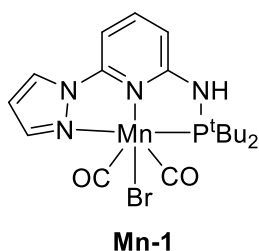
5.4 EXPERIMENTAL SECTION

5.4.1 General Experimental

All the manipulations were conducted under an argon atmosphere either in a glove box or using standard Schlenk techniques in pre-dried glasswares. The catalytic reactions were performed in reaction vessels with Teflon screw caps. Solvents were dried over Na/benzophenone or CaH₂ and distilled prior to use. Liquid reagents were flushed with argon prior to use. The PN³N based pincer ligand (**L**) synthesized by following the literature procedure. All other chemicals were obtained from commercial sources and were used without further purification. High resolution mass spectrometry (HRMS) mass spectra were recorded on a Thermo Scientific QExactive, Accela 1250 pump. NMR: (¹H and ¹³C) spectra were recorded at 400 *or* 500 MHz (¹H), 100 *or* 125 MHz (¹³C, DEPT (distortionless enhancement by polarization transfer)), 377 MHz (¹⁹F), respectively in CDCl₃ solutions, if not otherwise specified; chemical shifts (δ) are given in ppm. The ¹H and ¹³C NMR spectra are referenced to residual solvent signals (CDCl₃: δ H = 7.26 ppm, δ C = 77.2 ppm)

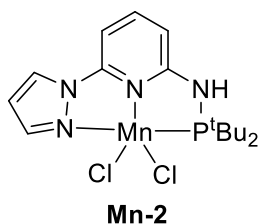
GC Method. Gas Chromatography analyses were performed using a Shimadzu GC2010 gas chromatograph equipped with a Shimadzu AOC-20s auto sampler and a Restek RTX-5 capillary column (30 m x 0.25 mm x 0.25 μ m). The instrument was set to an injection volume of 1 μ L, an inlet split ratio of 10:1, and inlet and detector temperatures of 250 and 320 °C, respectively. UHP-grade argon was used as carrier gas with a flow rate of 30 mL/min. The temperature program used for all the analyses is as follows: 80 °C, 1 min; 30 °C/min to 200 °C, 2 min; 30 °C/min to 260 °C, 3 min; 30 °C/min to 300 °C, 15 min.

5.4.2 Procedure for Synthesis of Manganese Complexes

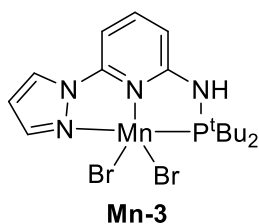


A solution of ligand **L** (0.304 g, 1.0 mmol) in THF (10 mL) was added dropwise to the Mn(CO)₅Br (0.275 g, 1.0 mmol) in THF (10 mL) and the reaction mixture was stirred at room temperature for 12 h. The saffron coloured precipitate obtained was filtered and washed with hexane (5 mL x 3). Upon drying under vacuum, the light saffron complex **Mn-1** was

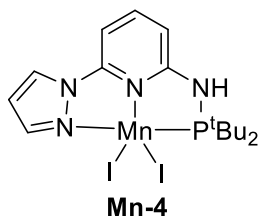
obtained. Yield: 0.406 g, 82%. Elemental Analysis Calcd (%) for C, 43.66; H, 5.09; N, 11.31; Found: C, 43.58; H, 5.47; N, 11.10.



A solution of ligand **L** (0.304 g, 1.0 mmol) in THF (10 mL) was added dropwise to the MnCl₂ (0.126 g, 1.0 mmol) in THF (10 mL) and the reaction mixture was stirred at room temperature for 12 h. The light yellow coloured precipitate obtained was filtered and washed with hexane (5 mL x 3). Upon drying under vacuum, the light yellow complex **2** was obtained. Yield: 0.378 g, 88%. Elemental Analysis Calcd (%) for C, 44.67; H, 5.86; N, 13.02; Found: C, 44.58; H, 5.67; N, 13.10.



A solution of ligand **L** (0.304 g, 1.0 mmol) in THF (10 mL) was added dropwise to the MnBr₂ (0.215 g, 1.0 mmol) in THF (10 mL) and the reaction mixture was stirred at room temperature for 12 h. The light yellow coloured precipitate obtained was filtered and washed with hexane (5 mL x 3). Upon drying under vacuum, the light yellow complex **Mn-3** was obtained. Yield: 0.378 g, 90%. Elemental Analysis Calcd (%) for C, 37.02; H, 4.85; N, 10.79; Found: C, 37.29; H, 4.80; N, 10.59.



A solution of ligand **L** (0.304 g, 1.0 mmol) in THF (10 mL) was added dropwise to the MnCl₂ (0.309 g, 1.0 mmol) in THF (10 mL) and the reaction mixture was stirred at room temperature for 12 h. The light yellow coloured precipitate obtained was filtered and washed with hexane (5 mL x 3). Upon drying under vacuum, the light yellow complex **Mn-4** was obtained. Yield: 0.513 g, 84%. The crystal suitable for a single-crystal X-ray diffraction was

obtained using slow evaporation method from the saturated solution of complex **Mn-4** in CH_2Cl_2 . Elemental Analysis Calcd (%) for C, 31.34; H, 4.11; N, 41.40; Found: C, 31.58; H, 4.47; N, 41.10.

5.4.3 Crystallographic Data

X-ray intensity data measurements of compound **Mn-4** was carried out on a Bruker D8 VENTURE Kappa Duo PHOTON II CPAD diffractometer equipped with Incoatech multilayer mirrors optics. The intensity measurements were carried out with Mo micro-focus sealed tube diffraction source ($\text{MoK}\alpha = 0.71073 \text{ \AA}$) at 100(2) K temperature. The X-ray generator was operated at 50 kV and 1.4 mA. A preliminary set of cell constants and an orientation matrix were calculated from three matrix sets of 36 frames (each matrix run consists of 12 frames). Data were collected with ω scan width of 0.5° at different settings of φ and 2θ with a frame time of 10 sec depending on the diffraction power of the crystals keeping the sample-to-detector distance fixed at 5.00 cm. The X-ray data collection was monitored by APEX3 program (Bruker, 2016). All the data were corrected for Lorentzian, polarization and absorption effects using SAINT and SADABS programs (Bruker, 2016). Using the APEX3 (Bruker) program suite, the structure was solved with the ShelXS-97 (Sheldrick, 2008) structure solution program, using direct methods. The model was refined with a version of ShelXL-2018/3 (Sheldrick, 2015) using Least Squares minimization. All the hydrogen atoms were placed in a geometrically idealized position and constrained to ride on their parent atoms. An ORTEP III view of the compounds was drawn with 50% probability displacement ellipsoids, and H atoms are shown as small spheres of arbitrary radii.

Table 5.2 Crystal data of Mn-4

Crystal Data	Mn-4
Formula	C ₁₆ H ₂₅ I ₂ MnN ₄ P, CH ₂ Cl ₂
Molecular weight	698.03
Crystal Size, mm ³	0.210 × 0.260 × 0.310
Temp. (K)	100(2)
Wavelength (Å)	0.71073
Crystal Syst.	monoclinic
Space Group	<i>P</i> 2 ₁ / <i>n</i>
<i>a</i> /Å	12.0702(15)
<i>b</i> /Å	15.0302(17)
<i>c</i> /Å	14.4008(17)
β /°	105.080(4)
<i>V</i> /Å ³	2522.6(5)
<i>Z</i>	4
<i>D</i> _{calc} /g cm ⁻³	1.838
μ /mm ⁻¹	3.256
<i>F</i> (000)	1348
<i>Ab. Correct.</i>	multi-scan
<i>T</i> _{min} / <i>T</i> _{max}	0.5971/0.7461
2 θ _{max}	60
Total reflns.	162696
Unique reflns.	7736
Obs. reflns.	6466
<i>h, k, l</i> (min, max)	(-17, 17), (-21, 21), (-20, 20)
<i>R</i> _{int} / <i>R</i> _{sig}	0.0881/ 0.0279
No. of parameters	250
<i>R</i> 1 [<i>I</i> > 2 σ (<i>I</i>)]	0.0253
<i>wR</i> 2 [<i>I</i> > 2 σ (<i>I</i>)]	0.0544
<i>R</i> 1 [all data]	0.0380
<i>wR</i> 2 [all data]	0.0612
goodness-of-fit	1.080
$\Delta\rho$ _{max} , $\Delta\rho$ _{min} (eÅ ⁻³)	+1.134, -0.998

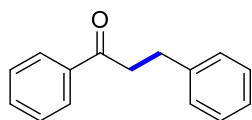
5.4.4 Representative Procedure for Hydrogenation

A Teflon screw-cap tube was introduced with catalyst **Mn-1** (0.002 g, 0.004 mmol), ammonia borane (0.003 g, 0.1 mmol) and (*E*)-chalcone (0.042 g, 0.2 mmol) inside the glove box. The solvent dioxane (1.0 mL) was added to the reaction vessel under the argon atmosphere. The reaction mixture was then stirred at room temperature (27 °C) for 2 h. At ambient temperature, the reaction mixture was diluted with ethyl acetate (5.0 mL) and resulting solution was concentrated under vacuum. The crude reaction mixture was purified by chromatography on silica gel using petroleum ether/EtOAc (30/1) to obtain 1,3-diphenylpropan-1-one (**6a**) (0.043 g, 94%).

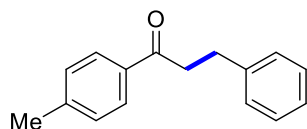
5.4.5 Gram Scale Synthesis

Representative procedure for the transfer hydrogenation followed, using 1.041 g (5 mmol) of **5a**, catalyst **Mn-1** (0.050 g, 0.1 mmol), NH₃-BH₃ (0.075 g, 2.5 mmol) and dioxane (15 mL). The reaction proceeded smoothly and gave an excellent yield of 1,3-diphenylpropan-1-one (**6a**) (0.904 g, 86 %) which highlights the synthetic applicability of the optimized protocol for the gram-scale synthesis.

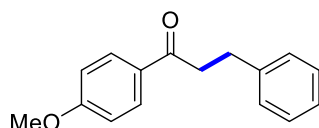
5.4.6 Characterization Data of Hydrogenated Compounds



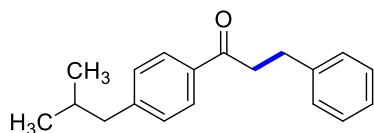
1,3-diphenylpropan-1-one (6a):⁷ The representative procedure was followed, using (*E*)-chalcone (**5a**; 0.042 g, 0.201 mmol), NH₃-BH₃ (0.0031 g, 0.10 mmol) and catalyst **Mn-1** (0.002 g, 0.004 mmol). Purification by column chromatography on silica gel (petroleum ether/EtOAc: 30/1) yielded **6a** as pale white solid. (0.043 g, 94%). ¹H-NMR (500 MHz, CDCl₃): δ = 7.95 (d, *J* = 7.4 Hz, 2H, Ar-H), 7.54 (t, *J* = 7.4 Hz, 1H, Ar-H), 7.44 (t, *J* = 7.6 Hz, 2H, Ar-H), 7.31-7.18 (m, 5H, Ar-H), 3.29 (t, *J* = 7.7 Hz, 2H, CH₂), 3.06 (t, *J* = 7.7 Hz, 2H, CH₂). ¹³C{¹H}-NMR (125 MHz, CDCl₃): δ = 199.4 (CO), 144.4 (C_q), 137.0 (C_q), 133.2 (CH), 128.8 (2C, CH), 128.7 (2C, CH), 128.6 (2C, CH), 128.2 (2C, CH), 126.3 (CH), 40.6 (CH₂), 30.3 (CH₂). HRMS (ESI): *m/z* Calcd for C₁₅H₁₄O + H⁺ [M + H]⁺ 211.1117; Found 211.1115. The ¹H and ¹³C spectra are consistent with those reported in the literature.



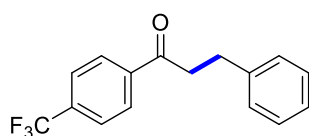
3-phenyl-1-(*p*-tolyl)propan-1-one (6b):⁴⁷ The representative procedure was followed, using (*E*)-3-phenyl-1-(*p*-tolyl)prop-2-en-1-one (**5b**; 0.044 g, 0.198 mmol), $\text{NH}_3\text{-BH}_3$ (0.0031 g, 0.10 mmol) and catalyst **Mn-1** (0.002 g, 0.004 mmol). Purification by column chromatography on silica gel (petroleum ether/EtOAc: 50/1) yielded **6b** as brown oil. (0.043 g, 95%). $^1\text{H-NMR}$ (500 MHz, CDCl_3): δ = 7.87-7.86 (d, J = 8.2 Hz, 2H, Ar-H), 7.32-7.29 (m, 2H, Ar-H), 7.27-7.24 (m, 4H, Ar-H), 7.21 (t, J = 7.2 Hz, 2H, Ar-H), 3.28 (t, J = 7.8 Hz, 2H, CH_2), 3.06 (t, J = 7.6 Hz, 2H, CH_2), 2.41 (s, 3H, CH_3). $^{13}\text{C}\{^1\text{H}\}\text{-NMR}$ (100 MHz, CDCl_3): δ = 199.1 (CO), 144.0 (C_q), 141.6 (C_q), 134.6 (C_q), 129.5 (2C, CH), 128.7 (2C, CH), 128.6 (2C, CH), 128.4 (2C, CH), 126.3 (CH), 40.5 (CH_2), 30.4 (CH_2), 21.8 (CH_3). HRMS (ESI): m/z Calcd for $\text{C}_{16}\text{H}_{16}\text{O} + \text{H}^+$ [M + H]⁺ 225.1274; Found 225.1272. The ^1H and ^{13}C spectra are consistent with those reported in the literature.



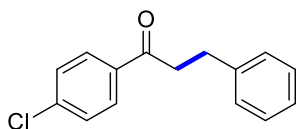
3-(4-methoxyphenyl)-1-phenylpropan-1-one (6c):²⁰ The representative procedure was followed, using (*E*)-3-(4-methoxyphenyl)-1-phenylprop-2-en-1-one (**5c**; 0.048 g, 0.201 mmol), $\text{NH}_3\text{-BH}_3$ (0.0031 g, 0.10 mmol) and catalyst **Mn-1** (0.002 g, 0.004 mmol). Purification by column chromatography on silica gel (petroleum ether/EtOAc: 10/1) yielded **6c** as colourless solid. (0.047 g, 98%). $^1\text{H-NMR}$ (400 MHz, CDCl_3): δ = 7.96 (d, J = 9.0 Hz, 2H, Ar-H), 7.33-7.20 (m, 5H, Ar-H), 6.94 (d, J = 9.0 Hz, 2H, Ar-H), 3.88 (s, 3H, CH_3), 3.27 (t, J = 7.8 Hz, 2H, CH_2), 3.02 (t, J = 7.8 Hz, 2H, CH_2). $^{13}\text{C}\{^1\text{H}\}\text{-NMR}$ (100 MHz, CDCl_3): δ = 198 (CO), 163.6 (C_q), 141.6 (C_q), 130.5 (2C, CH), 130.2 (C_q), 128.7 (2C, CH), 128.6 (2C, CH), 126.3 (CH), 113.9 (2C, CH), 55.6 (CH_3), 40.3 (CH_2), 30.5 (CH_2). HRMS (ESI): m/z Calcd for $\text{C}_{16}\text{H}_{16}\text{O}_2 + \text{H}^+$ [M + H]⁺ 241.1223; Found 241.1218. The ^1H and ^{13}C spectra are consistent with those reported in the literature.



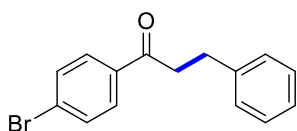
1-(4-isobutylphenyl)-3-phenylpropan-1-one (6d):⁴⁸ The representative procedure was followed, using (*E*)-1-(4-isobutylphenyl)-3-phenylprop-2-en-1-one (**5d**; 0.053 g, 0.20 mmol), $\text{NH}_3\text{-BH}_3$ (0.0031 g, 0.10 mmol) and catalyst **Mn-1** (0.002 g, 0.004 mmol). Purification by column chromatography on silica gel (petroleum ether/EtOAc: 30/1) yielded **6d** as yellow oil. (0.043 g, 81%). $^1\text{H-NMR}$ (500 MHz, CDCl_3): δ = 7.80 (d, J = 8.3 Hz, 2H, Ar-H), 7.24-7.10 (m, 7H, Ar-H), 3.20 (t, J = 7.8 Hz, 2H, CH_2), 2.98 (t, J = 7.8 Hz, 2H, CH_2), 2.44 (d, J = 7.3 Hz, 2H, CH_2), 1.81 (m, 1H, CH), 0.83-0.82 (d, J = 6.6 Hz, 6H, CH_3). $^{13}\text{C}\{^1\text{H}\}\text{-NMR}$ (125 MHz, CDCl_3): δ = 199.1 (CO), 147.7 (C_q), 141.6 (C_q), 134.8 (C_q), 129.5 (2C, CH), 128.7 (2C, CH), 128.6 (2C, CH), 128.2 (2C, CH), 126.3 (CH), 45.6 (CH_2), 40.5 (CH_2), 30.4 (CH_2), 30.3 (CH), 22.5 (CH_3). HRMS (ESI): m/z Calcd for $\text{C}_{19}\text{H}_{22}\text{O} + \text{H}^+$ $[\text{M} + \text{H}]^+$ 267.1743; Found 276.1740. The ^1H and ^{13}C spectra are consistent with those reported in the literature.



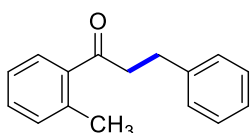
3-phenyl-1-(4-(trifluoromethyl)phenyl)propan-1-one (6e):²⁰ The representative procedure was followed, using (*E*)-3-phenyl-1-(4-(trifluoromethyl)phenyl)prop-2-en-1-one (**5e**; 0.055 g, 0.199 mmol), $\text{NH}_3\text{-BH}_3$ (0.0031 g, 0.10 mmol) and catalyst **Mn-1** (0.002 g, 0.004 mmol). Purification by column chromatography on silica gel (petroleum ether/EtOAc: 30/1) yielded **6e** as yellow oil. (0.030 g, 54%). $^1\text{H-NMR}$ (500 MHz, CDCl_3): δ = 8.05 (d, J = 8.3 Hz, 2H, Ar-H), 7.72 (d, J = 8.3 Hz, 2H, Ar-H), 7.33-7.29 (m, 2H, Ar-H), 7.26-7.20 (m, 3H, Ar-H), 3.33 (t, J = 7.6 Hz, 2H, CH_2), 3.09 (t, J = 7.6 Hz, 2H, CH_2). $^{13}\text{C}\{^1\text{H}\}\text{-NMR}$ (125 MHz, CDCl_3): δ = 198.4 (CO), 141.0 (C_q), 139.7 (C_q), 134.5 (q, $^2J_{\text{C-F}}$ = 32.8 Hz, C_q), 128.8 (2C, CH), 128.6 (2C, CH), 128.5 (2C, CH), 126.5 (CH), 125.9 (q, $^3J_{\text{C-F}}$ = 3.8 Hz, 2C, CH), 123.8 (q, $^1J_{\text{C-F}}$ = 272.6 Hz, C_q), 40.9 (CH_2), 30.1 (CH_2). HRMS (ESI): m/z Calcd for $\text{C}_{16}\text{H}_{13}\text{F}_3\text{O} + \text{H}^+$ $[\text{M} + \text{H}]^+$ 279.0991; Found 279.0988. The ^1H and ^{13}C spectra are consistent with those reported in the literature.



1-(4-chlorophenyl)-3-phenylpropan-1-one (6f):²⁰ The representative procedure was followed, using (*E*)-1-(4-chlorophenyl)-3-phenylprop-2-en-1-one (**5f**; 0.049 g, 0.202 mmol), $\text{NH}_3\text{-BH}_3$ (0.0031 g, 0.10 mmol) and catalyst **Mn-1** (0.002 g, 0.004 mmol). Purification by column chromatography on silica gel (petroleum ether/EtOAc: 30/1) yielded **6f** as white solid. (0.040 g, 82%). $^1\text{H-NMR}$ (400 MHz, CDCl_3): $\delta = 7.88$ (d, $J = 8.6$ Hz, 2H, Ar-H), 7.41 (d, $J = 8.6$ Hz, 2H, Ar-H), 7.31-7.27 (m, 2H, Ar-H), 7.24-7.18 (m, 3H, Ar-H), 3.26 (t, $J = 7.7$ Hz, 2H, CH_2), 3.05 (t, $J = 7.7$ Hz, 2H, CH_2). $^{13}\text{C}\{^1\text{H}\}\text{-NMR}$ (100 MHz, CDCl_3): $\delta = 198.1$ (CO), 141.2 (C_q), 139.6 (C_q), 135.3 (C_q), 129.6 (2C, CH), 129.1 (2C, CH), 128.7 (2C, CH), 128.6 (2C, CH), 126.4 (CH), 40.6 (CH_2), 30.2 (CH_2). The ^1H and ^{13}C spectra are consistent with those reported in the literature.

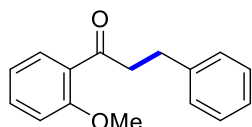


1-(4-bromophenyl)-3-phenylpropan-1-one (6g):²⁰ The representative procedure was followed, using (*E*)-1-(4-bromophenyl)-3-phenylprop-2-en-1-one (**5g**; 0.057 g, 0.198 mmol), $\text{NH}_3\text{-BH}_3$ (0.0031 g, 0.10 mmol) and catalyst **Mn-1** (0.002 g, 0.004 mmol). Purification by column chromatography on silica gel (petroleum ether/EtOAc: 50/1) yielded **6g** as white solid. (0.029 g, 50%). $^1\text{H-NMR}$ (400 MHz, CDCl_3): $\delta = 7.80$ (d, $J = 8.6$ Hz, 2H, Ar-H), 7.58 (d, $J = 8.6$ Hz, 2H, Ar-H), 7.31-7.18 (m, 5H, Ar-H), 3.25 (t, $J = 7.6$ Hz, 2H, CH_2), 3.05 (t, $J = 7.6$ Hz, 2H, CH_2). $^{13}\text{C}\{^1\text{H}\}\text{-NMR}$ (100 MHz, CDCl_3): $\delta = 198.3$ (CO), 141.2 (C_q), 135.7 (C_q), 132.1 (2C, CH), 129.7 (2C, CH), 128.7 (2C, CH), 128.6 (2C, CH), 128.4 (C_q), 126.4 (CH), 40.6 (CH_2), 30.2 (CH_2). The ^1H and ^{13}C spectra are consistent with those reported in the literature.

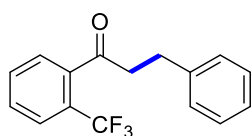


3-phenyl-1-(*o*-tolyl)propan-1-one (6h):⁴ The representative procedure was followed, using (*E*)-3-phenyl-1-(*o*-tolyl)prop-2-en-1-one (**5h**; 0.044 g, 0.198 mmol), $\text{NH}_3\text{-BH}_3$ (0.0031 g, 0.10 mmol) and catalyst **Mn-1** (0.002 g, 0.004 mmol). Purification by column chromatography on silica gel (petroleum ether/EtOAc: 50/1) yielded **6h** as yellow oil. (0.043

g, 96%). $^1\text{H-NMR}$ (400 MHz, CDCl_3): δ = 7.59 (d, J = 7.9 Hz, 1H, Ar-H), 7.35 (t, J = 7.4 Hz, 1H, Ar-H), 7.28 (t, J = 7.4 Hz, 2H, Ar-H), 7.24-7.17 (m, 5H, Ar-H), 3.22 (t, J = 7.7 Hz, 2H, Ar-H), 3.04 (t, J = 7.6 Hz, 2H, CH_2), 2.46 (s, 3H, CH_3). $^{13}\text{C}\{^1\text{H}\}$ -NMR (100 MHz, CDCl_3): δ = 203.6 (CO), 141.4 (C_q), 138.3 (C_q), 138.1 (C_q), 132.1 (CH), 131.4 (CH), 128.7 (2C, CH), 128.6 (2C, CH), 128.5 (CH), 126.3 (CH), 125.8 (CH), 43.4 (CH_2), 30.5 (CH_2), 21.4 (CH_3). HRMS (ESI): m/z Calcd for $\text{C}_{16}\text{H}_{16}\text{O} + \text{H}^+$ $[\text{M} + \text{H}]^+$ 225.1274; Found 225.1271. The ^1H and ^{13}C spectra are consistent with those reported in the literature.

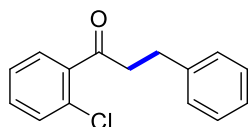


1-(2-methoxyphenyl)-3-phenylpropan-1-one (6i):⁴⁹ The representative procedure was followed, using (*E*)-1-(2-methoxyphenyl)-3-phenylprop-2-en-1-one (**5i**; 0.048 g, 0.201 mmol), $\text{NH}_3\text{-BH}_3$ (0.0031 g, 0.10 mmol) and catalyst **Mn-1** (0.002 g, 0.004 mmol). Purification by column chromatography on silica gel (petroleum ether/EtOAc: 50/1) yielded **6i** as yellow oil. (0.043 g, 96%). $^1\text{H-NMR}$ (400 MHz, CDCl_3): δ = 7.68 (dd, J = 7.6, 1.8 Hz, 1H, Ar-H), 7.44 (m, 1H, Ar-H), 7.29-7.26 (m, 2H, Ar-H), 7.25-7.21 (m, 2H, Ar-H), 7.21-7.16 (m, 1H, Ar-H), 6.99 (t, J = 7.6 Hz, 2H, Ar-H), 3.86 (s, 3H, OCH_3), 3.30 (t, J = 7.8 Hz, 2H, CH_2), 3.02 (s, J = 7.8 Hz, 2H, CH_2). $^{13}\text{C}\{^1\text{H}\}$ -NMR (100 MHz, CDCl_3): δ = 201.8 (C_q), 158.6 (C_q), 141.8 (C_q), 133.5 (C_q), 130.4 (CH), 128.5 (CH), 128.4 (2C, CH), 128.3 (2C, CH), 125.9 (CH), 120.7 (CH), 111.5 (CH), 55.5 (CH_3), 45.5 (CH_2), 30.5 (CH_2). HRMS (ESI): m/z Calcd for $\text{C}_{16}\text{H}_{16}\text{O} + \text{H}^+$ $[\text{M} + \text{H}]^+$ 225.1274; Found 225.1271. The ^1H and ^{13}C spectra are consistent with those reported in the literature.

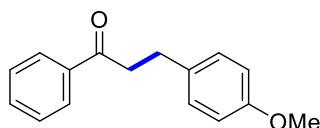


3-phenyl-1-(2-(trifluoromethyl)phenyl)propan-1-one (6j):⁵⁰ The representative procedure was followed, using (*E*)-3-phenyl-1-(2-(trifluoromethyl)phenyl)prop-2-en-1-one (**5j**; 0.055 g, 0.199 mmol), $\text{NH}_3\text{-BH}_3$ (0.0031 g, 0.10 mmol) and catalyst **Mn-1** (0.002 g, 0.004 mmol). Purification by column chromatography on silica gel (petroleum ether/EtOAc: 30/1) yielded **6j** as yellow oil. (0.045 g, 81%). $^1\text{H-NMR}$ (400 MHz, CDCl_3): δ = 7.69 (d, J = 7.8 Hz, 1H, Ar-H), 7.57-7.50 (m, 2H, Ar-H), 7.31-7.27 (m, 3H, Ar-H), 7.24-7.18 (m, 3H, Ar-H), 3.16 (t, J = 7.6 Hz, 2H, CH_2), 3.05 (t, J = 7.4 Hz, 2H, CH_2). $^{13}\text{C}\{^1\text{H}\}$ -NMR (100 MHz, CDCl_3): δ =

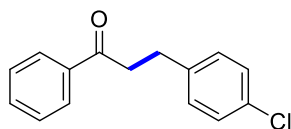
203.6 (C_q), 140.8 (C_q), 140.5 (q, ³J_{C-F} = 1.9 Hz, C_q), 132.0 (CH), 130.2 (CH), 128.7 (2C, CH), 128.5 (2C, CH), 127.0 (CH), 126.9 (q, ³J_{C-F} = 5.0 Hz, CH), 126.4 (CH), 122.4 (q, ¹J_{C-F} = 273.9 Hz, CF₃), 45.0 (d, ³J_{C-F} = 1.5 Hz, CH₂), 30.0 (CH₂). HRMS (ESI): *m/z* Calcd for C₁₆H₁₃F₃O + H⁺ [M + H]⁺ 279.0991; Found 279.0986. The ¹H and ¹³C spectra are consistent with those reported in the literature.



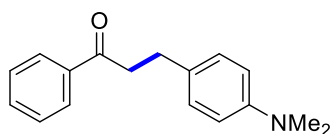
1-(2-chlorophenyl)-3-phenylpropan-1-one(6k):⁵¹ The representative procedure was followed, using (*E*)-1-(2-chlorophenyl)-3-phenylprop-2-en-1-one (**5k**; 0.049 g, 0.218 mmol), NH₃-BH₃ (0.0031 g, 0.10 mmol) and catalyst **Mn-1** (0.002 g, 0.004 mmol). Purification by column chromatography on silica gel (petroleum ether/EtOAc: 15/1) yielded **6k** as yellow oil. (0.035 g, 71%). ¹H-NMR (500 MHz, CDCl₃): δ = 7.90 (d, *J* = 8.6 Hz, 2H, Ar-H), 7.43 (d, *J* = 8.6 Hz, 2H, Ar-H), 7.31 (t, *J* = 7.3 Hz, 2H, Ar-H), 7.26-7.20 (m, 3H, Ar-H), 3.28 (t, *J* = 7.7 Hz, 2H, CH₂), 3.06 (t, *J* = 7.7 Hz, 2H, CH₂). ¹³C{¹H}-NMR (125 MHz, CDCl₃): δ = 198.2 (CO), 141.2 (C_q), 139.7 (C_q), 135.3 (C_q), 129.6 (2C, CH), 129.1 (2C, CH), 128.8 (2C, CH), 128.6 (2C, CH), 126.4 (CH), 40.6 (CH₂), 30.2 (CH₂). The ¹H and ¹³C spectra are consistent with those reported in the literature.



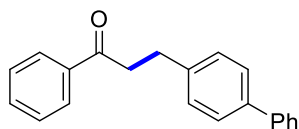
3-(4-methoxyphenyl)-1-phenylpropan-1-one (6l):²⁰ The representative procedure was followed, using (*E*)-3-(4-methoxyphenyl)-1-phenylprop-2-en-1-one (**5l**; 0.048 g, 0.201 mmol), NH₃-BH₃ (0.0031 g, 0.10 mmol) and catalyst **Mn-1** (0.002 g, 0.004 mmol). Purification by column chromatography on silica gel (petroleum ether/EtOAc: 10/1) yielded **6l** as white solid. (0.046 g, 96%). ¹H-NMR (400 MHz, CDCl₃): δ = 7.96 (d, *J* = 7.3 Hz, 2H, Ar-H), 7.56 (t, *J* = 7.4 Hz, 1H, Ar-H), 7.45 (vt, *J* = 7.6 Hz, 2H, Ar-H), 7.18 (d, *J* = 8.6 Hz, 2H, Ar-H), 6.85 (d, *J* = 8.6 Hz, 2H, Ar-H), 3.79 (s, 3H, CH₃), 3.27 (vt, *J* = 7.6 Hz, 2H, CH₂), 3.02 (vt, *J* = 7.6 Hz, 2H, CH₂). ¹³C{¹H}-NMR (100 MHz, CDCl₃): δ = 199.5 (CO), 158.2 (C_q), 137.1 (C_q), 133.5 (C_q), 133.2 (CH), 129.5 (2C, CH), 128.8 (2C, CH), 128.2 (2C, CH), 114.1 (2C, CH), 55.4 (OCH₃), 40.9 (CH₂), 29.5 (CH₂). HRMS (ESI): *m/z* Calcd for C₁₆H₁₆O₂ + H⁺ [M + H]⁺ 241.1223; Found 241.1220. The ¹H and ¹³C spectra are consistent with those reported in the literature.



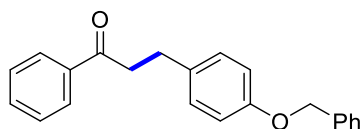
3-(4-chlorophenyl)-1-phenylpropan-1-one (6m):⁴⁹ The representative procedure was followed, using (*E*)-3-(4-chlorophenyl)-1-phenylprop-2-en-1-one (**5m**; 0.049 g, 0.202 mmol), $\text{NH}_3\text{-BH}_3$ (0.0031 g, 0.10 mmol) and catalyst **Mn-1** (0.002 g, 0.004 mmol). Purification by column chromatography on silica gel (petroleum ether/EtOAc: 30/1) yielded **6m** as pale white solid. (0.041 g, 84%). $^1\text{H-NMR}$ (500 MHz, CDCl_3): δ = 7.87-7.85 (m, 2H, Ar-H), 7.47 (t, J = 7.4 Hz, 1H, Ar-H), 7.37 (t, J = 7.6 Hz, 2H, Ar-H), 7.17 (d, J = 8.4 Hz, 2H, Ar-H), 7.10 (d, J = 8.6 Hz, 2H, Ar-H), 3.19 (t, J = 7.6 Hz, 2H, CH_2), 2.96 (t, J = 7.5 Hz, 2H, CH_2). $^{13}\text{C}\{^1\text{H}\}\text{-NMR}$ (125 MHz, CDCl_3): δ = 199 (CO), 139.9 (C_q), 136.9 (C_q), 133.3 (CH), 132.0 (C_q), 130.0 (2C, CH), 128.8 (2C, CH), 128.7 (2C, CH), 128.2 (2C, CH), 40.3 (CH_2), 29.5 (CH_2). The ^1H and ^{13}C spectra are consistent with those reported in the literature.



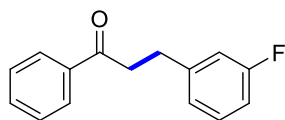
3-(4-(dimethylamino)phenyl)-1-phenylpropan-1-one (6n):⁵² The representative procedure was followed, using (*E*)-3-(4-(dimethylamino)phenyl)-1-phenylprop-2-en-1-one (**5n**; 0.050 g, 0.199 mmol), $\text{NH}_3\text{-BH}_3$ (0.0031 g, 0.10 mmol) and catalyst **Mn-1** (0.002 g, 0.004 mmol). Purification by column chromatography on silica gel (petroleum ether/EtOAc: 5/1) yielded **6n** as brown oil. (0.036 g, 71%). $^1\text{H-NMR}$ (500 MHz, CDCl_3): δ = 7.96 (d, J = 7.6 Hz, 2H, Ar-H), 7.56 (t, J = 8 Hz, 1H, Ar-H), 7.45 (t, J = 7.6 Hz, 2H, Ar-H), 7.14 (d, J = 8.8 Hz, 2H, Ar-H), 6.71 (d, J = 8.6 Hz, 2H, Ar-H), 3.26 (t, J = 7.8 Hz, 2H, CH_2), 2.98 (t, J = 7.8 Hz, 2H, CH_2), 2.92 (s, 6H, CH_3). $^{13}\text{C}\{^1\text{H}\}\text{-NMR}$ (125 MHz, CDCl_3): δ = 199.9 (CO), 149.4 (C_q), 137.1 (C_q), 133.1 (CH), 129.5 (C_q), 129.2 (2C, CH), 128.8 (2C, CH), 128.2 (2C, CH), 113.3 (2C, CH), 41.1 (CH_2), 41.1 (CH_3), 29.4 (CH_2). HRMS (ESI): m/z Calcd for $\text{C}_{17}\text{H}_{19}\text{NO} + \text{H}^+$ [$\text{M} + \text{H}$]⁺ 254.1539; Found 254.1536. The ^1H and ^{13}C spectra are consistent with those reported in the literature.



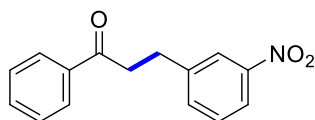
3-([1,1'-biphenyl]-4-yl)-1-phenylpropan-1-one (6o):⁵³ The representative procedure was followed, using (*E*)-3-([1,1'-biphenyl]-4-yl)-1-phenylprop-2-en-1-one (**5o**; 0.057 g, 0.20 mmol), $\text{NH}_3\text{-BH}_3$ (0.0031 g, 0.10 mmol) and catalyst **Mn-1** (0.002 g, 0.004 mmol). Purification by column chromatography on silica gel (petroleum ether/EtOAc: 30/1) yielded **6o** as pale white solid. (0.046 g, 80%). $^1\text{H-NMR}$ (400 MHz, CDCl_3): $\delta = 7.99$ (d, $J = 8.5$ Hz, 2H, Ar-H), 7.60-7.53 (m, 5H, Ar-H), 7.49-7.42 (m, 4H, Ar-H), 7.35-7.33 (m, 3H, Ar-H), 3.36 (t, $J = 7.6$ Hz, 2H, CH_2), 3.13 (t, $J = 7.6$ Hz, 2H, CH_2). $^{13}\text{C}\{^1\text{H}\}\text{-NMR}$ (100 MHz, CDCl_3): $\delta = 199.4$ (CO), 141.2 (C_q), 140.6 (C_q), 139.3 (C_q), 137.0 (C_q), 133.3 (CH), 129.0 (2C, CH), 128.9 (2C, CH), 128.8 (2C, CH), 128.2 (2C, CH), 127.5 (2C, CH), 127.3 (CH), 127.2 (2C, CH), 40.6 (CH_2), 29.9 (CH_2). HRMS (ESI): m/z Calcd for $\text{C}_{21}\text{H}_{18}\text{O} + \text{H}^+$ [$\text{M} + \text{H}$]⁺ 287.1430; Found 287.1425. The ^1H and ^{13}C spectra are consistent with those reported in the literature.



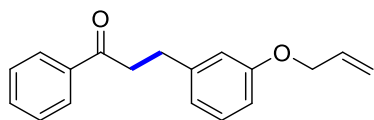
3-(4-(benzyloxy)phenyl)-1-phenylpropan-1-one (6p):⁵⁴ The representative procedure was followed, using (*E*)-3-(4-(benzyloxy)phenyl)-1-phenylprop-2-en-1-one (**5p**; 0.063 g, 0.20 mmol), $\text{NH}_3\text{-BH}_3$ (0.0031 g, 0.10 mmol) and catalyst **Mn-1** (0.002 g, 0.004 mmol). Purification by column chromatography on silica gel (petroleum ether/EtOAc: 10/1) yielded **6p** as yellow oil. (0.050 g, 79%). $^1\text{H-NMR}$ (500 MHz, CDCl_3): $\delta = 7.96$ (d, $J = 7.7$ Hz, 2H, Ar-H), 7.56 (vt, $J = 7.4$ Hz, 1H, Ar-H), 7.48-7.31 (m, 7H, Ar-H), 7.18 (d, $J = 8.6$ Hz, 2H, Ar-H), 6.92 (d, $J = 8.6$ Hz, 2H, Ar-H), 5.05 (s, 2H, CH_2), 3.28 (t, $J = 7.6$ Hz, 2H, CH_2), 3.02 (t, $J = 7.7$ Hz, 2H, CH_2). $^{13}\text{C}\{^1\text{H}\}\text{-NMR}$ (125 MHz, CDCl_3): $\delta = 199.6$ (CO), 157.4 (C_q), 137.4 (C_q), 137.1 (C_q), 133.8 (C_q), 133.2 (CH), 129.6 (2C, CH), 128.8 (2C, CH), 128.8 (2C, CH), 128.2 (2C, CH), 128.1 (CH), 127.6 (2C, CH), 115.1 (2C, CH), 70.3 (CH_2), 40.9 (CH_2), 29.5 (CH_2). HRMS (ESI): m/z Calcd for $\text{C}_{22}\text{H}_{20}\text{O}_2 + \text{H}^+$ [$\text{M} + \text{H}$]⁺ 317.1536; Found 317.1531. The ^1H and ^{13}C spectra are consistent with those reported in the literature.



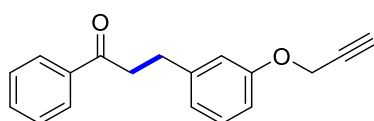
3-(3-fluorophenyl)-1-phenylpropan-1-one (6q):⁵⁵ The representative procedure was followed, using (*E*)-3-(3-fluorophenyl)-1-phenylprop-2-en-1-one (**5q**; 0.045 g, 0.199 mmol), $\text{NH}_3\text{-BH}_3$ (0.0031 g, 0.10 mmol) and catalyst **Mn-1** (0.002 g, 0.004 mmol). Purification by column chromatography on silica gel (petroleum ether/EtOAc: 30/1) yielded **6q** as pale white solid. (0.036 g, 79%). $^1\text{H-NMR}$ (400 MHz, CDCl_3): δ = 7.96 (d, J = 7.1 Hz, 2H, Ar-H), 7.56 (t, J = 7.4 Hz, 1H, Ar-H), 7.46 (tt, J = 7.6, 1.9 Hz, 2H, Ar-H), 7.28-7.22 (m, 1H, Ar-H), 7.04-7.03 (d, J = 7.6 Hz, 1H, Ar-H), 6.98-6.95 (m, 1H, Ar-H), 6.90 (td, J = 8.5, 2.4 Hz, 1H, Ar-H), 3.31 (t, J = 7.6 Hz, 2H, CH_2), 3.08 (t, J = 7.6 Hz, 2H, CH_2). $^{13}\text{C}\{^1\text{H}\}$ -NMR (100 MHz, CDCl_3): δ = 198.9 (CO), 163.1 (d, $^1J_{\text{C-F}}$ = 245.4 Hz, C_q), 144.0 (d, $^3J_{\text{C-F}}$ = 6.9 Hz, C_q), 136.9 (C_q), 133.3 (CH), 130.1 (CH), 130.1 (CH), 128.8 (2C, CH), 128.2 (2C, CH), 124.2 (d, $^3J_{\text{C-F}}$ = 3.1 Hz, CH), 115.5 (d, $^2J_{\text{C-F}}$ = 20.6 Hz, CH), 113.2 (d, $^2J_{\text{C-F}}$ = 21.4 Hz, CH), 40.1 (CH_2), 29.9 (d, $^4J_{\text{C-F}}$ = 1.5 Hz, CH_2). HRMS (ESI): m/z Calcd for $\text{C}_{15}\text{H}_{13}\text{FO} + \text{H}^+$ [$\text{M} + \text{H}$]⁺ 229.1023; Found 229.1021. The ^1H and ^{13}C spectra are consistent with those reported in the literature.



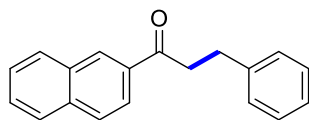
3-(3-nitrophenyl)-1-phenylpropan-1-one (6r): The representative procedure was followed, using (*E*)-3-(3-nitrophenyl)-1-phenylprop-2-en-1-one (**5r**; 0.051 g, 0.201 mmol), $\text{NH}_3\text{-BH}_3$ (0.0031 g, 0.10 mmol) and catalyst **Mn-1** (0.002 g, 0.004 mmol). Purification by column chromatography on silica gel (petroleum ether/EtOAc: 30/1) yielded **6r** as pale white solid. (0.025 g, 48%) as white solid. $^1\text{H-NMR}$ (400 MHz, CDCl_3): δ = 8.12 (s, 1H, Ar-H), 8.05 (d, J = 8.1 Hz, 1H, Ar-H), 7.95 (d, J = 7.8 Hz, 2H, Ar-H), 7.61 (d, J = 7.8 Hz, 1H, Ar-H), 7.57 (t, J = 7.4 Hz, 1H, Ar-H), 7.48-7.43 (m, 3H, Ar-H), 3.37 (t, J = 7.4 Hz, 2H, CH_2), 3.19 (t, J = 7.3 Hz, 2H, CH_2). $^{13}\text{C}\{^1\text{H}\}$ -NMR (100 MHz, CDCl_3): δ = 198.4 (C_q), 148.5 (C_q), 143.5 (C_q), 136.7 (C_q), 135.1 (CH), 133.5 (CH), 129.5 (CH), 128.9 (2C, CH), 128.1 (2C, CH), 123.4 (CH), 121.5 (CH), 39.7 (CH_2), 29.6 (CH_2). HRMS (ESI): m/z Calcd for $\text{C}_{15}\text{H}_{13}\text{NO}_3 + \text{H}^+$ [$\text{M} + \text{H}$]⁺ 256.0973; Found 256.0961.



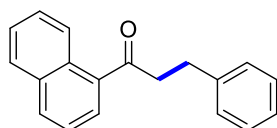
3-(3-(allyloxy)phenyl)-1-phenylpropan-1-one (6s): The representative procedure was followed, using (*E*)-3-(3-(allyloxy)phenyl)-1-phenylprop-2-en-1-one (**5s**; 0.053 g, 0.20 mmol), $\text{NH}_3\text{-BH}_3$ (0.0031 g, 0.10 mmol) and catalyst **Mn-1** (0.002 g, 0.004 mmol). Purification by column chromatography on silica gel (petroleum ether/EtOAc: 30/1) yielded **6s** as yellow oil. (0.043 g, 81%). $^1\text{H-NMR}$ (400 MHz, CDCl_3): δ = 7.54 (d, J = 7.6 Hz, 1H, Ar-H), 7.51-7.50 (m, 1H, Ar-H), 7.35 (t, J = 7.9 Hz, 1H, Ar-H), 7.32-7.29 (m, 2H, Ar-H), 7.26-7.19 (m, 3H, Ar-H), 7.13-7.10 (m, 1H, Ar-H), 6.10-6.01 (m, 1H, CH), 5.43 (dd, J = 17.3, 1.5 Hz, 1H, CH), 5.31 (dd, J = 10.5, 1.4 Hz, 1H, CH), 4.58 (d, J = 5.3 Hz, 2H, CH_2), 3.29 (t, J = 7.6 Hz, 2H, CH_2), 3.06 (t, J = 7.6 Hz, 2H, CH_2). $^{13}\text{C}\{^1\text{H}\}\text{-NMR}$ (100 MHz, CDCl_3): δ = 199.2 (CO), 159.0 (C_q), 141.4 (C_q), 138.4 (C_q), 133.0 (CH), 129.8 (CH), 128.7 (2C, CH), 128.6 (2C, CH), 126.3 (CH), 120.9 (CH), 120.4 (CH), 118.1 (CH_2), 113.5 (CH), 69.1 (CH_2), 40.7 (CH_2), 30.4 (CH_2). HRMS (ESI): m/z Calcd for $\text{C}_{18}\text{H}_{18}\text{O}_2 + \text{H}^+$ [$\text{M} + \text{H}$] $^+$ 267.1380; Found 267.1373.



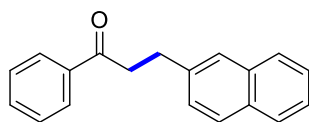
1-phenyl-3-(3-(prop-2-yn-1-yloxy)phenyl)propan-1-one (6t): The representative procedure was followed, using (*E*)-1-phenyl-3-(3-(prop-2-yn-1-yloxy)phenyl)prop-2-en-1-one (**5t**; 0.079 g, 0.301 mmol), $\text{NH}_3\text{-BH}_3$ (0.0046 g, 0.148 mmol) and catalyst **Mn-1** (0.003 g, 0.006 mmol). Purification by column chromatography on silica gel (petroleum ether/EtOAc: 20/1) yielded **6t** as yellow oil. (0.059 g, 74%). $^1\text{H-NMR}$ (500 MHz, CDCl_3): δ = 7.61-7.57 (m, 2H, Ar-H), 7.38 (t, J = 7.8 Hz, 1H, Ar-H), 7.31 (t, J = 7.3 Hz, 2H, Ar-H), 7.27-7.17 (m, 5H, Ar-H), 4.74 (d, J = 2.4 Hz, 2H, Ar-H), 3.30 (t, J = 7.6 Hz, 2H, CH_2), 3.08 (t, J = 7.7 Hz, 2H, CH_2), 2.54 (t, J = 2.4 Hz, 1H, CH). $^{13}\text{C}\{^1\text{H}\}\text{-NMR}$ (125 MHz, CDCl_3): δ = 198.9 (CO), 157.9 (C_q), 141.4 (C_q), 138.4 (C_q), 129.8 (CH), 128.7 (2C, CH), 128.6 (2C, CH), 126.3 (CH), 121.6 (CH), 120.4 (CH), 113.7 (CH), 78.2 (C_q), 76.1 (CH), 56.1 (CH_2), 40.7 (CH_2), 30.3 (CH_2). HRMS (ESI): m/z Calcd for $\text{C}_{18}\text{H}_{16}\text{O}_2 + \text{H}^+$ [$\text{M} + \text{H}$] $^+$ 265.1223; Found 265.1217.



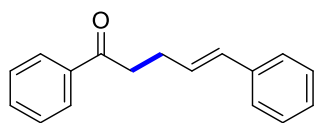
1-(naphthalen-2-yl)-3-phenylpropan-1-one (6u):⁴⁹ The representative procedure was followed, using (*E*)-1-(naphthalen-2-yl)-3-phenylprop-2-en-1-one (**5u**; 0.052 g, 0.201 mmol), $\text{NH}_3\text{-BH}_3$ (0.0031 g, 0.10 mmol) and catalyst **Mn-1** (0.002 g, 0.004 mmol). Purification by column chromatography on silica gel (petroleum ether/EtOAc: 30/1) yielded **6u** as brown solid. (0.046 g, 88%). $^1\text{H-NMR}$ (400 MHz, CDCl_3): δ = 8.41 (s, 1H, Ar-H), 8.01-7.98 (dd, J = 8.6, 1.8 Hz, 1H, Ar-H), 7.90 (d, J = 8.0 Hz, 1H, Ar-H), 7.83 (vt, J = 7.9 Hz, 2H, Ar-H), 7.57-7.48 (m, 2H, Ar-H), 7.30-7.24 (m, 4H, Ar-H), 7.20-7.15 (m, 1H, Ar-H), 3.40 (t, J = 7.8 Hz, 2H, CH_2), 3.09 (t, J = 7.8 Hz, 2H, CH_2). $^{13}\text{C}\{^1\text{H}\}\text{-NMR}$ (100 MHz, CDCl_3): δ = 199.3 (CO), 141.5 (C_q), 135.8 (C_q), 134.3 (C_q), 132.7 (C_q), 129.9 (CH), 129.7 (CH), 128.7 (2C, CH), 128.6 (2C, CH), 128.6 (CH), 128.6 (CH), 127.9 (CH), 126.9 (CH), 126.3 (CH), 124.0 (CH), 40.7 (CH_2), 30.5 (CH_2). HRMS (ESI): m/z Calcd for $\text{C}_{19}\text{H}_{16}\text{O} + \text{H}^+$ [$\text{M} + \text{H}$]⁺ 261.1274; Found 261.1270. The ^1H and ^{13}C spectra are consistent with those reported in the literature.



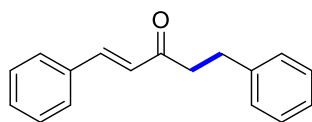
1-(naphthalen-1-yl)-3-phenylpropan-1-one (6v):⁵⁰ The representative procedure was followed, using (*E*)-1-(naphthalen-1-yl)-3-phenylprop-2-en-1-one (**5v**; 0.052 g, 0.201 mmol), $\text{NH}_3\text{-BH}_3$ (0.0031 g, 0.10 mmol) and catalyst **Mn-1** (0.002 g, 0.004 mmol). Purification by column chromatography on silica gel (petroleum ether/EtOAc: 30/1) yielded **6v** as white solid. (0.042 g, 80%). $^1\text{H-NMR}$ (400 MHz, CDCl_3): δ = 8.54 (d, J = 8.4 Hz, 1H, Ar-H), 7.96 (d, J = 8.3 Hz, 1H, Ar-H), 7.86 (d, J = 8.0 Hz, 1H, Ar-H), 7.81-7.80 (d, J = 7.1 Hz, 1H, Ar-H), 7.58-7.50 (m, 2H, Ar-H), 7.46 (t, J = 7.7 Hz, 1H, Ar-H), 7.31-7.18 (m, 5H, Ar-H), 3.38 (t, J = 7.6 Hz, 2H, CH_2), 3.13 (t, J = 7.6 Hz, 2H, CH_2). $^{13}\text{C}\{^1\text{H}\}\text{-NMR}$ (100 MHz, CDCl_3): δ = 203.7 (CO), 141.3 (C_q), 136.2 (C_q), 134.2 (C_q), 132.7 (CH), 130.3 (C_q), 128.7 (2C, CH), 128.6 (2C, CH), 128.6 (CH), 128.1 (CH), 127.6 (CH), 126.6 (CH), 126.3 (CH), 126.0 (CH), 124.5 (CH), 44.0 (CH_2), 30.8 (CH_2). HRMS (ESI): m/z Calcd for $\text{C}_{19}\text{H}_{16}\text{O} + \text{H}^+$ [$\text{M} + \text{H}$]⁺ 261.1274; Found 261.1270. The ^1H and ^{13}C spectra are consistent with those reported in the literature.



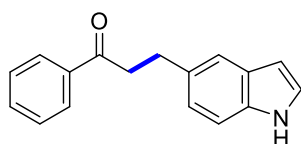
3-(naphthalen-2-yl)-1-phenylpropan-1-one (6w):²⁰ The representative procedure was followed, using (*E*)-3-(naphthalen-2-yl)-1-phenylprop-2-en-1-one (**5w**; 0.052 g, 0.201 mmol), $\text{NH}_3\text{-BH}_3$ (0.0031 g, 0.10 mmol) and catalyst **Mn-1** (0.002 g, 0.004 mmol). Purification by column chromatography on silica gel (petroleum ether/EtOAc: 30/1) yielded **6w** as white solid. (0.044 g, 85%). $^1\text{H-NMR}$ (400 MHz, CDCl_3): $\delta = 7.99$ (d, $J = 8.3$ Hz, 2H, Ar-H), 7.81 (t, $J = 7.8$ Hz, 3H, Ar-H), 7.70 (s, 1H, Ar-H), 7.56 (t, $J = 7.4$ Hz, 1H, Ar-H), 7.49-7.39 (m, 5H, Ar-H), 3.40 (t, $J = 7.7$ Hz, 2H, CH_2), 3.25 (t, $J = 7.7$ Hz, 2H, CH_2). $^{13}\text{C}\{^1\text{H}\}\text{-NMR}$ (100 MHz, CDCl_3): $\delta = 199.4$ (CO), 139.0 (C_q), 137.0 (C_q), 133.8 (C_q), 133.3 (CH), 132.3 (C_q), 128.8 (2C, CH), 128.3 (CH), 128.2 (2C, CH), 127.8 (CH), 127.6 (CH), 127.4 (CH), 126.7 (CH), 126.2 (CH), 125.5 (CH), 40.5 (CH_2), 30.4 (CH_2). HRMS (ESI): m/z Calcd for $\text{C}_{19}\text{H}_{16}\text{O} + \text{H}^+$ [M + H]⁺ 261.1274; Found 261.1270. The ^1H and ^{13}C spectra are consistent with those reported in the literature.



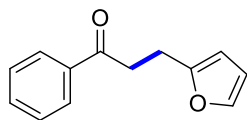
(*E*)-1,5-diphenylpent-4-en-1-one (6x):⁷ The representative procedure was followed, using (*2E,4E*)-1,5-diphenylpenta-2,4-dien-1-one (**5x**; 0.047 g, 0.20 mmol), $\text{NH}_3\text{-BH}_3$ (0.0031 g, 0.10 mmol) and catalyst **Mn-1** (0.002 g, 0.004 mmol). Purification by column chromatography on silica gel (petroleum ether/EtOAc: 30/1) yielded **6x** as brown solid. (0.037 g, 79%). $^1\text{H-NMR}$ (400 MHz, CDCl_3): $\delta = 8.0$ (d, $J = 7.8$ Hz, 2H, Ar-H), 7.58 (t, $J = 7.3$ Hz, 1H, Ar-H), 7.48 (t, $J = 7.6$ Hz, 2H, Ar-H), 7.36 (d, $J = 7.3$ Hz, 2H, Ar-H), 7.30 (t, $J = 7.6$ Hz, 2H, Ar-H), 7.21 (t, $J = 7.1$ Hz, 1H, Ar-H), 6.48 (d, $J = 15.8$ Hz, 1H, CH), 6.31 (dt, $J = 15.9, 6.8$ Hz, 1H, CH), 3.17 (t, $J = 7.4$ Hz, 2H, CH_2), 2.68 (q, $J = 6.9$ Hz, 2H, CH_2). $^{13}\text{C}\{^1\text{H}\}\text{-NMR}$ (100 MHz, CDCl_3): $\delta = 199.5$ (CO), 137.6 (C_q), 137.1 (C_q), 133.2 (CH), 130.9 (CH), 129.3 (CH), 128.8 (2C, CH), 128.7 (2C, CH), 128.2 (2C, CH), 127.2 (CH), 126.2 (2C, CH), 38.4 (CH_2), 27.7 (CH_2). HRMS (ESI): m/z Calcd for $\text{C}_{17}\text{H}_{16}\text{O} + \text{H}^+$ [M + H]⁺ 237.1274; Found 237.1271. The ^1H and ^{13}C spectra are consistent with those reported in the literature.



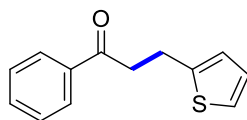
(E)-1,5-diphenylpent-1-en-3-one (6y):⁷ The representative procedure was followed, using (1*E*,4*E*)-1,5-diphenylpenta-1,4-dien-3-one (**5y**; 0.047 g, 0.20 mmol), NH₃-BH₃ (0.0031 g, 0.10 mmol) and catalyst **Mn-1** (0.002 g, 0.004 mmol). Purification by column chromatography on silica gel (petroleum ether/EtOAc: 40/1) yielded **6y** as pale white solid. (0.040 g, 85%). ¹H-NMR (400 MHz, CDCl₃): δ = 7.56-7.52 (m, 3H, Ar-H), 7.38 (br s, 3H, Ar-H), 7.29-7.16 (m, 5H, Ar-H), 6.73 (d, 1H, *J* = 16.1 Hz, Ar-H), 3.0 (s, 4H, CH₂). ¹³C{¹H}-NMR (100 MHz, CDCl₃): δ = 199.5 (CO), 142.9 (CH), 141.4 (C_q), 134.7 (C_q), 130.7 (CH), 129.1 (2C, CH), 128.7 (2C, CH), 128.6 (2C, CH), 128.4 (2C, CH), 126.3 (CH), 126.3 (CH), 42.6 (CH₂), 30.3 (CH₂). HRMS (ESI): *m/z* Calcd for C₁₇H₁₆O + H⁺ [M + H]⁺ 237.1274; Found 237.1273. The ¹H and ¹³C spectra are consistent with those reported in the literature.



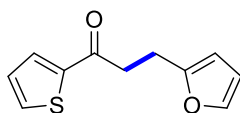
3-(1*H*-indol-5-yl)-1-phenylpropan-1-one (6z):⁷ The representative procedure was followed, using (*E*)-3-(1*H*-indol-5-yl)-1-phenylprop-2-en-1-one (**5z**; 0.049 g, 0.198 mmol), NH₃-BH₃ (0.0031 g, 0.10 mmol) and catalyst **Mn-1** (0.002 g, 0.004 mmol). Purification by column chromatography on silica gel (petroleum ether/EtOAc: 30/1) yielded **6z** as yellow oil. (0.026 g, 53%). ¹H-NMR (400 MHz, CDCl₃): δ = 8.19 (br s, 1H, NH), 7.99 (d, *J* = 7.4 Hz, 2H, Ar-H), 7.58-7.53 (m, 2H, Ar-H), 7.46 (t, *J* = 7.6 Hz, 2H, Ar-H), 7.33 (d, *J* = 8.4 Hz, 1H, Ar-H), 7.19 (t, *J* = 2.8 Hz, 1H, Ar-H), 7.11 (dd, *J* = 8.4, 1.6 Hz, 1H, Ar-H), 6.51 (t, *J* = 8.4 Hz, 1H, Ar-H), 3.36 (d, *J* = 7.8 Hz, 2H, CH₂), 3.18 (t, *J* = 7.7 Hz, 2H, CH₂). ¹³C{¹H}-NMR (100 MHz, CDCl₃): δ = 200.0 (CO), 137.1 (C_q), 134.7 (C_q), 133.1 (CH), 132.7 (C_q), 128.7 (2C, CH), 128.3 (C_q), 128.2 (2C, CH), 124.7 (CH), 123.0 (CH), 120.0 (CH), 111.2 (CH), 102.4 (CH), 41.7 (CH₂), 30.5 (CH₂). HRMS (ESI): *m/z* Calcd for C₁₇H₁₅NO + H⁺ [M + H]⁺ 250.1226; Found 250.1225.



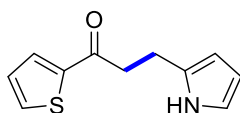
3-(Furan-2-yl)-1-phenylpropan-1-one (6A):²⁰ The representative procedure was followed, using (*E*)-3-(furan-2-yl)-1-phenylprop-2-en-1-one (**5A**; 0.040 g, 0.202 mmol), NH₃-BH₃ (0.0031 g, 0.10 mmol) and catalyst **Mn-1** (0.002 g, 0.004 mmol). Purification by column chromatography on silica gel (petroleum ether/EtOAc: 40/1) yielded **6A** as pale white solid. (0.024 g, 61%). ¹H-NMR (400 MHz, CDCl₃): δ = 7.98 (d, *J* = 7.8 Hz, 2H, Ar-H), 7.56 (tt, *J* = 7.4, 1.9 Hz, 1H, Ar-H), 7.46 (t, *J* = 7.6 Hz, 2H, Ar-H), 7.31 (d, *J* = 1.8 Hz, 1H, Ar-H), 6.29 (dd, *J* = 3.1, 1.9 Hz, 1H, Ar-H), 6.05 (dd, *J* = 3.1, 0.8 Hz, 1H, Ar-H), 3.34 (t, *J* = 7.4 Hz, 2H, CH₂), 3.10 (t, *J* = 7.5 Hz, 2H, CH₂). ¹³C{¹H}-NMR (100 MHz, CDCl₃): δ = 198.8 (CO), 154.9 (C_q), 141.2 (CH), 136.9 (C_q), 133.3 (CH), 128.8 (2C, CH), 128.2 (2C, CH), 110.4 (CH), 105.5 (CH), 37.1 (CH₂), 22.6 (CH₂). HRMS (ESI): *m/z* Calcd for C₁₃H₁₂O₂ + H⁺ [M + H]⁺ 201.0910; Found 201.0908. The ¹H and ¹³C spectra are consistent with those reported in the literature.



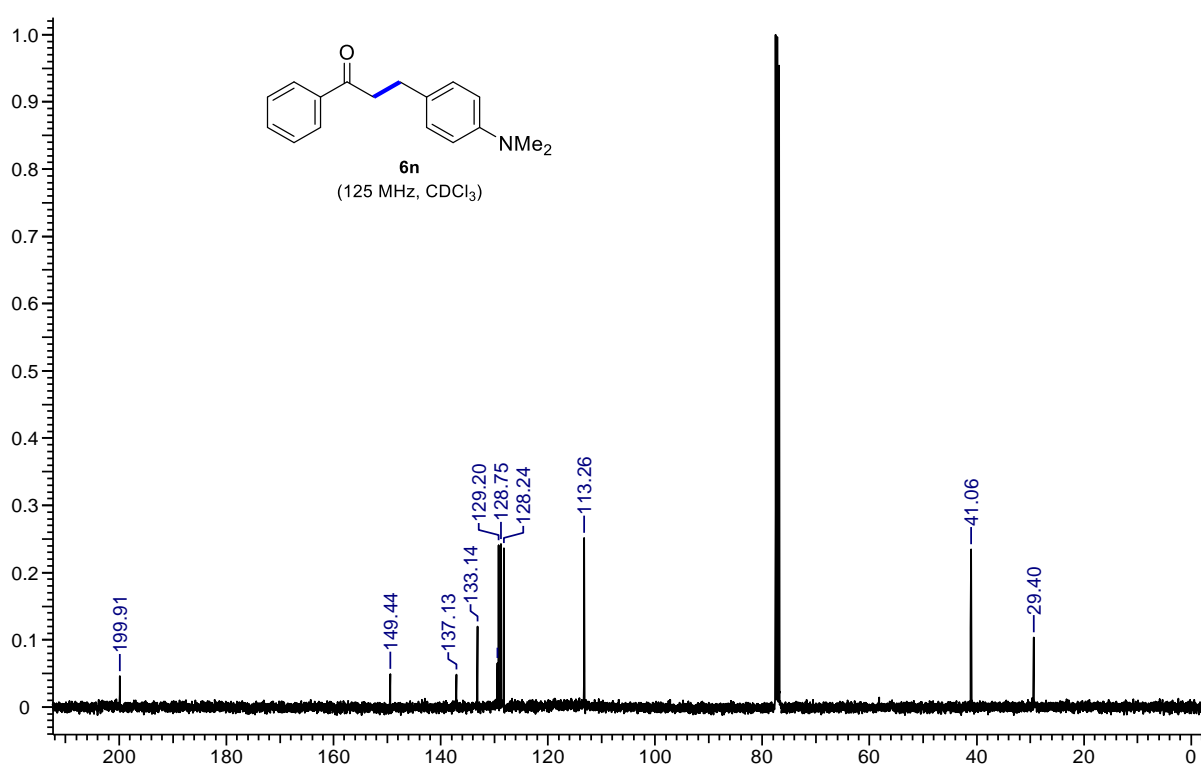
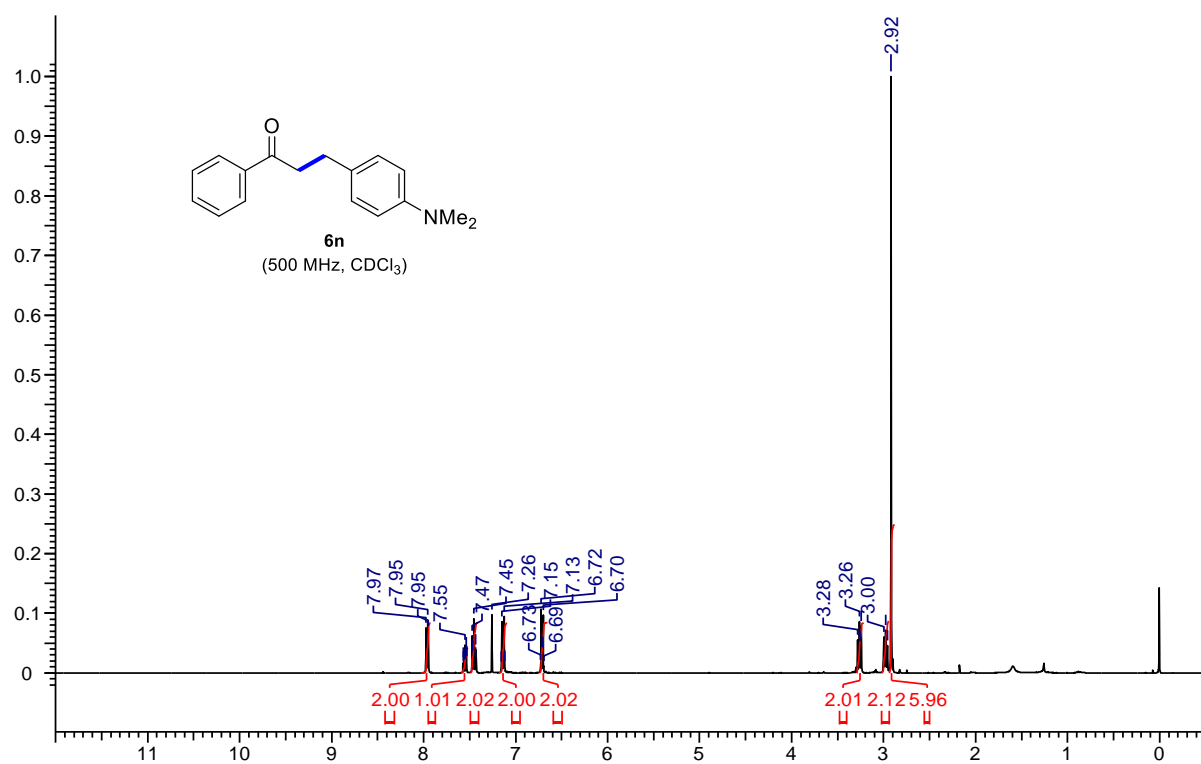
1-phenyl-3-(thiophen-2-yl)propan-1-one (6B):²⁰ The representative procedure was followed, using (*E*)-1-phenyl-3-(thiophen-2-yl)prop-2-en-1-one (**5B**; 0.043 g, 0.20 mmol), NH₃-BH₃ (0.0031 g, 0.10 mmol) and catalyst **Mn-1** (0.002 g, 0.004 mmol). Purification by column chromatography on silica gel (petroleum ether/EtOAc: 30/1) yielded **6B** as green oil. (0.030 g, 70%). ¹H-NMR (400 MHz, CDCl₃): δ = 7.97 (d, *J* = 7.8 Hz, 2H, Ar-H), 7.57 (t, *J* = 7.3 Hz, 1H, Ar-H), 7.47 (t, *J* = 7.6 Hz, 2H, Ar-H), 7.13 (d, *J* = 5.1 Hz, 1H, Ar-H), 6.94-6.92 (m, 1H, Ar-H), 6.87 (s, 1H, Ar-H), 3.37 (t, *J* = 6.8 Hz, 2H, CH₂), 3.30 (t, *J* = 6.6 Hz, 2H, CH₂). ¹³C{¹H}-NMR (100 MHz, CDCl₃): δ = 198.7 (CO), 144.1 (C_q), 136.9 (C_q), 133.3 (CH), 128.8 (2C, CH), 128.2 (2C, CH), 127.0 (CH), 124.8 (CH), 123.6 (CH), 40.7 (CH₂), 24.4 (CH₂). HRMS (ESI): *m/z* Calcd for C₁₃H₁₂S + H⁺ [M + H]⁺ 212.1070; Found 212.1068. The ¹H and ¹³C spectra are consistent with those reported in the literature.

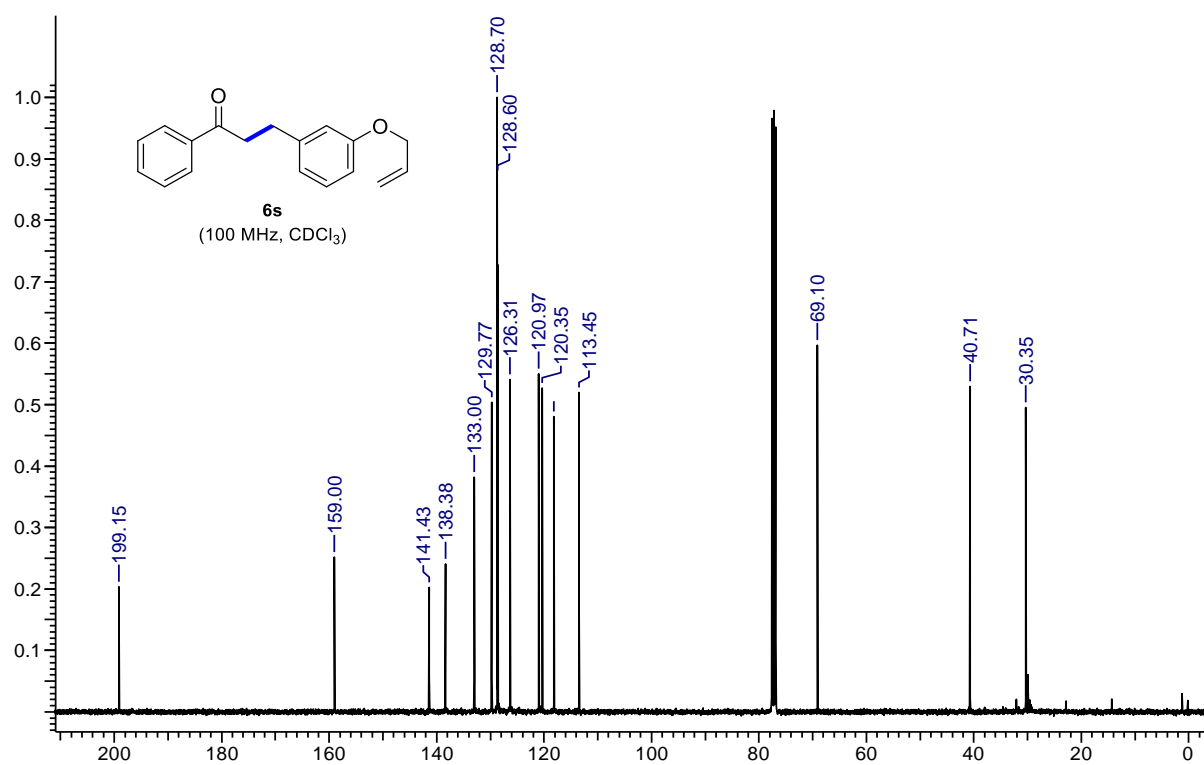
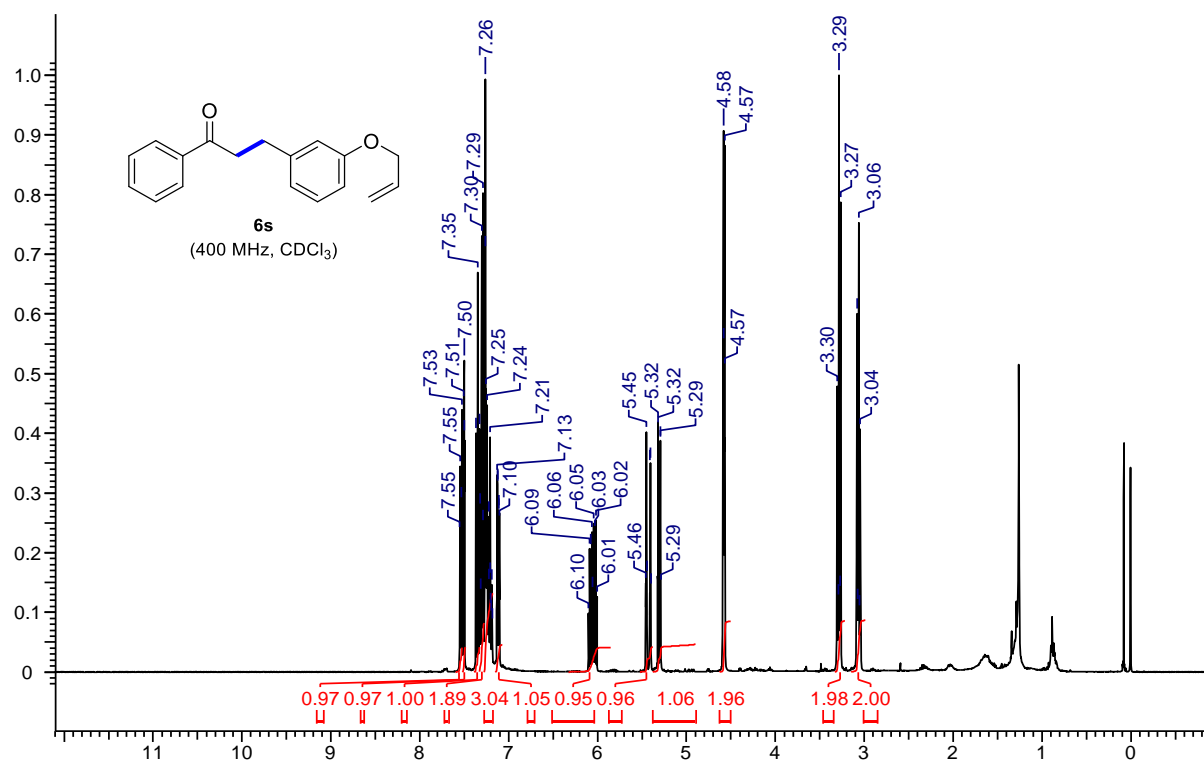


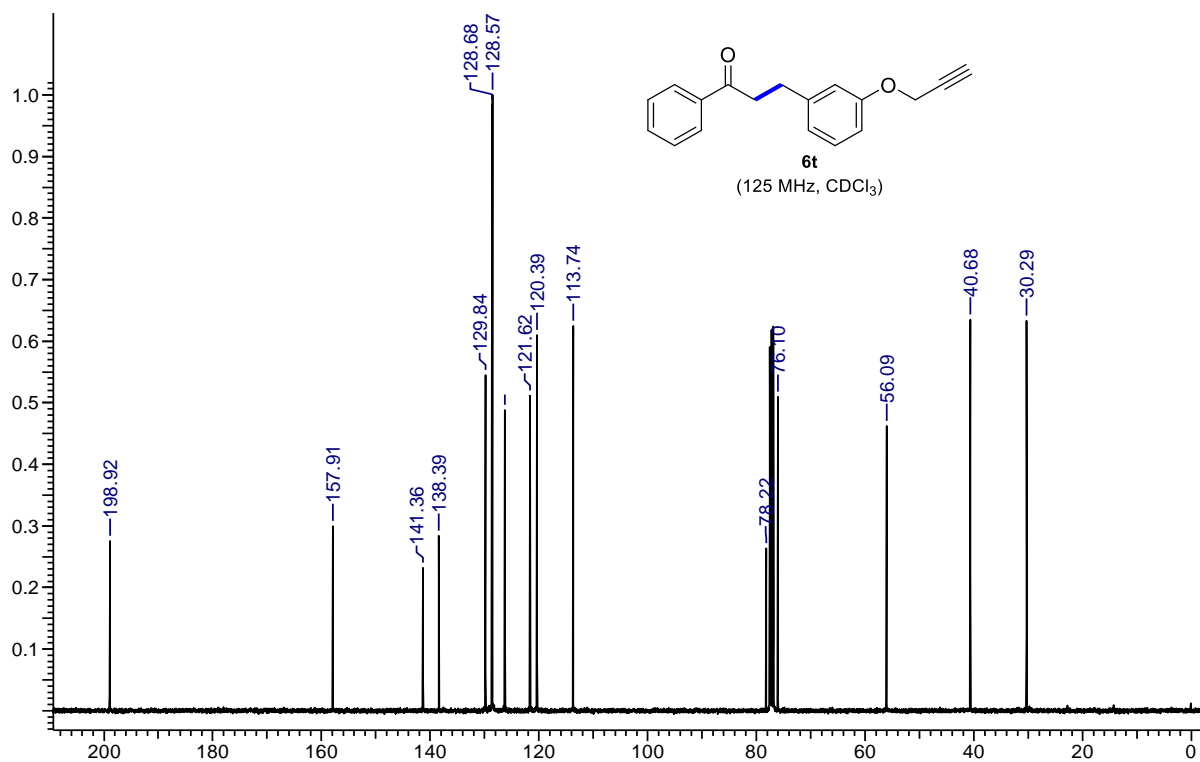
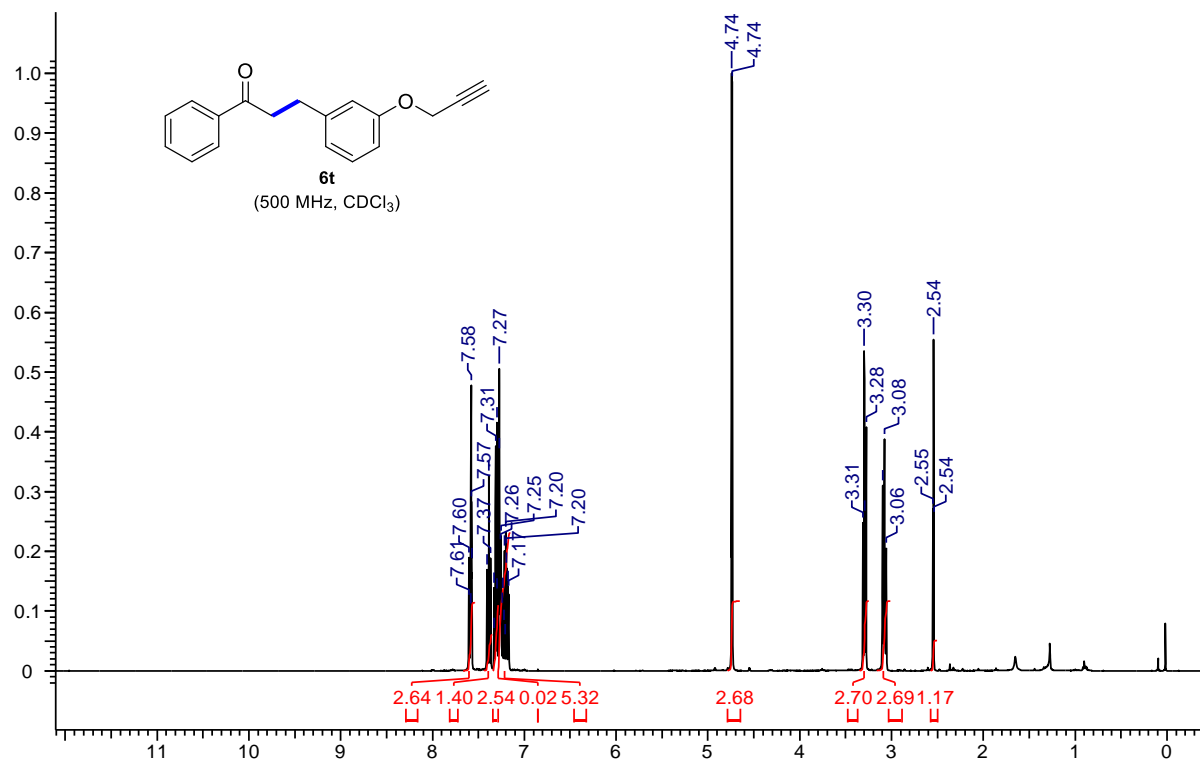
3-(furan-2-yl)-1-(thiophen-2-yl)propan-1-one (6C): The representative procedure was followed, using (*E*)-3-(furan-2-yl)-1-(thiophen-2-yl)prop-2-en-1-one (**5C**; 0.041 g, 0.201 mmol), $\text{NH}_3\text{-BH}_3$ (0.0031 g, 0.10 mmol) and catalyst **Mn-1** (0.002 g, 0.004 mmol). Purification by column chromatography on silica gel (petroleum ether/EtOAc: 30/1) yielded **6C** as yellow oil. (0.024 g, 58%). $^1\text{H-NMR}$ (400 MHz, CDCl_3): $\delta = 7.71$ (d, $J = 3.9$ Hz, 1H, Ar-H), 7.63 (d, $J = 5.0$ Hz, 1H, Ar-H), 7.30 (d, $J = 1.1$ Hz, 1H, Ar-H), 7.12 (dd, $J = 4.9, 3.9$ Hz, 1H, Ar-H), 6.27 (dd, $J = 2.9, 2.0$ Hz, 1H, Ar-H), 6.05 (d, $J = 3.0$ Hz, 1H, Ar-H), 3.26 (t, $J = 7.5$ Hz, 2H, CH_2), 3.08 (t, $J = 7.5$ Hz, 2H, CH_2). $^{13}\text{C}\{^1\text{H}\}\text{-NMR}$ (100 MHz, CDCl_3): $\delta = 191.7$ (CO), 154.6 (C_q), 144.1 (C_q), 141.3 (CH), 133.8 (CH), 132.0 (CH), 128.3 (CH), 110.4 (CH), 105.6 (CH), 37.7 (CH_2), 22.8 (CH_2). HRMS (ESI): m/z Calcd for $\text{C}_{11}\text{H}_{10}\text{O}_2\text{S} + \text{H}^+$ [$\text{M} + \text{H}$] $^+$ 207.0474; Found 207.0470.

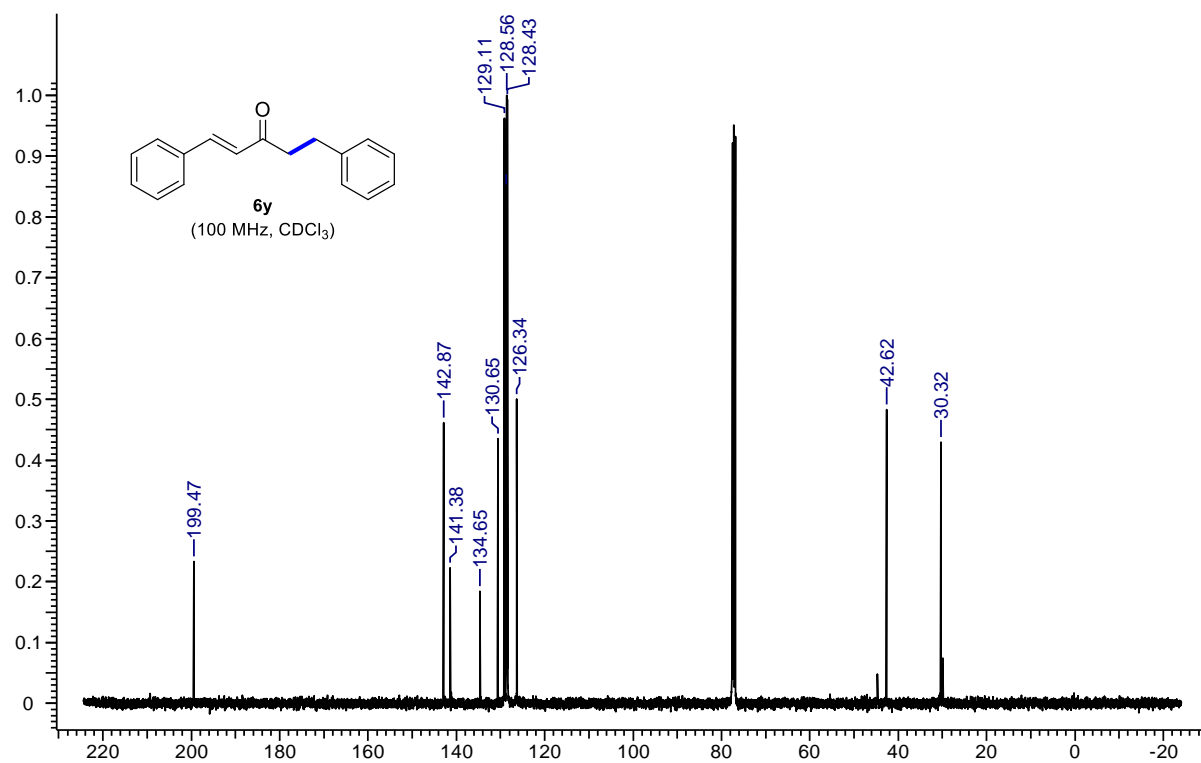
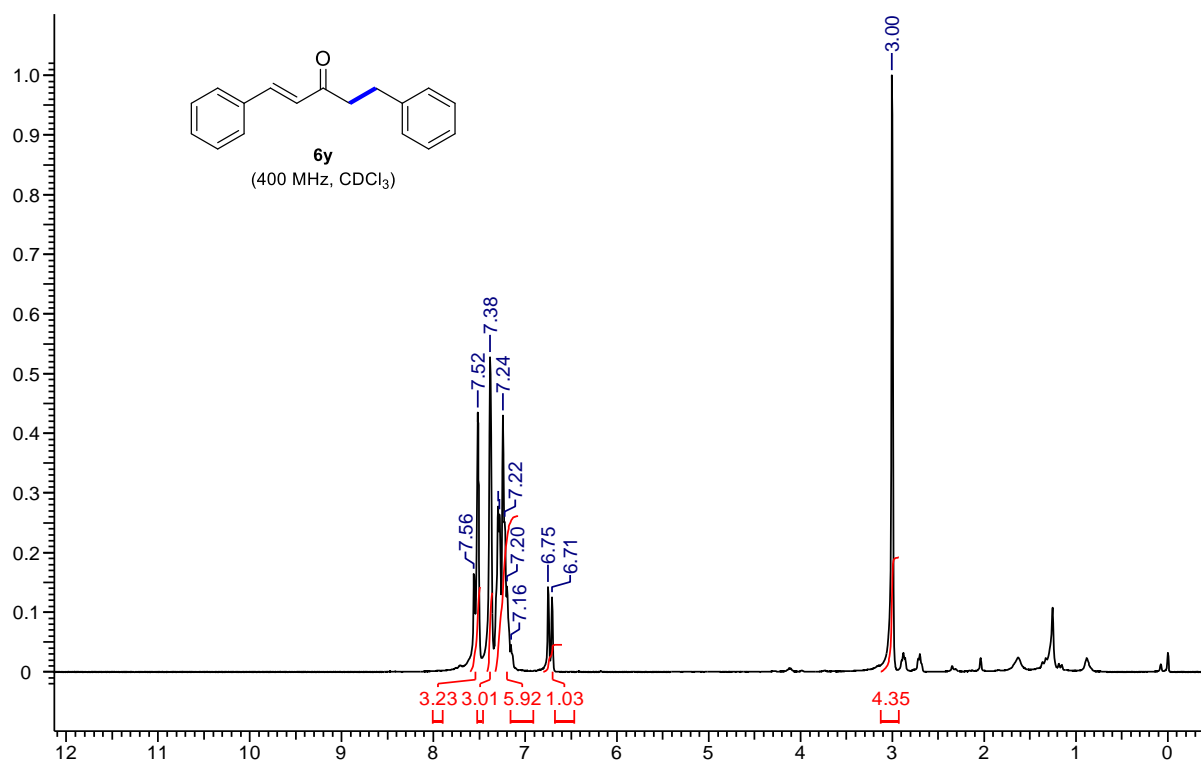


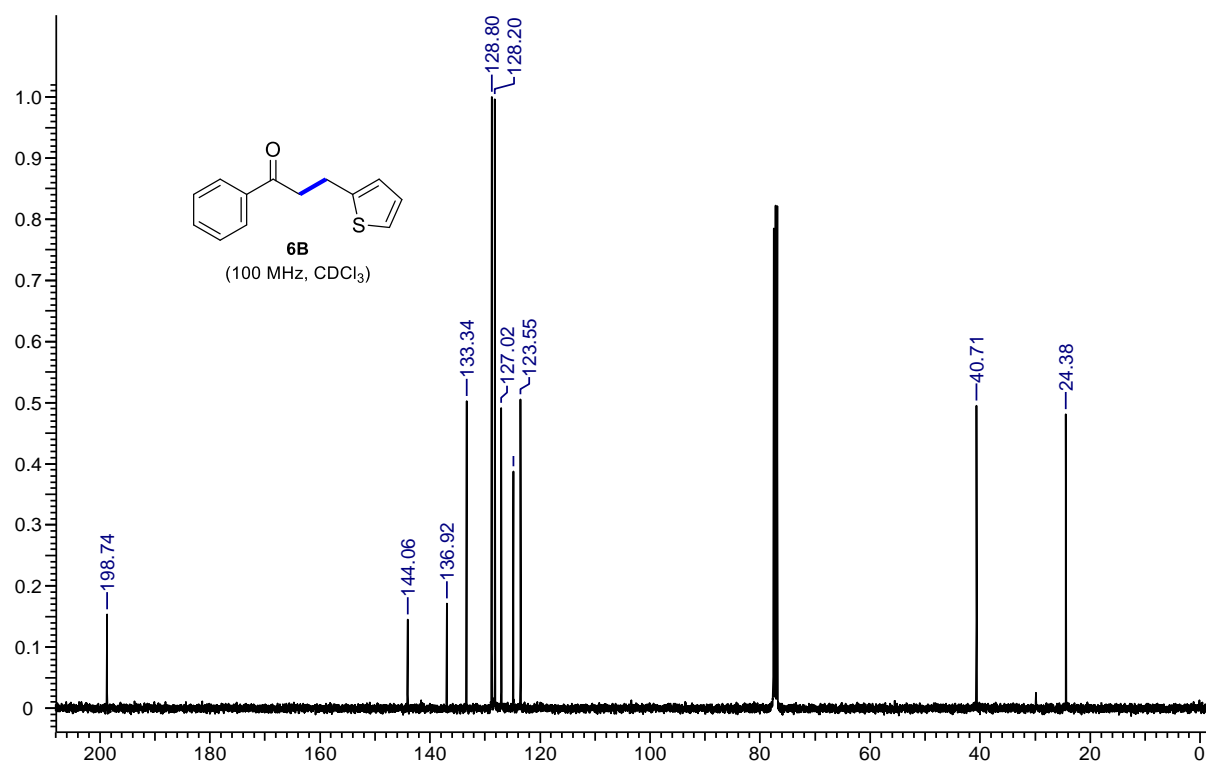
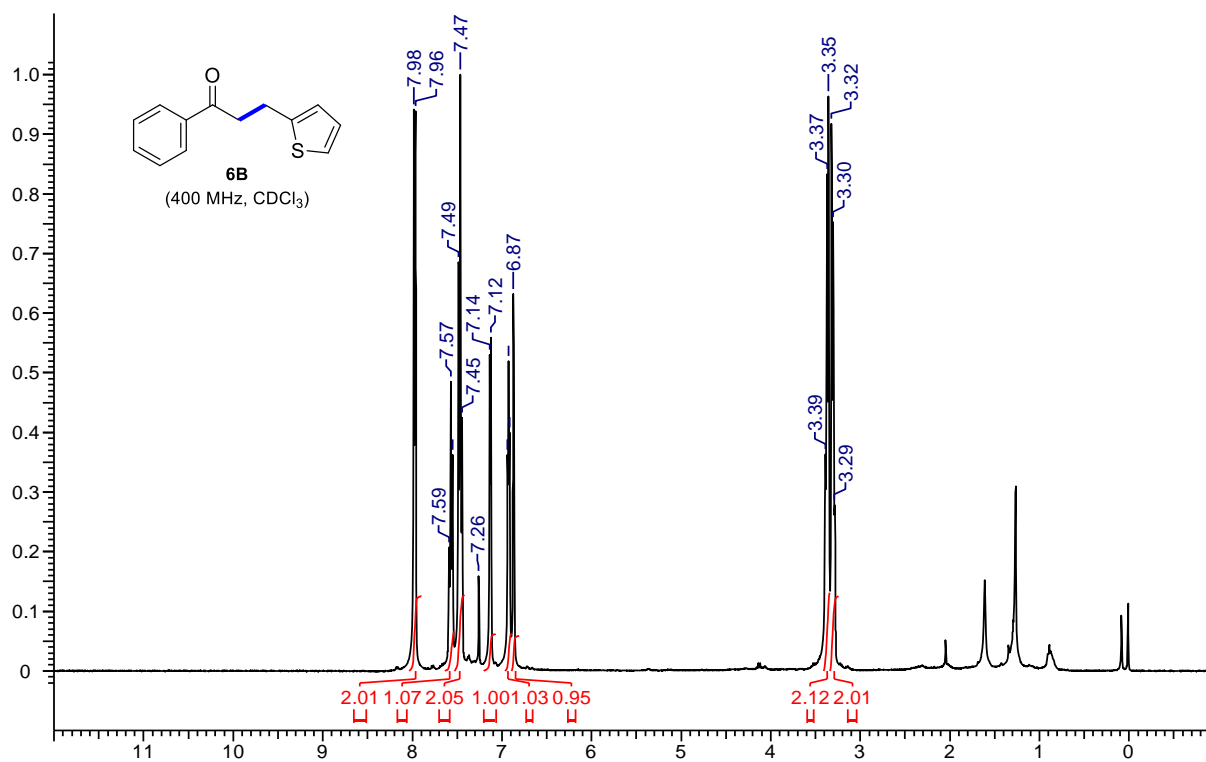
3-(1H-pyrrol-2-yl)-1-(thiophen-2-yl)propan-1-one (6D): The representative procedure was followed, using (*E*)-3-(1H-pyrrol-2-yl)-1-(thiophen-2-yl)prop-2-en-1-one (**5D**; 0.041 g, 0.202 mmol), $\text{NH}_3\text{-BH}_3$ (0.0031 g, 0.10 mmol) and catalyst **Mn-1** (0.002 g, 0.004 mmol). Purification by column chromatography on silica gel (petroleum ether/EtOAc: 30/1) yielded **6D** as yellow oil. (0.029 g, 71%). $^1\text{H-NMR}$ (400 MHz, CDCl_3): $\delta = 8.65$ (br s, 1H, NH), 7.72 (dd, $J = 3.8, 0.8$ Hz, 1H, Ar-H), 7.65 (dd, $J = 4.9, 0.8$ Hz, 1H, Ar-H), 7.13 (dd, $J = 4.8, 4.0$ Hz, 1H, Ar-H), 6.68-6.67 (m, 1H, Ar-H), 6.12-6.09 (m, 1H, Ar-H), 5.96 (s, 1H, Ar-H), 3.29 (t, $J = 6.4$ Hz, 2H, CH_2), 3.05 (t, $J = 6.4$ Hz, 2H, CH_2). $^{13}\text{C}\{^1\text{H}\}\text{-NMR}$ (100 MHz, CDCl_3): $\delta = 193.6$ (CO), 144.0 (C_q), 134.0 (CH), 132.3 (CH), 131.5 (C_q), 128.4 (CH), 178.0 (CH), 108.0 (CH), 105.6 (CH), 40.1 (CH_2), 21.8 (CH_2). HRMS (ESI): m/z Calcd for $\text{C}_{11}\text{H}_{11}\text{NOS} + \text{H}^+$ [$\text{M} + \text{H}$] $^+$ 206.0634; Found 206.0630.

5.4.7 ^1H and ^{13}C Spectra of Selected Saturated Ketone Compounds









5.5 REFERENCES

- (1) Cheenpracha, S.; Karalai, C.; Ponglimanont, C.; Subhadhirasakul, S.; Tewtrakul, S. *Bioorg. Med. Chem.* **2006**, *14*, 1710-1714.
- (2) Lowes, D. J.; Guiguemde, W. A.; Connelly, M. C.; Zhu, F.; Sigal, M. S.; Clark, J. A.; Lemoff, A. S.; Derisi, J. L.; Wilson, E. B.; Guy, R. K. *J. Med. Chem.* **2011**, *54*, 7477-7485.
- (3) Eglen, R. M.; Watson, N. *Pharmacol. Toxicol.* **1996**, *78*, 59-68.
- (4) Ding, B.; Zhang, Z.; Liu, Y.; Sugiya, M.; Imamoto, T.; Zhang, W. *Org. Lett.* **2013**, *15*, 3690-3693.
- (5) Ohkuma, T.; Ooka, H.; Ikariya, T.; Noyori, R. *J. Am. Chem. Soc.* **1995**, *117*, 10417-10418.
- (6) Sasson, Y.; Blum, J. *J. Org. Chem.* **1975**, *40*, 1887-1896.
- (7) Li, W.; Wu, X.-F. *Eur. J. Org. Chem.* **2015**, *2015*, 331-335.
- (8) Farrar-Tobar, R. A.; Wei, Z.; Jiao, H.; Hinze, S.; de Vries, J. G. *Chem. Eur. J.* **2018**, *24*, 2725-2734.
- (9) Puylaert, P.; van Heck, R.; Fan, Y.; Spannenberg, A.; Baumann, W.; Beller, M.; Medlock, J.; Bonrath, W.; Lefort, L.; Hinze, S.; de Vries, J. G. *Chem. Eur. J.* **2017**, *23*, 8473-8481.
- (10) Gu, Y.; Norton, J. R.; Salahi, F.; Lisnyak, V. G.; Zhou, Z.; Snyder, S. A. *J. Am. Chem. Soc.* **2021**, *143*, 9657-9663.
- (11) Wang, X.; Han, Z.; Wang, Z.; Ding, K. *Angew. Chem. Int. Ed.* **2012**, *51*, 936-940.
- (12) Fleischer, S.; Zhou, S.; Junge, K.; Beller, M. *Angew. Chem. Int. Ed.* **2013**, *52*, 5120-5124.
- (13) Gorgas, N.; Stöger, B.; Veiros, L. F.; Kirchner, K. *ACS Catal.* **2016**, *6*, 2664-2672.
- (14) Mazza, S.; Scopelliti, R.; Hu, X. *Organometallics* **2015**, *34*, 1538-1545.
- (15) Wienhöfer, G.; Westerhaus, F. A.; Junge, K.; Ludwig, R.; Beller, M. *Chem. Eur. J.* **2013**, *19*, 7701-7707.
- (16) Lator, A.; Gaillard, S.; Poater, A.; Renaud, J.-L. *Chem. Eur. J.* **2018**, *24*, 5770-5774.
- (17) Wei, Z.; Wang, Y.; Li, Y.; Ferraccioli, R.; Liu, Q. *Organometallics* **2020**, *39*, 3082-3087.
- (18) Beltran, F.; Bergamaschi, E.; Funes-Ardoiz, I.; Teskey, C. J. *Angew. Chem. Int. Ed.* **2020**, *59*, 21176-21182.

-
- (19) Jiang, B.-L.; Ma, S.-S.; Wang, M.-L.; Liu, D.-S.; Xu, B.-H.; Zhang, S.-J. *ChemCatChem* **2019**, *11*, 1701-1706.
- (20) Song, T.; Ma, Z.; Yang, Y. *ChemCatChem* **2019**, *11*, 1313-1319.
- (21) Li, X.; Wu, X.; Tang, L.; Xie, F.; Zhang, W. *Chem. Asian J.* **2019**, *14*, 3835-3839.
- (22) Zhang, G.; Hanson, S. K. *Chem. Commun.* **2013**, *49*, 10151-10153.
- (23) Zhang, G.; Scott, B. L.; Hanson, S. K. *Angew. Chem. Int. Ed.* **2012**, *51*, 12102-12106.
- (24) Rösler, S.; Obenauf, J.; Kempe, R. *J. Am. Chem. Soc.* **2015**, *137*, 7998-8001.
- (25) Huo, C.-F.; Li, Y.-W.; Beller, M.; Jiao, H. *Organometallics* **2004**, *23*, 2168-2178.
- (26) Alonso, F.; Osante, I.; Yus, M. *ChemInform* **2007**, *38*.
- (27) Shimizu, H.; Nagano, T.; Sayo, N.; Saito, T.; Ohshima, T.; Mashima, K. *Synlett* **2009**, *2009*, 3143-3146.
- (28) Mahoney, W. S.; Stryker, J. M. *J. Am. Chem. Soc.* **1989**, *111*, 8818-8823.
- (29) Chen, J.-X.; Daeuble, J. F.; Brestensky, D. M.; Stryker, J. M. *Tetrahed.* **2000**, *56*, 2153-2166.
- (30) Mendes-Burak, J.; Ghaffari, B.; Copéret, C. *Chem. Commun.* **2019**, *55*, 179-181.
- (31) Bruneau-Voisine, A.; Wang, D.; Dorcet, V.; Roisnel, T.; Darcel, C.; Sortais, J.-B. *Org. Lett.* **2017**, *19*, 3656-3659.
- (32) Perez, M.; Elangovan, S.; Spannenberg, A.; Junge, K.; Beller, M. *ChemSusChem* **2017**, *10*, 83-86.
- (33) Martínez-Ferraté, O.; Werlé, C.; Franciò, G.; Leitner, W. *ChemCatChem* **2018**, *10*, 4514-4518.
- (34) Demmans, K. Z.; Olson, M. E.; Morris, R. H. *Organometallics* **2018**, *37*, 4608-4618.
- (35) Schneekönig, J.; Junge, K.; Beller, M. *Synlett* **2019**, *30*, 503-507.
- (36) Zhang, C.; Hu, B.; Chen, D.; Xia, H. *Organometallics* **2019**, *38*, 3218-3226.
- (37) van Putten, R.; Benschop, J.; de Munck, V. J.; Weber, M.; Müller, C.; Filonenko, G. A.; Pidko, E. A. *ChemCatChem* **2019**, *11*, 5232-5235.
- (38) Azouzi, K.; Bruneau-Voisine, A.; Vendier, L.; Sortais, J.-B.; Bastin, S. *Catal. Commun.* **2020**, *142*, 106040.
- (39) Wei, D.; Bruneau-Voisine, A.; Chauvin, T.; Dorcet, V.; Roisnel, T.; Valyaev, D. A.; Lugan, N.; Sortais, J.-B. *Adv. Synth. Catal.* **2018**, *360*, 676-681.
- (40) Vielhaber, T.; Topf, C. *Appl. Catal. A: General* **2021**, *623*, 118280.
- (41) Weber, S.; Brünig, J.; Veiros, L. F.; Kirchner, K. *Organometallics* **2021**, *40*, 1388-1394.
-

-
- (42) Vigneswaran, V.; MacMillan, S. N.; Lacy, D. C. *Organometallics* **2019**, *38*, 4387-4391.
- (43) Li, H.; Gonçalves, T. P.; Lupp, D.; Huang, K.-W. *ACS Catal.* **2019**, *9*, 1619-1629.
- (44) Schlichter, P.; Werlé, C. *Synthesis* **2021**, *54*, 517-534.
- (45) Gholap, S. S.; Dakhil, A. A.; Chakraborty, P.; Li, H.; Dutta, I.; Das, P. K.; Huang, K.-W. *Chem. Commun.* **2021**, *57*, 11815-11818.
- (46) Yang, X.; Fox, T.; Berke, H. *Tetrahedron* **2011**, *67*, 7121-7127.
- (47) Bennedsen, N. R.; Mortensen, R. L.; Kramer, S.; Kegnæs, S. *J. Catal.* **2019**, *371*, 153-160.
- (48) Nallagangula, M.; Sujatha, C.; Bhat, V. T.; Namitharan, K. *Chem. Commun.* **2019**, *55*, 8490-8493.
- (49) Chen, S.-j.; Lu, G.-p.; Cai, C. *RSC Adv.* **2015**, *5*, 13208-13211.
- (50) Lan, X.-B.; Ye, Z.; Huang, M.; Liu, J.; Liu, Y.; Ke, Z. *Org. Lett.* **2019**, *21*, 8065-8070.
- (51) Zhu, Y.; Cai, C.; Lu, G. *Helvet. Chim. Acta* **2014**, *97*, 1666-1671.
- (52) Genç, S.; Gülcemal, S.; Günnaz, S.; Çetinkaya, B.; Gülcemal, D. *Org. Lett.* **2021**, *23*, 5229-5234.
- (53) Cao, X.-N.; Wan, X.-M.; Yang, F.-L.; Li, K.; Hao, X.-Q.; Shao, T.; Zhu, X.; Song, M.-P. *J. Org. Chem.* **2018**, *83*, 3657-3668.
- (54) Ding, Z.-C.; Li, C.-Y.; Chen, J.-J.; Zeng, J.-H.; Tang, H.-T.; Ding, Y.-J.; Zhan, Z.-P. *Adv. Synth. Catal.* **2017**, *359*, 2280-2287.
- (55) Luo, N.; Zhong, Y.; Wen, H.; Shui, H.; Luo, R. *Eur. J. Org. Chem.* **2021**, *2021*, 1355-1364.
- (56) Gong, D.; Zhang, X.; Huang, K.-W. *Dalton Trans.* **2016**, *45*, 19399-19407.

Summary and Outlook

Summary and Outlook

Summary

In this thesis work, we have made research attempts toward developing user-friendly and mild reaction protocols for the hydrogenative transformation of unsaturated functionalities. In the process, we could successfully synthesize nitrogen and phosphorus-based ligand systems to make manganese and cobalt-based pincer and non-pincer complexes. We have thoroughly characterized the newly made 3d metal-based complexes with different analytical techniques and have used them in the room temperature operated hydrogenation of alkynes, nitriles and chalcones. Furthermore, with the developed catalytic systems, we could achieve the chemo- and regio-selectivity in the aforementioned hydrogenation reaction. The chapter 1 of the thesis includes a collective summary of the recent progress made for the hydrogenation of alkynes, chalcones, and nitriles using 3d-transition metals. The catalytic systems made of manganese, iron, cobalt, nickel, and copper metal are highlighted in this chapter.

In chapter 2, we demonstrated the synthesis of the hemilabile and phosphine-free quinolinyl-based (*NNN*)-type pincer and non-pincer cobalt complexes for the chemo- and stereo-selective transfer hydrogenation of alkynes. The well-defined anionic non-pincer cobalt complexes $\kappa^2\text{-}(\text{QNN})\text{CoX}_2(\text{N}^{\text{C(O)HNEt}_2})$ ($\text{X} = \text{Cl}, \text{Br}$) efficiently catalyzed the semi-hydrogenation of diverse alkynes to deliver highly chemoselective and stereodivergent (*Z*)-alkenes at room temperature. This hydrogenation exhibited broad substrate scope with the tolerance of sensitive functional groups, such as $-\text{Cl}$, $-\text{Br}$, $-\text{I}$, $-\text{OH}$, $-\text{NH}_2$, $-\text{COOMe}$, and pyridinyl, employing a stable and friendly ammonia borane as the hydrogen source. The mechanistic studies put forward the crucial role of amide *N-H* of ligand backbone in room temperature activation of a non-pincer cobalt catalyst.

The chapter 3 of the thesis deals with a user-friendly and mild transfer hydrogenation protocol for synthesizing secondary amines from nitriles. This method avoids the synthesis of highly susceptible phosphine ligand systems as it is feasible with easy-to synthesize catalyst, i.e., $(\text{xantphos})\text{CoCl}_2$, which is made up of commercially available ‘xantphos’ ligand along with simple CoCl_2 . The optimized reaction condition is mild as it operates at room temperature using $\text{NH}_3\text{-BH}_3$ as a hydrogen source with vast functional group tolerance. In addition, the unsymmetrical secondary amines were afforded when the external amines were used for coupling. Also, the later mentioned synthesis requires commercially cheaper dimethylammonium-borane as hydrogen sacrificial.

The metal-catalyzed synthesis of secondary amines from nitriles is mainly explored by the transfer hydrogenation method. In this direction, we made efforts to optimize the protocol for the catalytic hydrogenation of nitriles to secondary amines/imines using molecular hydrogen (H_2). Thus, chapter 4 describes cobalt catalyzed hydrogenation of nitriles to afford secondary amines. This method worked with various substituted nitriles and resulted in moderate to good yields of the secondary amines. Albeit, an irregular formation of Co-particles limits the yields of the desired secondary amine products.

The final chapter of the thesis discusses the synthesis and characterization of phosphinamide-based $^{tBu}P^{Pyr}N^3N^{Pyz}-Mn(I)$ and $-Mn(II)$ complexes for the selective transfer hydrogenation of $C=C$ of α,β -unsaturated ketones. The optimization of the reaction condition revealed that the Mn(I) complex $^{tBu}P^{Pyr}N^3N^{Pyz}-Mn(CO)_3Br$ is an active catalyst that selectively hydrogenates $C=C$ of α,β -unsaturated ketones using a half equivalent of ammonia-borane (NH_3-BH_3). This protocol is very mild as it was tolerated by a variety of functional groups as well as heterocycles. In addition, the selectivity has remained towards disubstituted aromatic α,β -unsaturated ketones. The mechanistic investigation revealed that the amine N-H is essential for the desired hydrogenation and involved in metal-ligand cooperation.

Outlook

In the last two decades, considerable advancement has been observed in the transition metal-catalyzed hydrogenation reaction. Mainly, the first row 3d metal catalysts were given significant attention for the hydrogenation reaction. Although considerable progress has been made, many developed methods use extreme conditions, such as high temperature, sensitive additives, longer reaction time, etc., which limits the applicability of such processes. Thus, more environmentally benign and sustainable, and mild approaches are necessary. Moreover, base metal-catalyzed asymmetric hydrogenation to afford chiral reduced products remains a long-standing task in synthetic chemistry. Therefore, designing and developing suitable methodologies for enantioselective hydrogenation is imperative.

ABSTRACT

Name of the Student: Mr. Sharma Dipesh Mamraj

Registration No.: 10CC17J26006

Faculty of Study: Chemical Science

Year of Submission: 2022

AcSIR Academic Center/CSIR Lab:

Name of the Supervisor: Dr. Benudhar Punji

CSIR-National Chemical Laboratory, Pune

Title of the thesis: Synthesis and Implication of 3d Transition Metal Catalysts for the Hydrogenative Transformations of Alkynes, Chalcones and Nitriles

This thesis contains five different chapters. The first chapter deals with the compilation of literature survey on 3d transition metal catalyzed selective hydrogenative transformation of unsaturated bonds, i.e., alkynes, nitriles, and α,β -unsaturated ketones. In particular, advances made with the late 3d transition metals such as manganese, iron, cobalt, nickel, and copper catalysts in selective hydrogenation reactions are discussed; those proceed either *via* the transfer hydrogenation process or by using molecular hydrogen. Chapter-2 describes the synthesis of unified (NNN)-pincer and non-pincer anionic cobalt complexes and their application in selective room temperature transfer hydrogenation of internal aromatic alkynes to respective (*Z*)-alkenes. A preliminary mechanistic investigation has been performed, and a plausible reaction proposal is drawn. Chapter-3 presents the selective transfer hydrogenation of nitriles to secondary amines using a friendly (Xantphos)CoCl₂ catalyst. The ammonia-borane/dimethylammonia borane in the form of hydrogen source are been used to get the symmetrical/unsymmetrical secondary amines. Similarly, selective synthesis of secondary imines and symmetrical secondary amines from nitriles using cobalt(II) catalysts and molecular hydrogen (H₂) is illustrated in Chapter-4. Chapter-5 contains the synthesis and characterization of PN³N-based pincer Mn(I) and Mn(II) complexes for the selective transfer hydrogenation of C=C on chalcones using ammonia-borane as a hydrogen source. Lastly, the summary of the thesis work, including the future direction related to the field, is elaborated.

List of Publications Emanating from the Thesis Work

1. **D. M. Sharma**, C. Gouda, R. G. Gonnade and B. Punji, “Room Temperature Z-Selective Hydrogenation of Alkynes by Hemilabile and Non-innocent (NNN) Co(II) Catalyst” *Catal. Sci. Technol.*, **2022**, *12*, 1843-1849
2. **D. M. Sharma**, A. B. Shabade and B. Punji, “Synthesis of PN³N Based Mn(I) and Mn(II) Pincer Complexes and Application in Selective Transfer Hydrogenation of Chalcones”. (*Manuscript Under Preparation*)
3. **D. M. Sharma** and B. Punji, “Co(II)-Catalyzed Hydrogenation of Nitriles to Secondary Amines/Imines”. (*Manuscript Under Preparation*)

List of Publications Non-Emanating from the Thesis Work

1. **D. M. Sharma** and B. Punji, “Nickel-Catalysed Benzylic C–H Functionalization”, Book Chapter for "*Handbook of CH-Functionalization (CHF)*" **2021**
2. **D. M. Sharma** and B. Punji, “3 d Transition Metal-Catalyzed Hydrogenation of Nitriles and Alkynes” *Chem. Asian J.*, **2020**, *15*, 690–708 (Review article)
3. **D. M. Sharma** and B. Punji, “Selective Synthesis of Secondary Amines from Nitriles by a User-Friendly Cobalt Catalyst” *Adv. Synth. Catal.*, **2019**, *361*, 3930-3936
4. V. Soni, **D. M. Sharma** and B. Punji, “Nickel-Catalyzed Regioselective C (2)– H Difluoroalkylation of Indoles with Difluoroalkyl Bromides” *Chem. Asian J.*, **2018**, *13*, 2516–2521
5. H. Pandiri, **D. M. Sharma**, R. G. Gonnade and B. Punji, Synthesis and Characterization of Six-Membered Pincer Nickelacycles and Application in Alkylation of Benzothiazole” *J. Chem. Sci.*, **2017**, *129*, 1161–1169

List of Oral/Poster Presented with Details

1. National Science Day **Poster presentation** at CSIR-National Chemical Laboratory, Pune (February 26-27, **2019**):

Title: Cobalt-Catalyzed Reductive Amination of Aromatic Nitriles to Secondary Amines

Abstract: Secondary amines constitute one of the privileged compounds in organic synthesis that are often found in many medicinally important molecules, such as fluoxetine and amlodipine. Many methods are known for the synthesis of secondary amines from nitriles employing precious metals and defined catalysts. However, the multistep synthesis of ligands and catalysts, and harsh reaction conditions of the reaction limits the developed methods. Herein, we have developed a very simple and inexpensive $\text{CoCl}_2/\text{Xantphos}$ catalyst system for selective reduction of nitriles to secondary amines. Thus, the cobalt catalyst selectively reduces the aromatic nitriles to symmetrical secondary amines using ammonia borane ($\text{NH}_3\text{-BH}_3$) as a hydrogen source, whereas the use of external amine and dimethylammonia borane ($\text{Me}_2\text{NH-BH}_3$) afforded unsymmetrical secondary amines. Detailed optimization and scope of the reaction will be discussed in the presentation.

2. 3rd NCL-RF Annual Students' Conference - 2021 **Oral presentation** at CSIR - National Chemical Laboratory (November 29-30, **2021**):

Title: Room Temperature (*Z*)-Selective Hydrogenation of Alkyne by Hemilabile and Non-innocent NNN-Co(II) Catalyst

Abstract: Semi-hydrogenation of alkynes to stereoselective alkenes is a crucial transformation in organic synthesis. The use of different 3d-transition metals with bi/tridentate ligands explored widely for such (transfer) semi-hydrogenation reaction. Herein, we developed the hemilabile and phosphine-free quinolinylnyl-based NNN-type pincer and non-pincer cobalt complexes for the room temperature catalytic transfer semi-hydrogenation of alkynes to (*Z*)-alkenes. Treatment of quinolinylnyl-amine ligand, $[\text{C}_9\text{H}_6\text{N}(\text{NH})\text{CH}_2\text{CH}_2\text{NEt}_2]$ ($^{\text{Q}}\text{NNN}^{\text{CH}_2\text{NEt}_2}$)-H with CoX_2 afforded the pincer complexes $\kappa^3\text{-}(^{\text{Q}}\text{NNN}^{\text{CH}_2\text{NEt}_2})\text{CoX}_2$ ($\text{X} = \text{Cl}, \text{Br}$), whereas, the quinolinylnyl-amide ligand, $[\text{C}_9\text{H}_6\text{N}(\text{NH})\text{C}(\text{O})\text{CH}_2\text{NEt}_2]$ ($^{\text{Q}}\text{NNN}^{\text{C}(\text{O})\text{NEt}_2}$)-H gave chelate anionic complexes $\kappa^2\text{-}(^{\text{Q}}\text{NN})\text{CoX}_2(\text{NC}(\text{O})\text{HNEt}_2)$ ($\text{X} = \text{Cl}, \text{Br}$).

The well-defined anionic non-pincer cobalt Poster, Oral Presentations and Conferences complexes efficiently catalyzed the semi-hydrogenation of diverse alkynes to deliver highly chemoselective and stereo-divergent (*Z*)-alkenes at room temperature. This hydrogenation exhibited broad substrate scope with the tolerance of sensitive functional groups employing a stable and user-friendly $\text{NH}_3\text{-BH}_3$. The mechanistic investigation reveals the crucial role of acidic amido N–H which assist room temperature activation of non-pincer $\kappa^2\text{-}(\text{QNN})\text{CoX}_2(\text{NC}(\text{O})\text{HNEt}_2)$ catalyst. The abstraction of amidic N–H by nitrogen side-arm results in its deco-ordination from cobalt center by providing an active site for alkyne coordination.

Cite this: *Catal. Sci. Technol.*, 2022, 12, 1843

Room temperature Z-selective hydrogenation of alkynes by hemilabile and non-innocent (NNN)Co(II) catalysts†

Dipesh M. Sharma,^{ab} Chandrakant Gouda,^a
Rajesh G. Gonnade ^{bc} and Benudhar Punji ^{*ab}

Hemilabile and phosphine-free quinolonyl-based NNN-type pincer and non-pincer cobalt complexes were developed for the room temperature catalytic transfer semi-hydrogenation of alkynes to Z-alkenes. Treatment of the quinolonyl-amine ligand, [C₉H₆N(NH)CH₂CH₂NEt₂] (O⁻NNN^{CH₂NEt₂})-H with CoX₂ afforded the pincer complexes κ³-(O⁻NNN^{CH₂NEt₂})CoX₂ (X = Cl, Br), whereas, the quinolonyl-amide ligand, [C₉H₆N(NH)C(O)CH₂NEt₂] (O⁻NNN^{C(O)NEt₂})-H gave chelate anionic complexes κ²-(O⁻NN)CoX₂(N^{C(O)HNEt₂}) (X = Cl, Br). The well-defined anionic non-pincer cobalt complexes efficiently catalyzed the semi-hydrogenation of diverse alkynes to deliver highly chemoselective and stereodivergent Z-alkenes at room temperature. This hydrogenation exhibited broad substrate scope with the tolerance of sensitive functional groups, such as -Cl, -Br, -I, -OH, -NH₂, -COOMe, and pyridinyl, employing a stable and user-friendly ammonia borane hydrogen source.

Received 6th January 2022,
Accepted 7th February 2022

DOI: 10.1039/d2cy00027j

rsc.li/catalysis

Introduction

Stereo-defined alkenes represent a dominant functionality in various synthetic transformations and polyfunctionalized bioactive compounds.¹ Such stereoselective alkenes play a pivotal role in governing the peculiar characteristics of certain drugs and biomolecules, like in combretastatin A4,² cruentaren B,³ amphotericin,⁴ and lepidoptera pheromones (Fig. 1).⁵ Among the various routes of alkene synthesis,⁶ the selective hydrogenation of alkynes is considered the finest approach to achieve the olefins of interest.⁷ However, controlling the stereoselectivity of the resulting olefin and over-hydrogenation to alkane are the major concerns in regards to alkyne hydrogenation. Overcoming these challenges, in the last few decades, various noble metal catalysts, based on ruthenium,⁸ palladium,⁹ and iridium,¹⁰ are exploited for the catalytic hydrogenation of alkynes to get the desired reduced olefins with specific stereochemistry.¹¹

Particularly, in recent years, the high natural abundance and less bio-toxic 3d late transition metal complexes of Mn,¹² Fe,¹³ Ni,¹⁴ and Cu (ref. 15) have been substantially investigated as catalysts for the hydrogenation of alkynes with promising activity and selectivity.¹⁶

Cobalt, being one of the earth-abundant transition metals with biological significance, has substantially been explored for the hydrogenation of various unsaturated functional groups,¹⁷ including nitriles.¹⁸ In particular, the cobalt-catalyzed semi-hydrogenation of internal alkynes to (*E*) or (*Z*)-selective alkenes using molecular hydrogen is independently demonstrated by Fout, Zhang and Dong (Fig. 2).¹⁹ Considering the ease of transfer hydrogenation without requiring a special experimental setup, Luo and Liu demonstrated (PNP)Co(II) complexes for the semi-hydrogenation of alkynes to *Z*- or *E*-alkenes using NH₃-BH₃

^a Organometallic Synthesis and Catalysis Lab, Organic Chemistry Division, CSIR-National Chemical Laboratory (CSIR-NCL), Dr. Homi Bhabha Road, Pune – 411 008, Maharashtra, India. E-mail: b.punji@ncl.res.in; Fax: +91 20 2590 2621; Tel: +91 20 2590 2733

^b Academy of Scientific and Innovative Research (AcSIR), Ghaziabad – 201 002, India

^c Centre for Material Characterization, CSIR-National Chemical Laboratory, Dr. Homi Bhabha Road, Pune – 411 008, India

† Electronic supplementary information (ESI) available: ¹H and ¹³C NMR spectra of all compounds, CIF files for **2a** (CCDC-2119314) and **4a** (CCDC-2119313). For ESI and crystallographic data in CIF or other electronic format see DOI: 10.1039/d2cy00027j

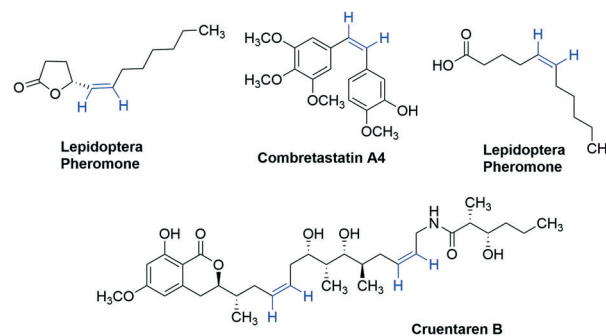


Fig. 1 Biologically important Z-alkene compounds.

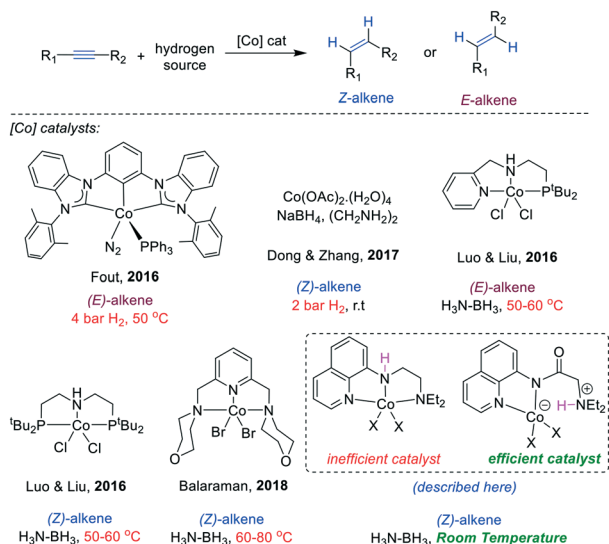


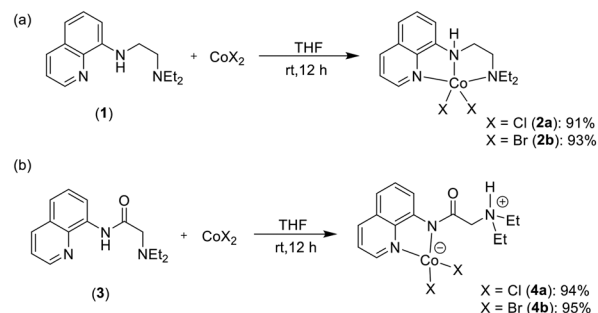
Fig. 2 Cobalt catalysts for the selective semi-hydrogenation of alkynes.

as a hydrogen source (Fig. 2).²⁰ Similarly, Balaraman, Zhou and Fan reported cobalt-catalyzed selective hydrogenation of alkynes to *Z*-alkenes using $\text{NH}_3\text{-BH}_3$ and H_2O as a hydrogen source, respectively.²¹ Though all these protocols efficiently provided *Z*-selective alkenes from alkynes, an elevated temperature of 60–80 °C is essential and/or they require the use of a phosphine-based ligand, whose synthesis involves a tedious multi-step process and an inert atmosphere. Therefore, developing a phosphine-free, nitrogen-ligated cobalt complex that can perform stereoselective hydrogenation at room temperature without requiring a special experimental setup would be an ideal and user-friendly approach. With this intention, we hypothesized to develop a nitrogen-based ligand with a dangling arm and acidic apical NH that can show hemilabile and non-innocent behavior during catalysis. Such a metal-bound ligand can provide suitable electronic features and vacant coordination sites for the incoming substrate and could activate the same *via* a unified mode of action. Thus, towards our goal to explore sustainable 3d metal catalysis,²² in this manuscript, we demonstrate the development of a set of phosphine-free and air-stable, 8-aminoquinolynyl-based (NNN) ligands and their coordination behavior. Depending on the ligand backbones, both pincer and non-pincer cobalt(II) complexes were obtained, and the non-pincer complex was found to be an efficient catalyst for the selective hydrogenation of alkyne derivatives at room temperature.

Results and discussion

Synthesis of cobalt catalysts

The quinolynyl-amide ligand, 2-(diethylamino)-*N*-(quinolin-8-yl)acetamide, ($^{\text{Q}}\text{NNN}^{\text{C}(\text{O})\text{NEt}_2}\text{-H}$ (**3**) was previously developed and explored for nickel catalysis.²³ We intended to investigate the reactivity of **3** and quinolynyl-amine ligand ($\text{C}_9\text{H}_6\text{N}(\text{NH})\text{CH}_2\text{CH}_2\text{NEt}_2$) [$^{\text{Q}}\text{NNN}^{\text{CH}_2\text{NEt}_2}\text{-H}$; **1**]²⁴ with cobalt



Scheme 1 Synthesis of cobalt complexes: (a) neutral pincer, (b) anionic chelate.

to understand the coordination reactivity and catalytic activity for the hydrogenation reaction. Thus, the reaction of ligand **1** with CoCl_2 and CoBr_2 at room temperature afforded the expected pincer complexes ($^{\text{Q}}\text{NNN}^{\text{CH}_2\text{NEt}_2}\text{CoCl}_2$ (**2a**) and ($^{\text{Q}}\text{NNN}^{\text{CH}_2\text{NEt}_2}\text{CoBr}_2$ (**2b**), respectively, as purple compounds (Scheme 1a). Both the compounds are NMR inactive, and thus, the chemical composition is determined by elemental analysis. Moreover, the molecular structure of complex **2a** was determined by X-ray analysis, wherein the NNN-ligand coordinated in a tridentate fashion resulting in the distorted trigonal bipyramidal (TBP) geometry around the $\text{Co}(\text{II})$ center (Fig. 3). In the structure of **2a**, the quinolynyl $\text{N}2$, amine $\text{N}3$ and one $\text{Cl}(1)$ ligands are in planar position with the average bond angle between them being 118.01°, whereas the central $\text{N}1$ and $\text{Cl}(2)$ are in axial position with the $\text{N}(1)\text{-Co}(1)\text{-Cl}(2)$ bond angle close to a straight angle (172.55(8)°).

Interestingly, the reaction of ligand ($^{\text{Q}}\text{NNN}^{\text{C}(\text{O})\text{NEt}_2}\text{-H}$ (**3**)^{23a} with CoCl_2 and CoBr_2 provided ($^{\text{Q}}\text{NN}$)-chelate complexes **4a** and **4b** in 94% and 95% yields, respectively (Scheme 1b). Both the complexes are air-stable and can be stored at room temperature for months. The chemical composition of both the complexes was verified by elemental analysis. The X-ray structural analysis of complex **4a** revealed the bidentate chelate coordination of ligand **3** to CoCl_2 with the amine nitrogen ($\text{N}3$) remaining uncoordinated (Fig. 4). Interestingly, the hydrogen atom of

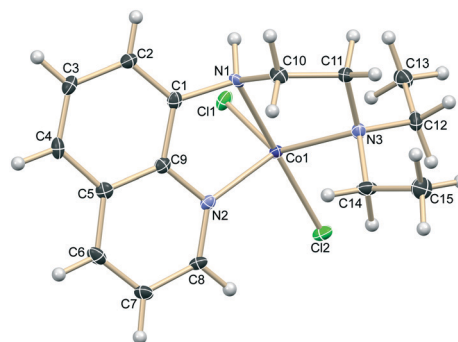


Fig. 3 Thermal ellipsoid plot of **2a**. Selected bond lengths (Å): $\text{Co}1\text{-N}1 = 2.201(3)$; $\text{Co}1\text{-N}2 = 2.099(3)$; $\text{Co}1\text{-N}3 = 2.163(3)$; $\text{Co}1\text{-Cl}1 = 2.3355(10)$; $\text{Co}1\text{-Cl}2 = 2.3103(10)$; $\text{N}1\text{-H}1 = 1.0$. Selected bond angles (°): $\text{N}1\text{-Co}1\text{-N}2 = 77.49(11)$; $\text{N}3\text{-Co}1\text{-N}1 = 80.67(11)$; $\text{N}1\text{-Co}1\text{-Cl}1 = 86.91(8)$; $\text{N}1\text{-Co}1\text{-Cl}2 = 172.55(8)$; $\text{Cl}1\text{-N}1\text{-C}10 = 112.1(3)$; $\text{C}10\text{-N}1\text{-Co}1 = 107.6(2)$; $\text{N}1\text{-C}10\text{-C}11 = 108.1(3)$.

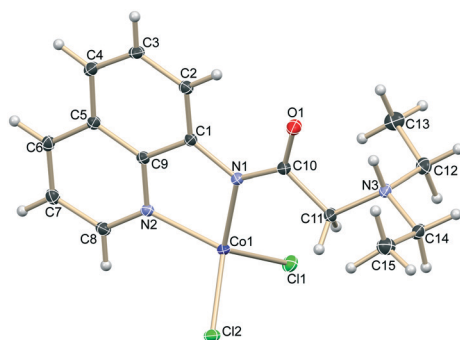


Fig. 4 Thermal ellipsoid plot of **4a**. Selected bond lengths (Å): Co1–N1 = 1.9982(10); Co1–N2 = 2.0269(10); Co1–Cl1 = 2.2658(3); O1–C10 = 1.2384(14); N3–H1 = 0.896(18). Selected bond angles (°): N1–Co1–N2 = 83.09(4); N1–Co1–Cl1 = 113.99(3); N1–Co1–Cl2 = 120.46(3); Cl2–Co1–Cl1 = 105.331(12); C1–N1–C10 = 121.29(9); C10–N1–Co1 = 126.01(8); N1–C10–C11 = 113.68(10).

N(1)–H migrated to N(3), thus making it an anionic Co(II) complex with the N(1)–Co(1) bond length of 1.9982(10) Å. The geometry around the cobalt is distorted tetrahedral, and that of the N(1) center is almost planar. We assume that the ligand **3** might initially form a tri-coordinated pincer complex (similar to that found with **1**), and later the hemilabile arm –NEt₂ decoordinates from cobalt upon abstracting an acidic N(1)–H bond. One can expect improved hemilability with ligand **3** (for complex **4a**) than with ligand **1** (for complex **2a**) because of the more flexible and wider N(1)–C(10)–C(11) bond angle (planar) in the former. The covalent bonding character of N(1)–Co(1) in complex **4a** could make it more electron-rich, whereas the tetraligation would give significant unsaturation for further reactivity.

Hydrogenation reaction

After the synthesis and characterization of the pincer complexes **2a,b** and non-pincer complexes **4a,b**, we investigated their catalytic activity for the selective transfer hydrogenation of internal alkyne to an alkene. Thus, in a typical reaction, diphenyl acetylene (**5a**; 1.0 equiv.) was chosen as a model substrate with ammonia borane as the hydrogen source (1.0 equiv.), and a cobalt catalyst (5 mol%) was used in MeOH (Table 1). At first, the use of both the pincer catalysts **2a,b** and non-pincer catalysts **4a,b** showed comparable activity at 65 °C with around 85% selectivity for *Z*-stilbene **6a** (entries 1–4). The employment of less expensive dimethylammonia-borane (Me₂NHBH₃) as a hydrogen source is less effective with **2a**, whereas quantitative hydrogenation was achieved in the presence of catalyst **4a** (Table S1, ESI†). Interestingly, the hydrogenation at 27 °C employing catalyst **2a** or **2b** led to low conversion; however, the reaction with the non-pincer catalyst **4a** retained the reactivity and provided 87% yield of *Z*-alkene **6a** (entries 5–7). The employment of analogous catalyst **4b** showed slightly higher selectivity for *Z*-alkene (91%) with complete hydrogenation (entry 8). Notably, the reduction in the loading of catalyst **4b** from 5 mol% to 2 mol% provided gratifyingly higher selectivity for

Table 1 Optimization of the reaction parameters for semi-hydrogenation^a

Entry	[Co]	T (°C)	GC conv.	6a (%)	7a (%)
1	2a	65	100	85	14
2	2b	65	100	88	12
3	4a	65	100	87	13
4	4b	65	100	84	16
5	2a	27	55	48	7
6	2b	27	61	45	16
7	4a	27	100	87	7
8	4b	27	100	91	8
9 ^b	4b	27	100	94 (89%) ^c	6
10 ^d	4b	27	81	73	7
11 ^{b,e}	4b	27	24–65	18–50	4–8
12 ^b	[Co] ^f	27	15–53	12–47	3–9
13 ^b	2a	27	23	18	4
14 ^b	2b	27	21	17	4

^a Reaction conditions: diphenyl acetylene (0.051 g, 0.50 mmol), [H]-source (0.50 mmol), solvent (1.5 mL). ^b 2 mol% loading of the catalyst. ^c Isolated yield. ^d 1 mol% loading of **4b**. ^e EtOH, ⁱPrOH, THF or toluene as a solvent. ^f CoCl₂, CoBr₂ or Co(OAc)₂ was employed as the catalyst.

Z-stilbene with up to 93% conversion (89% yield) (entry 9). Further lowering the catalyst loading led to a decrease in overall conversion (entry 10). The use of other protic (EtOH, ⁱPrOH) or aprotic (THF, toluene) solvents in place of MeOH led to a drastic reduction in hydrogenation (entry 11). The employment of simple CoCl₂, CoBr₂ or Co(OAc)₂ salts or the pincer complexes **2a** and **2b** as catalysts at 27 °C provided low to moderate yields of hydrogenated product **6a** (entries 12–14). All these studies suggest the importance of the ligand backbone in the non-pincer complexes **4a,b** with regards to the flexibility and hemilability of the dangling N-arm that might provide a vacant coordination sphere to the incoming substrate and stabilize the active cobalt species.

Scope for the synthesis of *Z*-alkene

With the optimized reaction conditions in hand, we started to explore the substrate scope by synthesizing *Z*-alkenes using 2–4 mol% of catalyst **4b** and ammonia borane (1 equiv.) at room temperature (Scheme 2). The biaryl alkynes with various substitutions at the *para*-position tolerated the reaction conditions to give respective *Z*-alkenes with high selectivity. The electron-donating groups on alkynes like methyl and methoxy showed very good selectivity for *Z*-alkene and yielded the respective compounds in 86% and 87% yields. The selectivity for *Z*-alkene was reduced when an electron-withdrawing group was attached to the *para*-position of the aryl alkyne, *i.e.* –CF₃ and –F groups (**6d,e**). Notably, a substantial amount of complete hydrogenation of alkynes to alkanes was observed for these substrates. The hydrogenation

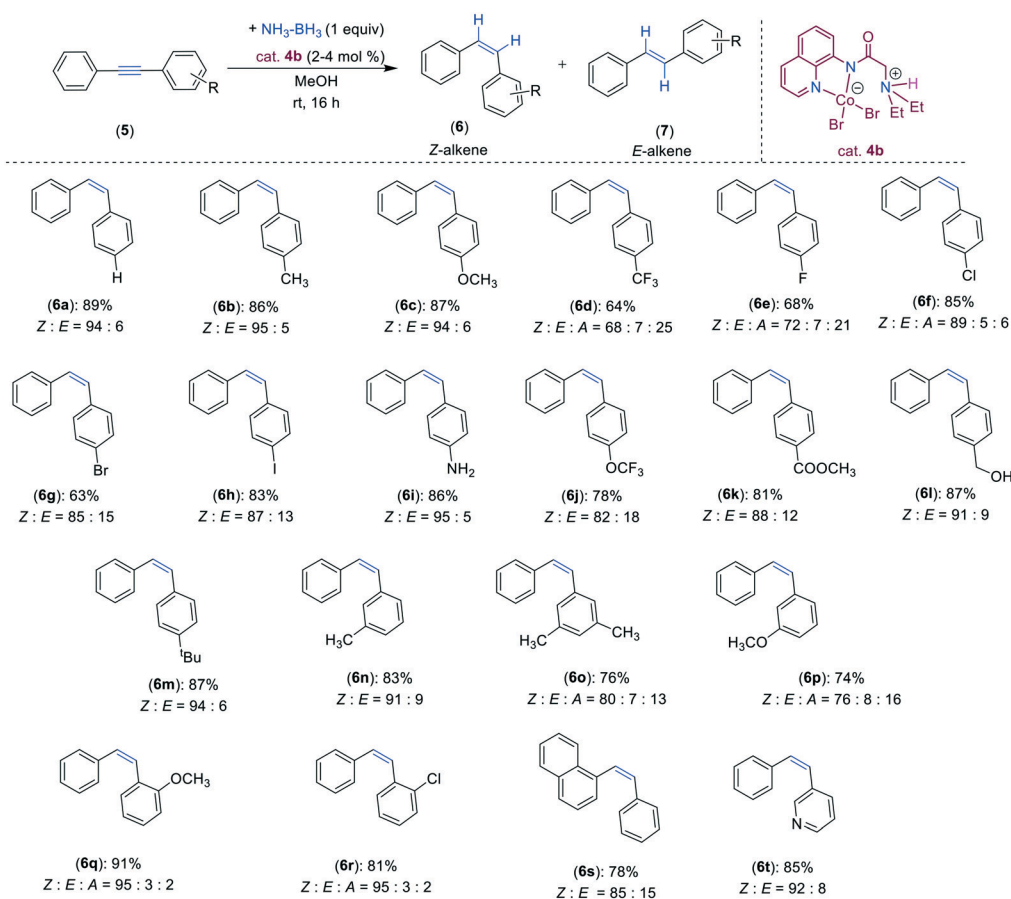
reaction could tolerate various halide substituents, *i.e.* chloro, bromo and iodo, affording the desired *Z*-alkenes **6f–h** in excellent yields. The tolerability of such functionalities is very important from the synthetic perspective as they can be used for further derivatization. The free amine and ester functional groups remained unaffected during the reaction and provided semi-hydrogenated *Z*-alkenes **6i** and **6k** in 86% and 81% yields, respectively. The chemo-selectivity of the catalyst for the alkyne hydrogenation over the ester group is noteworthy. Moreover, the benzylic alcohol functionality was tolerated well and gave 87% yield of **6l**. The alkynes with a $-\text{OCF}_3$ group or a bulky $-\text{tBu}$ moiety hydrogenated well under the reaction conditions to give **6j** and **6m** in good yields. In addition to the *para*-substituted aryl alkynes, both the *ortho*- and *meta*-substituted aryl alkynes hydrogenated smoothly to achieve selective *Z*-alkenes **6n–6r** in good yields. Similarly, the heterocycle, 3-pyridinyl alkyne–arene reacted efficiently to provide highly selective *Z*-alkene **6t** in 85% yield. The significance of this chemo- and stereoselective hydrogenation protocol can be highlighted for its facile reaction at room temperature and tolerance of diverse and valuable functionalities. Notably, the aryl alkyne substrates containing $-\text{NO}_2$, $-\text{CN}$, $-\text{COCH}_3$, $-\text{CHO}$, $-\text{OH}$, and $-\text{SH}$ functionalities were either decomposed under the reaction conditions or

failed to undergo desired hydrogenation (Sec 6, ESI†). Similarly, the alkylated alkynes remained unreactive under the optimized reaction conditions at room temperature.

Finally, a gram-scale synthesis of *Z*-stilbene was carried out using 1.082 g (6.0 mmol) of **5a** employing 2 mol% of catalyst **4b** in 15 mL of MeOH in a high-pressure reaction vessel. This experiment proceeded smoothly and gave an 84% yield of *Z*-stilbene that ensures the synthetic applicability of the optimized protocol in the gram-scale production.

Mechanistic study

We initiated the mechanistic investigation to understand the operational mode of the cobalt catalyst and the reaction pathway. The significance of the N–H proton on ligands **1** and **3** in complexes **2b** and **4b** was analyzed (Scheme 3a). The high activity of complex **4b** compared to that of **2b** in the hydrogenation of alkynes suggests that the acidity or lability of the N–H proton plays a crucial role in the desired intermediate formation. Moreover, the developed quinolinamide complex **8** showed good catalytic activity, whereas that of the quinolinamine cobalt complex **9** was very poor (Scheme 3a). These findings confirm that the acidity of N–H present in the ligand backbone plays a crucial role.



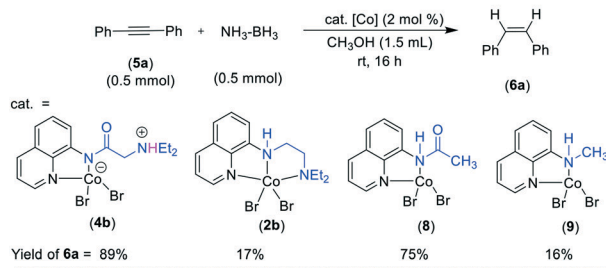
Scheme 2 Scope of semihydrogenation of diarylalkyne to *Z*-alkene. The yields (%) shown are for the isolated *Z*-alkenes. The *Z*:*E* ratios of alkenes are from the crude reaction mixture. A = alkane.

Comparing the activity of complexes **4b** and **8** highlighting the hemilability of the dangling $-\text{NEt}_2$ arm in complex **4b** may have little role in stabilizing active catalyst species. The kinetic analysis for the hydrogenation of **5c** and **5d** suggests that the electron-rich alkyne is slightly more reactive than the electron-deficient alkyne (Scheme 3b(i); Fig. S1 in the ESI[†]), which could be due to the better coordination of the former. A similar pattern of reactivity was observed in the competition experiment, upon performing the reaction in the same reaction vessel (Scheme 3b(ii)). The standard hydrogenation reaction in CD_3OD solvent provided the product **6a**-[D] with >99% deuterium incorporating into one of the alkenyl carbon (Scheme 3c), which highlights that one of the hydrogen atoms in the product arises from methanol, and the hydridic $-\text{H}$ comes from NH_3-BH_3 . However, NH_3-BH_3 would provide both the hydrogens to the product when the reaction is performed

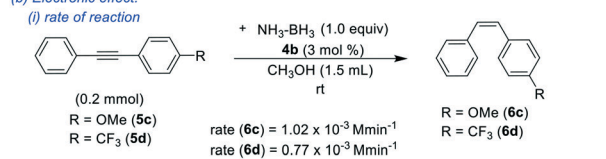
without methanol. Next, we treated alkyne **5a** with two equiv. of NH_3-BH_3 at room temperature, which led to its complete conversion into stilbene isomers (*Z/E*: 79/21) without forming any alkane product (Scheme 3d). This result highlights the greater reactivity of catalyst **4b** for the semi-reduction of alkyne to alkene than that for the complete reduction to the alkane. However, the formation of 21% yield of *E*-stilbene indicated the effectiveness of catalyst **4b** for the isomerization of alkene. Moreover, the attempted hydrogenation of *Z*-stilbene using catalyst **4b** and NH_3-BH_3 provided isomerized product *E*-stilbene **7a** and did not afford alkane even at elevated temperature (Scheme 3e). The isomerization of *Z*-stilbene (**6a**) to *E*-stilbene (**7a**) over the time course revealed that the isomerization is significant in the early time and equilibrates approximately in 60 min (Fig. S2[†]). Interestingly, the isomerization of **6a** to **7a** was not observed in the absence of a cobalt catalyst. All these findings suggest that the catalyst **4b** can be used for the isomerization of alkenes, and the catalyst is highly selective for alkyne to alkene hydrogenation.²⁰

Based on the preliminary investigation and literature precedents,^{19a,20} we have proposed a tentative catalytic cycle for the **4b**-catalyzed semi-hydrogenation of alkynes (Fig. 5). It is hypothesized that the initially formed pincer (NNN)CoX₂ would undergo rearrangement to non-pincer complex **4**. Complex **4** will be reduced by NH_3-BH_3 to an active Co(I) hydride complex **A**. Many attempts to synthesize and isolate the Co-H species **A** were unsuccessful, probably due to the non-stability of the electron-rich Co-H species ligated by an NNN-donor ligand. The formation of such cobalt hydride species from Co(II) complexes is well-documented for complexes bearing a phosphine ligand backbone.^{18a,25} The decoordination of the flexible nitrogen-arm followed by alkyne coordination would give intermediate **C**. Insertion of

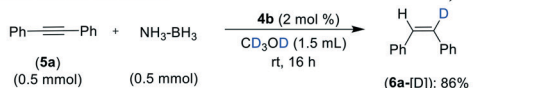
(a) Hydrogenation with different [Co] catalysts:



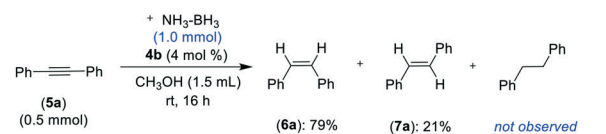
(b) Electronic effect:



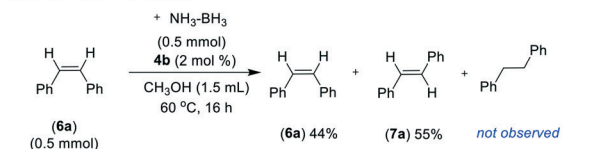
(c) Deuterium labelling experiment:



(d) Attempted over-reduction experiment:



(e) Isomerization experiment:



Scheme 3 Mechanistic experiments: (a) Hydrogenation with different [Co] catalysts, (b) Electronic effect: (i) rate of reaction and (ii) competition reaction, (c) Deuterium labelling experiment, (d) Attempted over-reduction experiment, and (e) Isomerization experiment.

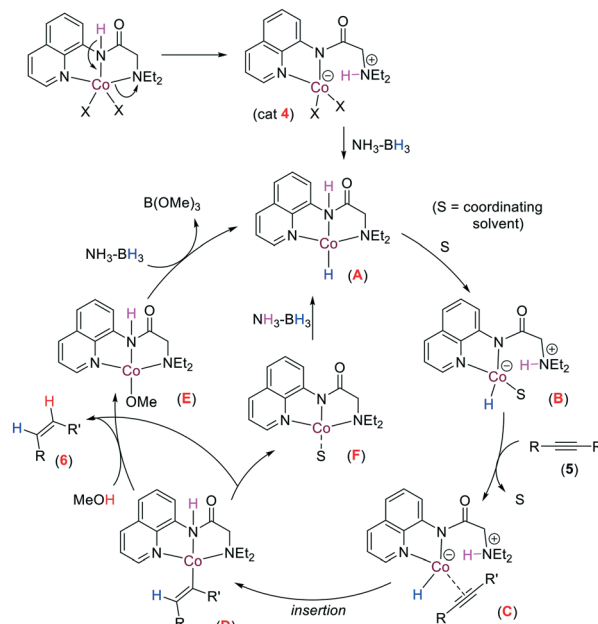


Fig. 5 Proposed mechanisms.

an alkyne into the Co–H bond will lead to pincer alkenyl-cobalt complex **D**, which will be followed by the protonation of a Co–alkenyl bond to afford product **6**.²⁰ The methoxy-cobalt intermediate **E** would react with NH₃–BH₃ to regenerate active catalyst **A**. Alternately, in the absence of a protic solvent, the intermediate **D** would undergo intramolecular trapping of N–H by a alkenyl moiety to produce product **6** and (NNN)Co complex **F**. The intermediate **F** can react with NH₃–BH₃ to regenerate active complex **A**. We assume that the ligand's hemilability and non-innocent behavior leads to the coordination and decoordination of the nitrogen-arm that provides desired stability and vacant coordination sphere, respectively, around the cobalt center. This might assist the catalyst to facilitate hydrogenation at room temperature.

Conclusions

In summary, we demonstrated the room temperature chemoselective and stereodivergent catalytic transfer semi-hydrogenation of alkynes to *Z*-alkenes using phosphine-free, hemilabile cobalt catalysts. Well-defined pincer cobalt complexes $\kappa^3\text{-}(\text{QNN}^{\text{CH}_2\text{NEt}_2})\text{CoX}_2$ were obtained from the quinolinyl-amine ligand, whereas the quinolinyl-amide ligand provided hemilabile, chelate anionic complexes $\kappa^2\text{-}(\text{QNN})\text{CoX}_2(\text{N}^{\text{C}(\text{O})\text{HNEt}_2})$. The anionic non-pincer cobalt complexes were very effective catalysts for the semi-hydrogenation of alkynes at room temperature using an air-stable and user-friendly ammonia borane hydrogen source. This system operates under extremely mild conditions and allows semi-hydrogenation of alkynes with excellent yields and selectivity.

Experimental

Representative procedure for hydrogenation

A Teflon screw-cap tube equipped with a magnetic bar was introduced with the catalyst **4b** (0.0048 g, 0.01 mmol), ammonia borane (0.0155 g, 0.5 mmol) and diphenylacetylene (**5a**; 0.089 g, 0.5 mmol) inside the glove box. Methanol (1.5 mL) was added to the reaction vessel under an argon atmosphere. The reaction mixture was then stirred at room temperature (27 °C) for 16 h. At ambient temperature, the reaction mixture was diluted with MeOH (5.0 mL) and the resulting solution was concentrated under vacuum. The crude reaction mixture was then purified by flash chromatography on silica gel (petroleum ether) to obtain *Z*-stilbene **6a** (0.080 g, 89%) as a colourless oil. ¹H-NMR (500 MHz, CDCl₃): δ 7.29–7.19 (m, 10H, Ar–H), 6.63 (s, 2H, CH). ¹³C{¹H}-NMR (125 MHz, CDCl₃): δ 137.4 (2C, C_q), 130.4 (2C, CH), 129.1 (4C, CH), 128.4 (4C, CH), 127.3 (2C, CH). HRMS (ESI): *m/z* calcd. for C₁₄H₁₂ + H⁺ [M + H]⁺ 181.1017; found 181.1012.

Conflicts of interest

There are no conflicts to declare.

Acknowledgements

This work was financially supported by SERB, New Delhi, India (CRG/2020/000554). DMS thanks CSIR-New Delhi for a research fellowship.

Notes and references

- (a) A. M. Kluwer and C. J. Elsevier, in *The Handbook of Homogeneous Hydrogenation*, 2006, p. 374; (b) C. Oger, L. Balas, T. Durand and J.-M. Galano, *Chem. Rev.*, 2013, **113**, 1313.
- (a) G. C. Tron, T. Pirali, G. Sorba, F. Pagliari, S. Busacca and A. A. Genazzani, *J. Med. Chem.*, 2006, **49**, 3033; (b) V. V. Semenov, A. S. Kiselyov, I. Y. Titov, I. K. Sagamanova, N. N. Ikizalp, N. B. Chernysheva, D. V. Tsyganov, L. D. Konyushkin, S. I. Firgang, R. V. Semenov, I. B. Karmanova, M. M. Raihstat and M. N. Semenova, *J. Nat. Prod.*, 2010, **73**, 1796.
- M. Fouché, L. Rooney and A. G. M. Barrett, *J. Org. Chem.*, 2012, **77**, 3060.
- K. C. Nicolaou, R. A. Daines, T. K. Chakraborty and Y. Ogawa, *J. Am. Chem. Soc.*, 1987, **109**, 2821.
- V. N. Odinokov, *Chem. Nat. Compd.*, 2000, **36**, 11.
- For example, see: (a) P. R. Blakemore, *J. Chem. Soc., Perkin Trans. 1*, 2002, 2563; (b) B. K. Keitz, K. Endo, P. R. Patel, M. B. Herbert and R. H. Grubbs, *J. Am. Chem. Soc.*, 2012, **134**, 693.
- (a) R. R. Schrock and J. A. Osborn, *J. Am. Chem. Soc.*, 1976, **98**, 2143; (b) M. Crespo-Quesada, F. Cárdenas-Lizana, A.-L. Dessimoz and L. Kiwi-Minsker, *ACS Catal.*, 2012, **2**, 1773.
- (a) B. M. Trost, Z. T. Ball and T. Jöge, *J. Am. Chem. Soc.*, 2002, **124**, 7922; (b) K. Radkowski, B. Sundararaju and A. Fürstner, *Angew. Chem., Int. Ed.*, 2013, **52**, 355; (c) M. Leutzsch, L. M. Wolf, P. Gupta, M. Fuchs, W. Thiel, C. Farès and A. Fürstner, *Angew. Chem., Int. Ed.*, 2015, **54**, 12431.
- (a) M. W. van Laren and C. J. Elsevier, *Angew. Chem., Int. Ed.*, 1999, **38**, 3715; (b) E. Shirakawa, H. Otsuka and T. Hayashi, *Chem. Commun.*, 2005, 5885; (c) R. Shen, T. Chen, Y. Zhao, R. Qiu, Y. Zhou, S. Yin, X. Wang, M. Goto and L.-B. Han, *J. Am. Chem. Soc.*, 2011, **133**, 17037.
- (a) K. E. Tani, A. Iseki and T. Yamagata, *Chem. Commun.*, 1999, 1821; (b) J. Yang, C. Wang, Y. Sun, X. Man, J. Li and F. Sun, *Chem. Commun.*, 2019, **55**, 1903; (c) Z. Huang, Y. Wang, X. Leng and Z. Huang, *J. Am. Chem. Soc.*, 2021, **143**, 4824.
- For a review, see: D. Wang and D. Astruc, *Chem. Rev.*, 2015, **115**, 6621.
- (a) Y.-P. Zhou, Z. Mo, M.-P. Luecke and M. Driess, *Chem. – Eur. J.*, 2018, **24**, 4780; (b) A. Brzozowska, L. M. Azofra, V. Zubar, I. Atodiressei, L. Cavallo, M. Rueping and O. El-Sepelgy, *ACS Catal.*, 2018, **8**, 4103; (c) M. Garbe, S. Budweg, V. Papa, Z. Wei, H. Hornke, S. Bachmann, M. Scalone, A. Spannenberg, H. Jiao, K. Junge and M. Beller, *Catal. Sci. Technol.*, 2020, **10**, 3994; (d) V. Zubar, J. Sklyaruk, A. Brzozowska and M. Rueping, *Org. Lett.*, 2020, **22**, 5423; (e) J. Sklyaruk, V. Zubar, J. C. Borghs and M. Rueping, *Org. Lett.*, 2020, **22**, 6067.

- 13 D. Srimani, Y. Diskin-Posner, Y. Ben-David and D. Milstein, *Angew. Chem., Int. Ed.*, 2013, **52**, 14131.
- 14 (a) R. Barrios-Francisco and J. J. Garcia, *Appl. Catal., A*, 2010, **385**, 108; (b) E. Richmond and J. Moran, *J. Org. Chem.*, 2015, **80**, 6922.
- 15 (a) K. Semba, T. Fujihara, T. Xu, J. Terao and Y. Tsuji, *Adv. Synth. Catal.*, 2012, **354**, 1542; (b) F. Pape, N. O. Thiel and J. F. Teichert, *Chem. – Eur. J.*, 2015, **21**, 15934; (c) N. O. Thiel and J. F. Teichert, *Org. Biomol. Chem.*, 2016, **14**, 10660; (d) T. Wakamatsu, K. Nagao, H. Ohmiya and M. Sawamura, *Organometallics*, 2016, **35**, 1354; (e) E. Korytiaková, N. O. Thiel, F. Pape and J. F. Teichert, *Chem. Commun.*, 2017, **53**, 732.
- 16 For reviews, see: (a) L. Alig, M. Fritz and S. Schneider, *Chem. Rev.*, 2019, **119**, 2681; (b) D. M. Sharma and B. Punji, *Chem. – Asian J.*, 2020, **15**, 690.
- 17 (a) A. Mukherjee and D. Milstein, *ACS Catal.*, 2018, **8**, 11435; (b) W. Liu, B. Sahoo, K. Junge and M. Beller, *Acc. Chem. Res.*, 2018, **51**, 1858; (c) W. Ai, R. Zhong, X. Liu and Q. Liu, *Chem. Rev.*, 2019, **119**, 2876.
- 18 (a) A. Mukherjee, D. Srimani, S. Chakraborty, Y. Ben-David and D. Milstein, *J. Am. Chem. Soc.*, 2015, **137**, 8888; (b) Z. Shao, S. Fu, M. Wei, S. Zhou and Q. Liu, *Angew. Chem., Int. Ed.*, 2016, **55**, 14653; (c) R. Adam, C. B. Bheeter, J. R. Cabrero-Antonino, K. Junge, R. Jackstell and M. Beller, *ChemSusChem*, 2017, **10**, 842; (d) K. Tokmic, B. J. Jackson, A. Salazar, T. J. Woods and A. R. Fout, *J. Am. Chem. Soc.*, 2017, **139**, 13554; (e) H. Dai and H. Guan, *ACS Catal.*, 2018, **8**, 9125; (f) H. Li, A. Al-Dakhil, D. Lupp, S. S. Gholap, Z. Lai, L.-C. Liang and K.-W. Huang, *Org. Lett.*, 2018, **20**, 6430; (g) D. M. Sharma and B. Punji, *Adv. Synth. Catal.*, 2019, **361**, 3930; (h) J. Schneekönig, B. Tannert, H. Hornke, M. Beller and K. Junge, *Catal. Sci. Technol.*, 2019, **9**, 1779.
- 19 (a) K. Tokmic and A. R. Fout, *J. Am. Chem. Soc.*, 2016, **138**, 13700; (b) C. Chen, Y. Huang, Z. Zhang, X.-Q. Dong and X. Zhang, *Chem. Commun.*, 2017, **53**, 4612; (c) J. Chen, X. Shen and Z. Lu, *J. Am. Chem. Soc.*, 2020, **142**, 14455; (d) K. Chen, H. Zhu, Y. Li, Q. Peng, Y. Guo and X. Wang, *ACS Catal.*, 2021, **11**, 13696.
- 20 (a) S. Fu, N.-Y. Chen, X. Liu, Z. Shao, S.-P. Luo and Q. Liu, *J. Am. Chem. Soc.*, 2016, **138**, 8588; (b) J. Chen, J. Guo and Z. Lu, *Chin. J. Chem.*, 2018, **36**, 1075.
- 21 (a) V. G. Landge, J. Pitchaimani, S. P. Midya, M. Subaramanian, V. Madhu and E. Balaraman, *Catal. Sci. Technol.*, 2018, **8**, 428; (b) K. Li, R. Khan, X. Zhang, Y. Gao, Y. Zhou, H. Tan, J. Chen and B. Fan, *Chem. Commun.*, 2019, **55**, 5663.
- 22 (a) V. Soni, D. M. Sharma and B. Punji, *Chem. – Asian J.*, 2018, **13**, 2516; (b) D. K. Pandey, S. B. Ankade, A. Ali, C. P. Vinod and B. Punji, *Chem. Sci.*, 2019, **10**, 9493; (c) R. A. Jagtap, C. P. Vinod and B. Punji, *ACS Catal.*, 2019, **9**, 431; (d) R. A. Jagtap, P. P. Samal, C. P. Vinod, S. Krishnamurty and B. Punji, *ACS Catal.*, 2020, **10**, 7312; (e) R. A. Jagtap, S. K. Verma and B. Punji, *Org. Lett.*, 2020, **22**, 4643; (f) S. B. Ankade, P. P. Samal, V. Soni, R. G. Gonnade, S. Krishnamurty and B. Punji, *ACS Catal.*, 2021, **11**, 12384; (g) S. B. Ankade, A. B. Shabade, V. Soni and B. Punji, *ACS Catal.*, 2021, **11**, 3268.
- 23 (a) V. Soni, R. A. Jagtap, R. G. Gonnade and B. Punji, *ACS Catal.*, 2016, **6**, 5666; (b) V. Soni, S. M. Khake and B. Punji, *ACS Catal.*, 2017, **7**, 4202; (c) R. A. Jagtap, V. Soni and B. Punji, *ChemSusChem*, 2017, **10**, 2242.
- 24 Q. Yan, Y. C. Fang, Y. X. Jia and X. H. Duan, *New J. Chem.*, 2017, **41**, 2372.
- 25 (a) L.-S. Zhang, Z. Zuo, X. Leng and Z. Huang, *Angew. Chem., Int. Ed.*, 2014, **53**, 2696; (b) S. P. Semproni, C. Milsmann and P. J. Chirik, *J. Am. Chem. Soc.*, 2014, **136**, 9211; (c) D. Srimani, A. Mukherjee, A. F. G. Goldberg, G. Leitius, Y. Diskin-Posner, L. J. W. Shimon, Y. Ben-David and D. Milstein, *Angew. Chem., Int. Ed.*, 2015, **54**, 12357.

